

Dissertation zur Erlangung des Doktorgrades
der Fakultät für Chemie und Pharmazie
der Ludwig-Maximilians-Universität München

**Proteotoxicity of polyglutamine expansion
proteins: Cellular mechanisms and their
modulation by molecular chaperones**

Christian Behrends

aus

Frankfurt am Main

2006

Erklärung

Diese Dissertation wurde im Sinne von §13 Abs. 3 bzw. 4 der Promotionsordnung vom 29. Januar 1998 von Prof. Dr. Franz-Ulrich Hartl betreut.

Ehrenwörtliche Versicherung

Diese Dissertation wurde selbstständig, ohne unerlaubte Hilfe erarbeitet.

München, den 4. Dezember 2006

Christian Behrends

Dissertation eingereicht am: 04.12.2006

1. Gutachter: Prof. Dr. Franz-Ulrich Hartl
2. Gutachter: Priv.-Doz. Dr. Konstanze F. Winklhofer

Mündliche Prüfung am: 07.03.2007

Danksagung

Die vorliegende Arbeit wurde in der Zeit von Oktober 2002 bis November 2006 am Max-Planck-Institut für Biochemie, Martinsried, in der Abteilung Zelluläre Biochemie angefertigt. An dieser Stelle möchte ich meinen Dank all jenen aussprechen, die zum Gelingen dieser Arbeit beigetragen haben.

Mein besonderer Dank gilt dabei Prof. Dr. F. Ulrich Hartl für die interessante und reizvolle Themenstellung, die großzügige Förderung und die hervorragenden Möglichkeiten, in seiner Abteilung wissenschaftliches Denken und Arbeiten zu erlernen. Für hilfreiche Anregungen und wertvolle Ratschläge danke ich auch Dr. Manajit Hayer-Hartl.

Dr. Konstanze F. Winklhofer danke ich ganz herzlich für konstruktive Diskussionen und die Erstellung des Zweitgutachtens.

Ein besonderer Dank gilt Dr. Peter Breuer und Dr. Gregor Schaffar für die langjährige, freundschaftliche und produktive Zusammenarbeit. Ihr Interesse, ihre Ideen und ihre Diskussionsbereitschaft haben wesentlich zum Erfolg dieser Arbeit beigetragen. Dr. Katja Siegers und Dr. Sarah Broadley danke ich für ihre Hilfsbereitschaft und Unterstützung sowie viele wertvolle Anregungen. Dr. Raina Boteva und Carola Langer danke ich für die hervorragende Zusammenarbeit. Dr. Jose Baral, Dr. Martin Vabulas, Dr. Jason Young und Dr. Zoya Ignatova danke ich für viele inspirierende Diskussionen.

Weiterer Dank gilt allen momentanen und ehemaligen Mitarbeitern der Abteilung für die freundschaftliche und hilfsbereite Atmosphäre, ohne die ein erfolgreiches Arbeiten nicht möglich gewesen wäre. Insbesondere danke ich in diesem Zusammenhang Alice, Angela, Christian, Chun, Iris, Jose, Juliane, Geli, Michael, Niclas, Sathish, Sophia, Shruti, Chi, Uli und Ulrike. Tobi danke ich für die vielen erfrischenden Stunden im und außerhalb des Labors.

Zum Abschluss gilt mein besonderer Dank aber meiner Familie, die meine Arbeit wohlwollend begleitet und mich in jeglicher Form unterstützt haben. Meinen Eltern, meiner Schwester und meiner Großmutter Charlotte danke ich von ganzem Herzen für die vielen aufmunternden Worte, das stete Daumendrücken und ihre gedankliche Anwesenheit. Susanne möchte ich für ihre Freude, Tränen und Liebe danken.

“Au football, tout est compliqué par la présence de l'équipe adverse”

Jean-Paul Sartre

1 Summary	1
2 Introduction	2
2.1 Protein folding	2
2.1.1 Protein folding problem	3
2.1.2 Protein folding mechanisms and energy landscapes	3
2.1.3 Folding of small and large proteins	5
2.2 Protein folding <i>in vivo</i>	6
2.2.1 Protein aggregation	6
2.2.2 Macromolecular crowding	6
2.2.3 Nascent polypeptide chains	7
2.2.4 Molecular chaperones	9
2.3 A chaperone network in the eukaryotic cytosol	10
2.3.1 Ribosome associated factors	10
2.3.2 The Hsp70 chaperones	11
2.3.3 The chaperonin TRiC	13
2.3.4 GimC/Prefoldin	16
2.3.5 Hsp90	17
2.3.6 Chaperone-mediated protein degradation	17
2.4 Aberrant protein folding and conformational diseases	19
2.4.1 Protein aggregation and amyloid-like deposits	20
2.4.1.1 Structure and formation of amyloid fibrils	20
2.4.1.2 Protein aggregation and toxicity	22
2.4.2 Huntington's disease	24
2.4.2.1 Huntingtin	24
2.4.2.2 PolyQ aggregation	25
2.4.2.3 The nature of toxic species in polyQ aggregation	27
2.4.2.4 Mechanisms of polyQ aggregation mediated toxicity	28
2.4.2.5 Transcriptional dysregulation	29
2.4.2.6 Molecular chaperones in polyQ aggregation and toxicity	31
2.5 Aim of thesis	34
3 Material and Methods	35
3.1 Material	35
3.1.1 Instruments	35
3.1.2 Chemicals	35
3.1.3 Buffers and Media	37
3.1.4 Antisera	38
3.1.5 Bacterial and yeast strains, mammalian cell lines	39
3.1.6 Plasmids and oligonucleotides	40
3.2 Methods	41
3.2.1 Molecular biological methods	41

3.2.1.1	Plasmid DNA purification.....	41
3.2.1.2	Determination of DNA concentration.....	41
3.2.1.3	Plasmid DNA sequencing.....	41
3.2.1.4	DNA restriction digestion.....	41
3.2.1.5	Dephosphorylation of DNA fragments.....	42
3.2.1.6	5'-DNA end overhand fill in.....	42
3.2.1.7	DNA purification.....	42
3.2.1.8	DNA agarose gel electrophoresis.....	42
3.2.1.9	DNA extraction from agarose gels.....	42
3.2.1.10	Polymerase chain reaction (PCR).....	43
3.2.1.11	Oligonucleotides annealing.....	43
3.2.1.12	Site-directed mutagenesis.....	43
3.2.1.13	Ligation of DNA fragments.....	44
3.2.1.14	Preparation and transformation of competent E. coli cells.....	44
3.2.2	Yeast methods.....	45
3.2.2.1	Culture and storage.....	45
3.2.2.2	Determination of cell density.....	45
3.2.2.3	Preparation and transformation of competent yeast cells.....	45
3.2.2.4	Purification of DNA from yeast cells.....	46
3.2.2.5	Protein expression in yeast cells.....	46
3.2.2.6	Growth assays.....	47
3.2.2.7	Luciferase assay.....	47
3.2.2.8	β -Galactosidase assay.....	47
3.2.2.9	Preparation of yeast cell lysates.....	48
3.2.2.10	Immunofluorescence.....	48
3.2.3	Mammalian cell culture methods.....	49
3.2.3.1	Cultivation of adherent cells.....	49
3.2.3.2	Transient transfection.....	49
3.2.3.3	Preparation of cell lysates.....	50
3.2.3.4	Immunofluorescence.....	50
3.2.3.5	Luciferase assay.....	50
3.2.4	Biochemical methods.....	51
3.2.4.1	Determination of protein concentration.....	51
3.2.4.2	SDS polyacrylamide gel electrophoresis (SDS-PAGE).....	51
3.2.4.3	Western Blotting.....	51
3.2.4.4	Dot blot assay.....	52
3.2.4.5	In vitro HttExon1-Aggregation.....	52
3.2.4.6	Filter retardation assay.....	52
3.2.4.7	Size exclusion chromatography.....	53
3.2.4.8	Immunoprecipitation.....	53
3.2.4.9	Ni-NTA pull down of His-tagged proteins.....	53
3.2.4.10	Trichloroacetic acid (TCA)-precipitation.....	53
4	Results.....	54
4.1	PolyQ toxicity mediated by transcription factor deactivation.....	54
4.1.1	PolyQ aggregation and sequestration of the transcription factor TBP.....	55
4.1.1.1	Aggregation of mutant Htt and TBP.....	56

4.1.1.2	Requirements for Htt aggregation and TBP recruitment.....	57
4.1.2	Impairment of transcription factors by soluble, misfolded polyQ proteins	61
4.1.2.1	Growth impairment upon expression of nuclear targeted polyQ-expanded Htt	63
4.1.2.2	Correlation between soluble, oligomeric polyQ-expanded Htt and cellular toxicity.....	66
4.1.2.3	Functional interference of TBP upon expression of nuclear targeted mutant Htt	68
4.1.2.4	Transcriptional dysregulation due to aberrant interactions of mutant Htt and TBP	70
4.1.2.5	General impairment of transcription factors by soluble, oligomeric mutant Htt	72
4.1.2.6	Influence of flanking sequences on TBP mediated polyQ protein toxicity	74
4.2	Chaperonin TRiC as modulator of polyQ protein aggregation and toxicity	80
4.2.1	TRiC deficiency modulates the properties of polyQ-expanded Htt.....	81
4.2.1.1	Pronounced polyQ aggregation due to TRiC impairment	81
4.2.1.2	Ambivalent effect of TRiC impairment on polyQ toxicity.....	83
4.2.2	Influence of TRiC overexpression on the properties of mutant Htt.....	88
4.2.2.1	Suppression of detergent-resistant aggregate formation.....	88
4.2.2.2	Generation and accumulation of detergent-soluble polyQ oligomers	91
4.2.2.3	Cooperative and effective modulation of toxic, oligomeric aggregation intermediates	93
4.2.2.4	Structural differences between toxic and benign Htt oligomers.....	97
5	Discussion.....	100
5.1	PolyQ-induced transcriptional dysregulation.....	102
5.1.1	Contribution of aggregated polyQ-expanded Htt.....	103
5.1.1.1	Sequestration and co-aggregation of TBP	104
5.1.1.2	Prerequisites for Htt aggregation and TBP co-aggregation	105
5.1.2	Contribution of soluble, misfolded polyQ-expanded Htt to toxicity	106
5.1.2.1	Influence of cellular localization on polyQ aggregation and toxicity.....	107
5.1.2.2	Significance of soluble, misfolded polyQ intermediates	108
5.1.2.3	Mechanism of transcription factor deactivation	109
5.1.2.4	Influence of sequence context on polyQ aggregation and toxicity.....	111
5.2	Molecular chaperones and polyQ expansion proteins	113
5.2.1	Modulation of polyQ aggregation and toxicity by the chaperonin TRiC	114
5.2.2	TRiC deficiency.....	114
5.2.3	TRiC overexpression	116
5.2.3.1	Modulation of aggregated polyQ-expanded Htt.....	116
5.2.3.2	Modulation of soluble, misfolded and toxic polyQ-expanded Htt	118
5.2.4	Cooperation of TRiC with Hsp70 in altering aggregation and toxicity	119
5.3	Existence of distinct polyQ oligomeric states	122
5.4	Implications in neurodegenerative diseases	124
5.5	Perspective.....	125
6	References	126
7	Appendix	145
7.1	Abbreviations	145
7.2	Publications and Presentations.....	146
7.3	Curriculum vitae.....	147

1 Summary

Proteins are central to all biological processes. To become functionally active, newly synthesized protein chains must fold into unique three-dimensional conformations. A group of proteins, known as molecular chaperones, are essential for protein folding to occur with high efficiency in cells. Their main role is to prevent off-pathway reactions during folding that lead to misfolding and aggregation. A number of human diseases are known to result from aberrant folding reactions. The formation of insoluble protein aggregates in neurons is a hallmark of neurodegenerative diseases including Huntington's disease (HD). These disorders are thought to result from the acquisition of dominant, toxic functions of misfolded proteins.

HD is caused by a CAG trinucleotide expansion that results in the expansion of a polyglutamine (polyQ) tract in the protein Huntingtin (Htt). The disorder is characterized by a progressive loss of specific neurons and the formation of inclusions containing aggregated Htt. Aggregate formation is causally linked to the progressive HD neuropathology, though it is not clear whether large insoluble, fibrillar structures or smaller assemblies of Htt are the toxic agents. Toxicity could arise from the recruitment of other polyQ-containing proteins, i.e. transcription factors, into the inclusions resulting in a loss of their normal cellular functions.

Here, soluble Htt oligomers have been found to accumulate in the nucleus and to inhibit the function of the transcription factors TBP and CBP in cells. Aberrant interaction of toxic Htt with the benign polyQ repeat of TBP structurally destabilized the transcription factor, independent of the formation of insoluble coaggregates and caused transcriptional dysregulation. Chaperones of the Hsp70 family protect against this deactivation by modulating the conformation of Htt.

This protective effect of Hsp70 was found to be based on a cooperation between Hsp70 and the chaperonin TRiC. Both chaperone systems cooperate in eliminating toxic polyQ oligomers, which may resemble the potentially pathogenic, prefibrillar states of other amyloidogenic disease proteins, and in stabilizing mutant Htt in a soluble, oligomeric state that is not associated with toxicity. TRiC and Hsp70 appear to be part of an effective chaperone network preventing the formation of harmful, amyloidogenic proteins species. They act synergistically on Htt, reminiscent of their sequential action in assisting the folding of newly-synthesized proteins.

2 Introduction

Proteins are the most abundant macromolecules in cells and are involved in virtually every biological process. Humans contain perhaps 100,000 different types of proteins, and their functions range from catalysis of chemical reaction to maintenance of the electrochemical potential across cell membranes. Prerequisite for their specific function is the unique three-dimensional structure of a given protein. Acquisition and maintenance of protein structure is safeguarded by a class of specially evolved proteins termed molecular chaperones. Despite the existence of this highly sophisticated quality control system, a growing number of human diseases are associated with pathologically misfolded and aggregated proteins.

2.1 Protein folding

The structure of proteins is generally described by four successive levels of architecture. The basic structural units of proteins are amino acids, which consist of an amino group, a carboxyl group, a hydrogen atom and a variable side chain bound to a carbon atom (α -carbon). Different side chains distinguish the twenty amino acids commonly found in proteins. Polypeptide chains are formed by covalent peptide bonds between the α -carboxyl group of one amino acid and the α -amino group of another amino acid; the consecutive sequence of amino acids is referred to as the primary structure of a protein. The peptide bond is a rigid planar unit due to its partial double bond character, and therefore, rotational freedom exists only for the bonds on either side of the peptide group. The conformation of amino acids in the main chain can be described by the torsion angles ψ and ϕ , referring to rotations about the α -carbon and the carboxyl carbon and rotations about the α -carbon and the amino group, respectively. The range of different conformations is limited by several steric constraints on the torsion angles imposed by the rigid spherical nature of atoms. The relative stabilities of various conformations can be obtained by calculating the potential energy of nonbonded interactions (Venkatachalam and Ramachandran, 1969) and the most prominent and stable examples of allowed conformations are α helix and β sheet. The conformation of a polypeptide chain is referred to as secondary structure. It describes local three-dimensional structures, which are usually restricted to only parts of a polypeptide chain. The arrangement of secondary structures within the complete polypeptide chain to an overall fold and shape of

a protein is assigned to as tertiary structure. This physiologically folded i.e. native state is defined as the energetically most stable structure. In tertiary structure, specific contacts can be formed between sections of a polypeptide chain that are widely separated in the primary structure. Additionally, the spatial arrangement of several polypeptide chains in a multisubunit protein complex is referred to as quaternary structure.

2.1.1 Protein folding problem

The information required to reach the native state of a protein is solely encoded in its primary structure. *In vitro*, heat-denatured i.e. unfolded Ribonuclease A was shown to refold spontaneously into its native and enzymatically active structure at a biologically relevant rate (Anfinsen, 1973). How a polypeptide sequence codes for its fold represents one of the most perplexing problems in molecular biology. Protein sequences must satisfy thermodynamic and kinetic requirements so that polypeptide chains adopt a unique folded conformation within a reasonable time. The complexity of this task is referred to as ‘the folding problem’ and is often exemplarily illustrated by the Levinthal paradox. That is, the total number of possible conformations of even a small polypeptide chain is so large that a systematic search for this particular structure would take an astronomical length of time (Levinthal, 1969). However, real average-sized proteins fold rapidly, frequently in less than one second (Karplus, 1997). Thus to remove the need to systematically search all possible conformations, protein folding was considered to occur along specific, defined pathways, as a series of sequential steps between increasingly native-like species, until the final native structure is formed.

2.1.2 Protein folding mechanisms and energy landscapes

The framework model (Kim and Baldwin, 1982) assumed a rapid formation of local secondary structure that functioned as scaffold for the subsequent acquisition of tertiary structure and was controversially discussed to occur either via a ‘nucleation-growth’ mechanism (Wetlaufer, 1973) or a ‘diffusion-collision’ mechanism (Karplus and Weaver, 1976). The former proposed that tertiary structure propagates rapidly from an initial nucleus of local secondary structure, and the latter that secondary structure forms first, followed by diffusion, collision and coalescence of the preformed secondary structural units to yield the native, folded protein. Alternatively, the ‘hydrophobic collapse’ model proposed involvement

of the hydrophobic collapse as initial folding step followed by acquisition of secondary structure and correct packing interactions in a confined volume (Ptitsyn and Rashin, 1975). Unification of features of both the hydrophobic collapse and framework models led to formulation of the “nucleation-condensation” mechanism (Fersht, 1997). Long range and other native hydrophobic contacts are formed in the transition state, in which otherwise weak secondary structural elements are stabilized by tertiary interactions. Whether any or all of the mechanisms occur in general, and whether there is an underlying unifying mechanism remains unclear.

The perception of pathways changed after computer simulation studies of protein folding revealed that the folding process involves a stochastic search of the many conformations accessible to a polypeptide chain (Wolynes *et al.*, 1995; Dill and Chan, 1997; Karplus, 1997). Residues at different position in the primary structure contact each other due to inherent fluctuations in the conformation of the unfolded or incompletely folded polypeptide chain. Since native-like interactions between residues are on average more stable than nonnative ones, these interactions are more persistently resulting in a search mechanism to find the lowest energy structure by a process of trial and error (Dinner *et al.*, 2000).

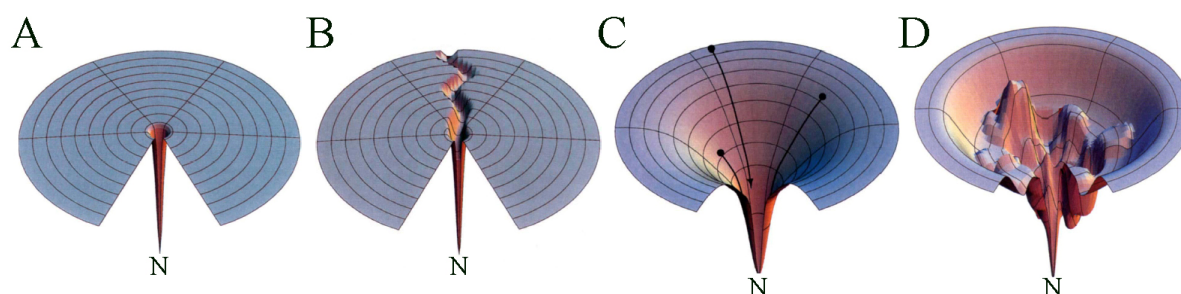


Figure 1: Energy landscape of protein folding.

(A) Levinthal ‘golf course’ landscape. The chain searches randomly for the native state (N). (B) The ‘pathway’ solution to the random search problem. (C) Idealized funnel landscape. (D) Rugged energy landscape with kinetic traps, energy barriers and narrow throughway paths to native state (Adapted from Dill and Chan, 1997).

For the description of such a search mechanism, energy surfaces i.e. energy landscapes have been of great conceptual benefit (Bryngelson *et al.*, 1995; Wolynes *et al.*, 1995; Dobson and Ellis, 1998). They represent the free energy of polypeptide chains as a function of their conformational properties and can be used to determine the trajectories along which molecules move from reactants to products and the position of transition states. Individual polypeptide chains are likely to follow different trajectories in which the native contacts are

formed in different orders giving rise to many transition states. The energy landscape resembles a funnel since the conformational space accessible to the polypeptide chain is reduced upon approaching the native state (Wolynes *et al.*, 1995). Thus, the polypeptide chain needs to sample only a relative small number of conformations during its transition to the native structure due to the restrictive nature of the energy surface, providing a solution to the Levinthal paradox.

2.1.3 Folding of small and large proteins

Small single domain proteins with less than 100 amino acids in length generally fold into their native state on a sub-second timescale. The folding landscape of these proteins is relatively smooth. Only two species are stably populated during this folding reaction, the ensemble of unfolded structures and the native state (Fersht, 2000). These proteins fold by a two-state mechanism by which a folding nucleus of a small number of key residues forms, about which the remainder of the structure can then condense (Daggett and Fersht, 2003). Collapse of the polypeptide chain to a compact structure occurs as soon as the majority of the interactions involving the key residues have been formed followed by rapid conversion to the fully folded state.

Proteins larger than 100 residues in length generally fold on a rougher energy surface. A higher proportion of hydrophobic residues provide among other factors a greater driving force for chain collapse. Compact folding states with substantial elements of native-like structure form prior to the stage at which folding can progress rapidly to the native state (Dobson and Hore, 1998). Reorganization of inter-residue contacts in these compact states may involve a high-energy barrier, leading to a transient population of partially folded or intermediate states. There is ongoing discussion about whether such intermediates assist folding by limiting the search process or whether they are traps that inhibit rapid folding (Roder and Colon, 1997; Khan *et al.*, 2003; Sanchez and Kiefhaber, 2003). In large multidomain proteins, folding is suggested to occur largely independently among different segments or domains of the protein allowing parallel topology searches (Vendruscolo *et al.*, 2001). Key interactions define the fold within domains and other specific interactions ensure the appropriate interlocking of initially folded regions to the correct overall structure. A final cooperative folding step establishes all native intra- and interdomain contacts defining the final functional form (Radford *et al.*, 1992).

2.2 Protein folding *in vivo*

In the living cell, proteins are synthesized on the ribosome, an organelle-sized ribonucleoprotein complex that translates the genetic information from the nucleic acid into the polypeptide chain. In contrast to the situation *in vitro*, protein folding inside the cell is not generally a spontaneous process. Folding of a polypeptide chain *in vivo* reaches an additional level of complexity as the physiological conditions inside the cell differ considerably from those of *in vitro* refolding in the test tube and do not necessarily favor folding. For examples, some newly translated polypeptide chains must be guided to their correct location within the cell or must be kept in a folding or assembly-competent state until assembly partners are present in order to complete their folding.

2.2.1 Protein aggregation

Cooperative and reversible folding *in vitro* is generally observed only for small, single-domain proteins where exposed hydrophobic residues are rapidly buried upon initiation of folding. The majority of cellular proteins, especially large and multi-domain proteins, refold inefficiently. Kinetically trapped, slow folding and/or formation of stable interactions between regions of the polypeptide chain that are separated in the native protein result in the population of partially folded and misfolded (i.e. non-productive but compact) intermediates. Typically, both types of intermediates expose hydrophobic residues and segments of unstructured polypeptide backbone to the solvent and therefore favor aggregation. Hydrophobic forces and interchain hydrogen bonding drive the self-association into ordered complexes (Dobson and Karplus, 1999; Radford, 2000). Since aggregation is generally irreversible, proteins are removed from their productive folding pathways.

2.2.2 Macromolecular crowding

The interior of a cell is a crowded and dynamic environment in which protein concentration has been estimated to be as high as 300 mg/ml (Zimmerman and Trach, 1991). The term ‘crowded’ is used instead of ‘concentrated’ because no single macromolecule species occurs at high concentration, but taken together, the macromolecules occupy a significant fraction (20 – 30 %) of the total volume. This fraction is physically unavailable to other molecules. The mutual impenetrability of all solute molecules implicates a non-specific steric repulsion that has been described as molecular crowding or excluded volume effect

(Ellis, 2001; Minton, 2001). Steric exclusion generates considerable effects on the thermodynamic and kinetic properties of macromolecules. While restriction of the available volume for macromolecules leads to an increase in the effective concentration (i.e. thermodynamic activity) of each macromolecule species, the diffusion rates for macromolecules are reduced. Since aggregation is highly concentration dependent, molecular crowding enhances aggregation of non-native polypeptide chains. Aggregation would be more pronounced for small polypeptides, as large polypeptides have their diffusion slowed resulting in reduced encounter rate. In biochemical equilibria, molecular crowding favors association of macromolecules and can increase equilibrium constants for such reactions by two to three orders of magnitude (Zimmerman and Trach, 1991). This effect arises from reduction in excluded volume, i.e. concomitant increase in available volume, obtained when macromolecules bind to each other. Consequently, small structures are favoured over large structures, and this applies to the collapse of nascent polypeptide chains into compact functional proteins as well as to the aggregation of unfolded polypeptides into highly ordered structures.

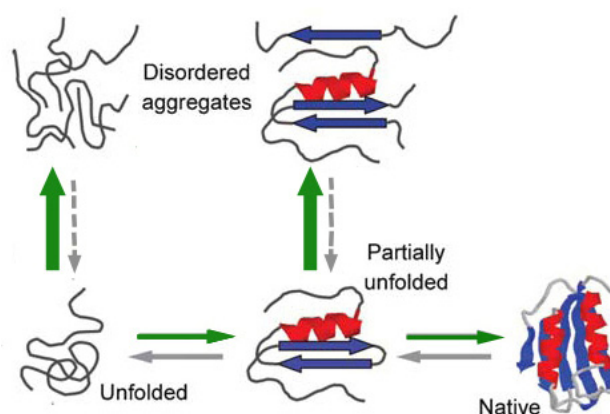


Figure 2: Aggregation of non-native polypeptide chains as a side-reaction of productive folding.

Enhancement of aggregation and chain compaction by macromolecular crowding (green arrows). Schematic representation of unfolded polypeptide chain released from the ribosome, partially folded intermediate and native, folded protein (Adapted from Dobson and Karplus, 1999).

2.2.3 Nascent polypeptide chains

A major difference between refolding of a denatured protein *in vitro* and *de novo* folding inside a cell is the vectorial synthesis from the amino (N) terminus towards the carboxy (C) terminus by which newly synthesized polypeptide chains emerge from the

ribosome. Although the N terminus is available for folding before the remaining polypeptide chain is synthesized, stable folding of a domain (100 – 300 amino acids) can only occur after its complete synthesis (Creighton, 1990; Jaenicke, 1991). Furthermore, during translation, about 40 residues of a nascent chain are sequestered within the polypeptides exit channel of the ribosome. As the channel is approximately 100 Å long and 10 – 20 Å wide at its narrowest point, folding beyond helix formation would not be allowed unless the channel is conformationally dynamic (Ban *et al.*, 2000). Translation occurs on a timescale of seconds in bacteria to several minutes in eukaryotes and is therefore much slower than the millisecond timescale of the hydrophobic collapse. Since hydrophobic stretches of a nascent polypeptide chain cannot immediately be buried upon correct folding, they are exposed to the solution, rendering the polypeptide chain aggregation prone. Consequently, translating polypeptides populate non-native conformations until sufficient structural information is available for folding. The tendency to aggregate is even more pronounced due to the high concentration of unfolded polypeptides, especially occurring during translation on neighboring ribosomes (Ellis and Hartl, 1996). Thus, nascent polypeptides chains temporarily face the quandary of being unable to fold into stable structures or to remain in an extended state. However, they must avoid formation of misfolded intermediates as well as aggregation with other nascent polypeptide chains.

For larger proteins composed of multiple domains, the vectorial nature of the translation process actually facilitates advantageous domain-wise folding of a polypeptide chain. Cotranslational and sequential domain folding of large proteins has been shown to avoid intramolecular misfolding and aggregation as it may occur upon their attempted refolding *in vitro* (Netzer and Hartl, 1997; Frydman, 2001). Concomitant with a much greater number of multidomain proteins in eukaryotes, the eukaryotic translation and folding machineries seem to have evolved to facilitate cotranslational domain folding (Hartl and Hayer-Hartl, 2002). Nevertheless, until sufficient sequence information of a nascent polypeptide chain is provided in order to allow formation of its correct domain structures, non-productive inter- and intramolecular interaction as well as premature misfolding of nascent polypeptide chains must be prevented.

2.2.4 Molecular chaperones

To counteract these dangers of misfolding and aggregation and to ensure that polypeptides reach their native state with high efficiency, cells have evolved a complex machinery which includes several conserved protein families that are collectively termed molecular chaperones (Ellis *et al.*, 1989; Gething and Sambrook, 1992; Hartl, 1996; Frydman, 2001; Hartl and Hayer-Hartl, 2002). By counteracting aggregation and misfolding of non-native proteins, chaperones assist in the folding of newly synthesized polypeptides as soon as they emerge from the ribosome and rescue existing proteins from partial stress-induced denaturation. Additionally, chaperones function in protein transport to subcellular compartments and may facilitate oligomer assembly. Many chaperones are constitutively expressed, but are synthesized at greatly increased levels under stress conditions and thus are classified as stress-response or heat-shock proteins (Hsps) (Gething and Sambrook, 1992). Their respective molecular weight determines their name, for example, the 70-kDa heat-shock protein is termed Hsp70. Molecular chaperones generally recognize exposed hydrophobic residues as well as unstructured segments of the main chain in their substrates. Such structural elements are typically present in non-native intermediates, but absent in the native state due to burial upon compact folding (Dobson and Ellis, 1998). Efficient folding is achieved by sequential cycles of substrate (client protein) binding and its release from the chaperone, often controlled by ATPase activity and cofactors proteins. Binding of chaperones shields non-productive intramolecular interacting surfaces and likely blocks intermolecular aggregation of polypeptides. By avoiding the formation of non-native intramolecular contacts, chaperones may also prevent misfolding of kinetically trapped intermediates. Furthermore, one chaperone family, the Hsp100s, is able to resolubilize protein aggregates by an energy dependent process in order to pass misfolded polypeptides back to the productive folding pathway (Ben-Zvi and Goloubinoff, 2001). Importantly, chaperones do not contribute steric information to the folding process. Instead of actively folding their substrates (client proteins), chaperones provide a local environment in which productive folding is favoured over functionally non-productive side reactions (Feldman and Frydman, 2000). Thus, chaperones increase the efficiency of the overall process by reducing the probability of competing reactions, particularly aggregation. Consequently, molecular chaperones can be distinguished from folding catalysts that accelerate specific rate-limiting steps in the folding process, like peptidyl-prolyl cis/trans isomerases (PPIase) or protein disulfide isomerases (PDIs).

2.3 A chaperone network in the eukaryotic cytosol

Despite the similar general role of various chaperones in enabling efficient folding and assembly, their specific cellular functions can differ substantially. Distinct chaperones cooperate in a topologically and timely ordered manner. The cytosol provides a well-developed network of chaperone pathways that can handle polypeptides at all stages of folding (Ellis and Hartl, 1996; Frydman and Hartl, 1996; Hartl and Hayer-Hartl, 2002; Young *et al.*, 2004). The cytosolic chaperone pathways in eukaryotes start with several structurally unrelated ribosome-bound factors that function during the translation of polypeptides. Proteins of the Hsp70 family, such as the 70-kDa heat-shock cognate protein (Hsc70) in mammals or Ssb and Ssa (the Hsc70 homologue) in *Saccharomyces cerevisiae*, are also important in chaperoning nascent polypeptide chains and continue to assist in the folding of newly translated polypeptides together with the chaperonin TRiC. GimC/prefoldin binds to a subset of newly synthesized polypeptides and cooperates with TRiC. Another subset of polypeptides uses chaperones of the Hsp90 family together with the Hsp70 family to complete their folding. Several co-chaperones contribute to the chaperoning functions of Hsp70 and Hsp90 proteins. The Hsp104 can resolubilize aggregated polypeptides and cooperates with small heat shock proteins and the Hsp70 system to return them to a productive folding trajectory.

2.3.1 Ribosome associated factors

Once emerged from the ribosomal exit tunnel, nascent polypeptides are received by ribosome-bound chaperones, which then recruit further chaperone components. In *Saccharomyces cerevisiae*, the ribosome-associated complex, RAC, is a heterodimer consisting of the DnaJ-related co-chaperone zuotin, which mediates ribosome binding, and the Hsp70-related Ssz1/Pdr13 (Yan *et al.*, 1998; Michimoto *et al.*, 2000; Gautschi *et al.*, 2001). RAC might recruit Hsp70s of the Ssb class to stabilize nascent polypeptides and assist in their folding (Gautschi *et al.*, 2002; Huang *et al.*, 2005). In mammals, RAC is composed of the homologues of zuotin and Ssz1, Mpp11 and Hsp70L1, respectively. Mpp11 associates with ribosomes and forms a stable complex with Hsp70L1 (Otto *et al.*, 2005). Together Mpp11 and Hsp70L1 may target cytosolic Hsp70 to the nascent chain (Wegrzyn *et al.*, 2006). Additionally, in *Saccharomyces cerevisiae* and mammals, the nascent-polypeptide-associated

complex, NAC, represents yet another ribosome bound complex. NAC is a heterodimer and contacts nascent polypeptides chains as they emerge from the ribosomal exit tunnel (Wiedmann *et al.*, 1994; Shi *et al.*, 1995). However, a clear chaperone activity has not been demonstrated so far. At present, it is unclear whether these factors interact in a hierarchical manner with nascent chains or whether they display specific functions for a particular subset of nascent polypeptides.

2.3.2 The Hsp70 chaperones

Hsp70s are a highly conserved family of proteins, distributed ubiquitously in all prokaryotes and in compartments of eukaryotic organisms (Bukau and Horwich, 1998; Hartl and Hayer-Hartl, 2002). In *Saccharomyces cerevisiae*, the cytosol contains four partially functional redundant Hsp70 homologues termed Ssa1-4, of which Ssa1p and Ssa2p are constitutively expressed and Ssa3p and Ssa4p are stress-inducible. Additionally, three ribosome-associated Hsp70s are present, namely Ssb1p, Ssb2p and Ssz1p/Pdr13p. In the mammalian cytosol, the stress-induced form of Hsp70 is named Hsp70 and the constitutively expressed homologue is termed Hsp70 cognate protein (Hsc70) (Frydman, 2001). The cytosolic Hsp70 chaperones are monomers and composed of two functionally coupled domains, namely the 44-kDa N-terminal ATPase domain and the 27-kDa C-terminal peptide-binding domain (Zhu *et al.*, 1996; Harrison *et al.*, 1997). Hsp70 proteins recognize short hydrophobic polypeptide stretches in extended conformation as their substrates (Hartl, 1996; Rudiger *et al.*, 1997). Binding and release of substrates is regulated by cycles of ATP binding and hydrolysis in the ATPase domain, thereby modulating the intrinsic peptide affinity (Hartl, 1996; Bukau and Horwich, 1998). These ATPase cycles consist of an alternation between the ATP state with low affinity and fast exchange rates for substrates and the ADP state with high affinity and low exchange rates for substrates.

Cycling between these different nucleotide-bound states is regulated by cofactors, mainly the Hsp40 co-chaperones. Hsp40 proteins characteristically possess an amino-terminal J-domain that stimulates the ATP hydrolysis of Hsp70 and often a carboxy-terminal chaperone domain, which binds unfolded polypeptides. Thereby, substrate polypeptides are transferred from Hsp40 to Hsp70 and stably bound by it in its ADP-bound state. In *Saccharomyces cerevisiae*, Ssa interacts with one of the two Hsp40 proteins Ydj1p or Sis1p and Ssb is thought to work together with Zuotin. The mammalian Hsc70 cooperates either

with the Hsp40 co-chaperones Hdj1 or Hdj2 (Johnson and Craig, 2001). In contrast to the bacterial Hsp70 reaction cycle, ADP-release is not the rate-limiting step when Hsp70 is in a complex with Hdj1 or Hdj2, but rather ATP hydrolysis (Ziegelhoffer *et al.*, 1995; Minami *et al.*, 1996). However, nucleotide exchange by Hsc70 can be stimulated through the mammalian co-chaperone BCL2-associated athanogene-1 (BAG1) or its homologues (Young *et al.*, 2003). The mammalian co-chaperone Hsp70-interacting protein (Hip) counteracts BAG1 by stabilizing the polypeptide-binding ADP-bound state of Hsc70 (Hohfeld *et al.*, 1995). Mammalian HSP70-binding protein (HSPBP1) and its *Saccharomyces cerevisiae* homologue Fes1 form yet another class of Hsp70 nucleotide exchange factors (Shomura *et al.*, 2005; Dragovic *et al.*, 2006).

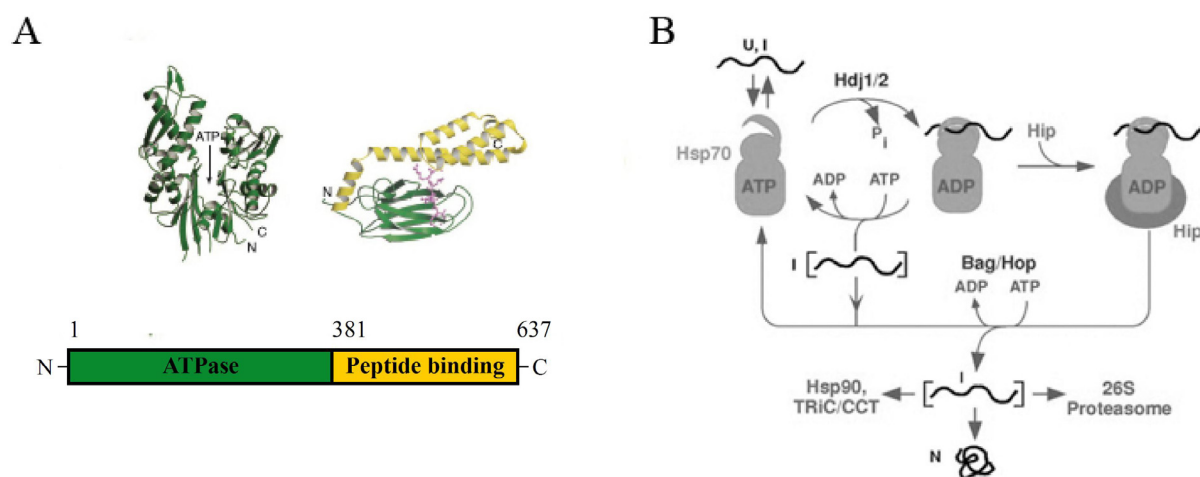


Figure 3: Hsp70 structure and model of its reaction cycle in the mammalian cytosol.

(A) Structures of the ATPase domain and the peptide-binding domain of Hsp70 shown representatively for *E. coli* DnaK (B) Hsp70 reaction cycle. Unfolded polypeptide (U), folding intermediate (I), native state (N) (Adapted from Frydman, 2001; and Hartl and Hayer-Hartl, 2002).

After release from Hsp70, an unfolded polypeptide can partition between progressive folding to its native state and rebinding to Hsp70. Slow-folding intermediates can undergo multiple rounds of binding and release by Hsp70. Association with Hsp70 stabilizes segments of the substrate protein in an extended conformation, thereby inhibiting intramolecular misfolding and intermolecular aggregation. As non-native polypeptides presumably expose multiple hydrophobic peptide stretches, several Hsp70 molecules may bind to the same polypeptide. Optimal folding would then require the coordinated release of the polypeptide from several Hsp70 monomers. However, yet there is no experimental evidence for the existence of a coordinated mechanism. Released polypeptide substrates may also bind

sequentially to other cytosolic chaperones, such as the chaperonin TRiC or Hsp90, in order to complete their folding. In *Saccharomyces cerevisiae*, Ssa assists the folding of proteins that were initially bound by Ssb. Ssa also cooperates with the chaperonin TRiC and folds substrates such as the Von-Hippel-Landau (VHL) tumor suppressor (Melville *et al.*, 2003). Ssb has been shown to interact, among others, with certain WD40 repeat proteins during their translation and continues to bind them post-translationally until their folding is completed by TRiC. In mammals, Hsc70 binds nascent polypeptide chains and is thought to assist in their co-translational folding (Beckmann *et al.*, 1990; Frydman *et al.*, 1994). Alternatively, polypeptide substrates can be passed onto Hsp90. The co-chaperone Hsp-organizing protein (HOP) links Hsc70 and Hsp90 for subsequent folding of a subset of polypeptide substrates.

2.3.3 The chaperonin TRiC

The Chaperonins are a conserved class of large cylindrical double-ring protein complexes of approximately 900 kDa. They are found in all cells and are strictly required for viability. Chaperonins comprise two subclasses that are similar in architecture but distantly related in sequence: Members of Group I are found in eubacteria and organelles of endosymbiotic origin, mitochondria and chloroplast (Bukau and Horwich, 1998; Ellis and Hartl, 1999), and Group II chaperonins occur in archaea and in the cytosol of eukaryotic cells (Gutsche *et al.*, 1999; Llorca *et al.*, 1999). Chaperonins differ substantially from Hsp70 in architecture and mechanism. However, as in Hsp70, ATP binding and hydrolysis generates conformational changes which drive cycles of substrate binding and release.

The eukaryotic chaperonin TRiC (tailless complex polypeptide-1 [TCP1] ring complex) also known as CCT (for chaperonin containing TCP1) is a double-ring shaped hetero-oligomeric complex that consists of eight orthologous subunits per ring ranging between 50 and 60 kDa (Hartl and Hayer-Hartl, 2002). The crystal structure of the archetype group II chaperonin, the thermosome complex from *Thermoplasma acidophilum*, revealed that individual subunits have a domain arrangement similar to those in the bacterial GroEL (Klumpp *et al.*, 1997; Ditzel *et al.*, 1998). The equatorial domain harbors the ATP binding site and is connected through a hingelike domain to the apical domain. Most sequence divergence between TRiC subunits is found in the apical domains, which likely contain the substrate binding sites (Kim *et al.*, 1994). Given the hetero-oligomeric nature of the TRiC subunits and ensuing sequence diversity in apical domains, the contribution of each of the eight TRiC

subunits for the folding of different proteins is however an open question. The backbone trace of the chaperonin II apical domain is virtually identical to that of GroEL, with the exception of a α -helical insertion that protrudes from the ring opening. One of the substantial differences between group I and II chaperonins relates to the functional dependency of GroEL function on the ring-shaped cofactor GroES. Following binding, GroES acts as a detachable lid for the cavity and creates a folding chamber that encloses polypeptide substrates (Sigler *et al.*, 1998). In the absence of a separate GroES-like cofactor, this α -helical protrusion is thought to function as a built-in lid of the central cavity. In the crystal structure of the thermosome, the apical protrusions form an iris-like structure that restricts access to the central cavity, in which a polypeptide of up to 60 kDa could be encapsulated (Ditzel *et al.*, 1998). TRiC function likely comprises enclosure of substrate polypeptides in this cavity as part of an ATP-dependent cycle as observed with the structurally related chaperonins from archaea (Klumpp *et al.*, 1997; Ditzel *et al.*, 1998).

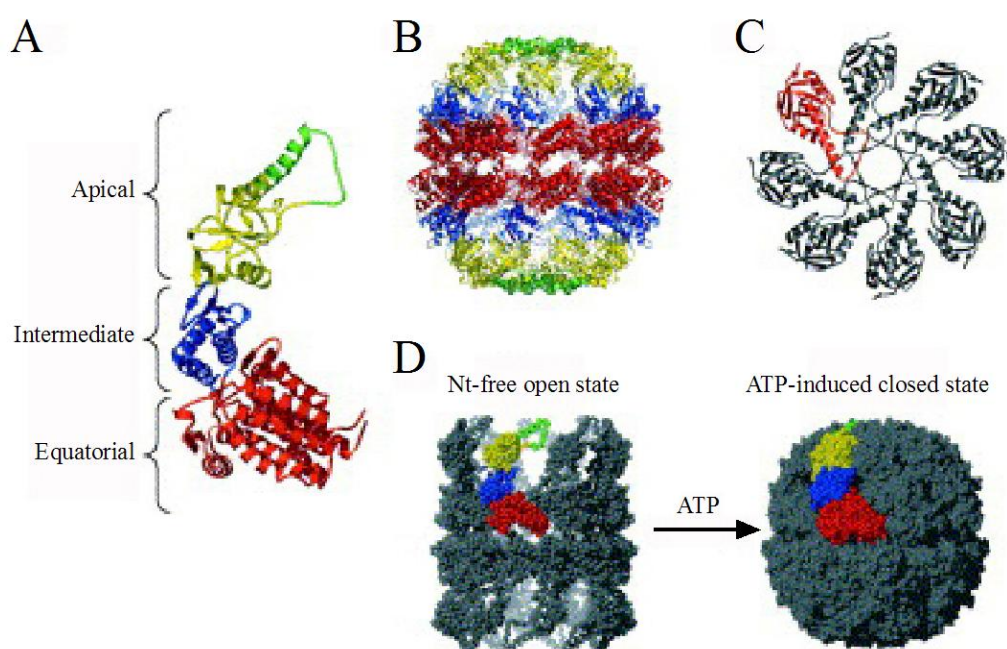


Figure 4: Architecture of group II chaperonins.

(A) Subunit of the thermosome from *Thermoplasma acidophilum*. (B) Side view of closed conformation observed in the X-ray structure of thermosome. (C) Top view of the closed thermosome structure from (B). (D) Bead models of the ATP-induced transition from the open to closed state (Adapted from Spiess *et al.*, 2004).

Indeed, ATP-dependent movements of the apical domains were demonstrated to be involved in TRiC-mediated folding similar to GroEL (Llorca *et al.*, 2001b). The apical domains bind substrate polypeptides through hydrophobic contacts and release them into the enclosed central cavity where they fold protected from aggregating with other nonnative proteins (Meyer *et al.*, 2003). In contrast to the group I chaperonin, TRiC binds to nascent polypeptide chains (Frydman *et al.*, 1994; Agashe and Hartl, 2000; McCallum *et al.*, 2000). This capacity may allow TRiC to assist the folding of an individual domain of a multidomain protein by encapsulation while the rest of the protein remains outside and extends through a gap in the apical domain (Frydman *et al.*, 1994; Ditzel *et al.*, 1998). Indeed, TRiC may be able to support folding without complete sequestration of a protein (Llorca *et al.*, 2001a).

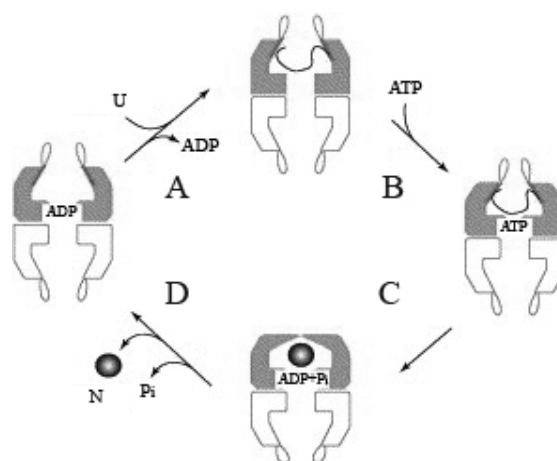


Figure 5: Model of the nucleotide cycle of the eukaryotic chaperonin.

(A) In the absence of nucleotide, the open complex can bind to unfolded substrates (U-substrate). (B) ATP binding. (C) Lid closure and confinement of the substrate in the central cavity. Folding probably occurs at this stage of the cycle. (D) Bond scission or inorganic phosphate (Pi) dissociation is likely to trigger reopening of the lid and the release of folded substrate (Adapted from Spiess *et al.*, 2004).

The essential role of TRiC relates to its absolute requirement for folding of a subset of essential proteins. TRiC is responsible for the folding of actin and tubulin as well as for *Ga*-transducin, cyclin E and the Von Hippel-Landau (VHL) tumor suppressor (Gao *et al.*, 1992; Yaffe *et al.*, 1992; Farr *et al.*, 1997; Won *et al.*, 1998; Feldman *et al.*, 1999). In *Saccharomyces cerevisiae*, TRiC is required for the folding of several WD40 repeat proteins. In these proteins, several consecutive WD40 repeats fold into a β -propeller domain in which each blade is a four-stranded β -sheet. The WD40 repeat proteins represent the first structural class of proteins, which is handled by chaperonins, and include the Stec4 transducin subunit, the Cdc55 regulatory phosphatase subunit, the Pex27 peroxisomal import receptor as well as

the Cdc20 and Cdh1 activators of the anaphase-promoting complex (Camasses *et al.*, 2003). WD40 repeat proteins have cooperatively folded structures and function as components in either homo- or hetero-oligomeric complexes. Thus, these presumably complex folding requirements might explain their strict TRiC dependency. In addition to the folding of subunits, TRiC may also be involved in assisting oligomeric assembly, since TRiC is known to mediate the folding of interacting subunits in the case of G α - and G β -transducin as well as Cdc55 and Sit4 (Farr *et al.*, 1997; Siegers *et al.*, 2003). Furthermore, for some substrates, such as tubulin, VHL and CDC20, release from TRiC occurs only in the presence of their partner proteins and is coupled to substrate assembly into the oligomeric complex (Spiess *et al.*, 2004). In *Saccharomyces cerevisiae*, TRiC cooperates with the Hsp70 Ssb in the folding of WD40 repeat proteins and with the Hsp70 Ssa in the folding of VHL. In contrast, TRiC works together with GimC/Prefoldin in the folding of actin and tubulin. One controversial aspect of TRiC-mediated folding is whether substrates bind in either a native-like or an unstructured state. Protease sensitivity of TRiC-bound actin and the location of TRiC-binding sites in the core of the native structure of VHL indicate a unstructured conformation of these substrates (Feldman *et al.*, 2003; Meyer *et al.*, 2003). By contrast, electron microscopy revealed that TRiC binds to compact folding intermediate of actin and tubulin (Llorca *et al.*, 2000).

2.3.4 GimC/Prefoldin

The cytosolic Gim1-6 complex (GimC)/prefoldin is composed of six different subunits. Initially, the yeast GimC and its mammalian homologue prefoldin were shown to support folding and assembly of tubulin as well as delivering unfolded actin to TRiC *in vitro*, respectively (Geissler *et al.*, 1998; Vainberg *et al.*, 1998). GimC functions independently of ATP and recognizes substrates via hydrophobic extensions at the ends of its six coiled-coil domains (Vainberg *et al.*, 1998; Siegers and Schiebel, 2000). These extensions also mediate weak interactions with TRiC, possibly a mechanism for polypeptide transfer to the chaperonin (Martin-Benito *et al.*, 2002). GimC interacts with actin and tubulin nascent polypeptides during their translation (Hansen *et al.*, 1999), and in cooperation with TRiC, GimC assists in post-translational folding of actin. Additionally, GimC protects polypeptides from non-productive intermolecular interactions (Siegers *et al.*, 1999). Consistent with its post-translational role in folding, GimC is capable of binding to a compact folding intermediate of

actin (Martin-Benito *et al.*, 2002). Thus, GimC might recognize some yet unknown specific features of its substrates, in addition to exposed hydrophobic surfaces.

2.3.5 Hsp90

In eukaryotic cells, Hsp90 is a highly abundant and essential chaperone that acts at late stages of protein folding. Hsp90 is a homodimer in which each subunit consists of an N-terminal ATP-binding domain linked by an extended region to a C-terminal dimerization site. ATP binding and hydrolysis regulates the activity of Hsp90. In the ATP-bound state, the N-termini can transiently dimerize, thereby presumably closing the structure around a substrate polypeptide. The opening of the structure after ATP hydrolysis might release the bound substrate and allow reloading of substrate onto Hsp90. The exact mechanism of polypeptide substrate binding and folding remains to be determined. Since Hsp90 often cooperates with Hsc70, these two chaperones might be considered as part of a multichaperone complex. The activities of this Hsc70-Hsp90 machinery are modulated by a wide range of cofactors (Richter and Buchner, 2001; Young *et al.*, 2001; Pratt and Toft, 2003). Several of these co-chaperones (e.g. tetratricopeptide repeat protein 2; p23, activator of Hsp90 ATPase or Cdc37) affect the ATPase cycles of Hsc70 or Hsp90 and thereby influence substrate binding by the chaperones (Young *et al.*, 2004). Among these are co-chaperones (e.g. HOP) that can physically link Hsc70 and Hsp90 to facilitate substrate transfer (Prodromou *et al.*, 1999; Scheufler *et al.*, 2000). Another group of co-chaperones interacts preferentially with subsets of Hsp90 substrates and might either target them to Hsp90 or provide a specifically required chaperoning activity (e.g. UNC-45) (Barral *et al.*, 2002). Hsp90 substrates include signal-transduction molecules (e.g. steroid hormone receptor), transcription factors, regulatory kinases (e.g. v-src, Wee-1, Cdk4 or Raf) and other proteins.

2.3.6 Chaperone-mediated protein degradation

Eukaryotic cells have a sophisticated system for protein degradation, in which multimers of the ubiquitin polypeptide (Ub) are covalently attached to proteins and are thus earmarked for targeting to and degradation by the 26S proteasome (Hershko and Ciechanover, 1998). This multi-subunit, self-compartmentalized protease comprises a 20S core complex bearing different, rather non-specific proteolytic sites within its cavity, and two axial 19S regulatory caps (Pickart and Cohen, 2004). This system removes misfolded proteins and

destroys native proteins for regulatory purposes. Under certain conditions, when chaperones cannot repair misfolded proteins, chaperone-mediated targeting to the ubiquitin-proteasome system (UPS) results in selective degradation. Hsp70 and Hsp90 cooperate with the UPS through the co-chaperones Chip (carboxyl terminus of Hsp70-interaction protein) and Bag1. In addition to its Hsc70 regulatory activity, Bag1 also contains a ubiquitin-like domain that mediates the contact with the proteasome (Hohfeld *et al.*, 2001). Chip contains a TPR-clamp domain, which recognizes either Hsc70 or Hsp90, and a E3 ubiquitin ligase activity that promotes the ubiquitinylation and degradation of some Hsc70-Hsp90 substrate polypeptides (Cyr *et al.*, 2002). Bag1 and Chip interact with each other and might present non-native polypeptides as ubiquitylated substrates to the proteasome for degradation (Demand *et al.*, 2001).

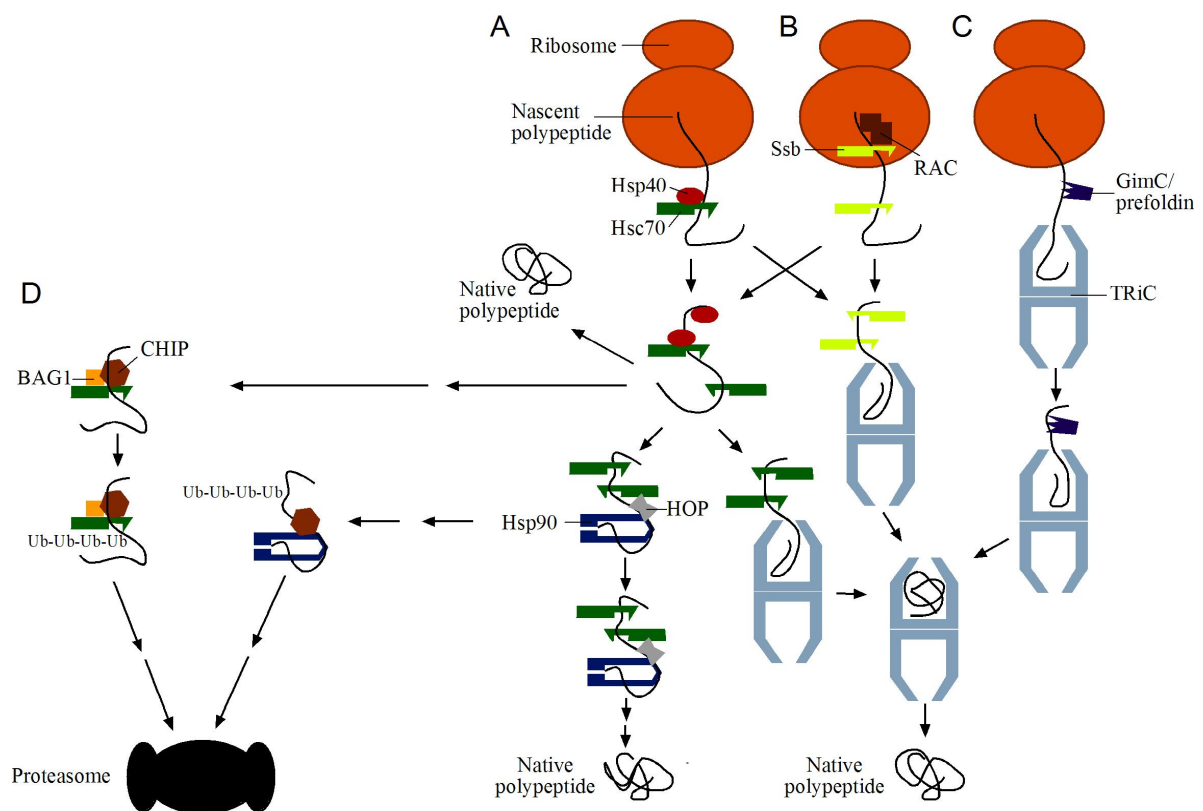


Figure 6: Schematic representation of the chaperone network in eukaryotic cytosol.

(A) In mammals, nascent polypeptides are met by Hsc70 and its Hsp40 cofactors. (B) In *Saccharomyces cerevisiae*, RAC recruits Ssb to bind nascent chains. Some proteins, initially bound by Ssb, are assisted in folding by Ssa, the *S. cerevisiae* homologue of Hsc70. (C) Actin and tubulin nascent chains are bound by GimC/prefoldin and TRiC. Hsc70 (Ssa) and Ssb also cooperate with TRiC in folding. Other newly synthesized polypeptides can fold spontaneously or be assisted by Hsc70. Alternatively, HOP mediates their transfer from Hsc70 to Hsp90. (D) CHIP contacts Hsc70 or Hsp90 to attach polyubiquitin onto polypeptides, targeting these substrates, in assistance with BAG1, to the proteasome for degradation. (Adapted from Young *et al.*, 2004).

2.4 Aberrant protein folding and conformational diseases

The failure of proteins to fold appropriately or to remain correctly folded is associated with a large number of disease related cellular malfunctions. Proteins that do not fold correctly are not able to exert their proper functions and may give rise to disease (loss of function diseases, e.g. cystic fibrosis). In the case of amyloid diseases, misfolded proteins escape all protective mechanism and form aggregates within cells or in the extracellular space. These aggregates, or the pathway of their formation, are toxic independently of the function of the normal protein they derived from (gain of function disease). An increasing number of pathologies, including neurodegenerative disorders such as Alzheimer's and Huntington's disease, are known to be directly associated with the deposition of such aggregates, suggesting a causative link between aggregate formation and pathological symptoms. These diseases can be inherited, sporadic or even infectious.

Table 1: Summary of some of the main amyloidoses and the proteins or peptides involved.

Disease	Protein
Alzheimer's disease (AD)	A β peptide/Tau/ γ -secretase
Spongiform encephalopathies	Prion (PrP ^c /PrP ^{sc})
Parkinson's disease (PD)	α -synuclein/parkin
Senile systemic amyloidosis	Transthyretin (TTR)
Haemodialysis-related amyloidoses	β_2 -microglobulin (β_2 -m)
Huntington's disease (HD)	Huntingtin (Htt)
Spinal and bulbar muscular atrophy (SBMA)	Androgen receptor (AR)
Dentatorubal-palidolusian atrophy (DRPLA)	Atrophin
Spinocerebella ataxias 1, 2, 3, 6, 7 (SCA1/2/3/6/7)	Ataxin 1, 2, 3, 6, 7
Spinocerebella ataxia 17 (SCA17)	TATA box-binding protein (TBP)

Many of the mutations associated with familial deposition diseases populate partially unfolded states by decreasing the stability or cooperativity of the native state or increasing the stability of intermediates. Other familial diseases are associated with the accumulation of fragments of the native proteins, often produced by aberrant processing or incomplete degradation. Such species are unable to fold into aggregation-resistant native-like states. The mechanism(s) by which protein aggregation results in pathology are not yet understood in detail. In the case of systemic diseases, the sheer mass of insoluble protein may physically disrupt the functioning of specific organs (Tan and Pepys, 1994). However, for the neurodegenerative disorders AD, PD and HD, the primary symptoms apparently occur through the destruction of neurons by a toxic gain-of-function that results from the aggregation process (Koo *et al.*, 1999; Caughey and Lansbury, 2003).

2.4.1 Protein aggregation and amyloid-like deposits

In the amyloid diseases, the protein deposits contain intractable aggregates, often fibrillar in nature. Each amyloid disease is associated primarily with one protein or fragment of a protein that forms the core structure of the deposits (Sunde and Blake, 1997). Remarkably, although the polypeptides that aggregate in these disorders are unrelated in size or primary amino acid sequence, they form amyloid-like structures with common biochemical and biophysical characteristics. These commonalities may indicate that a conserved mechanism of aggregation, and perhaps toxicity, might connect these phenotypically diverse diseases.

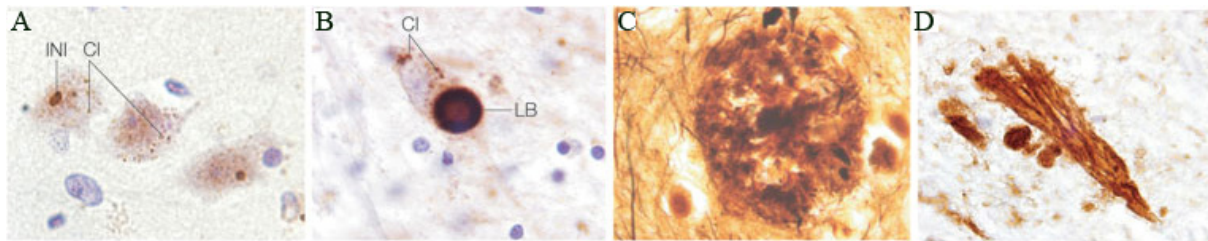


Figure 7: Intracellular, cytoplasmic and extracellular aggregates and inclusion bodies.

(A) Intranuclear (INI) and cytoplasmic (CI) polyglutamine inclusions in the motor cortex of HD brain. (B) Lewy body (LB) and other cytoplasmic inclusions (CI) in substantia nigra of PD brain. (C) Neuritic plaque of AD in the cerebral cortex. (D) Neurofibrillary tangles of AD in the hippocampus (Ross and Poirier, 2005).

2.4.1.1 Structure and formation of amyloid fibrils

Amyloid fibrils are long, straight and unbranched filamentous structures with a width of ~10 nm and a length of 0.1-10 μm (Sunde and Blake, 1997). The fibrils typically consist of between 2 and 6 protofilaments that are often twisted around each other to form a supercoiled rope-like structure (Serpell, 2000). The defining feature of amyloid fibrils is the so-called cross- β structure (Eanes and Glenner, 1968; Sunde and Blake, 1997). In this structural motif, ribbonlike β -sheets are formed by β -strands running nearly perpendicular to the long axis of the fibril and hydrogen bonds that run nearly parallel to the long axis. The core structure of $A\beta$, α -synuclein and polyglutamine aggregates appears to involve both β -strands and β -turns (Benzinger *et al.*, 2000; Thakur and Wetzel, 2002; Williams *et al.*, 2004). Consistent with a common core structure, monoclonal conformation-specific antibodies recognize the amyloid fibril state of $A\beta$ peptide and of other proteins of unrelated sequences including polyglutamine (polyQ), Transthyretin (TTR) and β_2 -microglobulin (β_2 -m) but neither the

soluble monomeric state of A β nor native polymers such as collagen or gelatin (O'Nuallain and Wetzel, 2002). Furthermore, a monoclonal antibody raised against human light chain amyloid fibrils also stains amyloid deposits from tissue containing other types of amyloid such as A β and TTR (Hrncic *et al.*, 2000).

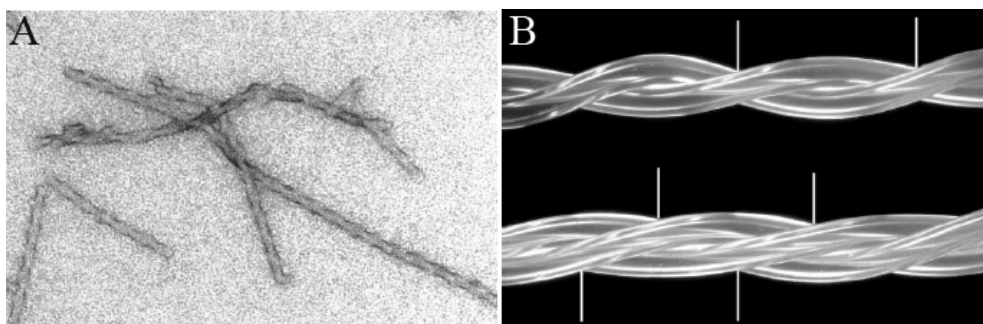


Figure 8: Fibers and protofibrils.

(A) Electron micrograph of fibers made of the glutamine- and asparagine-rich region of prion protein Sup35. **(B)** Models of bundles of plastic tubes wound around each other and representing protofibrils (Perutz *et al.*, 2002a).

In vitro, many proteins unrelated to known amyloid disease (e.g., myoglobin) have been shown to form fibrillar structures under certain conditions with all characteristics of those found associated with the clinical amyloidoses (Chiti *et al.*, 1999; Fandrich *et al.*, 2001; Fandrich and Dobson, 2002). Thus, the ability to form amyloid fibrils was suggested to be a generic property of polypeptide chains (Dobson and Karplus, 1999). The stability of the amyloid core structure results primarily from hydrogen bonds that link the β -strands and involve the amide and carbonyl groups of the polypeptide main chain, which is common to all polypeptides (Dobson, 2002). In amyloid fibrils, the main chain dominates the structure and the side chains are incorporated in the most favorable manner, in contrast to the evolved globular structures. The residues that nucleate the folding of a globular protein appear to be distinct from those that nucleate its aggregation into amyloid fibrils (Chiti *et al.*, 2002).

The common core structure of amyloid fibrils supports the assumption of similarities in their assembly pathways. Unfolded or aberrantly folded polypeptides acquire the ability to self-assemble into higher-order structures (Dobson and Karplus, 1999). However, in a globular protein, the polypeptide main chain and hydrophobic side chains are largely buried within the folded structure. Thus, only conditions that favor their exposure, such as partial unfolding (i.e.: low pH) or fragmentation (i.e.: proteolysis), will allow the conversion into amyloid fibrils. *In vitro*, fibrils form in a nucleation-dependent manner typically characterized

by a lag phase, which is followed by a period of rapid growth (Rochet and Lansbury, 2000). The formation of soluble oligomeric species appears to be involved early in amyloid formation. In this context, oligomers have been defined as clusters of small numbers of protein or peptide molecules without a fibrillar appearance (Chiti and Dobson, 2006). The first structures observed by electron and atomic force microscopy resemble isolated or clustered spherical beads of 2-5 nm in diameter and are termed protofibrils (Dobson, 2004; Glabe, 2004; Chiti and Dobson, 2006). These metastable, nonfibrillar species are generally characterized by extensive β -sheet structure (Chiti and Dobson, 2006). Protofibrils can be on- or off-pathway with regard to fibril formation (Serio *et al.*, 2000; Gosal *et al.*, 2005). Later on, species with a more distinct morphology, commonly described as fibrillar, develop and are termed protofilaments (Caughey and Lansbury, 2003). These structures may anneal or undergo conformational changes to form mature fibrils (Bouchard *et al.*, 2000; Goldsbury *et al.*, 2000). The exact order of events in the aggregation process is unknown. Protein aggregation could follow a linear pathway – from monomers to oligomers to protofibrils to fibrils – or a series of parallel processes in which monomers are added directly to growing fibers, with alternative species originating from side pathways (Ross and Poirier, 2005).

2.4.1.2 Protein aggregation and toxicity

Abnormal protein conformation and protein aggregation are emerging as common pathological features of amyloid diseases such as neurodegenerative disorders. However, there is an ongoing controversy about the role of aggregation in the disease process. The presence of inclusions correlates poorly with other markers of neurodegeneration, or with clinical features (Ross and Poirier, 2005). In AD, there is only a weak correlation between the density of A β peptide derived amyloid plaques in human post-mortem material and the clinical severity of AD (Terry *et al.*, 1991). Similarly in PD, only little correlation exists between the presence of Lewis bodies and cell death in the Substantia nigra in the brain (Tompkins and Hill, 1997). Thus, paradoxically, the process of aggregation might be related to toxicity, but the inclusion bodies might be neutral by-products or even protective. Presumably, inclusions represent an end-stage manifestation of a multi-step aggregation process with several possible intermediate species, including oligomeric and protofibrillar forms. Early events before the formation of inclusion bodies might cause toxicity and possible culprits include abnormal monomers of the disease proteins or small assemblies of abnormal

aggregated protein (oligomer). Indeed, early pre-fibrillar aggregates of proteins associated with neurological diseases can be highly damaging to cells, in contrast to mature fibrils that are relatively benign or even protective (Walsh *et al.*, 2002; Caughey and Lansbury, 2003; Arrasate *et al.*, 2004). The toxic oligomer hypothesis is supported by the finding that a single polyclonal antibody can equally recognize a common conformational epitope that is displayed by several disease-associated proteins, including A β , α -synuclein and polyQ-containing peptides (Kayed *et al.*, 2003). Co-incubation of the anti-oligomer antibody with oligomers of the aforementioned disease proteins blocks their toxicity when applied to cultured cells, indicating that oligomeric structures formed by distinct disease proteins might confer toxicity through a similar mechanism (Kayed *et al.*, 2003). Furthermore, pre-fibrillar aggregates of several proteins that are not connected with any known disease are as cytotoxic as A β (Bucciantini *et al.*, 2002), conceptually supporting the generic toxic nature of early pre-fibrillar aggregates (Dobson, 2004).

A general proposal for the relationship between aggregation and toxicity is supported by studies of polyglutamine-expanded proteins. Therein, toxicity may depend on interactions of polyglutamine-expanded proteins with, and possibly recruitment into aggregates of, other cellular constituents during the aggregation process (Preisinger *et al.*, 1999; McCampbell *et al.*, 2000; Chen *et al.*, 2001; Nucifora *et al.*, 2001). Exposure of moieties that are usually hidden in globular proteins, such as hydrophobic side chains or main chain NH and CO groups in an abnormal β -conformation could lead to the formation of aberrant, non-native hydrogen bonds with other proteins in the cell (Dobson, 2003). Such a toxicity mechanism could be exerted by particular molecular species (for example oligomers or protofibrils). Alternatively, toxicity might not be exclusively due to any specific species, but to the dynamics of the aggregation process, as there seems to be structures shared by various aggregating proteins. This would imply the maintenance of a common toxic fold upon assembly into dimers, oligomers or fibrils (Stefani and Dobson, 2003). Based on the same concept, abnormal interaction with cellular membranes through the formation of membrane pores is being discussed (Lashuel *et al.*, 2002; Quist *et al.*, 2005).

2.4.2 Huntington's disease

HD is an autosomal dominant inherited disorder characterized by irrepressible motor dysfunction, cognitive decline and psychiatric disturbance, which lead to progressive dementia and death approximately 15-20 years after disease onset (Bates, 2000). HD is caused by expansion of a CAG repeat coding for polyglutamine (polyQ) in the amino terminus of the protein huntingtin (Htt) (HDCRG, 1993; Nasir *et al.*, 1995). This type of mutation is responsible for a number of neurodegenerative diseases, including DRPLA, SBMA, SCA 1-3, 6, 7 and SCA 17, that are collectively termed polyglutamine disease and which are likely to be caused by common pathogenic mechanisms (Orr and Zoghbi, 2001). Apart from their polyQ repeats, the proteins involved are structurally unrelated, and although they are all widely expressed in the central nervous system and peripheral tissue, each leads to a distinct characteristic pattern of neurodegeneration (Zoghbi and Orr, 2000). In HD, the selective neurodegeneration of the γ -aminobutyric acid-releasing spiny-projection neurons of the striatum is predominant, although loss of neurons in many other brain regions has also been reported. The length of the normal polyQ tract is polymorphic, typically ranging from 10 to 36 glutamine residues, whereas in HD there is an unstable expansion beyond the normal range, with longer expansion correlating with earlier onset and more severe disease (Bates, 2003). The expanded polyQ domain seems to induce a conformational change in the protein, which causes it to form aggregates (Scherzinger *et al.*, 1997). There is a correlation between the polyQ threshold of aggregation *in vitro* and the polyQ threshold for disease in humans, consistent with the idea that aggregation is related to pathogenesis (Davies *et al.*, 1997; Scherzinger *et al.*, 1999). HD has a prevalence of 5-10 cases per 100,000 worldwide, which makes it the most common inherited neurodegenerative disorder (Tobin and Signer, 2000).

2.4.2.1 Huntingtin

Htt is an essential 348-kDa multidomain protein that contains a polymorphic glutamine/proline-rich domain at its amino terminus. The function of normal Htt and the mechanism whereby mutant Htt mediates harmful effects remains unclear. Htt contains very little sequence homology to other known proteins and its expression is ubiquitous but greatest in neurons (Trottier *et al.*, 1995a). Moreover, Htt is localized in many subcellular compartments, including nucleus, cell body, dendrites as well as nerve terminals (DiFiglia *et al.*, 1995; Trottier *et al.*, 1995a) and is associated with a number of organelles, namely Golgi

apparatus, endoplasmatic reticulum, synaptic vesicle and mitochondria (DiFiglia *et al.*, 1995; Sharp *et al.*, 1995; Gutekunst *et al.*, 1998). Htt interacts with a range of proteins suggesting that it may act as a molecular scaffold, regulating several cellular processes including endocytosis, vesicle transport, excitatory synapses, mitochondrial function and transcriptional events (Harjes and Wanker, 2003; Li and Li, 2004). Interestingly, Htt can protect neuronal cells from apoptotic stress and therefore may have a pro-survival role (Rigamonti *et al.*, 2000). Transgenic animal studies support a toxic gain-of-function mechanism that leads to neuronal dysfunction and death (Zoghbi and Orr, 2000), although loss-of-function has not been excluded in contributing to disease pathogenesis (Reiner *et al.*, 2001; Cattaneo, 2003).

2.4.2.2 PolyQ aggregation

Mutant Htt forms microscopically distinct inclusions in the cytoplasm and nucleus of affected neurons (DiFiglia *et al.*, 1997; Becher *et al.*, 1998), indicating that the aggregation is dominated by the expanded polyQ stretch. PolyQ aggregation has been reproduced *in vitro*, using either a fragment of mutant Htt or synthetic polyQ peptides (Perutz *et al.*, 1994; Scherzinger *et al.*, 1997; Chen and Wetzel, 2001). Their aggregation results in the accumulation of β -sheet rich fibrillar structures and displays nucleated-growth polymerization kinetics, with a rate-limiting lag-phase accounting for the formation of an aggregation nucleus, followed by a fast elongation phase during which additional polyQ monomers or oligomers rapidly join the growing aggregates (Scherzinger *et al.*, 1999; Chen and Wetzel, 2001).

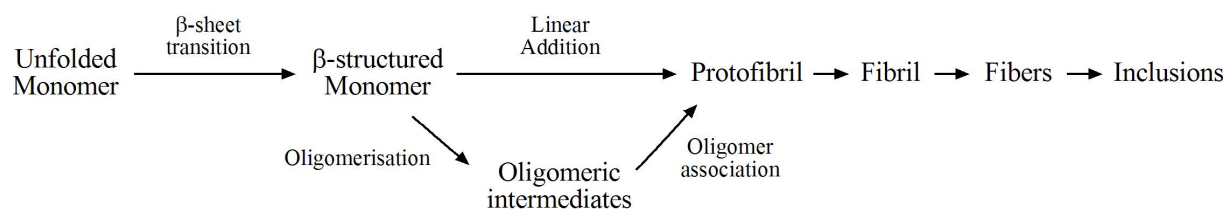


Figure 9: Hypothetical pathway of polyQ-mediated aggregation and inclusion formation.

Unstructured polyQ monomer undergoes a structural conversion to β -sheet, resulting in the formation of protofibrillar intermediates. This step may proceed through a linear growth mechanism or through assembly of oligomeric intermediates. Protofibril assembly is followed by fibril and finally inclusion formation (Adapted from Ross *et al.*, 2003).

Detailed structural information on polyQ has been difficult to obtain due to intrinsic insolubility. Whereas monomeric polyQ peptides with repeat length of 5 – 44, have been shown to be unstructured (Altschuler *et al.*, 1997; Chen and Wetzel, 2001; Masino *et al.*, 2002), aggregates derived from expanded polyQ peptides or proteins adopt β -sheet structure (Chen *et al.*, 2002; Perutz *et al.*, 2002b; Poirier *et al.*, 2002). Thus, a conversion from disordered to β -strand is likely to occur in an individual polyQ chain (Chen *et al.*, 2002) and fibril formation by addition of other polyQ chains to these monomeric β -strand nuclei. The structure of polyQ segments was proposed to be an anti-parallel β -sheet termed “polar zipper”, held together by hydrogen bonds between main-chain and side-chain amides (Perutz *et al.*, 1994). Refinement predicted a polyQ β -helix with a cylindrical, parallel β -sheet and 20 residues per turn, structurally addressing the aggregation threshold of polyQ tracts. A single 20-residue helical turn would be unstable and, therefore only polyQ monomers above the pathological threshold would favor a conformational change (Perutz *et al.*, 2002b). In contrast, a mutational study suggested that polyQ aggregation begins by the formation of a compact β -structure with alternating β -strands and β -turns, with an optimal length of seven glutamines per β -strand (Thakur and Wetzel, 2002) (Figure 7). This alternative model would support a compact β -structure, rather than an extended strand model, but would be compatible in parts with the polar zipper model, as hydrogen bonds are formed between main chain atoms and do not involve the side chains (Ross *et al.*, 2003). Yet, the precise organization of polyQ molecules within the aggregate is still largely unknown.

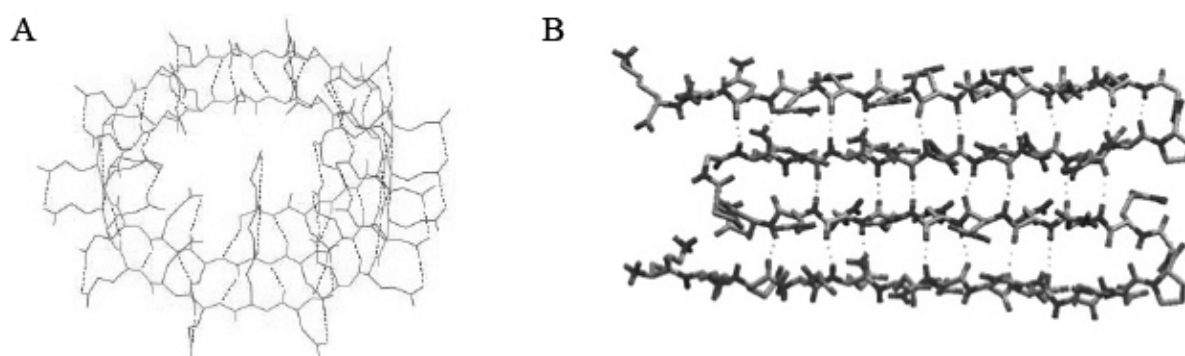


Figure 10: Schematic representation of proposed structural models for aggregated mutant polyQ. (A) Computer-generated model of a polyQ helix with 20 residues per turn (Perutz *et al.*, 2002a). (B) Sketch of expanded polyQ, with β -turns constrained by proline-glycine insertions that is purported to be similar to the structure of expanded pure polyQ (Adapted from Ross and Poirier, 2004).

The aggregation process might be initiated by proteolytic cleavage of full-length Htt. Inclusions in HD post-mortem tissue are selectively labeled with antibodies to epitopes near the amino terminus of Htt (DiFiglia *et al.*, 1997; Becher *et al.*, 1998). Short amino terminal fragments containing the expanded polyQ repeat are substantially more toxic, in most cell culture and mouse models, than longer or full-length Htt (Saudou *et al.*, 1998; Peters *et al.*, 1999; de Almeida *et al.*, 2002). Htt can be cleaved by several proteases, including caspases, calpain and an unidentified aspartyl protease (Gafni and Ellerby, 2002; Lunkes *et al.*, 2002; Wellington *et al.*, 2002). Recently, transgenic mice carrying caspase-6-resistant mutant Htt were shown to maintain normal neuronal function and did not develop striatal neurodegeneration (Graham *et al.*, 2006), suggesting that cleavage of Htt at the caspases-6 site generates polyQ-expanded N-terminal Htt fragments.

2.4.2.3 *The nature of toxic species in polyQ aggregation*

The role of aggregation in the pathogenesis of HD remains contentious; it may be pathogenic, represent an epiphenomenon, or be beneficial and neuroprotective (Sakahira *et al.*, 2002; Bates, 2003). There is a good correlation between the length of the CAG repeat and the density of inclusions (Vonsattel *et al.*, 1985; Becher *et al.*, 1998). However, in the cerebral cortex, which undergoes only moderate degeneration, inclusions are denser than in the cells of the striatum, which undergoes massive degeneration (Gutekunst *et al.*, 1999). Striatal inclusions are most prevalent in large interneurons, which are spared in HD, rather than in medium spiny neurons, which are selectively lost in the disease (Kuemmerle *et al.*, 1999). Transgenic mouse models provide evidence for a lack of association between inclusions and neurodegeneration or dysfunction (Slow *et al.*, 2005). Moreover, in cell culture models, inclusion body formation showed little correlation with neuronal toxicity and even predicted neuronal survival, whereas the level of diffuse huntingtin correlates significantly with cell death (Saudou *et al.*, 1998; Arrasate *et al.*, 2004). Interestingly, formation of inclusion bodies seems to be a regulated cellular process that requires an intact microtubule cytoskeleton and might have evolved as a protective mechanism to sequester toxic, misfolded protein entities that could otherwise disrupt cellular homeostasis (Waelter *et al.*, 2001; Muchowski *et al.*, 2002; Taylor *et al.*, 2003). Despite the chemical stability, inclusions are not necessarily permanent cellular components. The cell is able to degrade polyQ aggregates after expression of the soluble mutant protein is discontinued (Yamamoto *et al.*, 2000). Alternatively, once

collected in an aggresome, abnormally folded proteins could potentially be disposed of by autophagy (Ravikumar and Rubinsztein, 2004; Rideout *et al.*, 2004; Iwata *et al.*, 2005). Thus, although aggregates are thought to be protective, the aggregation processes itself seems to trigger toxicity.

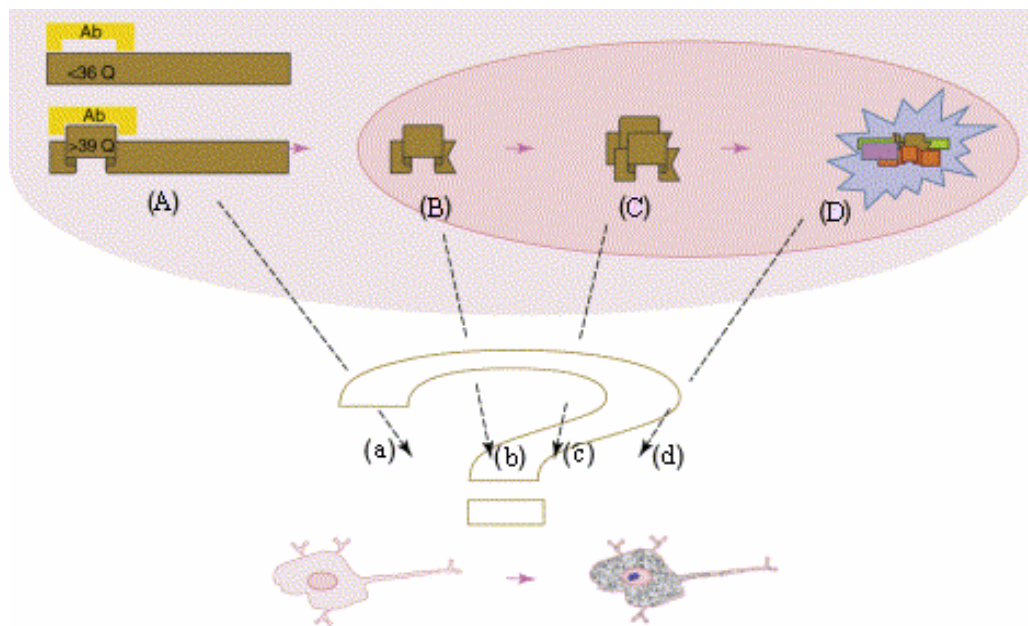


Figure 11: Likely cellular events in the pathogenesis of HD.

(A) Htt becomes pathogenic when its polyQ tract exceeds ~39 repeats (top left). Monoclonal antibodies (yellow) selectively recognize the polyQ-expanded Htt, indicating that the polyQ expansion entails a conformational change. (B) Mutant Htt is selectively subject to cleavage, and its N-terminal fragment can enter the nucleus. (C) These fragments can self-aggregate and, (D) form inclusions that also contain other proteins. Neuronal function is compromised (bottom), but it is not precisely known whether the proximate cause of compromised function is (a) full-length mutant Htt, (b) a fragment of Htt, (c) a fragment aggregate or (d) an inclusion that contains Htt and other molecules. The pathomechanism is also not known precisely (Adapted from Tobin and Signer, 2000).

2.4.2.4 Mechanisms of polyQ aggregation mediated toxicity

Several non-exclusive hypotheses have been developed to explain how the unusually long polyQ tract causes neurodegeneration. The expansion of the polyQ domain is likely to impart a novel, presumably aberrant, conformation. The unprotected β -sheets in intracellular polyQ oligomers or even in the monomeric polyQ fragments may interact unfavorably with the surface of other proteins thereby impairing various cellular functions (Sakahira *et al.*, 2002). Intriguingly, the transient association of transcriptional regulators into their transcriptional complexes is commonly facilitated by interactions between glutamine-rich regions within these proteins (Gerber *et al.*, 1994). These presumably flexible and unstructured regions may act as molecular ‘fishing lines’ that allow a single protein within a

complex to recruit additional factors or to bridge large distances, such as is required in transcription (Faux *et al.*, 2005). Hence, monomeric or oligomeric soluble expanded polyQ species could aberrantly bind to transcriptional mediators harboring polyQ tracts in the non-pathogenic range, disrupt the organization of transcriptional complexes and lead to transcriptional dysregulation (Cha, 2000; Sakahira *et al.*, 2002).

The accumulation of molecular chaperones and components of the ubiquitin-proteasome system (UPS) in polyQ aggregates suggests that insufficient protein folding and degradation plays a role in the pathogenesis of polyQ diseases (Sakahira *et al.*, 2002; Ciechanover and Brundin, 2003). Therefore, polyQ diseases might arise from impaired folding or proteolysis, either when proteins become inherently difficult to refold or degrade. Consistently, overexpression of molecular chaperones in fly and mouse models suppresses toxicity (Chan *et al.*, 2000; Cummings *et al.*, 2001). The role of UPS impairment is still controversial (Yamamoto *et al.*, 2000; Bence *et al.*, 2001; Verhoef *et al.*, 2002; Kaytor *et al.*, 2004; Bennett *et al.*, 2005; Bowman *et al.*, 2005). Impaired axonal and dendritic trafficking as well as mitochondrial dysfunction are also implicated in HD (Sipione and Cattaneo, 2001; Feany and La Spada, 2003).

2.4.2.5 Transcriptional dysregulation

The cAMP-responsive element (CRE-) and the SP1-mediated transcription pathways have been shown to be affected in HD and intriguingly are involved in the expression of genes essential for neuronal survival (Lonze *et al.*, 2002; Landles and Bates, 2004). Deletion of cAMP-responsive element binding protein (CREB) results in an HD-like phenotype with progressive neurodegeneration in the hippocampus and striatum (Mantamadiotis *et al.*, 2002) and downregulation of CRE-regulated genes has been detected in transgenic mice, cell-culture models and in HD patients (Glass *et al.*, 2000; Luthi-Carter *et al.*, 2000; Wytttenbach *et al.*, 2001). Furthermore, CBP overexpression alleviates polyQ toxicity in neuronal cells (McC Campbell *et al.*, 2000). Mutant Htt also interferes with Sp1-mediated transcription of genes such as the dopamine-D2-receptor gene that are compromised in HD patients (Dunah *et al.*, 2002). Consistently, glutamine-rich transcription regulators involved in these transcription pathways including the CREB-binding protein (CBP), specificity protein 1 (Sp1) and TATA-binding protein (TBP)-associated factor (TAF_{II}130) have been shown to interact directly with soluble polyQ species and this interaction is enhanced by expansion of the polyQ tract into

the pathological range (Nucifora *et al.*, 2001; Dunah *et al.*, 2002; Li *et al.*, 2002). CBP cooperates with the transcription factor CREB in activating the expression of cAMP-responsive genes and Sp1 recruits the general transcription factor TFIID that contains TBP and multiple TBP-associated factors including TAF_{II}130 to DNA. TAF_{II}130 directly interacts with Sp1 and stimulates transcriptional activation of genes. Mutant Htt seems to disturb these orchestrated interactions. Increased binding of mutant Htt to Sp1 reduces the association of Sp1 with TAF_{II}130 and with its promoter region. Only overexpression of both SP1 and TAF_{II}130 can overcome the inhibition of dopamine-D2-receptor gene expression (Dunah *et al.*, 2002). Furthermore, *in vitro* transcription analysis revealed that Sp1 and selective components of the core transcription apparatus, including the transcription initiation factors TFIID and TFIIF, are direct targets inhibited by mutant Htt in a polyQ-length dependent manner (Zhai *et al.*, 2005). However, CBP, Sp1, and TAF_{II}130 have also been found to localize to inclusions (Kazantsev *et al.*, 1999; McCampbell *et al.*, 2000; Shimohata *et al.*, 2000; Steffan *et al.*, 2000; Nucifora *et al.*, 2001). Whether recruitment of these factors into aggregates is mediated by toxic monomeric or oligomeric intermediates during the aggregation process or by the final fibrils is still unclear. Thus, expanded polyQ might disturb transcription whether soluble or aggregated (Michalik and Van Broeckhoven, 2003). Importantly, characteristic alterations in gene expression that are normally regulated by these factors can be observed in transgenic and cell-culture models which are not necessarily associated with the formation of inclusions (Kita *et al.*, 2002; Luthi-Carter *et al.*, 2002a; Sipione *et al.*, 2002).

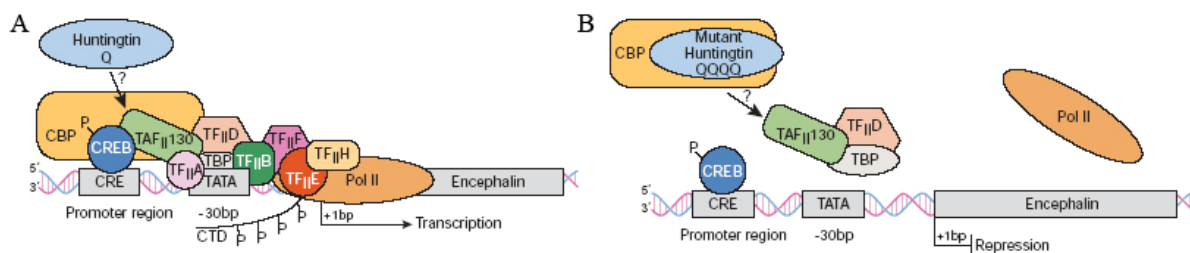


Figure 12: Dysregulation of CRE-mediated transcription in HD.

(A) CREB binds to CRE elements in promoters such as in the enkephalin gene, the activation of which is important in neuronal survival. CREB recruits CBP and the TAF_{II}130 subunit of TFIID, followed by the general transcriptional machinery (transcription factors TFIIA, B, D, E, F, H and TBP) and RNA polymerase II (Pol II). Once correctly targeted, transcription is initiated (B) Mutant Htt disrupts transcription by directly interacting with or sequestering CBP, and possibly TAF_{II}130, in aggregates in the nucleus. CBP and TAF_{II}130 are prevented from binding to CRE regions, so the general transcription apparatus along with Pol II are not correctly targeted and transcriptional activation is impaired. (Adapted from Landles and Bates, 2004).

In addition to CBP, Sp1 and TAF_{II}130, several other important transcription factors appear to interact with Htt. The Gln-Ala repeat transcriptional activator CA150 has been found associated with both normal and mutant Htt (Holbert *et al.*, 2001). In HD brain samples, CA150 protein levels increase as the disease progress, implying accumulation of CA150 in response to Htt aggregation and hence interference with transcription (Holbert *et al.*, 2001). Furthermore, the general transcription factor TBP has been localized to inclusions (Perez *et al.*, 1998) and strikingly, an expanded polyQ stretch in TBP causes SCA17 which resembles HD in many aspects (Nakamura *et al.*, 2001; Stevanin *et al.*, 2003), suggesting that altered function of TBP could similarly contribute to the pathology of HD. Htt might also function as a transcriptional repressor owing to its direct and polyQ dependent interaction with nuclear corepressor protein (N-CoR) and Sin3A, which both act in concert with other transcriptional DNA-binding proteins to repress the transcriptional activation of nuclear receptors such as thyroid and retinoic acid receptors (Boutell *et al.*, 1999). Consistently, microarray analysis indicates an involvement of Htt in the regulation of N-CoR and Sin3A-mediated transcription in HD transgenic mice (Luthi-Carter *et al.*, 2000). Finally, the tumor protein p53 was also found in inclusions, reinforcing the hypothesis of a role for transcriptional dysregulation (McC Campbell *et al.*, 2000; Steffan *et al.*, 2000).

Another harmful interaction takes place between expanded polyQ tracts and the acetyltransferase domain of several histone acetylases, including CBP, p300 and P/CAF (Steffan *et al.*, 2001) whose function is to maintain chromatin in a transcriptionally active state through acetylation of histones (Grewal and Moazed, 2003). Expanded polyQ inhibits histone acetylases and impairs histone acetylation. Furthermore, the role of defective histone acetylation in polyQ pathogenesis has been substantiated by the observation that histone deacetylase inhibitors alleviate neurodegeneration in animal and cellular models of polyQ toxicity (McC Campbell *et al.*, 2001; Steffan *et al.*, 2001).

2.4.2.6 *Molecular chaperones in polyQ aggregation and toxicity*

Molecular chaperones are localized to polyQ aggregates in both cellular and animal models of polyQ diseases as well as in patient tissue samples (Cummings *et al.*, 1998; Chai *et al.*, 1999), suggesting that cellular quality-control mechanisms act to prevent aggregation (Sherman and Goldberg, 2001). Thus, impairment of protein folding might give rise to HD pathology (Sakahira *et al.*, 2002). Chronic expression or generation of aggregation-prone

polyQ protein could have global consequences on protein homeostasis and may affect folding or stability of proteins, which harbor folding defects (Gidalevitz *et al.*, 2006), such as metastable polymorphic proteins (Rutherford and Lindquist, 1998). Moreover, sequestration of chaperones into aggregates decreases the amount of available chaperones in the cell and thereby presumably enhances abnormal protein folding (Hay *et al.*, 2004). Consistently, overexpression of the Hsp70/Hsp40 chaperone system suppressed polyQ-induced neurotoxicity in fly models (Warrick *et al.*, 1999; Chan *et al.*, 2000; Fernandez-Funez *et al.*, 2000; Kazemi-Esfarjani and Benzer, 2000) and mouse models of polyQ disease (Cummings *et al.*, 2001; Bonini, 2002; Adachi *et al.*, 2003) whereas expression of a dominant negative mutant form of Hsp70 increased polyQ toxicity (Cummings *et al.*, 2001). Intriguingly, overexpression of Hsp70 and Hsp40 did neither prevent the formation nor alter the microscopic appearance of the neuronal inclusions, indicating that the protective effect of Hsp70 does not require inclusion body clearance. *In vitro* analysis revealed that Hsp70 and Hsp40 inhibited the self-assembly of polyQ proteins into amyloid-like fibrils in an ATP-dependent manner and caused the formation of amorphous (as opposed to protofibrillar or fibrillar) detergent-soluble aggregates (Muchowski *et al.*, 2000). Since fibril prevention was most effective when Hsp70 and Hsp40 acted synergistically during the lag phase of the aggregation reaction, their substrate is presumably in an intermediate, pre-fibrillar state. Yeast and mammalian cell models of polyQ aggregation as well as a *Drosophila* model of polyQ-induced neurodegeneration confirmed the synergistic effect of the Hsp70/Hsp40 chaperones (Sittler *et al.*, 2001; Bonini, 2002). Furthermore, Hsp70 and Hsp40 were found to partition monomers and decrease spherical and annular oligomers, which seem to be intermediates on the pathway to fibril assembly (Wacker *et al.*, 2004). Hsp70 and Hsp40 might bind to expanded polypeptide segments and inhibit the formation of intramolecular β -sheet conformation, thereby blocking nucleation and fibril growth. Binding of Hsp70 to the polyQ segments must be transient and of low affinity, because Hsp70 cycles its substrates in an ATP-dependent manner and glutamine is not a preferred residue in Hsp70-binding peptides (Rudiger *et al.*, 1997). In addition to Hsp70/Hsp40 chaperones, genetic screens implicated various chaperones in modulating polyQ aggregation (Nollen *et al.*, 2004).

Considering that chaperones are multifunctional proteins, their protection against neurodegeneration may result from more than one activity in the cell. Failure of housekeeping mechanisms during ageing may be in part a result of the need for greater protective capacity

in old age as aggregation becomes more prevalent, perhaps as a result of the gradual increased accumulation of misfolded and damaged proteins (Csermely, 2001). With progressive age, it is likely that the activity of our chaperone response and degradatory mechanism declines, resulting in an increased probability that the protective mechanisms are overwhelmed (Keller *et al.*, 2002; Cohen and Kelly, 2003). Marginally stable or folding-defective proteins may misfold due to this stressed folding capacity and in turn contribute to the progressive disruption of the folding environment (Gidalevitz *et al.*, 2006). Apparently, aged organisms and senescent cultures of mammalian cells are less able to induce Hsps in response to protein-damaging conditions (Rattan and Derventzi, 1991; Heydari *et al.*, 1994). Thus, a shift in the balance between cellular chaperone capacity and production of polyQ-expanded protein may be crucial in triggering the onset of disease (Muchowski *et al.*, 2000). Longer polyQ stretches would require more chaperone binding to avoid a toxic aggregation pathway, and therefore patients expressing such sequences would develop neuronal dysfunction earlier in life.

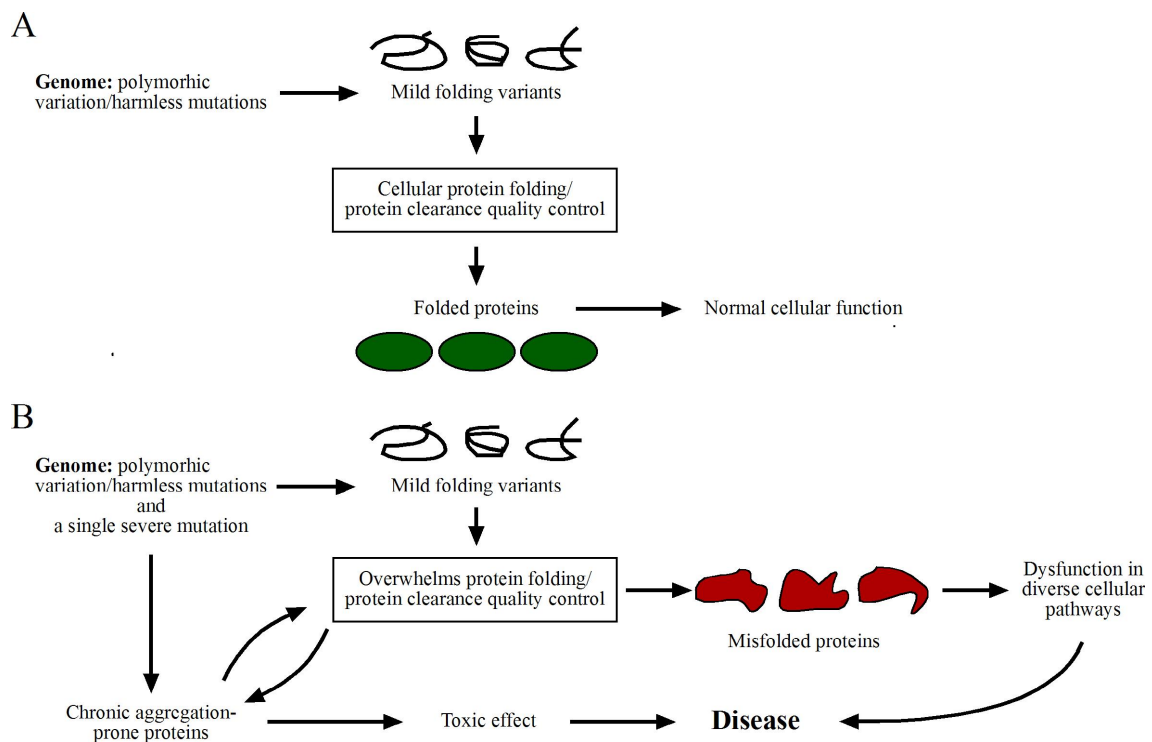


Figure 13: The global consequences of an aggregation-prone protein on protein folding homeostasis.

(A) Under normal physiological conditions, polymorphisms in genes can result in the expression of proteins that are mild folding variants, which are correctly folded or cleared out of the cell by protein quality control mechanisms. (B) In the presence of a chronic aggregation-prone protein, the protein folding and clearance process may become overwhelmed. Innocuous proteins may no longer be correctly folded, leading to dysfunction in a diverse set of cellular pathways. In turn, these structurally and functionally unrelated proteins might generate a positive feedback loop and could exacerbate the misfolding of the aggregation-prone protein, acting as modifiers of this process (Adapted from Bates, 2006).

2.5 Aim of thesis

There is increasing evidence that aggregate formation by a mutant version of Huntingtin (Htt), the disease protein in HD, is causally linked to the progressive neuropathology of this disease. However, whether large insoluble, fibrillar structures or smaller, monomers or oligomeric assemblies of Htt are the toxic agents responsible for cellular malfunction and eventual neuronal loss, is far from clear. Toxicity could arise from the recruitment of other polyQ-containing proteins, i.e. transcription factors, into the neuronal inclusions, which would result in a loss of their normal cellular function. Alternatively, such factors might form abnormal protein-protein interactions with misfolded β -sheet rich Htt monomers or small soluble oligomers.

The main aim of the project was to mechanistically dissect the contribution of soluble and aggregated forms of polyQ-expanded Htt exon 1 to cellular toxicity. This problem was addressed in the context of transcriptional dysregulation as a possible pathomechanism. Specifically, the interaction of polyQ-expanded Htt constructs with the transcription factors TBP and CBP was investigated in yeast model *in vivo*. These experiments were designed to determine whether destabilization of the transcription factors can occur by polyQ-mediated aberrant interactions independent of the formation of insoluble coaggregates. Furthermore, the role of intramolecular determinants flanking the expanded polyQ stretch in modulating polyQ aggregation and cellular toxicity was analyzed.

In a second part of the study, the interaction of different classes of molecular chaperones with polyQ-expanded fragments of Htt was investigated focusing on their ability to modulate oligomerization, aggregation and toxicity. In particular, the role of the cytosolic chaperonin TRiC was investigated in this context for the first time. Given the fact that chaperones assist in the folding of newly-synthesized proteins in a concerted and sequential manner of sequential actions, the cooperativity of chaperones in handling misfolded, aggregation-prone and toxic proteins was investigated.

3 Material and Methods

3.1 Material

3.1.1 Instruments

Abimed (Langenfeld, Germany): Gilson Pipetman (2, 10, 20, 100, 200, 1000 μ l).

Amersham Pharmacia Biotech (Freiburg, Germany): electrophoresis power supply EPS 600, FPLC systems, SMART-System, prepacked chromatography columns: Superdex200, Superose6.

Beckman (Munich, Germany): DU 640 UV/VIS spectrophotometer; Avanti J-25, Avanti 30 and GS-6R centrifuge; Optima TLX ultracentrifuge.

Biometra (Göttingen, Germany): T3 PCR-Thermocycler.

Bio-Rad (München, Germany): electrophoresis chambers MiniProtean 2 and 3; electrophoresis power supply Power PAC 300.

Eppendorf (Hamburg, Germany): centrifuges 5415C and 5417R, Thermomixer Comfort.

EG&G Berthold (Bad Wildbad, Germany): Lumat LB9507.

Fisher Scientific (Schwerte, Germany): pH meter Accumet Basic.

Hoefer Scientific Instruments (San Francisco, USA): SemiPhore blotting transfer unit.

Mettler Toledo (Gießen, Germany): balances AG285, PB602.

Millipore (Eschborn, Germany): deionization system MilliQ plus PF, Millix-HA filters 0.22 μ m.

New Brunswick Scientific (Nürtingen, Germany): orbital shaker and incubator Innova 4430.

Sartorius (Goettingen, Germany): vacuum filtration unit (0.2 μ m).

WTW (Weilheim, Germany): pH meter pH535.

Zeiss (Jena, Germany): Microscope Axiovert 200M

3.1.2 Chemicals

All chemicals were of quality *pro analysi* and purchased from *Sigma-Aldrich* (Deisenhofen, Germany) if not stated otherwise. Solutions were prepared with deionised, double distilled and sterile-filtered water. Concentration in percent of liquids are given as (v/v) and of solid chemicals as (w/v).

Amersham Pharmacia Biotech (Freiburg, Germany): Protein G Sepharose™, LMW and HMW gel filtration Calibration kits.

BioMol (Hamburg, Germany): HEPES.

BioRad (München, Germany): ethidiumbromide.

BD Bioscience (Heidelberg Germany): doxycycline.

Calbiochem (Bad Soden, Germany): TWEEN-20.

Difco (Heidelberg, Germany): Bacto agar, Bacto yeast extract, Bacto pepton, Bacto trypton, Yeast nitrogen base w/o amino acids.

Fermentas (St. Leon-Rot, Germany): PageRuler™ protein ladder, GeneRuler™ 100bp and 1 kb DNA ladder.

Fluka (Deisenhofen, Germany): DMSO.

Invitrogen (Karlsruhe, Germany): Lipofectamine™-reagent.

New England Biolabs (Frankfurt/Main, Germany), T4 DNA Ligase, DNA polymerase I (Klenow fragment), restriction endonucleases, prestained protein marker broad range.

Merk (Darmstadt, Germany): Benzoylase, EDTA, 2-Mercaptoethanol, paraformaldehyde.

Molecular Probes (Karlsruhe, Germany): DAPI.

Qiagen (Hilden, Germany): NiNTA resin, QIAprep spin miniprep Kit, QUIAGEN Plasmid Midi Kit, QIAprepEndoFree Plasmid Maxi kit, QIAquick PCR purification and gel extraction kits.

Pierce (Bonn, Germany): Coomassie protein assay reagent.

Promega (Mannheim, Germany): Wizard®PlusSV Minipreps, PureYield™ Plasmid Midiprep system, Wizard®SV gel and PCR clean-up system, Beetle Luciferin-potassium salt, Luciferase Assay System.

Roche (Basel, Switzerland): ampicillin, aprotinin, Complete Protease inhibitor, DTT, Expand™ Long Template PCR system, leupeptin, Pefabloc Protease inhibitor, pepstatinA, shrimp alkaline phosphatase.

Schleicher & Schuell (Dassel, Germany): Protran™ nitrocellulose transfer membrane, nitrocellulose acetate membrane filter.

Seikagaku (Tokyo, Japan): Zymolyase-20T

Serva (Heidelberg, Germany): Coomassie, Serva BlueR, PEG, PMSF, Acrylamide-Bis solution 30% (37:5:1), Citifluor.

Stratagene (La Jolla, USA): PfuTurbo™ DNA Polymerase II, QuickChange™ site-directed mutagenesis kit, Yeast Carrier DNA.

3.1.3 Buffers and Media

Buffers were prepared with ddH₂O.

PBS	137 mM NaCl, 2.7 mM KCl, 8.4 mM KH ₂ PO ₄ , 1.5 mM K ₂ HPO ₄ , pH 7.4, adjusted with HCl
PBST	PBS + 0.05 % (v/v) Tween 20
TE	10 mM Tris-HCl pH 8.0, 1 mM EDTA

Media were prepared with ddH₂O and autoclaved, unless stated otherwise.

LB medium:	10 g/l Bacto™tryptone, 5 g/l Bacto™yeast extract, 5 g/l NaCl, (+ 15 g/l agar for solid medium), Adjusted to pH 7.0 with NaOH, ampicillin 100 mg/ml in ddH ₂ O (sterile filtered and added to media after autoclaving).
YPD medium:	20 g/l Difco™peptone, 10 g/l Bacto™yeast extract, 20 g glucose, ddH ₂ O to 1 l final volume, adjust pH 5.8.
SC-synthetic complete	6.7 g/l Yeast Nitrogen Base without amino acids, 20 g/l glucose, 2 g/l drop-out mix, (+ 20 g/l agar for solid medium), ddH ₂ O to 1 l final volume, adjust pH 5.8.
Drop-out mix	0,5 g adenine, 0,2 g <i>para</i> -aminobenzoic acid, 10 g leucine, 2 g each of alanine, arginine, asparagine, aspartic acid, cyteine, glutamine, glutamic acid, glycine, histidine, inositol, isoleucine, lysine, methionine, phenylalanine, proline, serine, threonine, tryptophan, tyrosine, uracil, valine (For selection, components were left out for which the strain was prototroph.)
Sugar stock solutions	20 %glucose, 20 % raffinose, 20 % galactose (Solutions were sterile filtered and added to sterile media).
DMEM	inclusive 3.7 g/l NaHCO ₃ and 4.5 g/l glucose (BiochromAG, F0435)
FCS	Tet system improved FCS (BD Bioscience, 8637, Lot G20951)
200 mM L-glutamine	(Invitrogen, 25030-024)
Penicillin/Streptomycin (100x)	each 10000 U/ml
Geneticin (G-418)	100 mg/ml (Sigma, 9516)
OptiMEM-I	(Invitrogen, 31985-04)
PBS	w/o CaCl ₂ /MgCl ₂ (Invitrogen, 20012-019)
Trypsin/EDTA-Solution	0.25 % trypsin (BiochromAG, L2163), 0.002 % EDTA

3.1.4 Antisera

All antisera were used in 2×10^{-3} to 10^{-5} dilutions in PBS-T supplemented either with 0.3 % BSA or with 0.4 % non-fat milk powder.

Table 2: Antisera used in this study.

Primary antibody	Species	Reference
anti-c-myc	mouse, monoclonal	SantaCruz sc-40
anti-c-myc-Cy3	mouse clone 9E10, monoclonal	Sigma C 6594
anti-HA	rabbit, polyclonal	Babco MMS-101R
anti-Flag M2	mouse, monoclonal	Babco MMS-101R
anti-GFP	mouse clones 7.1&13.1, monoclonal	Roche 11814 460 001
anti-GST	goat, monoclonal	Amersham 27-4577
anti-CBP	mouse, monoclonal	abcam ab2832
anti-TBP	mouse, monoclonal	abcam ab818
anti-1C2	mouse, monoclonal	Chemicon MAB1574
anti-A11	rabbit, polyclonal	C. Glabe
anti-Ssa1	rabbit, polyclonal	K. Siegers
anti-Ssb1	rabbit, polyclonal	E. Craig
anti-Ydj1	rabbit, polyclonal	E. Craig
anti-GroEL	rabbit, polyclonal	Dean Naylor
anti-TCP-1 α	rat, polyclonal	Stressgen CTA-191
anti-TCP1	rabbit, polyclonal	K. Siegers
anti-TCP3	rabbit, polyclonal	K. Siegers
anti-TCP5	rabbit, polyclonal	K. Siegers
anti-TCP7	rabbit, polyclonal	K. Siegers

Secondary antibody	Species	Reference
anti-mouse IgG HRP	goat, polyclonal	DakoCytomation P0447
anti-mouse IgG Cy3	goat, polyclonal	Dianova 115-165-062
anti-mouse IgG FITC	goat, polyclonal	Dianova 115-096-062
anti-rabbit IgG HRP	goat, polyclonal	Sigma A9169
anti-rabbit IgG Cy3	goat, polyclonal	Dianova 111-165-045
anti-rabbit IgG FITC	goat, polyclonal	Sigma F6005
anti-rat IgG FITC	goat, polyclonal	Sigma F 6258
anti-rat IgG Cy3	goat, polyclonal	abcam ab6953

3.1.5 Bacterial and yeast strains, mammalian cell lines

Table 3: *E. coli* strains used in this study.

Strain	Genotype	Reference
DH5 α	<i>F'</i> <i>endA1 hsdR17</i> (<i>r_K-m_K</i> ⁺) <i>supE44 thi-1 recA1 gyrA</i> (<i>Nal</i> ^r) <i>relA1 D(lacZYA-argF)</i> _{U169} (<i>m80lacZDM15</i>)	Novagene
SURE	<i>e14- (McrA-)</i> <i>D(mcrCB-hsdSMR-mrr)</i> <i>171 endA1 supE44 thi-1 gyrA96 relA1 lac recB</i>	Novagene
XL1-Blue	<i>recA1 endA1 gyrA96 thi-1 hsdR17 supE44 relA1 lac [F⁺proAB lacIqZDM15 Tn10 (Tetr)]</i>	Stratagene

Table 4: *Saccharomyces cerevisiae* strains used in this study.

Strain	Genotyp	Reference
YPH499	<i>MATa ura3-52 lys2-801 ade2-101 trp1Δ63 his3Δ200 leu2Δ1</i>	(Sikorski and Hieter, 1989)
GSY2	<i>MATa ura3-52 lys2-801 ade2-101 trp1Δ63 his3Δ200 leu2Δ1 Δspt15::HIS3 pRS415yhTBP38Q</i>	(Schaffar <i>et al.</i> , 2004)
GSY2	<i>MATa ura3-52 lys2-801 ade2-101 trp1Δ63 his3Δ200 leu2Δ1 ssa1Δ ssa2Δ</i>	Gregor Schaffar
KSY185.7	<i>MATa ura3-52 lys2-801 ade2-101 trp1Δ63 his3Δ200 leu2Δ1 ssb1Δ ssb2Δ</i>	(Siegers <i>et al.</i> , 2003)
KSY515	<i>MATa ura3-52 lys2-801 ade2-101 trp1Δ63 his3Δ200 leu2Δ1 tcp1Δ pRS414-TCP1</i>	(Siegers <i>et al.</i> , 2003)
KSY333	<i>MATa ura3-52 lys2-801 ade2-101 trp1Δ63 his3Δ200 leu2Δ1 tcp1Δ pRS414-tcp1-2</i>	(Siegers <i>et al.</i> , 2003)

Table 5: Neuroblastoma cell lines used in this study.

Cell line	Description	Reference
Neuro-2a (N2a) -Tet-off	(adherent) mouse neuroblastoma cell line stable transfected with tetracycline-inducible transactivator tTA	(Schaffar <i>et al.</i> , 2004)
SH-SY5Y	(adherent) human neuroblastoma cell line	ATCC CRL-2266

3.1.6 Plasmids and oligonucleotides

Table 6: Plasmids used in this study.

Vector	Description	Reference
pGEX-6P1	<i>E. coli</i> cloning vector, T7 and T3 promoters	Stratagene
pRS317	Yeast Shuttle vector (<i>CEN6</i> , <i>LYS2</i>)	(Sikorski and Boeke, 1991)
pRS413	Yeast Shuttle vector (<i>CEN6</i> , <i>HIS3</i>)	(Sikorski and Hieter, 1989)
pRS414	Yeast Shuttle vector (<i>CEN6</i> , <i>TRP1</i>)	(Sikorski and Hieter, 1989)
pRS415	Yeast Shuttle vector (<i>CEN6</i> , <i>LEU2</i>)	(Sikorski and Hieter, 1989)
pRS416	Yeast Shuttle vector (<i>CEN6</i> , <i>URA3</i>)	(Sikorski and Hieter, 1989)
p415ADH	Yeast expression vector (<i>CEN6</i> , <i>LEU2</i>), <i>ADH1</i> promoter	(Mumberg <i>et al.</i> , 1994)
p415Gal	Yeast expression vector (<i>CEN6</i> , <i>Leu2</i>), <i>GAL1</i> promoter	(Mumberg <i>et al.</i> , 1994)
p416Gal	Yeast expression vector (<i>CEN6</i> , <i>URA3</i>), <i>GAL1</i> promoter	(Mumberg <i>et al.</i> , 1994)
p425Gal	Yeast expression vector (2 μ , <i>LEU2</i>), <i>GAL1</i> promoter	(Mumberg <i>et al.</i> , 1994)
p426Gal	Yeast expression vector (2 μ , <i>URA3</i>), <i>GAL1</i> promoter	(Mumberg <i>et al.</i> , 1994)
p423tet	Yeast expression vector (<i>CEN6</i> , <i>HIS3</i>), <i>tetO</i> promoter	K. Siegers
pSI215	Yeast expression vector (2 μ , <i>TRP1</i>), <i>CUP1</i> promoter	K. Siegers
pSI244	Yeast expression vector (2 μ , <i>LEU2</i>), <i>CUP1</i> promoter	K. Siegers
YEp105	Yeast expression vector (2 μ , <i>TRP1</i>), <i>CUP1</i> promoter	(Ecker <i>et al.</i> , 1987)
pTRE2hygro	mammalian expression vector, tet- <i>CMV</i> promoter	BD Bioscience
pcDNA3.1	mammalian expression vector, <i>CMV</i> promoter	Invitrogene
pEF-BOS-EX	mammalian expression vector, <i>EF-1-α</i> promoter	(Mizushima and Nagata, 1990)

Table 7: Oligonucleotides used in this study.

Name	Nucleotide sequence
5'-myc-Htt-BglII	5'-CTAGCTAGCATGTGTGAACAAAAGCTTATTTCTGAAGAAGACTTGGGTA TGCAATCATGGCGACCCCTGGAAAGGCTG-3'
5'-NLS-myc-BglII	5'-CTAGCTAGCATGCGCCAAAAAAGAAGAGAAAGGTAGAATTAGGAACA GCATGTGAACAAAAGCTTATTTCTG-3'
5'-myc-PstI	5'-AACTGCAGATGTGTGAACAAAAGCTTATTTCTGAAG-3'
3'-Htt-SalI	5'-GAGGTCGACTCACGGTCGGTGCAGCGGCTCCTCAGCC-3'
3'-Htt-NotI	5'-CTTTTGGCGCCGCTCACGGTCGGTGCAGCGGCTCC-3'
5'-GST-BglII	5'-GGAAGATCTATGTCCCCTATACTAGGTTATTGG-3'
3'-HA-stop-SalI	5'-GACGTCGACTTACGCGTAATCTGGAACGTCATACGG-3'
5'-GST-NheI	5'-CTAGCTAGCATGTCCCCTATACTAGGTTATTGGAAAATTAAGGG-3'
3'-GFP-SalI	5'-CTGCAGCTGGCTTTTGTATAGTTCATCCATGCC-3'
5'-PKI-NES	5'-CTAGTAATGAATTAGCCTTGAAATTAGCAGGCTTTGATATCAACAAGACA A-3'
3'-PKI-NES	5'-ATTACTTAATCGGAACTTTAATCGTCCAGAACTATAGTTGTTCTGTTTCGA- 3'
5'-Luc-BamHI	5'-CGGATCCATGGAAAACATGGAGAACGATGAAAATATTGTG-3'
3'-Luc-SalI	5'-TGACGTCGACTTACAATTTGGACTTTCCGCCCTTCTTGGC-3'
5'- <i>GALI</i> -TGTA	5'-GGTTATGCAGTTTTTGCATTTACATATCTGTTAATAGAT-3'
3'- <i>GALI</i> -TGTA	5'-GATCTATTAACAGATATGTAATGCAAAAACGTCATAACC-3'
5'-hTBP-NotI	5'-ATTTGCGGCCGCGATGGATCAGAACACAGCCTGCCACC-3'
3'-hTBP-XhoI	5'-GGCTCGAGCCTTACGTCGCTTCTGAATCCCTTTAGAAT-3'
5'-yTBP-NotI	5'-CAGGCGCGAGCTCATGGCCGATGAGGAACG-3'
3'-yTBP-XhoI	5'-CAGGCGCCTCGAGTCACATTTTCTAAATTCAC-3'
5'-mut3hTBP	5'-GTTATGAGCCAGAGTTATTTCTGGTTTATTCTACAGAATGATCAAACC CAGAATTACTCTCGTTATTTTGTCTGGAAAAG-3'
3'-mut3hTBP	5'-CTTTTCCAGAAACAAAATAACGAGAGTAATTCTGGGTTTGTATCATTCT GTAGAATAAACAGGAAATAACTCTGGCTCATAAC-3'

3.2 Methods

3.2.1 Molecular biological methods

All solutions were autoclaved or sterile filtered before usage. All methods were adapted from “Molecular Cloning“(Sambrook J., 1989), if not stated elsewhere.

3.2.1.1 Plasmid DNA purification

5 ml or 100 ml LB medium, for small or large-scale plasmid DNA purification, respectively, were inoculated with a single *E.coli* colony harboring the plasmid of interest and grown to saturation over night at 37 °C. Cells were harvested and further processed according to instructions of the following plasmid purification kits: QIAprep spin miniprep Kit, QUIAGEN Plasmid Midi Kit and QIAprep Endofree Plasmid Maxi Kit (Quiagen) or Wizard® PlusSV Miniprep and PureYield™ Plasmid Midiprep system (Promega).

3.2.1.2 Determination of DNA concentration

DNA concentration of purified Plasmid DNA was measured by UV absorption spectroscopy at a wavelength of 260 nm. In H₂O, a solution of 50 µg/ml of double-stranded DNA exhibits approximately an absorbance $A_{260} = 1$.

3.2.1.3 Plasmid DNA sequencing

DNA sequencing was performed either by Medigenomix GmbH (Martinsried, Germany) or by Sequiserve (Vaterstetten, Germany).

3.2.1.4 DNA restriction digestion

DNA fragmentation for analysis and cloning was carried out by digesting plasmid DNA or PCR products with restriction endonucleases. Enzymes and supplied buffers were used as recommended by the manufacturer. 0.5-1 µg plasmid DNA was used for analysis and 8-15 µg plasmid DNA or 20 µl purified PCR product for cloning purposes. The reaction was incubated at the recommended temperature for 2-4 h. The restriction digest was incubated typically at 65°C for 20 min to heat-inactivate enzyme for further cloning or separated by agarose gel electrophoresis for DNA fragment analysis.

3.2.1.5 *Dephosphorylation of DNA fragments*

Prior to ligation of DNA fragments carrying identical ends, 5'-end dephosphorylation was carried out in order to prevent self-ligation of plasmid DNA fragments. The removal of 5' phosphate groups was catalysed by Shrimp alkaline phosphatase (SAP). 5 – 10 µg plasmid DNA were incubated with 1 U SAP and supplied buffer for 1 h at 37 °C. Subsequently, the reaction was heat inactivation by incubation at 65 °C for 15 min.

3.2.1.6 *5'-DNA end overhand fill in*

For generation of blunt ends, 3'-recessed ends were filled-in by Klenow fragment. 15 U Klenow fragment and 30 µM dNTP were added to a 100µl DNA restriction digest and incubated at 25°C for 15 min. Klenow fragment was heat inactivated at 75°C for 20 min.

3.2.1.7 *DNA purification*

Enzymatically modified DNA or PCR products were purified according to QIAquick PCR purification kit (Qiagen) or to Wizard[®]SV PCR clean-up system (Promega).

3.2.1.8 *DNA agarose gel electrophoresis*

For separation of DNA fragments or analysis of plasmid digests, DNA agarose gel electrophoresis was performed in TAE buffer and 1 – 2 % TAE-agarose gels, supplemented with 1 mg/ml ethidiumbromide, at 4 – 6 V/cm. Ethidiumbromide interchelates with DNA and can be visualized under UV light. A DNA mass standard was used for identification of DNA length. The DNA was loaded in loading buffer on agarose gel.

DNA sample buffer	30 % glycerol, 0.25 % bromphenol blue, 0.25 % xylencyanol FF
TAE	40 mM Tris-acetate, 1 mM EDTA, pH 8.0

3.2.1.9 *DNA extraction from agarose gels*

After separation by agarose gel electrophoresis and staining, bands of interest were cut out and purified by Wizard[®]SV gel clean-up system (Promega) or QIAquick gel extraction kit (Quiagen) in order to isolate DNA fragments.

3.2.1.10 Polymerase chain reaction (PCR)

For amplification of DNA fragments, the polymerase chain reaction (PCR) was performed according to the following protocol:

Table 8: Standard protocol for PCR.

Reaction mixture	Reaction			
0.25 μ M primer 1 (sense)	1st cycle	denaturation	95 °C	5 min
0.25 μ M primer 1 (antisense)	25 cycle	denaturation	95 °C	30 sec
10 μ l 10x Pfu polymerase buffer		annealing	60 °C	30 sec
10 μ l DMSO		extension	72 °C	1 min/kb
50 – 100 μ g template DNA	last cycle	extension	72 °C	8 min
250 μ M dNTPs			4 °C	
1 – 2 U Pfu DNA polymerase II				
ddH ₂ O to 100 μ l final volume				

3.2.1.11 Oligonucleotides annealing

100 pmol/ μ l sense and antisense oligonucleotides were mixed at a 1:1 ratio, incubated first for 3 min at 95 °C, following 10 min at 65 °C, and finally for 2 h at 37 °C. The annealed oligonucleotides were ligated into vector DNA

3.2.1.12 Site-directed mutagenesis

Site-directed mutagenesis was performed using the QuickChange™ System (Stratagene) following the manufacturers' instructions. Vector DNA containing the gene of interest was amplified by PCR using a complementary set of sense and antisense primers, which introduced site-specific the desired mutation. A mutagenesis PCR reaction was typically performed using the following protocol:

Table 9: Standard protocol for site-directed mutagenesis.

Reaction mixture	Reaction			
125 ng primer 1 (sense)	1st cycle	denaturation	95 °C	30 sec
125 ng primer 2 (antisense)	25 cycle	denaturation	95 °C	30 sec
5 μ l 10x Pfu polymerase buffer		annealing	55 °C	1 min
5 – 50 ng template DNA		extension	68 °C	2 min/kb
250 μ M dNTPs	last cycle	extension	68 °C	20 min
1 μ l PfuTurbo™ DNA polymerase II			4 °C	∞
ddH ₂ O to 50 μ l final volume				

PCR products were treated with 1 μ l endonuclease DpnI (20000U/ml) for 1 hour at 37 °C to digest specifically methylated and hemimethylated parental template DNA. 1 – 5 μ l of the reactions were transformed in *E.coli* XL1-Blue supercompetent cells and mutations were confirmed by DNA sequencing.

3.2.1.13 Ligation of DNA fragments

Ligation reaction was carried out to fuse compatible DNA ends. Usually vector and fragment DNA were mixed at 1:7 ratios with 0.5 U T4 DNA Ligase and supplied buffer. The reaction was incubated at 20 °C for 15 min in case of cohesive ends and for 2 h in case of blunt ends followed by transformation into chemical competent *E.coli* cells.

3.2.1.14 Preparation and transformation of competent *E. coli* cells

Chemical competent cells were prepared as described (Hanahan, 1983). 5 ml LB were inoculate with a single colony and grown to saturation at 37 °C. 2 ml of this pre-culture were used to inoculate 200 ml LB medium and grown to an OD₆₀₀ of 0.3. Cells were chilled on ice for 15 min and centrifuged at 1500 x g for 15 min at 4 °C. Pelleted cells were resuspended in 30 ml ice-cold TB1 and incubated on ice for 10 min. Then, cells were centrifuged again and resuspended in 4 ml ice-cold TB2. Aliquots were frozen in liquid nitrogen and stored at -80 °C. For transformation, 50 μ l competent cells were mixed with 0.05 – 0.2 μ g plasmid DNA or 1 – 5 μ l ligation reaction and incubated on ice for 30 min. The cells were then heat shocked at 42 °C for 45 – 60 s and placed on ice for 2 min. After addition of 1 ml of LB medium, cells were incubated at 37 °C for 1 h with shaking. The cell suspension was subsequently plated on selective plates and incubated at 37 °C until colonies had developed.

TB1	100 mM RbCl, 250 mM MnCl ₂ , 30 mM KAc, 10 mM CaCl ₂ , 15 % glycerol, pH 5.8 (adjusted with 0.2 HOAc)
TB2	75 mM CaCl ₂ , 10 mM RbCl ₂ , 10 mM MOPS, 15 % glycerol, pH 6.5 (adjusted with KOH)

3.2.2 Yeast methods

All solutions required for cultivation of yeast were autoclaved or sterile filtered before usage. All yeast methods were adapted from “Yeast Protocols” (Evans, 1996), if not stated otherwise.

3.2.2.1 Culture and storage

Saccharomyces cerevisiae yeast strains were cultivated on YPD or SC medium containing agar plates or as liquid culture with vigorous agitation at the required temperature in YPD or SC medium. Media were supplemented with 0,003 % adenine, since all used yeast strains harbor an auxotroph *ade2-101* mutation within the adenine gene. For short-term storage, yeast was streaked on agar plates, grown until colony formation and stored at 4 °C. For long-term storage, glycerol stocks were performed by mixing a liquid culture, grown to saturation, in 1:1 ration with 50 % glycerol. Cell suspension is shock frozen in liquid nitrogen and stored at -80 °C.

3.2.2.2 Determination of cell density

The density of cells in a culture was determined spectrophotometrically by measuring its optical density (OD) at 600 nm. For reliable measurements, cultures were diluted such that the OD₆₀₀ was below 1. In this range, each 0.1 OD₆₀₀ unit corresponds to ~ 3x10⁶ cells/ml. Consequently, an OD₆₀₀ of 1 is equal to 3x10⁷ cells/ml.

3.2.2.3 Preparation and transformation of competent yeast cells

For generation of competent yeast cells, 5 ml appropriated media was inoculated with a single yeast colony and grown to stationary phase at 30 °C. This preculture was used to inoculated 50 ml main culture to a cell density of OD₆₀₀ = 0.15 and incubated as described above. Cells were harvested at OD₆₀₀ = 0.5 – 0.6 by centrifugation at 1000 x g for 3 min at room temperature, resuspended in 50 ml ddH₂O and centrifuged again. Cells were resuspended in 12.5 ml lithium/sorbitol-buffer and pelleted once more. After an additional centrifugation step in order to remove the supernatant completely, pellets were finally resuspended in 300 µl lithium/sorbitol-buffer and mixed with 30 µl yeast carrier DNA (10 mg/ml). Next, cell suspension was aliquoted and stored at -80 °C. For transformation, 50 µl cells were incubated with 1 µg plasmid DNA and 300 µl lithium/PEG-buffer for 20 min at

RT. 35 μ l DMSO were added to the cells suspension followed by heat shock incubation at 42 °C for 15 min. Cells were pelleted at 4000 x g for 5 min, resuspended in appropriated medium and plated on selective plates followed by incubation at 30 °C until colonies developed.

Lithium/sorbitol buffer	100 mM LiOAc, 10 mM Tris-HCl pH 8.0, 1 mM EDTA 1 M sorbitol
Lithium/PEG buffer	100 mM LiOAc, 10 mM Tris-HCl pH 8.0, 1 mM EDTA 40% PEG3350

3.2.2.4 Purification of DNA from yeast cells

2 ml yeast cultures were grown overnight to early stationary phase at 30 °C. Cells were pelleted by centrifugation at 2000 x g, washed once with ddH₂O and resuspended in 200 μ l buffer A followed by incubation for 1 h at 30 °C with gently agitation. Subsequently, 200 μ l buffer B were added and incubated for 20 min at 65 °C. Cells were placed on ice prior to addition of 200 μ l KAc and 15 min incubation. Cells were centrifuged at 20.000 x g and supernatant transferred to fresh Eppendorf tube. DNA was precipitated from supernatant by addition of 600 μ l isopropanol. After short incubation at RT, DNA was pelleted by centrifugation at 20.000 x g for 10 min, washed once with 70 % ethanol and incubated at RT for 10 min. DNA was pelleted again by centrifugation at 20.000 x g for 10 min, air-dried and resuspended in 30 μ l TE buffer.

Buffer A	100 mM Tris-HCl pH 7.5, 10 mM EDTA pH 7.5, 10 μ l/ml 2-mercaptoethanol, 0.2 mg/ml Zymolase-20T
Buffer B	0.2 M NaOH, 1 % SDS

3.2.2.5 Protein expression in yeast cells

For expression of proteins in yeast, galactose, copper and doxycycline regulated promoters, *GALI*, *CUPI* and *tetO* respectively, were used. Since glucose inhibits the *GALI* promoter, glucose was only used as carbon source for yeast in media when expression was driven by *CUPI* promoter. For galactose inducible expression, raffinose was used as carbon source instead of glucose. A stationary phase preculture was used to inoculated a main culture to an optical density of OD₆₀₀ = 0.15 and grown at 30 °C while shaking (230 rpm). Expression of the protein of interest was induced with 2 % Galactose or 100 μ M CuSO₄, for *GALI* or *CUPI* promoter respectively, once the culture reached OD₆₀₀ = 0.4 – 0.5 and cells were incubated for desired period of time at 30 °C with vigorous agitation (230 rpm). *tetO* driven

expression was induced by withdrawal of doxycycline from the media. Cells were washed 3 times in media and were allowed to grow for desired period.

3.2.2.6 *Growth assays*

Growth curves and plate assays were performed to compare viability of various yeast strains. For plate assays, a serial dilution was performed with the appropriated medium starting from an exponential phase culture adjusted to a cell density of $OD_{600} = 1$. 5 μ l of each dilution was dropped on selective plate and incubated at the required temperature until colonies developed. Sensitivity to the microtubule-destabilizing drug benomyl was assayed by spotting cells on YPD agar plates containing 0 and 40mg/ml benomyl. For growth curves, cell density was recorded in liquid media supplemented with 50 mM 3-AT at 30 °C by reading OD_{600} at various time points.

3.2.2.7 *Luciferase assay*

Luciferase activity was measured by mixing approximately 5 μ l exponential phase cells with 50 μ l of beetle luciferin (Promega). The samples were immediately transferred into a luminometer (EG&G Berthold) and measured for 5 – 30 seconds. Each measurement was repeated at least three times and the results were averaged. Cell density was determined by measuring OD_{600} in order to calculate relative luciferase activity.

3.2.2.8 *β -Galactosidase assay*

β -galactosidase converts the colorless ONPG substrate into galactose and the chromophore o-nitrophenol, yielding a bright yellow solution. 100 μ l lysate were incubated with 700 μ l Z buffer and 160 μ l ONPG at 30 °C. 400 μ l Stop solution were added when all samples showed a weak yellow coloring and absorbance were measured at 420 nm. β -galactosidase activity was expressed in nmoles of β -galactose formed per minutes per mg of lysates at 30 °C (Nielsen *et al.*, 1983).

Z Buffer	100 mM NaH_2PO_4 pH 7.0, 10 mM KCl, 1 mM $MgSO_4$, 50 mM β -mercaptoethanol
ONPG	4 mg/ml in Z Buffer
Stop solution	1 M Na_2CO_3

3.2.2.9 Preparation of yeast cell lysates

Glass bead lysis was performed for preparation of lysates under native conditions. Yeast cultures were harvested by centrifugation at 2000 x g. Pellets were washed once with ddH₂O and mixed with 0.5 – 1 ml ice-cold lysis buffer and one volume of acid-washed glass beads (diameter 0.45 – 0.5 mm). Lysis buffers TG&I or TP were only used for gel filtration and immunoprecipitation or NiNTA pull down of TRiC, respectively. Suspensions were repeatedly shaken vigorously for 1 min and chilled on ice in between. Cell debris and beads were pelleted at 1000 x g at 4 °C and supernatants were transferred to new tubes.

Lysis buffer	25 mM Tris-HCl pH 7.5, 50 mM KCl, 10 mM MgCl ₂ , 1 mM EDTA, 5% glycerol, 1% Triton-X-100, 1x protease-inhibitor-mix
Lysis buffer TG&I	1 x PBS, 1 mM EDTA, 1x protease-inhibitor-mix
Lysis buffer TP	1 x PBS, 10 mM MgCl ₂ , 5 % glycerol, 0.1% Triton-X-100, 1x protease-inhibitor-mix

3.2.2.10 Immunofluorescence

For immunofluorescence microscopy, 5 ml exponential phase culture were fixed by addition of 0.5 M K₃PO₄ (pH 6.5) and 3.7% formaldehyde for one hour at RT. Cells were harvested by centrifugation at 1000 x g, washed five times with sorbitol buffer and resuspended in 1 ml sorbitol buffer supplemented with 2.5 mg Zymolase T20 and 19 µM 2-mercaptoethanol. Suspension was incubated at 30 °C under agitation until ~ 90 % of cells were spheroblasts. After thoroughly washing with sorbitol buffer, spheroblasts were resuspended in 500 µl sorbitol buffer. 20 µl of suspension were transferred onto a multiwell microscopy slide coated with 0,3 % poly-L-lysine and incubated for 10 min. Unbound spheroblasts were washed away with PBS supplemented with 1 % BSA (PBS-B) before air-drying slides. For permeabilization, slides were incubated 5 min in ice-cold 100 % ethanol following 30 sec in ice-cold 100 % acetone. After air-drying, cells were incubated with PBS-B for one hour at RT to prevent unspecific antibodies binding. Spheroblasts were incubated with appropriate primary antibody (20 – 50 mg/ml in PBS-B) for one hour. After thoroughly washing with PBS-B, cells were incubated with corresponding fluorescent-labeled secondary antibody (5 – 10 µg/ml in PBS-B) as before. Slides were washed as before, overlaid with mounting medium and covered with coverslip sealed by nail polisher.

Sorbitol buffer	0.1 M KPO ₄ , pH 6.5, 1.2 M sorbitol
Mounting medium	75% Citifluor, 25% PBS, 0.25 µg/ml DAPI

3.2.3 Mammalian cell culture methods

All media and material, utilized for mammalian cell culture, were either sterile filtered, autoclaved or UV-light radiated prior to usage.

3.2.3.1 *Cultivation of adherent cells*

The adherent cell lines N2a and SH-SY5S were grown in DMEM medium supplemented with 10 % FCS, 2 mM L-glutamine 1x Penicillin/Streptomycin, if not stated otherwise. Cells were cultured in tissue culture plates at 37 °C in 5 % CO₂. For maintenance, cells reached approximately 90 % confluency were washed once with PBS and then detached from tissue culture plates using 1x trypsin/EDTA. Cells were then diluted in fresh medium as required and plated into appropriated tissue culture plates for further cultivation. For long-term storage, cells were trypsinized, pelleted at 200 x g for 5 min and resuspended in medium supplemented with 10 % DMSO. Next, cells were frozen at -80 °C over night and then transferred into liquid nitrogen. For regeneration, cells were thaw at 37 °C in a water bath followed by dilution into pre-warmed medium. After centrifugation at 200 x g for 5 min, cells were resuspended in medium, transferred into tissue culture plates and incubated as described above. In order to remove DMSO completely, medium was exchanged the following day.

3.2.3.2 *Transient transfection*

Cell lines were transfected with the liposome based LipofectAMINE™ reagent (Invitrogen) according to the manufacturers' instructions. Transfection was enhanced by the use of Plus™ reagent (Invitrogen) to pre-complex DNA prior to the preparation of transfection complexes. The day prior to transfection, cells were diluted and plated in order to reach approximately 60 % confluency at the day of transfection. Per 6 cm dish, 2 µg DNA were mixed with 8 µl Plus™ reagents in 250 µl OptiMEM-I medium and incubated for 15 min at room temperature to pre-complex DNA. 12 µl LipofectAMINE™ diluted in 250 µl OptiMEM-I medium were added and incubated for another 15 min. While DNA-liposome complexes were forming, medium was replaced by serum free OptiMEM-I medium. DNA-liposome mixture was then transferred on to the cells and incubated for 3 h at 37 °C. Finally, serum containing growth medium was added and cells were grown for 24 to 48 h.

3.2.3.3 Preparation of cell lysates

Cell lysates were prepared 24 h to 48 h after transient transfection. Cells were washed twice with ice-cold PBS and incubated with 0.5 ml ice-cold lysis buffer on ice for 10 min. Complete detachment of cells was achieved using a cell scraper. Cell lysates were separated from intact cells upon centrifugation at 1000 x g for 5 min at 4 °C.

Lysis buffer	150 mM NaCl, 10 mM Tris-HCl pH 7.5, 1% Triton-X-100, 0.5% deoxycholat, 0.1% SDS, 1x protease-inhibitor-mix
--------------	--

3.2.3.4 Immunofluorescence

Cells were grown on coverslips to about 50 % confluency. Cells were washed three times with pre-warmed PBS prior to fixation and permeabilization in methanol for 5 min at -20 °C. C. After removing of methanol, cells were washed once again three times with PBS and incubated in PBS supplemented with 1 % BSA (PBS-B) for 1 h at RT to reduce unspecific binding of antibodies. The first antibody was applied at concentration of 20 – 50 µg/ml in PBS-B for 1 h. Cells were then washed three times with PBS before applying the secondary, fluorescent-labeled antibody at concentration of 10 – 20 µg/ml in PBS-B together with 1 µg/ml DAPI for 1 h. DAPI was used to stain the nucleus. Prior to fixation on microscopy slide with Prolong®Antifade kit (Molecular Probes) cells were washed three times with PBS and once in ddH₂O in order to remove salts. Finally, slides were sealed with nail polisher and stored in the dark at 4 °C.

3.2.3.5 Luciferase assay

Transfected cells were washed once in PBS, lysed in 200 µl reporter lysis buffer (Promega) and separated from intact cells upon low spin centrifugation. Luciferase activity was tested by diluting 5 µl lysates into 50 µl luciferase reagent (Promega). The samples were immediately transferred into a luminometer (EG&G Berthold) and measured for two seconds. Each measurement was repeated at least twice and the results were averaged. Total protein concentration was determined in order to calculate relative luciferase activity.

3.2.4 Biochemical methods

3.2.4.1 Determination of protein concentration

Total protein concentration of cell lysates was determined spectrophotometrically at OD₅₉₅ using Bradford reagent (Pierce) (Bradford, 1976) and compared to a BSA standard dilution series. The concentration of the samples was then normalized.

3.2.4.2 SDS polyacrylamide gel electrophoresis (SDS-PAGE)

Proteins were analyzed by SDS-PAGE using a discontinuous buffer system under denaturing and reducing conditions (Laemmli, 1970). 4x concentrated SDS loading buffer was added to protein samples prior to denaturation at 95 °C for 5 min and gel loading. Gels (0.75 or 1 mm width) had varying polyacrylamide concentrations (7.5 – 15 %) depending on the required resolution. Electrophoresis was performed in BioRad Mini-Protean II employing a constant voltage of 200 V in SDS running buffer.

Stacking Gel	5.1 % acrylamide/bisacrylamide (37.5:1), 125 mM Tris HCl, pH 6.8, 0.1 % SDS, 0.1 % TEMED, 0.1 % APS
Separating Gel	7.5 - 15 % acrylamide/bisacrylamide (37.5:1), 750 mM Tris HCl, pH 8.8, 0.1 % SDS, 0.075 % TEMED, 0.05 % APS
4x SDS loading buffer	62.5 mM Tris-HCl, pH 6.8, 20 % glycerol, 2 % SDS, 0,005 % bromphenol blue, 750 mM 2-mercaptoethanol
SDS running buffer	50 mM Tris-Base (pH8.3), 380 mM glycine, 0.1 % SDS

3.2.4.3 Western Blotting

Proteins, separated by SDS-PAGE, were transferred onto nitrocellulose membranes (Protran, Schleicher&Schuell) in a semi-dry blotting unit (SemiPhore). The electrophoretic protein transfers were achieved in Western blot buffer at a constant current of approximately 0.5 – 0.8 mA/cm² gel size for 1 h (Towbin *et al.*, 1979). Transfer efficiency was verified by brief incubation of nitrocellulose membranes into PonceauS solution. Membranes were blocked in PBS-T supplemented either with 3 % BSA or with 4 % skim milk powder for 1 h at RT or at over night at 4 °C. Subsequently membranes were incubated with the primary antibody diluted 1:200-1:10000 in PBS-T supplemented with either 0.3 % BSA or 0.4 % skim milk powder for 1 h at RT. After extensively washing in PBST, membranes were incubated with a 1:1000-1:10000 dilution of secondary antibody conjugated to horseradish peroxidase as above described. Finally, membranes were washed as before. Protein bands were detected

by incubating membranes with ECL solutions A and B at 1:1 ratio and exposing to either X-ray films (Amersham) or luminescent image analyzer LAS3000 (Fujifilm).

Western blot buffer	50 mM Tris (pH 8.4), 192 mM glycine, 20 % methanol
PonceauS solution	2.5 % PonceauS, 40 % methanol, 5 % acetic acid
PBS-T	PBS, 0.05 % TWEEN-20
ECL-A	1 ml 250 mM 3-aminophthalhydrazid (Luminol), 444 μ l 90 mM p-coumarin acid, 10 ml 1 M Tris-HCl, pH 8.5, ddH ₂ O to 100 ml final volume.
ECL-B	61.4 μ l 30 % ddH ₂ O, 10 ml 1 M Tris-HCl, pH 8.5, ddH ₂ O to 100 ml final volume.

3.2.4.4 Dot blot assay

Dot blot assay was also used to detect proteins but in contrast to Western blot, protein samples were neither denatured nor separated electrophoretically. Typically, 5 μ l protein samples (total cell extracts or gel filtration fractions) were spotted directly onto nitrocellulose membrane. The membrane was then air-dried and processed as described above.

3.2.4.5 *In vitro* HttExon1-Aggregation

Purified GST-Htt20Q and GST-Htt53Q (Muchowski *et al.*, 2000) were obtained from the laboratory stock of the Department of Cellular Biochemistry, Max-Planck Institute of Biochemistry, Martinsried, Germany. Aggregation of GST-Htt proteins (3 μ M) was initiated by addition of 2.5 U PreScission protease (Amersham) in aggregation buffer at 30°C for 5 h. For recruitment analysis, 45 μ l of gel filtration fraction were added.

Aggregation buffer	50 mM Tris-HCl, pH 7.5, 150 mM KCl, 1 mM DTT, 0.1 mg/ml Ovalbumin, 1x protease inhibitor mix
--------------------	--

3.2.4.6 Filter retardation assay

To detect SDS-insoluble aggregates, cell extracts or *in vitro* aggregation reactions were mixed with an equal volume of 4% SDS and 100 mM DTT and heated (95°C, 5 min), followed by filtration through a cellulose acetate membrane (0.2 μ m pore size) and immunodetection (Scherzinger *et al.*, 1997; Muchowski *et al.*, 2000).

3.2.4.7 *Size exclusion chromatography*

Total cell extracts were centrifuged at either 20.000 x g or 100.000 x g for 30 min or 1 h and subjected to size exclusion chromatography on FPLC or SMART system with Superdex200 or Superose6 column at 4 °C or 15 °C, respectively. The appropriate lysis buffer was used as running buffer. Fractions were analyzed by immunoblotting and quantification software AIDA. The chromatographic resolution was between 2000 and 17 kDa determined by protein standards.

3.2.4.8 *Immunoprecipitation*

Cell lysates were blocked with 50 µl protein A sepharose and BSA at a final concentration of 1 % for 1 h at 4 °C in order to prevent unspecific binding. After removal of protein A sepharose by centrifugation at 2000 x g, cell lysates were transferred to mini-columns and incubated with 1 – 2 µg primary antibodies over night at 4 °C with agitation. Subsequently 50 µl protein A sepharose were added to the antigen-antibody complex and incubated for 1 – 2 h at 4 °C. Protein A sepharose was washed extensively with cell lysis buffer TG&P. Finally, the bound antibody and antigen complex was incubated in SDS loading buffer at 95 °C for 5 min and eluted by centrifugation.

3.2.4.9 *Ni-NTA pull down of His-tagged proteins*

Cell lysates were incubated with Ni-NTA resin pre-equilibrated in lysis buffer TP (Qiagen; 50 µl of 1:1 slurry) in micro spin columns (*MoBiTec*, Germany) over night at 4 °C. Beads were washed three times with lysis buffer TP. Bound proteins were eluted from the resin with lysis buffer TP (supplemented with 400 mM Imidazole pH 7.5). Samples were removed during washing for analysis. Equal amount of eluate and control samples were mixed with 4x SDS loading buffer and incubated at 95 °C for 5 min.

3.2.4.10 *Trichloroacetic acid (TCA)-precipitation*

TCA precipitation was performed to concentrate protein samples prior to SDS-PAGE analysis. Protein samples were mixed at 1:1 ratio with a 20 % TCA solution and incubated for 30 min on ice. After centrifugation at 20.000 x g for 20 min at 4 °C, pellets were washed with 500 µl of acetone (-20 °C) and pelleted again. Proteins were then resuspended in SDS loading buffer.

4 Results

Huntington's disease (HD) is caused by the expansion of a polyglutamine (polyQ) repeat in the N-terminal exon 1 segment of huntingtin (Htt). The pathogenic length of the polyQ stretch is typically greater than ~37 Q. Cytotoxicity presumably results from interference of polyQ-expanded Htt with various cell functions, including transcriptional regulation and protein quality control and is associated with aberrant folding of mutant Htt, leading to its deposition in the form of insoluble, fibrillar aggregates (inclusions). Aggregation-competent N-terminal fragments of a size similar to Htt exon 1 are produced by proteolysis and are thought to be critical in cellular toxicity.

This study investigated the interactions of polyQ-expanded Htt exon 1 with the transcription factors TBP and CBP and their contributions to polyQ protein toxicity. Small oligomers formed by polyQ expanded Htt rather than aggregates have been related to cellular toxicity. Furthermore, for the first time, the chaperonin TRiC was demonstrated not only to inhibit polyQ protein aggregation, but also to conformationally modulate soluble polyQ-expanded Htt oligomers, thereby reducing their toxicity.

4.1 PolyQ toxicity mediated by transcription factor deactivation

Mainly two nonexclusive ideas have been put forward to explain how polyQ expansion proteins may cause cellular dysfunction (Sakahira *et al.*, 2002). In one model, expanded polyQ proteins may engage the quality control machinery in a non-productive manner, thereby reducing the chaperone capacity and/or interfering with the function of the ubiquitin-proteasome system (Bence *et al.*, 2001; Berke and Paulson, 2003). In the second model, neurotoxicity originates from the ability of the polyQ proteins to induce the coaggregation of other proteins essential for cell viability, among them several transcription components, which possess non-pathogenic polyQ repeats. These factors include the TATA box binding protein (TBP), a central component of the general transcription initiation complex, and the transcriptional coactivator CREB binding protein (CBP). TBP, CBP, and other transcription factors have been reported to colocalize with the aggregates of disease-related polyQ proteins (Perez *et al.*, 1998; Kazantsev *et al.*, 1999; McCampbell *et al.*, 2000). Hence, the coaggregation of TBP and CBP might result in their sequestration and loss of

function (Chai *et al.*, 2002; Kim *et al.*, 2002). Indeed, transcriptional dysregulation has been implicated in several polyQ diseases (Sugars and Rubinsztein, 2003); however, the underlying mechanism is far from clear. PolyQ-induced transcriptional dysregulation in neurons can manifest itself before cellular aggregates are detectable (Sugars and Rubinsztein, 2003), and the formation of aggregates has even been suggested to be a protective mechanism (Saudou *et al.*, 1998; Cummings *et al.*, 1999). The increased expression of molecular chaperones such as Hsp70 and Hsp40 can suppress the neurotoxicity of polyQ-expanded proteins without preventing the formation of polyQ inclusions (Warrick *et al.*, 1999; Cummings *et al.*, 2001), although the chaperones do modulate the aggregation process (Chan *et al.*, 2000; Krobitch and Lindquist, 2000; Muchowski *et al.*, 2000). These findings seemed to question the general significance of the sequestration model for the disruption of transcriptional pathways in polyQ diseases. Alternatively, aberrant interactions of soluble expanded polyQ proteins with transcription factors may render them non-functional. To clarify the role of aggregates as well as of monomers and small soluble oligomers, this study investigated the interaction of polyQ-expanded Htt exon1 fragments with TBP and CBP and the differential contribution of transcription factor sequestration and deactivation to polyQ protein toxicity.

4.1.1 PolyQ aggregation and sequestration of the transcription factor TBP

Sequestration represents a widely proposed hypothesis describing how select cellular factors might be depleted away from their usual localization, thereby compromising their function and leading to toxicity (Ross, 2002). Accordingly, recruitment of TBP, which carried a non-pathogenic polyQ stretch of 38 glutamines, into Htt aggregates was analyzed in mouse neuronal and yeast cells. Htt fusion to GST was demonstrated to allow purification of mutant Htt from *E. coli* in soluble form (Scherzinger *et al.*, 1997; Muchowski *et al.*, 2000; Schaffar *et al.*, 2004). Aggregation and recruitment properties of Htt and GST-Htt fusion were compared to dissect the requirements for sequestration of transcription factors *in vivo*.

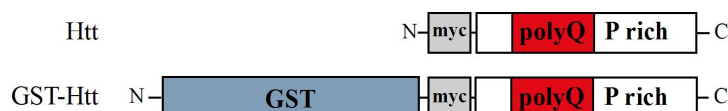


Figure 14: Schematic overview of Htt exon 1 constructs.

myc tag (myc), polyQ stretch of 20, 53 or 96 Q, proline rich domain (P rich), Glutathione S-transferase (GST).

4.1.1.1 Aggregation of mutant Htt and TBP

myc-tagged Htt exon 1 fragments with 20, 53 and 96Q (Htt20Q, Htt53Q and Htt96Q) as well as N-terminal GST fusion to these constructs (GST-Htt20Q, GST-Htt53Q and GST-Htt96Q) were cloned under control of the CMV promoter into mammalian expression vectors and transiently expressed in mouse neuroblastoma cells (N2a) (Figure 14). These cells have been used previously to study polyQ expansion proteins (Jana *et al.*, 2000; Schaffar *et al.*, 2004; Haacke *et al.*, 2006). Transfection efficiency was on average ~30 %. Expression of constructs was analyzed in lysates 48 h after transfection by SDS-PAGE and Western blot. Htt constructs and GST-Htt fusions were produced to roughly similar levels (Figure 15A). Noteworthy, Htt polypeptides exhibited a mobility in SDS-PAGE that was proportional to predicted molecular mass but demonstrated a systematic relative decrease in electrophoretic mobility consistent with previous reports (Preisinger *et al.*, 1999). Remarkably, this effect was less pronounced when Htt was fused to GST.

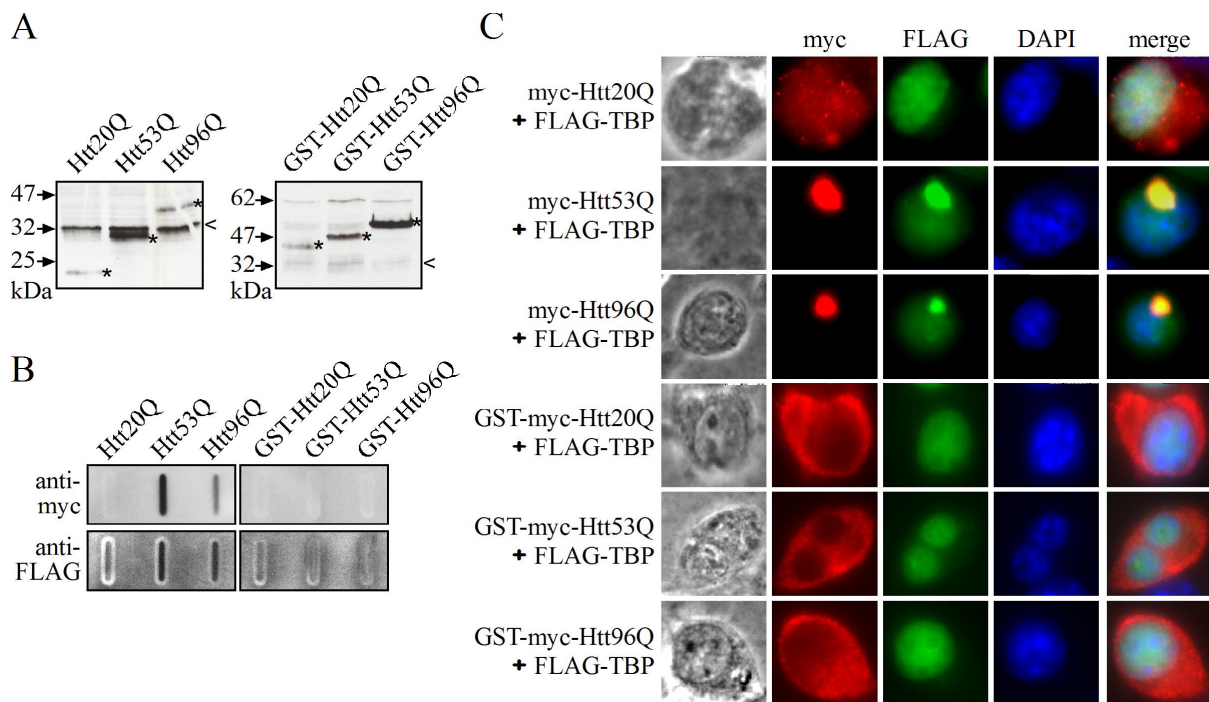


Figure 15: Recruitment of human TBP into Htt aggregates in N2a cells.

(A) myc-tagged Htt20Q, Htt53Q and Htt96Q with or without N-terminal GST fusion were transiently expressed in N2a cells for 48 h. Lysates were analyzed by Western blot and Htt constructs were detected with anti-myc antibody. * indicates specific protein band and < endogenous c-myc protein. (B) Constructs used in (A) were transiently coexpressed with FLAG-tagged human TBP as described above. SDS-resistant aggregates in lysates were detected by filter assay and immunostaining for Htt constructs with anti-myc and for recruited human TBP with anti-FLAG antibody. (C) Cells derived from (B) were fixed and immunolabeled with anti-myc or anti-FLAG antibody coupled either to Cy3- or FITC-conjugated secondary antibodies, respectively. Nuclei were counterstained with DAPI.

For TBP recruitment analysis, Htt constructs were transiently coexpressed with FLAG-tagged human TBP cloned under control of EF-1 α promoter. In this experimental setup, co-transfection efficiency was on average ~10 %. Htt53Q and Htt96Q but not Htt20Q formed SDS-resistant aggregates detectable in N2a cell extracts by the filter assay (Figure 15B). Unexpectedly, aggregation of Htt53Q was markedly increased compared to Htt96Q, presumably due to instability of Htt96Q in N2a cells. Whereas coexpression of Htt20Q and TBP did not lead to co-aggregation, substantial amount of TBP were recovered in SDS-resistant aggregates formed by Htt53Q and Htt96Q (Figure 15B). Furthermore, recruitment of TBP has been demonstrated to depend on the ongoing production of mutant Htt and on the presence of its polyQ segment (Schaffar *et al.*, 2004), consistent with a polyQ-mediated recruitment process.

Intriguingly, Htt exon 1 fragments fused to GST formed neither SDS-resistant aggregates nor induced co-aggregation of TBP (Figure 15B). Immunofluorescence analysis confirmed these findings. Htt53Q and Htt96Q formed large cytoplasmic inclusions, whereas normal Htt with 20 Q was diffusely distributed in the cytoplasm. TBP was located in the nucleus upon transient coexpression with Htt20Q, while substantial amounts of TBP were dislocated to the cytoplasm and colocalized with the Htt53Q and Htt96Q aggregates. Consistently, GST-Htt fusions were diffusely distributed in the cytoplasm and coexpressed TBP located to the nucleus (Figure 15C). Thus, aggregation of mutant Htt is inhibited in the sequence context of the GST fusion. Furthermore, recruitment of transcription factor appears to require mutant Htt in an aggregation-prone conformation, which is perturbed by the attachment of the GST part.

4.1.1.2 Requirements for Htt aggregation and TBP recruitment

Besides neuronal cells, the baker's yeast *Saccharomyces cerevisiae* was used as model systems in this work to study polyQ protein interaction, aggregation and toxicity as described previously in several other studies (Krobitsch and Lindquist, 2000; Muchowski *et al.*, 2000; Meriin *et al.*, 2002). Several independent studies demonstrate that at a basic level, the yeast model faithfully recapitulates the molecular basis of polyQ length-dependent aggregation and toxicity (Colby *et al.*, 2004; Cashikar *et al.*, 2005; Vacher *et al.*, 2005; Zhang *et al.*, 2005). The yeast system offers the unique opportunity to dissect modulators of polyQ aggregation and toxicity in a defined and uniform cellular environment. In fact, an advantage of yeast cells

is that they are not confounded by the perplexing variations in cellular proteome that characterize distinct cell types in whole organisms or in cultured mammalian cells. In addition, numerous genetic tools available in yeast make it a powerful instrument to explore the intra- and intermolecular factors that govern polyQ aggregation and toxicity.

To confirm the recruitment of human TBP into Htt aggregates in the yeast system, myc-tagged Htt and GST-Htt fusion constructs as well as HA-tagged human TBP were cloned into yeast expression vectors under control of copper- and galactose-inducible promoters, respectively, and coexpressed in the wild-type strain YPH499 (Sikorski and Hieter, 1989).

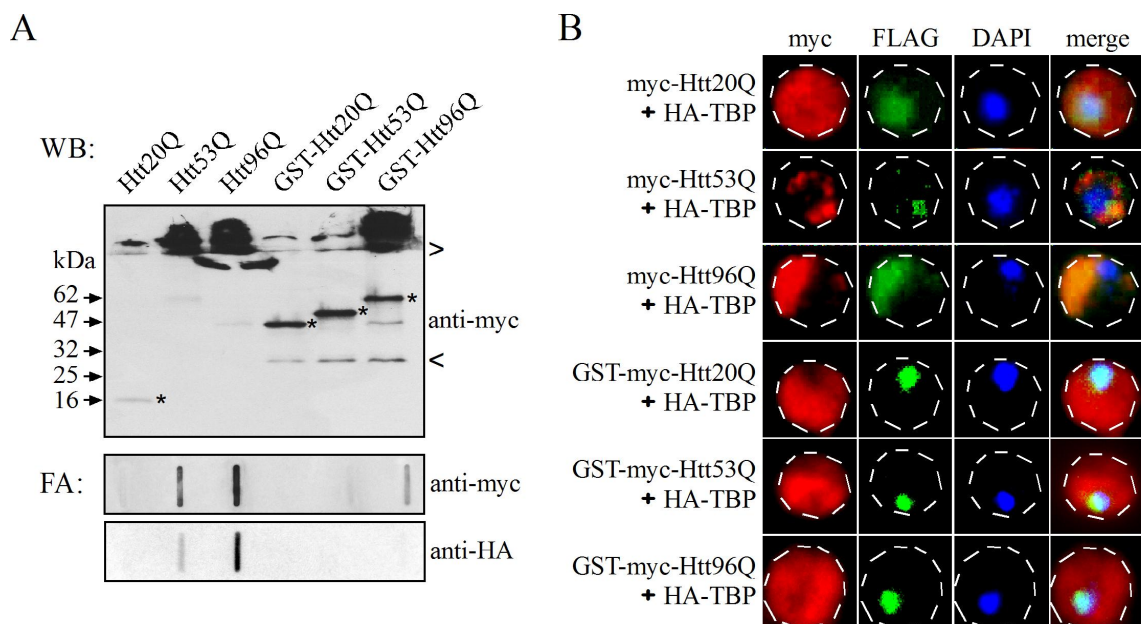


Figure 16: Recruitment of human TBP into Htt aggregates in wild-type yeast cells.

(A) myc-tagged Htt20Q, Htt53Q and Htt96Q with or without N-terminal GST fusion under *CUP1* control were coexpressed with HA-tagged human TBP under control of *GAL1* in wild-type cells for 12 h at 30 °C. Lysates were analyzed by Western blot (WB) and by filter assay (FA). Htt constructs and recruited human TBP were immunodetected with anti-myc and anti-HA antibody, respectively. * indicates specific protein band, < GST cleavage products and > stacking gel. (B) Cells derived from (A) were analyzed by indirect immunofluorescence with anti-myc or anti-HA antibody coupled either to Cy3- or FITC-conjugated secondary antibodies, respectively. Nuclei were counterstained with DAPI.

Small amounts of Htt20Q were detected as a protein band on SDS-PAGE, while Htt53Q and Htt96Q did not migrate into the gel and were only detectable in the stacking gel (Figure 16A). Consistently, GST-Htt20Q and GST-Htt53Q were produced similarly in substantial amounts and almost exclusively in SDS soluble form. To a minor extent, GST-Htt96Q was detected as a protein band but additionally also in the stacking gel (Figure 16A). Htt53Q and Htt96Q displayed polyQ-length dependent formation of SDS-insoluble

aggregates and recruitment of TBP. Htt20Q did neither aggregate nor recruit TBP (Figure 16A). Fusion to GST inhibited aggregation of Htt53Q completely and of Htt96Q to some residual extent. Recruitment of TBP could not be observed for any GST-Htt construct (Figure 16A). These results were confirmed by immunofluorescence analysis: TBP resided in the nucleus when coexpressed with Htt20Q or any of the GST-Htt constructs and redistributed from the nucleus to cytoplasmic Htt aggregates when coexpressed with Htt53Q and Htt96Q (Figure 16B).

Expression of mutant Htt fused to GST was without any effect on the recruitment of TBP (Figure 16A and Figure 16B). These proteins did not form aggregates by themselves, although their polyQ segments were exposed, based on the observation by filter assay that GST-Htt53Q but not GST alone co-aggregated with Htt96Q (Figure 17A). Consistently, GST-Htt53Q coalesced with Htt96Q in aggregates observable by immunofluorescence (Figure 17B). Hence, since mutant Htt when fused to GST is not per se aggregation-incompetent, a conformational rearrangement of Htt occurring upon its release from the GST moiety might be a prerequisite for initiating aggregation and recruitment of TBP. *In vitro* FRET experiments with GST-Htt53Q indicated that a rapid conformational compaction occurs in the Htt fragment upon its proteolytic release from a protective sequence context (Schaffar *et al.*, 2004).

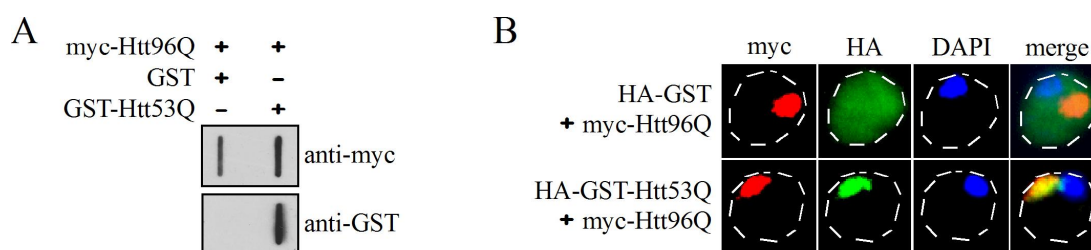


Figure 17: Accessibility of the Q stretch in GST-Htt fusions protein

(A) myc-tagged Htt96Q under control of *CUP1* was coexpressed with HA-tagged GST or GST-Htt53Q under control of *GAL1* in wild-type cells for 12 h at 30 °C. SDS-resistant aggregates in lysates were detected by filter assay and immunostaining for Htt with anti-myc and for recruited GST-Htt with anti-GST antibody. (B) Cells derived from (A) were analyzed by indirect immunofluorescence with anti-myc or anti-HA antibody coupled either to Cy3- or FITC-conjugated secondary antibodies, respectively. Nuclei were counterstained with DAPI.

In order to verify whether liberation of mutant Htt from its GST fusion partner initiates its aggregation and recruitment of TBP, GST-Htt fusions were constructed that harbor an internal, highly specific tobacco etch virus (TEV) protease cleavage site between the GST part and the myc-tagged mutant Htt exon 1 fragment. TEV protease was cloned under a

doxycycline-controllable promoter and coexpressed with GST-TEV-myc-Htt constructs in wild-type yeast. Expression and proteolytic cleavage of GST-TEV-myc-Htt constructs were analyzed by SDS-PAGE and immunoblotting. GST-TEV-myc-Htt53Q and GST-TEV-myc-Htt96Q were produced to similar levels and migrated according to their nominal size in the gel. Only minor amounts of unspecific cleavage products could be detected in the absence of TEV protease (Figure 18A). Upon induction of TEV protease, protein bands corresponding to GST-TEV-myc-Htt constructs diminished and substantial amounts of cleaved GST accumulated. Concurrently, myc-Htt53Q and myc-Htt96Q were almost exclusively detectable in the stacking gel (Figure 18A). GST-TEV-myc-Htt53Q and GST-TEV-myc-Htt96Q did not form SDS-insoluble aggregates detectable by filter assay unless TEV protease was induced (Figure 18B). Thus, analogous to *in vitro* experiments (Scherzinger *et al.*, 1997; Schaffar *et al.*, 2004), aggregation of formerly soluble mutant Htt fused to GST can be initiated *in vivo* in yeast cells by cleavage of the Htt part from the GST moiety. Similarly, aggregation of full-length polyQ expanded Ataxin-3 was demonstrated to be initiated by proteolytical cleavage at an engineered TEV protease cleavage site (Haacke *et al.*, 2006).

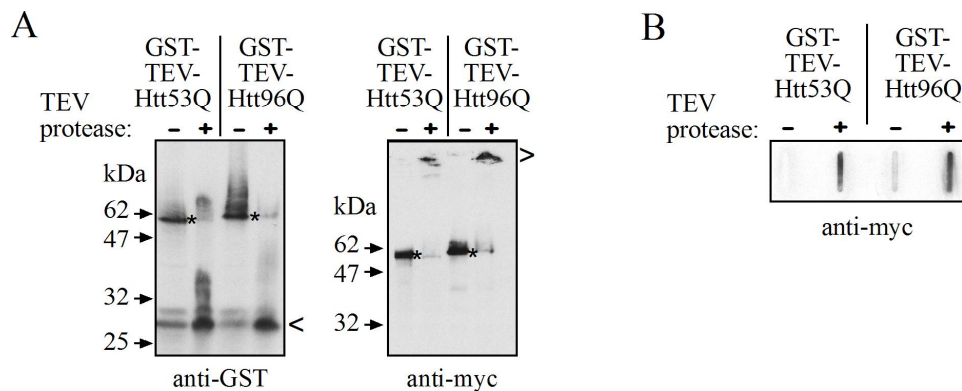


Figure 18: Initiation of Htt aggregation upon cleavage of the GST-Htt fusion protein.

(A) GST-TEV-myc-Htt53Q and GST-TEV-myc-Htt96Q were expressed under control of *CUP1* in wild-type cells for 12 h at 30°C with and without expression of TEV protease from a doxycycline-regulated promoter. Cell lysates were analyzed by Western blot, and cleaved and uncleaved GST-Htt constructs were detected with anti-GST and anti-myc antibodies, respectively. * indicates specific protein band, < GST cleavage products and > stacking gel. (B) SDS-resistant aggregates in lysates from (A) were detected by filter assay and immunostaining for Htt constructs with anti-myc antibody.

To determine whether recruitment of TBP could be initiated similarly, proteolytic cleavage of GST-Htt *in vivo* was analyzed in parallel by filter assay and immunofluorescence. GST-TEV-myc-Htt96Q and HA-tagged human TBP were coexpressed in the absence of TEV protease. Formation of SDS-insoluble aggregates in lysates could be detected neither for

Htt96Q nor for TBP. Remarkably, continuous coexpression of GST-TEV-myc-Htt96Q and TBP in the presence of TEV protease but not in its absence led to substantial aggregation of Htt96Q and TBP (Figure 19A). In the absence of TEV protease, GST-TEV-myc-Htt96Q was diffusely distributed throughout the cytosol and TBP located to the nucleus. Consistently, TBP was dislocated from the nucleus and coalesced with Htt96Q in aggregate in the presence of TEV protease (Figure 19B). Hence, mutant Htt acquires, presumably by a structural rearrangement, the ability to aggregate and consequently to recruit TBP upon its release from the GST moiety.

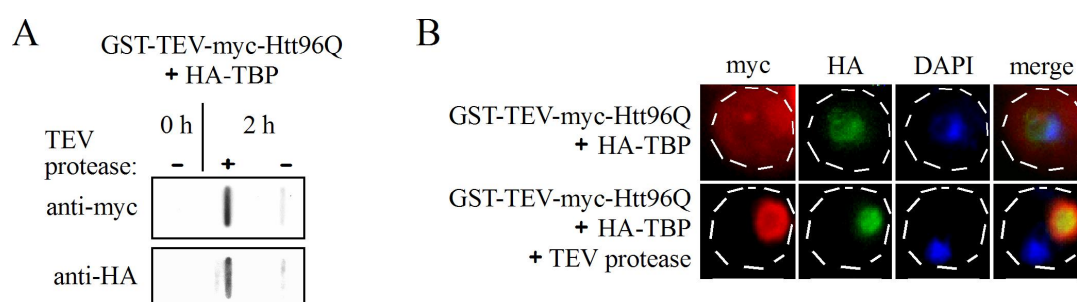


Figure 19: Initiation of TBP recruitment into aggregates upon cleavage of the GST-Htt fusion protein. (A) GST-TEV-myc-Htt96Q and HA-tagged human TBP under control of *CUP1* and *GAL1*, respectively, were coexpressed in wild-type cells for 4 h at 30 °C followed by 2 h with and without induction of TEV protease. SDS-resistant aggregates in lysates from samples taken after 0 and 2 h induction of TEV protease were detected by filter assay and immunostaining for Htt96Q with anti-myc and recruited TBP with anti-HA antibody. (B) Cells derived from (A) were analyzed by indirect immunofluorescence with anti-myc or anti-HA antibody coupled either to Cy3- or FITC-conjugated secondary antibodies, respectively. Nuclei were counterstained with DAPI.

4.1.2 Impairment of transcription factors by soluble, misfolded polyQ proteins

Alternatively but mutually non-exclusive to the sequestration hypothesis, polyQ toxicity may arise by aberrant non-productive interactions of soluble polyQ protein with select cellular factors, including transcription factors, thereby leading to their inactivation. To examine the relevance of soluble mutant Htt for cellular toxicity, a yeast model was designed in which toxicity arising from polyQ-mediated TBP deactivation can be detected without interference from other possible mechanisms of polyQ toxicity. Wild-type yeast cells tolerate the expression of mutant Htt exon 1 fragment (Htt96Q) without overt toxicity under standard growth conditions (Krobitsch and Lindquist, 2000; Muchowski *et al.*, 2000). Human and yeast TBP share 80 % homology in their C-terminal DNA binding (basic) domains, but differ substantially in their N-terminal domain that is almost absent in yeast TBP including the polyQ stretch (Hahn *et al.*, 1989; Peterson *et al.*, 1990) (Figure 20). Yeast TBP is essential for

growth but can be functionally replaced by human TBP, carrying the mutation R231K, at temperatures up to 35 °C (Cormack *et al.*, 1994). Taking advantage of the fact that yeast TBP lacks the polyQ stretch, yeast strain *yTBPΔ/hTBP* was constructed, in which yeast TBP was deleted and human TBP (R231K) was expressed complementarily under the control of the endogenous yeast TBP promoter. A toxic effect of mutant Htt on human TBP function should result in reduced growth of the host cells.

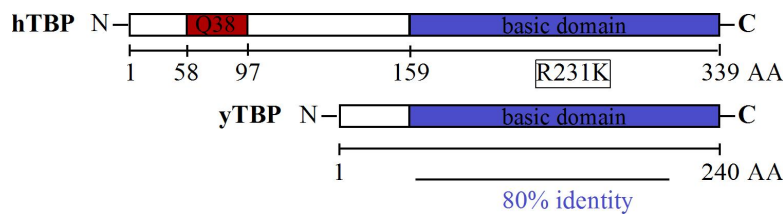


Figure 20: Comparison of human and yeast TBP.

yTBPΔ/hTBP cells grew indistinguishably from wild-type cells up to 34 °C, but showed temperature sensitivity upon incubation at 37 °C (Figure 21A). DNA analysis of wild-type and *yTBPΔ/hTBP* cells by PCR using primers against yTBP and hTBP revealed the absence of yTBP and the presence of hTBP in *yTBPΔ/hTBP* cells and vice versa in wild-type cells (Figure 21B). Expression of hTBP was investigated by SDS-PAGE and immunoblotting of lysates derived from wild-type and *yTBPΔ/hTBP* cells. hTBP was produced to substantial amounts in *yTBPΔ/hTBP* and was absent in wild-type cells (Figure 21C). Hence, hTBP functionally replaced yTBP in *yTBPΔ/hTBP* cells.

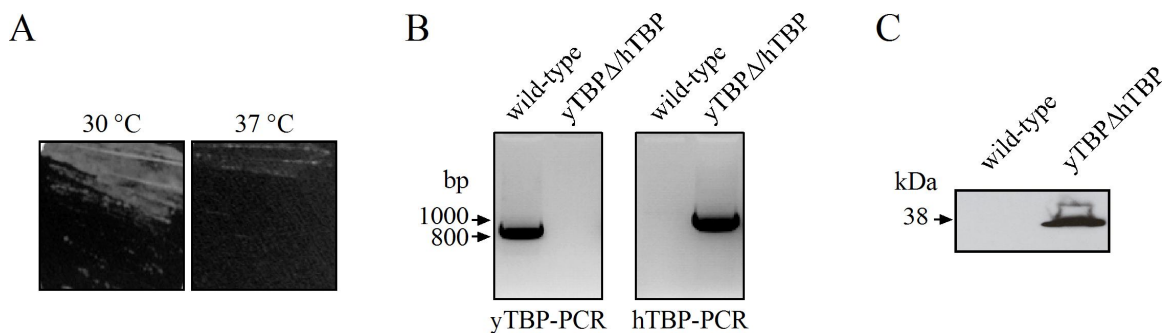


Figure 21: Initial characterization of *yTBPΔ/hTBP* yeast strain.

(A) Wild-type and *yTBPΔ/hTBP* cells were grown for 24 h at 30 °C. Growth was examined on SC-plates after 2 d at 37 °C. (B) PCR analysis of DNA derived from (A). (C) Lysates derived from (A) were analyzed by Western blot, and hTBP was detected by anti-hTBP antibody, which recognizes the N-terminus of hTBP.

4.1.2.1 Growth impairment upon expression of nuclear targeted polyQ-expanded Htt

To investigate the effect of a polyQ expanded protein in *yTBPΔ/hTBP* cells, myc-tagged Htt exon 1 fragments with 20, 53 and 96 Q (Htt20Q, Htt53Q and Htt96Q) and their corresponding GST fusions (GST-Htt20Q, GST-Htt53Q and GST-Htt96Q) were cloned with and without nuclear localization sequence (NLS) under copper-inducible promoters into yeast expression vectors. The expression and aggregation of the proteins in *yTBPΔ/hTBP* cells was analyzed by SDS-PAGE followed by immunoblotting and filter assay after 24 h induction at 30 °C. While Htt20Q and NLS-Htt20Q showed protein bands according to their size and did not form SDS-insoluble aggregates, Htt53Q and Htt96Q were only detectable in the stacking gel. Surprisingly, considerable amounts of NLS-Htt53Q and NLS-Htt96Q migrated into the gel and were detectable in the stacking gel only to a minor extent (Figure 22A).

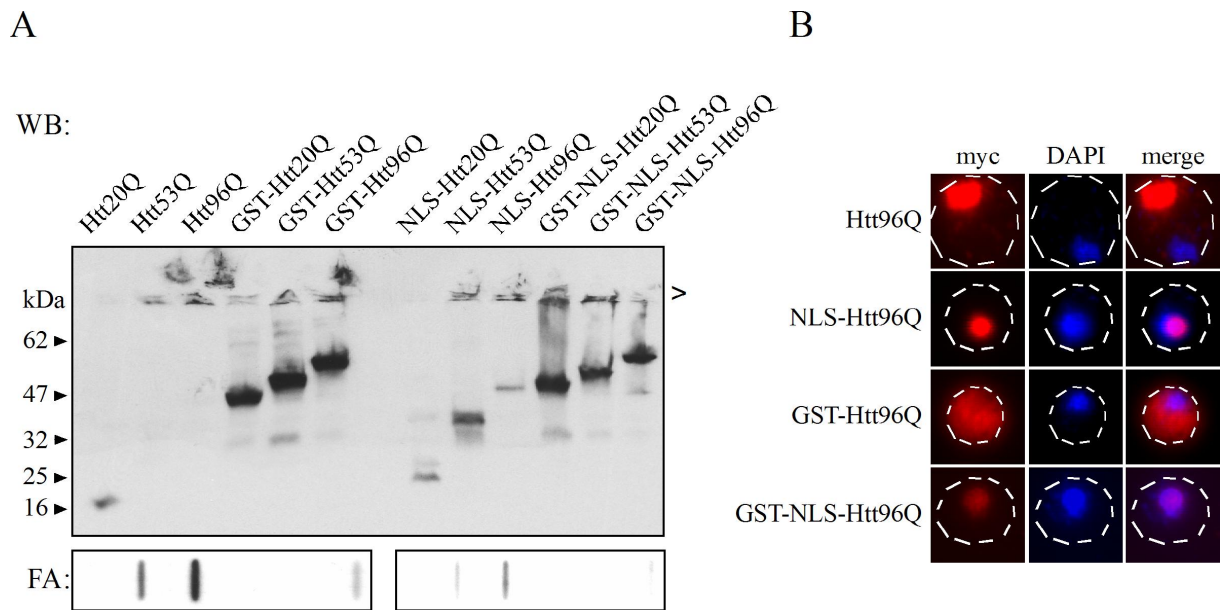


Figure 22: Expression, aggregation and localization of Htt constructs in *yTBPΔ/hTBP* cells.

(A) myc-tagged Htt20Q, Htt53Q and Htt96Q with or without NLS and/or N-terminal GST fusion were expressed under control of *CUPI* in *yTBPΔ/hTBP* cells for 24 h at 30 °C. Htt constructs in lysates were analyzed by Western blot (WB) and filter assay (FA) and immunodetected with anti-myc antibody. > indicates stacking gel. (B) Cells from (A) were analyzed by indirect immunofluorescence. Htt constructs were immunolabeled with anti-myc antibody coupled to Cy3-conjugated secondary antibodies, and nuclei were counterstained with DAPI.

Htt53Q and Htt96Q as well as NLS-Htt53Q and NLS-Htt96Q showed a polyQ-length dependent aggregation, but in contrast to their cytosolic counterparts, aggregation of NLS-Htt53Q and NLS-Htt96Q was significantly reduced, consistent with their increased SDS-solubility detected by Western blot (Figure 22A). Importantly, the presence of the NLS did

not influence Htt aggregation *in vitro* (data not shown). All GST Htt fusions were produced in substantial amounts and migrated to their corresponding size in the gel. Similar to their expression in wild-type cells, fusion to GST prevented aggregation of Htt53Q completely and of Htt96Q to some residual extent. Remarkably, GST fusion to nuclear Htt constructs inhibited their aggregation entirely (Figure 22A). Localization of cytosolic and nuclear Htt exon 1 constructs was verified by indirect immunofluorescence. While Htt96Q formed a large bright aggregate in the cytosol and aggregates of NLS-Htt96Q located to the nucleus, GST-Htt96Q was diffusely distributed throughout the cytosol and GST-NLS-Htt96Q was found to be nuclear (Figure 22B). The remaining Htt constructs were found to localize to the cytosol or nucleus according to the presence or absence of NLS, respectively (data not shown). Thus, Htt fusion to GST and the nuclear environment seem to have an inhibitory effect on Htt aggregation.

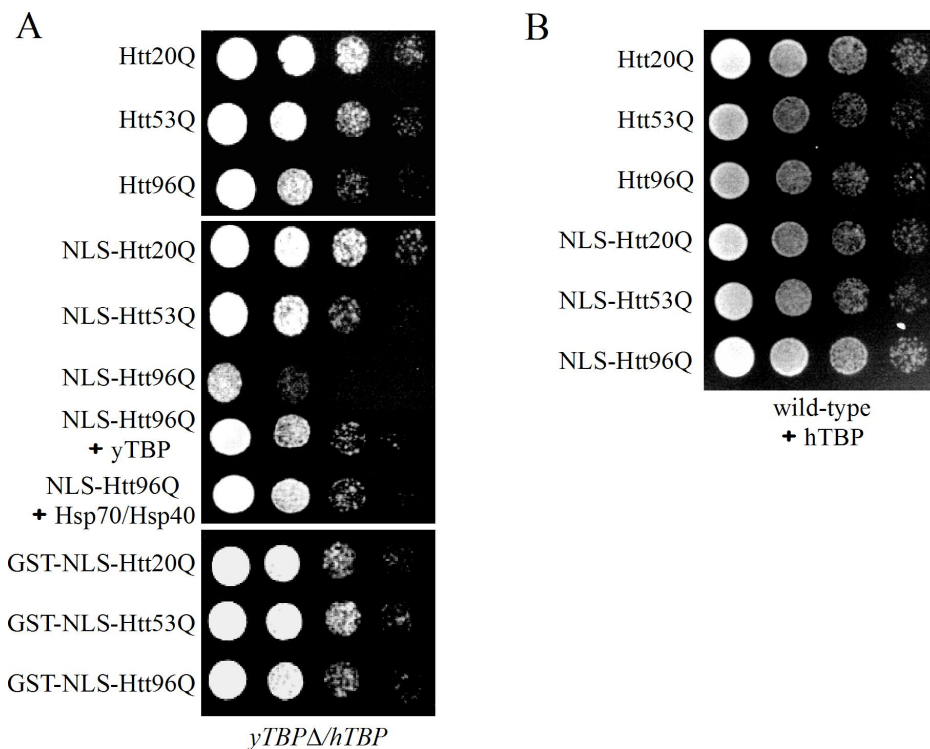


Figure 23: Growth defect in *yTBPΔ/hTBP* upon Htt expression targeted to the nucleus.

(A) myc-tagged Htt, NLS-Htt and GST-NLS-Htt constructs were expressed under control of *CUPI* in *yTBPΔ/hTBP* cells for 24 h at 30 °C. Growth was examined by serial dilutions of cells on SC-plates after 2 d at 34 °C. Growth defect was suppressed upon simultaneous expression of yTBP or human Hsp70/Hsp40 under control of galactose-regulated promoter. (B) myc-tagged Htt and NLS-Htt constructs under control of *CUPI* were coexpressed with hTBP under control of *GALI* in wild-type cells for 24 h at 30 °C. Growth was examined as in (A).

Expression of Htt53Q and Htt96Q resulted only in a mild growth defect of *yTBPΔ/hTBP* cells, although the mutant Htt proteins formed large cytoplasmic aggregates (Figure 23A). However, expression of NLS-Htt53Q and NLS-Htt96Q resulted in a pronounced, polyQ length-dependent growth impairment (Figure 23A). This effect can be attributed to a (partial) polyQ-mediated deactivation of human TBP, because it was suppressed by coexpression of yeast TBP (Figure 23A). Rescue of the growth defect was also achieved by coexpression of human Hsp70 and Hsp40 (Hdj1) (Figure 23A). Intriguingly, no growth defect was observed in wild-type yeast expressing the NLS-Htt constructs, whether or not these cells also expressed human TBP (Figure 23B and data not shown). The expression of mutant Htt fused to GST in the nucleus or cytosol was without any effect on the growth of *yTBPΔ/hTBP* cells (Figure 23A and data not shown). Thus, toxicity of mutant Htt in this yeast model appears to depend on interference with the function of TBP and to require a conformational re-arrangement of Htt occurring upon its release from the GST moiety, as shown to be a prerequisite for the recruitment of TBP.

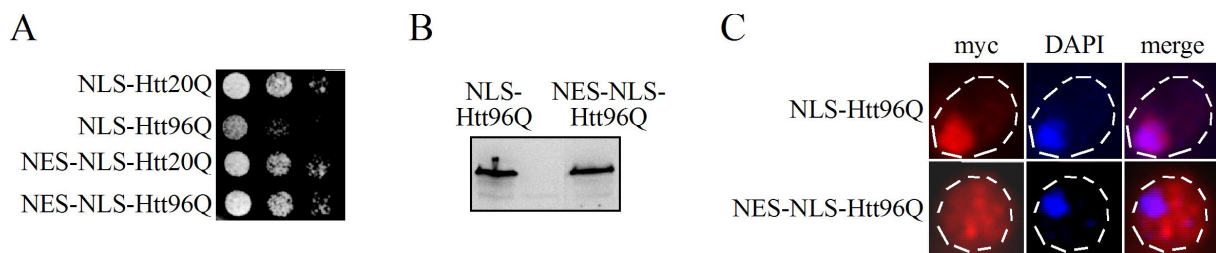


Figure 24: Nuclear location is prerequisite for transcription factor mediated polyQ toxicity.

(A) myc-tagged NLS-Htt20Q, NLS-Htt96Q with or without NES were expressed under control of *CUP1* in *yTBPΔ/hTBP* cells for 24 h at 30 °C. Growth was examined by serial dilutions of cells on SC-plates after 2 d at 34 °C. (B) Htt constructs in lysates from (A) were analyzed by Western blot with anti-myc antibody. (C) Cells from (A) were analyzed by indirect immunofluorescence. Htt constructs were immunolabeled with anti-myc antibody coupled to Cy3-conjugated secondary antibodies, and nuclei were counterstained with DAPI.

To further demonstrate that the nuclear localization of mutant Htt is a prerequisite for toxicity, the nuclear export sequence (NES) of protein kinase inhibitor α (PKI- α) was fused N-terminal to NLS-Htt constructs. The polyQ-length dependent growth defect was suppressed by targeting mutant Htt to the cytoplasm (Figure 24A). Importantly, the fusion of NES to NLS-Htt96Q did not alter its expression level or aggregation propensity (Figure 24B and data not shown) and, indeed, led to redistribution of the fusion protein to the cytosol (Figure 24C). Thus, the presence of mutant Htt in the nucleus seems to be necessary for toxicity in this yeast system.

4.1.2.2 Correlation between soluble, oligomeric polyQ-expanded Htt and cellular toxicity

Growth of *yTBPΔ/hTBP* yeast in liquid medium was monitored to determine when the reduction in growth rate sets in relative to the appearance of Htt aggregates. Remarkably, expression of NLS-Htt96Q for one hour resulted already in a marked growth defect (Figure 25A). In contrast, no substantial impairment was observed upon expression of Htt96Q or GST-Htt96Q in the cytosol and GST-NLS-Htt96Q in the nucleus, as compared to cells expressing Htt20Q (Figure 25A). Interestingly, while the cytoplasmic Htt96Q aggregated rapidly, the nuclear NLS-Htt96Q formed insoluble aggregates more slowly after a delay of several hours. Their GST fusions did not form any aggregates within this time (Figure 25B).

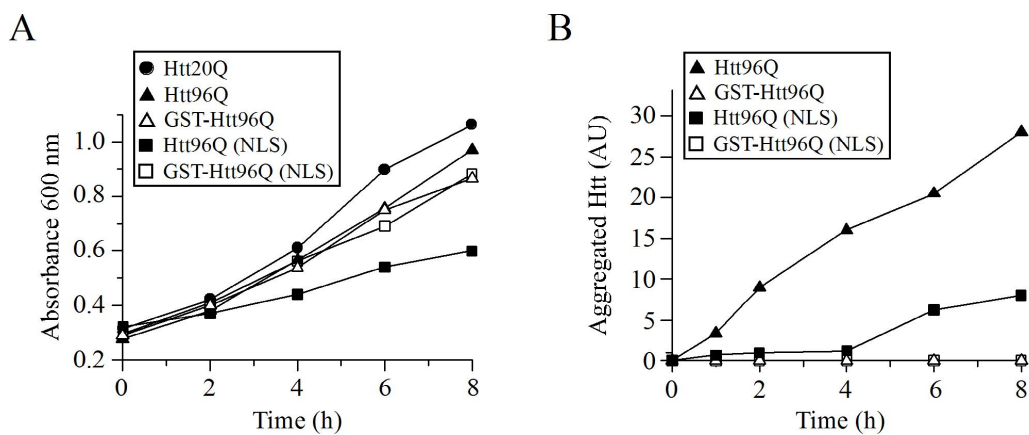


Figure 25: Lack of correlation between the presence of insoluble aggregates and toxicity.

(A) *yTBPΔ/hTBP* cells were grown in liquid medium over night and adjusted to an OD of ~0.3 before expression of indicated Htt constructs was induced. Growth at 30 °C in medium containing 50 mM 3-AT was followed over 8 h. (B) Accumulation of SDS-insoluble aggregates was determined in cells analyzed in (A) by filter assay and immunodetection with anti-myc antibody. Amounts of aggregates are expressed in arbitrary units (AU).

Strikingly, lysates of yeast cells expressing NLS-Htt96Q for up to 4 hours contained Htt protein that was exclusively soluble upon centrifugation at 100,000 x g (Figure 26A). In contrast, soluble Htt protein was absent in cells expressing Htt96Q in the cytoplasm but was detected in cells expressing GST-Htt96Q (Figure 26A). Thus, the soluble mutant Htt in the nucleus must be responsible for the early growth defect observed in *yTBPΔ/hTBP* cells. This soluble NLS-Htt96Q fractionated upon size exclusion chromatography between 70 and 170 kDa (Figure 26B). Taking into account that the Htt constructs tend to fractionate greater than their nominal mass, this protein would represent monomers and/or small oligomers of Htt (dimers and trimers), although it is also possible that the NLS-Htt is associated with other cellular factors.

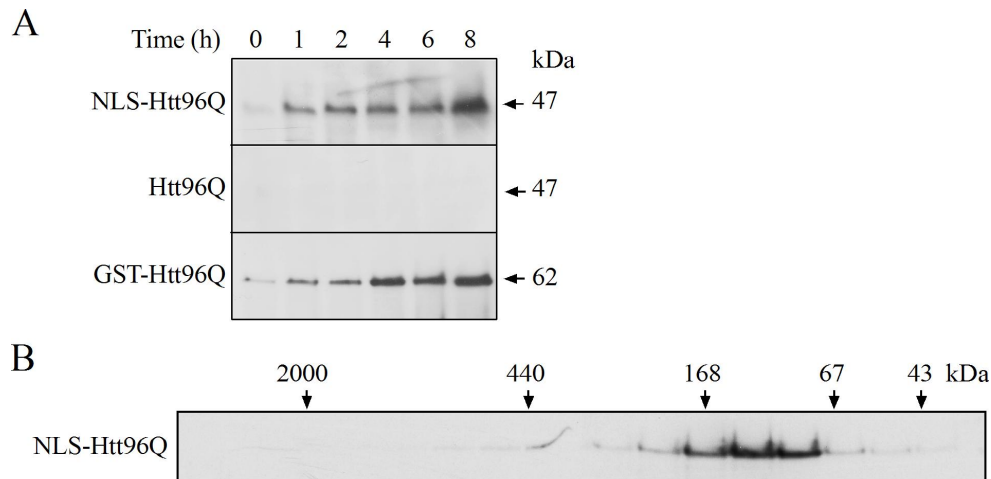


Figure 26: NLS-Htt96Q forms toxic soluble oligomers of ~70 – 170 kDa size.

(A) Solubility of myc-tagged NLS-Htt96Q, Htt96Q and GST-Htt96Q (100,000 x g, 30 min) in extracts of *yTBPΔ/hTBP* cells after different times of induction, as detected by Western blot with anti-myc antibody. (B) Size exclusion chromatography of soluble fractions from *yTBPΔ/hTBP* cells expressing NLS-Htt96Q for 1 h. The distribution of Htt constructs in the fractions was analyzed by Western blot with anti-myc antibody. The position of molecular weight markers is indicated.

To dissect the mechanism by which the soluble nuclear mutant Htt exon 1 fragment impairs growth in *yTBPΔ/hTBP* cells, its effect on TBP was analyzed. The solubility of TBP did not change significantly over time regardless of which Htt construct was expressed (Figure 27A). Intriguingly, expression of NLS-Htt96Q affected the size fractionation properties of TBP. In cells expressing Htt96Q in the cytoplasm or in the absence of any Htt, TBP was present in a well-defined complex of ~200 kDa (Figure 27B and data not shown). However, upon expression of NLS-Htt96Q for one hour, a substantial amount of TBP was recovered in high molecular weight fractions between 200 and 800 kDa. This effect was not observed upon expression of GST-fused NLS-Htt96Q (Figure 27C). Thus, an interaction with the toxic soluble form of nuclear Htt changes the conformational properties of TBP (or TBP containing transcription complexes), presumably resulting in the formation of aggregates. This interaction between TBP and soluble mutant Htt must be transient since it did not result in the formation of TBP/Htt co-aggregates (data not shown), which were however observed when both Htt and TBP were expressed to high levels in wild-type yeast cells (Figure 16).

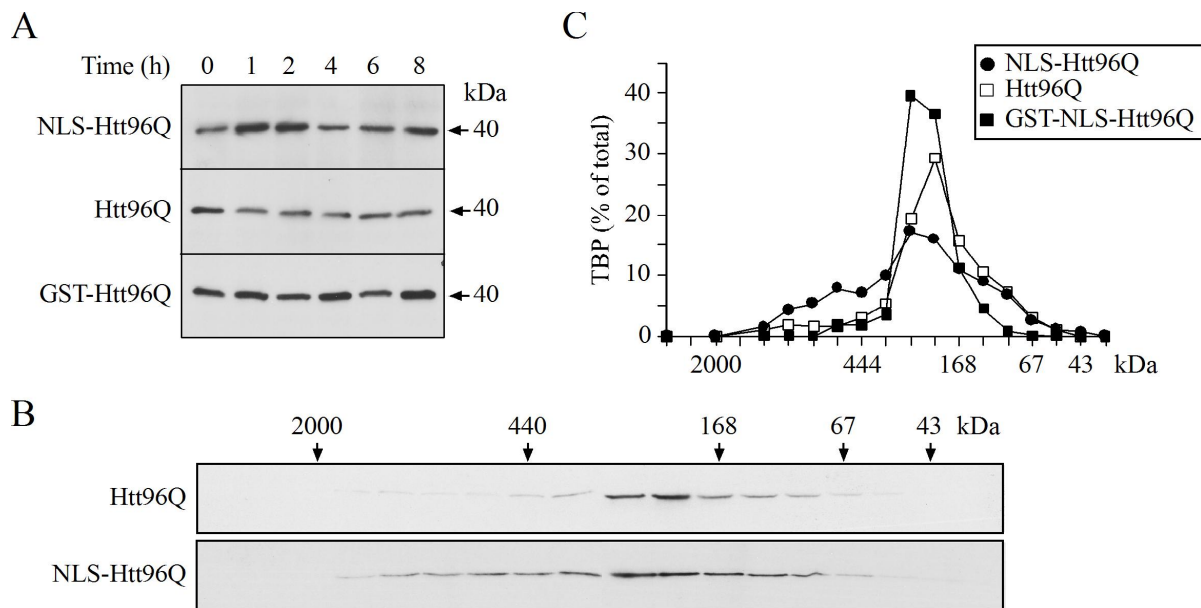


Figure 27: Soluble NLS-Htt96Q oligomers affect size fractionation properties of TBP.

(A) Solubility of hTBP (100,000 x g) in extracts of $yTBP\Delta/hTBP$ cells expressing myc-tagged NLS-Htt96Q, Htt96Q or GST-Htt96Q after different times of induction, as detected by Western blot with anti-TBP antibody. (B) Soluble fractions of $yTBP\Delta/hTBP$ cells expressing NLS-Htt96Q and Htt96Q for 1 h were subjected to size exclusion chromatography (Superdex 200 column). Distribution of hTBP in fractions was analyzed by Western blot. (C) Size fractionation of hTBP in $yTBP\Delta/hTBP$ cells expressing NLS-Htt96Q, Htt96Q and GST-NLS-Htt96Q for 1 h quantified by densitometry.

4.1.2.3 Functional interference of TBP upon expression of nuclear targeted mutant Htt

For a detailed analysis of the functional impairment of human TBP by mutant Htt, a reporter system was designed in wild-type instead of $yTBP\Delta/hTBP$ yeast cells to exclude any secondary effects, such as global down regulation of transcription or translation in response to toxicity upon expression of mutant Htt. This reporter system takes advantage of the fact that TBP binds to DNA at the TATA box and serves as a platform for the assembly of the transcription initiation complex. Three point mutations (I194P, V202T and L205V) in the basic DNA binding domain of human TBP were shown to allow transcription almost exclusively from a modified TATA box, which contained the DNA sequence TGTA instead of TATA (Strubin and Struhl, 1992). In this reporter system, intra- and intermolecular effectors of the TBP impairment, such as a dependence of the polyQ stretch in TBP and modulation by chaperones, respectively, could be directly dissected. Therefore, the above mentioned mutations were introduced by site-directed mutagenesis into human TBP (mut3hTBP) which was subsequently cloned under control of the constitutive *ADHI* promoter into a yeast expression vector. The TATA box in the *GALI* promoter was mutated

accordingly and coupled to the luciferase gene (Figure 28A). Coexpression of wild-type human TBP and TGTA-luc reporter resulted in a basal luciferase activity in wild-type yeast cells upon induction of the TGTA-luc reporter construct (Figure 28B). However, coexpression of mut3hTBP and TGTA-luc reporter markedly increased luciferase activity (Figure 28B). Thus, the mutated human TBP specifically allows transcription from the modified TATA box in wild-type yeast cells. Deactivation of TBP by mutant Htt should suppress transcription of the luciferase gene and lead to a decrease in luciferase activity.

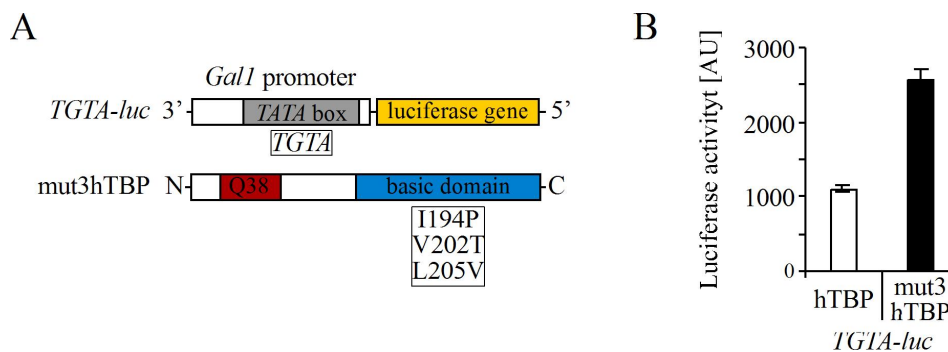


Figure 28: Reporter system to assay TBP mediated transcription in wild-type yeast.

(A) Schematic representation of the TGTA-luc reporter and mutated human TBP (mut3hTBP). (B) NLS-Htt20Q, NLS-Htt96Q, mut3hTBP and TGTA-luc were coexpressed in wild-type cells for 12 h at 30 °C. Growth was examined by serial dilutions of cells on SC-plates after 2 d at 34 °C. (C) hTBP or mut3hTBP under control of *ADHI* were coexpressed with TGTA-luc and NLS-Htt20Q in wild-type cells for 2 h at 30 °C followed by 1 h induction of TGTA-luc. Luciferase activity was recorded and expressed in arbitrary units (AU).

Various Htt constructs were coexpressed with the reporter system and assayed for their ability to interfere with TBP mediated transcription of the luciferase gene by recording luciferase activity. Expression of NLS-Htt20Q or NLS-Htt96Q did not cause any growth defect in wild-type yeast, whether or not these cells also expressed TGTA-luc reporter construct and mutated human TBP (Figure 23B and data not shown). Strikingly, NLS-Htt96Q caused a substantial decrease in luciferase activity compared to NLS-Htt20Q, whereas Htt96Q did not affect the activity (Figure 29A). The decrease in luciferase activity upon expression of NLS-Htt96Q depended on the presence of the polyQ segment in TBP (Figure 29B). Furthermore, the amount of TBP in these cells was reduced upon induction of NLS-Htt96Q compared to NLS-Htt20Q as revealed by immunoblot analysis (Figure 29C). In agreement with these results, soluble mutant Htt has been demonstrated to structurally destabilize TBP and to inhibit TBP binding to DNA *in vitro* (Schaffar *et al.*, 2004). Thus, based on these combined data, nuclear mutant Htt seems to impair the transcription initiation function of TBP, presumably by destabilizing its structure, which in turn inhibits its binding to DNA.

This interference seems to be mediated by polyQ-polyQ interaction. The alteration of the size fractionation properties of TBP might reflect the production of structurally distorted TBP or TBP containing transcription complexes. This reporter system now offers the opportunity to investigate the effect of chaperones on the aberrant interaction and, more general, to screen a human cDNA library to find new modulators of polyQ-mediated transcription impairment.

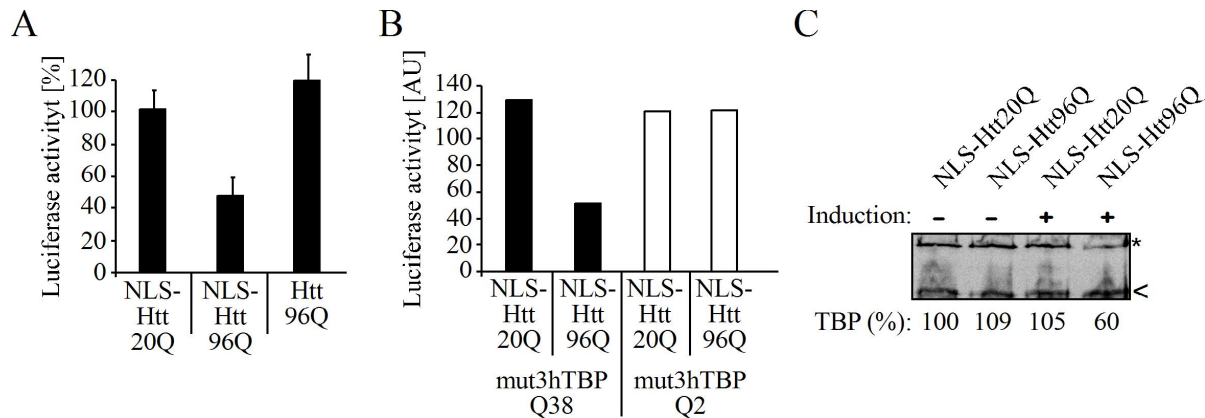


Figure 29: NLS-Htt96Q interferes with TBP mediated transcription.

(A) NLS-Htt20Q, NLS-Htt96Q or Htt96Q were coexpressed with mut3hTBP and TGTA-luc for 2 h at 30 °C followed by 1 h induction of TGTA-luc. Luciferase activity was recorded and set to 100 % in cells expressing NLS-Htt20Q. (B) Cells coexpressing NLS-Htt20Q or NLS-Htt96Q with either mut3hTBP38Q or mut3hTBP2Q and TGTA-luc were assayed as in (A). Luciferase activity is expressed in arbitrary units ($\times 10^4$) (AU). (C) mut3hTBP and TGTA-luc were coexpressed as in (A) with and without induction of NLS-Htt20Q and NLS-Htt96Q. TBP in lysates was detected by Western blot with anti-TBP antibody and quantified. * marks TBP protein and < unspecific background. Amount of TBP in cells expressing NLS-Htt20Q was set to 100 %.

4.1.2.4 Transcriptional dysregulation due to aberrant interactions of mutant Htt and TBP

In order to reproduce and validate the findings obtained from the yeast model system, the properties of soluble mutant Htt exon 1 fragment targeted to the nucleus were investigated in mouse neuroblastoma cells. Therefore, myc-tagged Htt96Q and NLS-Htt96Q were cloned into mammalian expression vectors, transiently expressed in N2a cells and analyzed by the filter assay and Western blot as described above. Aggregation of NLS-Htt96Q was reduced markedly compared to Htt96Q (Figure 30A) and consistently, NLS-Htt96Q accumulated to higher levels in SDS-soluble form than Htt96Q (Figure 30B). Whereas no Htt96Q could be recovered from the gel filtration column, NLS-Htt96Q fractionated between ~70 – 170 kDa upon size exclusion chromatography (Figure 30C). Hence, a fraction of nuclear targeted mutant Htt exists in a soluble, well-defined species similar to those found to be toxic in *yTBP*/*hTBP* yeast cells. Preliminary experiments showed that expression of NLS-Htt96Q caused polyQ-length dependent toxicity in mouse neuroblastoma cells (Schaffar, 2004).

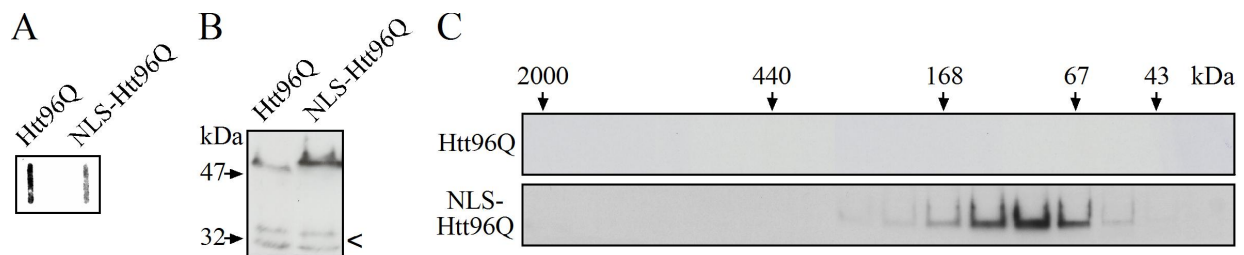


Figure 30: Soluble NLS-Htt96Q forms oligomers of ~70-170 kDa size in N2a cells.

(A) myc-tagged Htt96Q and NLS-Htt96Q were transiently expressed in N2a cells for 48 h. SDS-resistant Htt aggregates in lysates were detected by filter assay and immunostaining with anti-myc antibody. (B) Htt constructs in lysates from (A) were detected by Western blot with anti-myc antibody. (C) Size exclusion chromatography of soluble fractions from (B) followed by Western blot. Htt constructs were detected with anti-myc antibody. Positions of size markers are indicated in kDa.

Interference with the size fractionation properties of TBP by soluble mutant Htt in *yTBPΔ/hTBP* cells suggested at least a transient association with TBP. Therefore, interaction of soluble Htt and human TBP was investigated by co-immunoprecipitation experiment. myc-tagged NLS-Htt20Q and NLS-Htt96Q were transiently coexpressed in N2a cells with FLAG-tagged human TBP and subsequently radioactively-labeled. NLS-Htt20Q and NLS-Htt96Q were produced to similar levels (Figure 31A). Strikingly, although TBP was present at equal amounts in cells expressing NLS-Htt20Q and NLS-Htt96Q, TBP could only be co-precipitated with NLS-Htt96Q (Figure 31B). Thus, soluble Htt exon 1 fragment associates with human TBP in a polyQ-length dependent manner.

To dissect whether transient association of mutant Htt and TBP leads to functional impairment of the transcription factor, the reporter assay for TBP mediated transcription established in yeast was applied in N2a cells. Mutated human TBP (mut3hTBP) and luciferase were subcloned into mammalian expression vectors under control of the EF-1 α and the CMV promoter, respectively; the latter contained a modified TATA box. N2a cells were transiently co-transfected with mut3hTBP, TGTA-luc reporter construct and either NLS-Htt20Q or NLS-Htt96Q for 48 h and assay for luciferase activity. Expression of NLS-Htt96Q markedly reduced the luciferase activity compared to NLS-Htt20Q (Figure 31C). Thus, an aberrant association of soluble oligomers formed by mutant Htt is likely to impair the function of the transcription factor TBP in the nucleus.

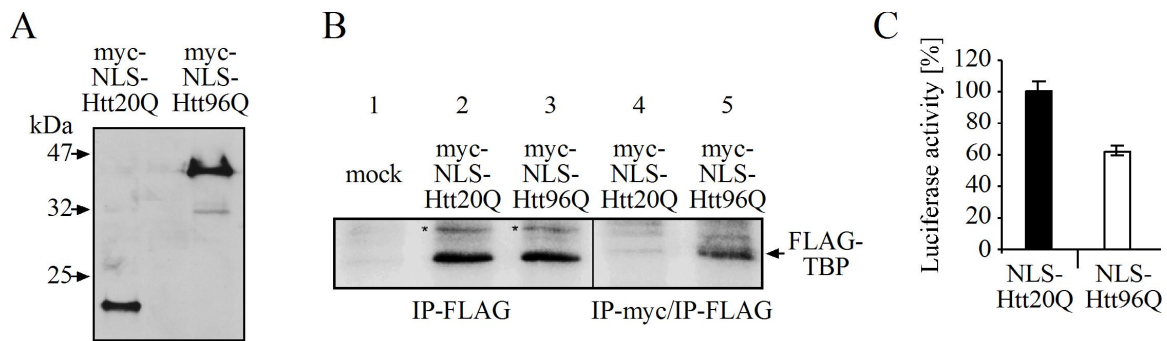


Figure 31: Coimmunoprecipitation of FLAG-tagged human TBP with antibodies against myc-tagged Htt. (A) myc-NLS-Htt20Q and NLS-Htt96Q were transiently expressed in N2a cells for 48 h. Htt constructs in lysates were detected by Western blot with anti-myc antibody. (B) myc-NLS-Htt20Q, NLS-Htt96Q and FLAG-hTBP were coexpressed as in (A). Cells were labeled for 2 h with 400 μ Ci/ml 35 S-Met/ 35 S-Cys (Promix, Amersham) and 100,000 \times g supernatants of cell extracts prepared in lysis buffer. FLAG-hTBP was immunoprecipitated from the 100,000 \times g supernatants of mock-transfected and of NLS-Htt20Q- and NLS-Htt96Q-expressing cells (lanes 1, 2 and 3). Equivalent aliquots of 100,000 \times g supernatant of NLS-Htt20Q- and NLS-Htt96Q-expressing cells (lanes 4 and 5) were first immunoprecipitated with anti-myc antibody. The precipitates were redissolved in lysis buffer/1 % SDS, followed by 10-fold dilution in lysis buffer and immunoprecipitation with anti-FLAG antibody. Reactions were analyzed by SDS-PAGE and fluorography. * marks an unidentified band precipitating with anti-FLAG antibody. This experiment was performed in cooperation with Dr. Peter Breuer. (C) NLS-Htt20Q, NLS-Htt96Q, mut3hTBP and TGTA-luciferase reporter were transiently coexpressed in N2a cells for 48 h. Cell lysates were assayed for luciferase activity. Luciferase activity without induction of Htt construct was set to 100 %.

4.1.2.5 General impairment of transcription factors by soluble, oligomeric mutant Htt

To address whether soluble polyQ expanded Htt exon 1 fragments similarly impair the function of endogenous transcription factors, Htt constructs were transiently expressed in human neuroblastoma cells (SH-SY5Y) and analyzed for their effect on endogenous human TBP and CBP. These cells were used previously to study polyQ-expansion proteins (Wytttenbach *et al.*, 2000; Ding *et al.*, 2002). While NLS-Htt96Q fractionated between \sim 70 – 170 kDa upon size exclusion chromatography, Htt96Q could not be recovered from the gel filtration column (Figure 32A). Surprisingly, NLS-Htt20Q was found to fractionate at a higher molecular weight than NLS-Htt96Q. Both proteins were present at roughly similar amounts (Figure 32A). Size fractionation of the transcription factors TBP and CBP were altered by NLS-Htt96Q (Figure 32B and Figure 32C). In cells expressing NLS-Htt20Q, TBP was in a well-defined complex of \sim 200 kDa, as observed previously and, CBP fractionated at \sim 400 kDa. However, upon expression of NLS-Htt96Q, substantial amount of TBP and CBP were recovered in higher molecular weight fractions. Thus, the soluble form of nuclear Htt seems to modulate the conformational properties of TBP and CBP (or transcription complexes containing these factors).

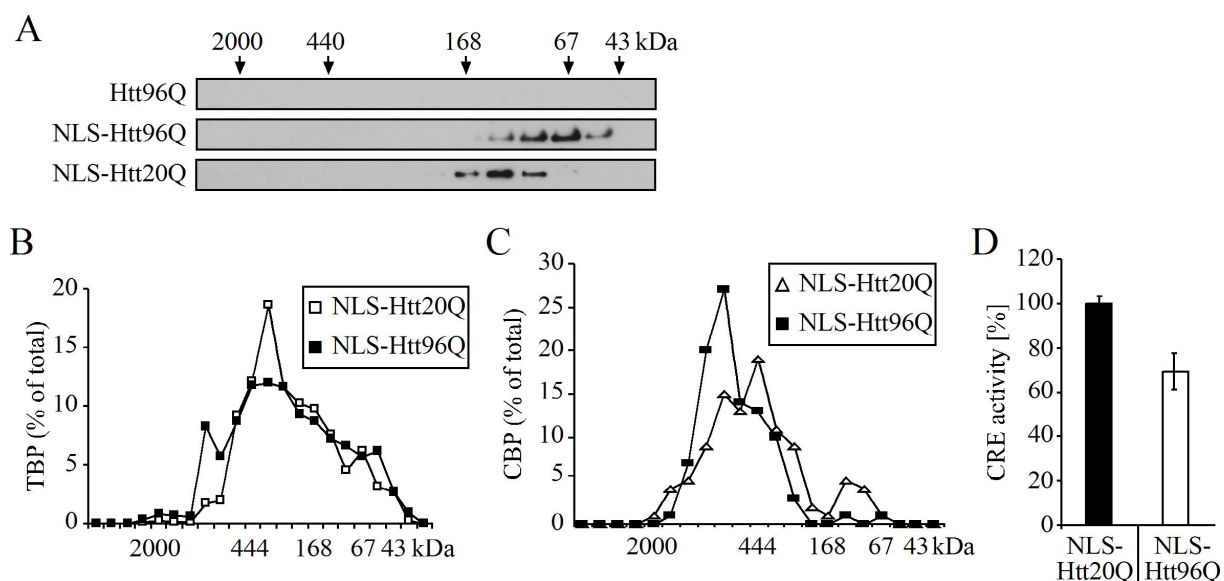


Figure 32: NLS-Htt96Q affects unproductively properties of transcription factors in SH-SY5Y cells.

(A) myc-tagged Htt96Q, NLS-Htt20Q and NLS-Htt96Q were transiently expressed in SH-SY5Y cells for 48 hours. Soluble fractions of lysates were subjected to size exclusion chromatography on a Superdex 200 column followed by Western blot with anti-myc antibody. Positions of size markers are indicated in kDa. (B) and (C) Distribution of endogenous TBP and CBP in the fractions from (A) was analyzed by Western blot with anti-TBP and anti-CBP antibody, respectively, and quantified by densitometry. (D) myc-tagged NLS-Htt20Q, NLS-Htt96Q and CRE-luc construct were transiently coexpressed as in (A). Cell lysates were assayed for luciferase activity. Luciferase activity in cells expressing NLS-Htt20Q was set to 100 %

Disease associated polyQ proteins have been shown to cause dysregulation of CRE-mediated transcription (Nucifora *et al.*, 2001; Shimohata *et al.*, 2001). To assess whether the altered fractionation properties of the transcription factors TBP and CBP are connected to transcriptional dysregulation, NLS-Htt20Q and NLS-Htt96Q were transiently coexpressed with a CRE luciferase reporter construct in SH-SY5Y cells for 48 h. Strikingly, expression of NLS-Htt96Q caused a reduction in luciferase activity compared to NLS-Htt20Q (Figure 32D). Thus, soluble polyQ expanded Htt exon 1 fragment seems to interfere with the function of endogenous transcription factors in the nucleus of human neuronal cells, leading to a downregulation of CRE mediated transcription. Whether this transcriptional dysregulation also leads to cellular toxicity remains to be determined.

4.1.2.6 Influence of flanking sequences on TBP mediated polyQ protein toxicity

Specific amino acids sequences flanking the polyQ region of Htt exon 1 are believed to modulate polyQ-length dependent toxicity (Steffan *et al.*, 2004; Duennwald *et al.*, 2006b). To dissect the influence of flanking sequences on the toxicity of polyQ expansion proteins, a set of Htt exon 1 fragments was constructed that varied in the length of their polyQ stretch, presence or absence of the endogenous proline-rich region juxtaposed C-terminally to the polyQ sequence, C-terminal fusion to green fluorescent protein (GFP), or presence of a N-terminal epitope tag (myc or FLAG) (Figure 33).

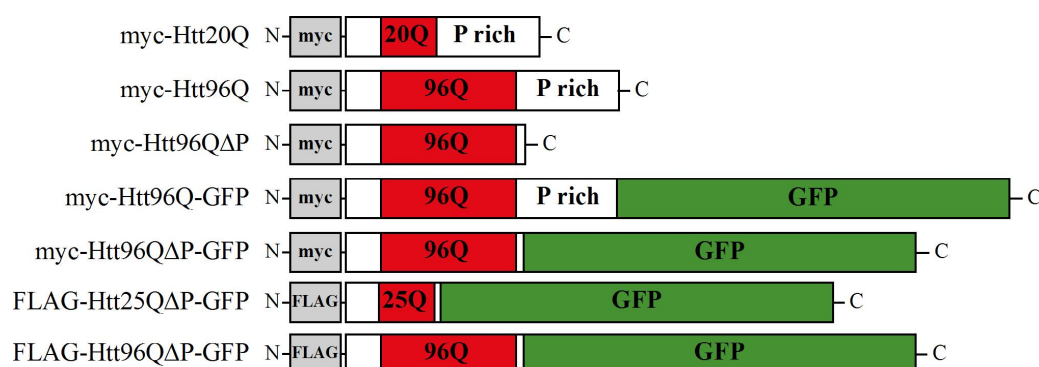


Figure 33: Schematic overview of different Htt exon 1 constructs.

N-terminal myc tag (myc) or FLAG-tag (FLAG), polyQ stretch of 20 or 96 Q (20Q or 96Q), proline rich domain (P rich), green fluorescent protein (GFP).

All Htt constructs were cloned into copper-inducible yeast expression vectors. FLAG-tagged Htt Δ Prich-GFP fragments have been demonstrated to cause a polyQ length-dependent growth defect in yeast (Meriin *et al.*, 2002), and it was proposed that toxicity of this particular Htt exon 1 construct arises from the combined effect of the amino-terminal epitope (FLAG) tag and deletion of the proline rich domain (Duennwald *et al.*, 2006b). FLAG-tagged Htt25Q Δ P-GFP and FLAG-tagged Htt96Q Δ P-GFP used in this study were identical to constructs described previously with the exceptions that the expanded polyQ stretch contains 96 glutamines instead of 103 and that expression was originally driven from the *GALI* promoter (Meriin *et al.*, 2002). Since FLAG-tagged Htt96Q Δ P-GFP was described to be toxic in wild-type yeast, the effect of these different Htt exon 1 constructs on viability was first analyzed in wild-type cells by serial dilution on plates containing selective media. Expression of Htt20Q and Htt96Q did not cause any toxicity as described previously (Krobitsch and Lindquist, 2000; Muchowski *et al.*, 2000) (Figure 34A). Whereas Htt96Q-GFP did also not

affect cell viability, Htt96Q Δ P-GFP showed a pronounced growth defect (Figure 34A). This growth defect was also observed at 30 °C and 34 °C, but was less pronounced at these temperatures (data not shown). To exclude the possibility that the growth defect caused by Htt96Q Δ P-GFP was only due to deletion of the proline domain, viability of wild-type cells expressing Htt96Q Δ P was analyzed. Intriguingly, Htt96Q Δ P did not cause any toxicity (Figure 34B). Moreover, to address whether the epitope tag has any influence on toxicity, FLAG- and myc-tagged Htt96Q Δ P-GFP were expressed in wild-type cells. The toxicity caused by Htt96Q Δ P-GFP was independent of its N-terminal epitope tag (Figure 34C). As FLAG (DYKDDDDK) and myc ((EQKLISEEDL) tags differ substantially in amino acid composition, charge and hydrophobicity, it seems unlikely that the epitope tags are responsible for toxicity as previously reported (Duennwald *et al.*, 2006b). Thus, toxicity of Htt96Q Δ P-GFP is likely to arise from the combined effect of deletion of the proline rich domain and fusion to GFP.

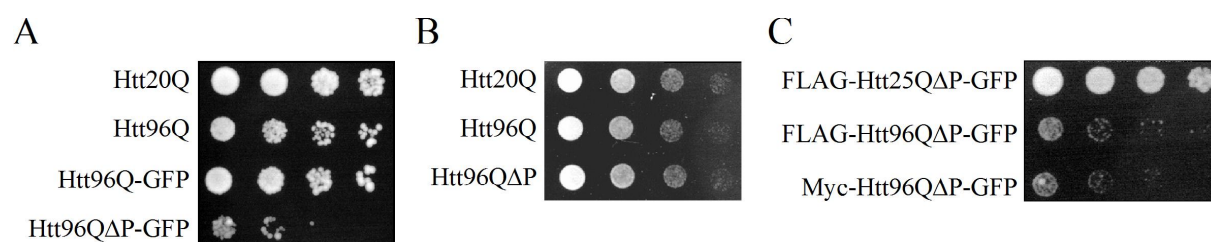


Figure 34: Growth defect upon expression of Htt constructs.

(A) myc-tagged Htt20Q, Htt96Q, Htt96Q-GFP or Htt96Q Δ P-GFP was expressed under *CUP1* for 12 h in wild-type cells at 30 °C. Growth was examined by 5-fold serial dilutions on SC plate after 2 days at 37 °C. (B) Wild-type cells expressing myc-tagged Htt20Q, Htt96Q or Htt96Q Δ P were cultured and analyzed as in (A). (C) FLAG-tagged Htt25Q Δ P-GFP, FLAG-tagged Htt96Q Δ P-GFP and myc-tagged Htt96Q Δ P-GFP were cultured and analyzed as in (A).

Expression and formation of SDS-resistant aggregates of the different Htt constructs was investigated as before in order to correlate aggregation properties and toxicity. Dot blot analysis revealed that Htt96Q, Htt96Q-GFP and Htt96Q Δ P-GFP were expressed at comparable levels (Figure 35A). Whereas Htt96Q and Htt96Q-GFP formed similar amounts of SDS-resistant aggregates detectable by filter-trap assay, Htt96Q Δ P-GFP formed 90 % less detergent-resistant aggregates (Figure 35A). Furthermore, Htt96Q Δ P formed 4 – 5 times more SDS resistant aggregates compared to Htt96Q (Figure 35B). Similar to their effect on cell viability, the investigated epitope tags (Myc and FLAG) did not change the aggregation propensity of Htt96Q Δ P-GFP fragment governed by the polyQ stretch (Figure 35C). Thus, the

combined effect of deletion of the proline segment and fusion to GFP seems not only to be responsible for toxicity but also for inhibition of aggregation. The GFP moiety might possibly exert a kinetic block on the aggregation of Htt, retarding the formation of detergent-resistant inclusions. Similarly, the propensity of Htt to aggregate is reduced by the nuclear environment.

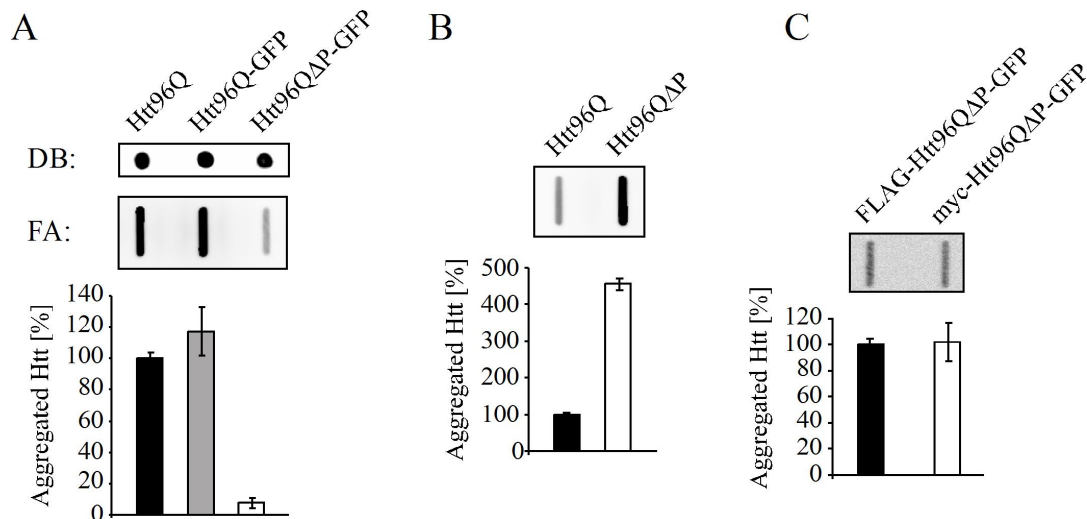


Figure 35: Expression and aggregation of Htt constructs.

(A) myc-tagged Htt96Q, Htt96Q-GFP or Htt96QΔP-GFP was expressed under *CUP1* control for 12 h in wild-type cells at 30 °C. Lysates were analyzed by dot blot (DB) and filter assay (FA) followed by detection of Htt constructs with anti-myc antibody. The amount of Htt96Q aggregates was set to 100 %. (B) myc-tagged Htt96Q and Htt96QΔP were expressed and analyzed as in (A). (C) FLAG-tagged Htt96QΔP-GFP and myc-tagged Htt96QΔP-GFP were expressed and analyzed as in (A). Htt constructs were immunodetected with anti-GFP antibody. The amount of FLAG-Htt96QΔP-GFP aggregates was set to 100 %.

Intriguingly the amount of SDS-resistant aggregates did not correlate with the observed growth defect. In addition to the analysis of SDS-resistance of aggregates, SDS-solubility of the various Htt constructs was determined in lysates from wild-type yeast by SDS-PAGE and immunoblot analysis. Htt96Q and Htt96Q-GFP did not migrate into the gel and were only detectable in the stacking gel consistent with the formation of detergent-resistant aggregates observed for these constructs. A substantial amount of Htt96QΔP-GFP migrated into the gel and was detected as a single protein band of ~50 kDa (Figure 36A).

To assess the oligomeric state of different Htt constructs, size exclusion chromatography was carried out on supernatants of lysates obtained by centrifugation at 20,000 x g. Whereas neither Htt96Q nor Htt96Q-GFP could be recovered from the gel filtration column, SDS-soluble oligomers of Htt96QΔP-GFP fractionated around ~200 kDa

(100-230 kDa) (Figure 36B). Interestingly, the detergent-soluble 200 kDa oligomers formed by Htt96Q Δ P-GFP correlate with the growth defect caused by the same construct. Thus, soluble polyQ species exert toxicity rather than large aggregates.

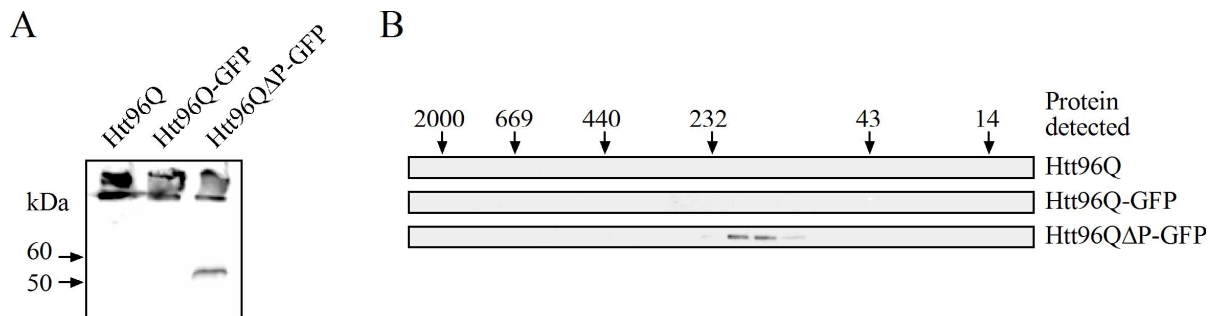


Figure 36: Soluble Htt96Q Δ P-GFP forms oligomers of ~200 kDa.

(A) Myc-tagged Htt exon 1 constructs with 96 Q (Htt96Q, Htt96Q-GFP and Htt96Q Δ P-GFP) were expressed under *CUP1* control for 12 h in wild-type cells at 30 °C. Lysates were analyzed by Western blot with anti-myc antibody. (B) Soluble lysate fractions analyzed in (A) were subjected to size exclusion chromatography on a Superdex 200 column. Htt proteins were detected by Western blot with anti-myc antibody. Positions of size markers are indicated in kDa.

The ability of Htt exon 1 fragments to recruit other polyQ proteins into aggregates is thought to play an important role in toxicity (Kazantsev *et al.*, 1999; Schaffar *et al.*, 2004; Duennwald *et al.*, 2006a). To address whether toxicity of Htt96Q Δ P-GFP could be mitigated by enhanced aggregation and/or recruitment of the ~200 kDa oligomer into aggregates formed by Htt96Q, both Htt exon 1 fragments were coexpressed in wild-type cells. Therefore, myc-tagged Htt20Q and Htt96Q were expressed from copper-inducible promoters and FLAG-tagged Htt25Q Δ P-GFP and Htt96Q Δ P-GFP as previously described (Meriin *et al.*, 2002). Differences in abundance or toxicity of Htt96Q Δ P-GFP were not observable regardless which promoter drove its expression. Intriguingly, the growth defect caused by Htt96Q Δ P-GFP could not be suppressed by coexpression of Htt96Q (Figure 37A). Although Htt25Q Δ P-GFP and Htt96Q Δ P-GFP were found to co-aggregate upon coexpression with Htt96Q as detected with filter trap assay, aggregation of Htt96Q Δ P-GFP was not increased compared to Htt25Q Δ P-GFP under the same conditions (Figure 37B). Size exclusion chromatography revealed the persistence of the ~200 kDa Htt96Q Δ P-GFP oligomer upon coexpression with Htt96Q (Figure 37C), indicating that Htt96Q Δ P-GFP cannot be efficiently recruited by Htt96Q. Thus, in agreement with the results above, the presence of the ~200 kDa Htt96Q Δ P-GFP oligomer correlates with toxicity.

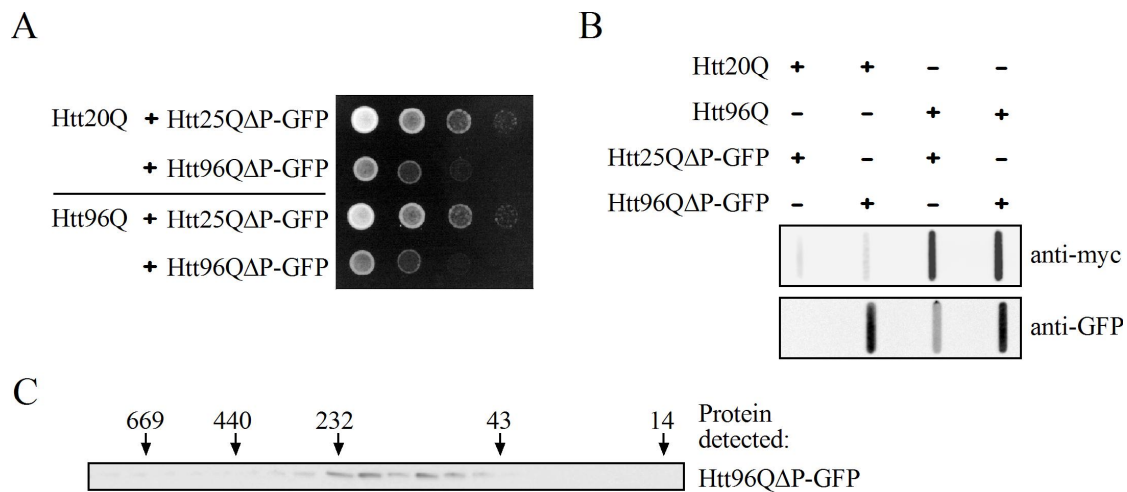


Figure 37: Toxicity of Htt96QΔP-GFP oligomers cannot be mitigated by recruitment into Htt aggregates. (A) Myc-tagged Htt20Q or Htt96Q under *CUP1* control were coexpressed with Htt25QΔP-GFP or Htt96QΔP-GFP under *GALI* control in wild-type cells for 24 h at 30 °C. Growth was examined by 5-fold serial dilutions on SC plates after 2 days at 37 °C. (B) SDS-resistant aggregates in lysates from (A) were analyzed by filter assay and immunodetected as indicated. (C) Soluble fraction from cells coexpressing myc-tagged Htt96Q and Htt96QΔP-GFP as in (A) was subjected to size exclusion chromatography. Htt96QΔP-GFP was detected by Western blot with anti-GFP antibody. Positions of size markers are indicated in kDa.

Intriguingly, in *yTBPΔ/hTBP* cells, similar soluble oligomers as those observed for Htt96QΔP-GFP were formed by nuclear targeted Htt96Q. These species interfered with the function of the transcription factor TBP and caused cellular toxicity. Since the aggregation propensity of Htt96QΔP-GFP is reduced compared to the non-toxic Htt96Q, the toxicity of Htt96QΔP-GFP is likely to arise as well from aberrant protein-protein interaction rather than from a sequestration mechanism. To address whether Htt96QΔP-GFP also causes a growth defect in *yTBPΔ/hTBP* cells, Htt constructs were expressed in these cells and their growth was assayed at 34 °C. At this temperature, expression of Htt96QΔP-GFP in wild-type cells resulted only in mild growth impairment (Figure 38). In contrast, in *yTBPΔ/hTBP* cells, Htt96QΔP-GFP expression led to a severe growth defect (Figure 38). Neither Htt96Q nor Htt96Q-GFP showed any toxicity in *yTBPΔ/hTBP* cells (Figure 38). Although growth of *yTBPΔ/hTBP* cells is to some extent slower compared to wild-type cells, expression of Htt96QΔP-GFP causes the most pronounced growth defect in *yTBPΔ/hTBP* cells (Figure 38). Thus, Htt96QΔP-GFP oligomers, which are correlated to toxicity in wild-type cells, appear to exercise increased toxicity in *yTBPΔ/hTBP* cells, presumably due to functional interference with the transcription factor TBP, as observed for oligomers formed by NLS-Htt96Q.

Whether Htt96Q Δ P-GFP is also found in the nucleus of *yTBP* Δ /*hTBP* cells, as primary site of cellular toxicity, remains to be determined.

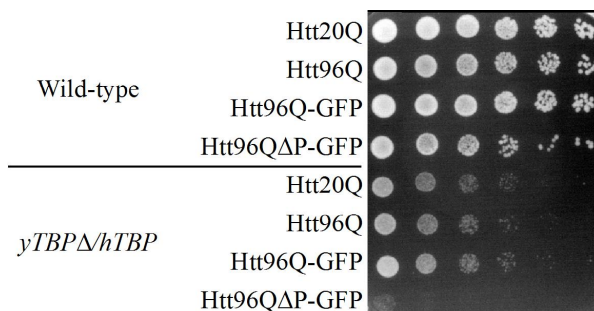


Figure 38: Increased growth defect upon expression of Htt96Q Δ P-GFP in *yTBP* Δ /*hTBP* cells.

Htt20Q, Htt96Q, Htt96Q-GFP or Htt96Q Δ P-GFP was expressed under CUP1 for 12 h in wild-type or *yTBP* Δ /*hTBP* cells at 30 °C. Growth was examined by 5-fold serial dilutions on SC plate after 2 days at 34 °C.

In summary, the interaction of polyQ-expanded Htt with the transcription factors TBP and CBP was investigated in mouse and human neuronal cells as well as in a yeast model. Monomers and/or small soluble oligomers of mutant Htt were shown to deactivate the transcription factors by a polyQ-mediated interaction, independent of the formation of insoluble coaggregates. These soluble toxic forms are possibly generated through a conformational rearrangement in mutant Htt and accumulated to high levels when the polyQ-expanded protein is targeted to the nucleus. Soluble oligomers of a distinct size (and presumably conformation) might generally represent a toxic species since similar effects could be observed for oligomers formed by a polyQ-expanded Htt fragment with largely modified flanking sequences

4.2 Chaperonin TRiC as modulator of polyQ protein aggregation and toxicity

Hsp70 and its cochaperone Hsp40 have been demonstrated to interfere with polyQ toxicity early in the aggregation pathway by retarding the conformational compaction of the polyQ disease protein and presumably also by transiently shielding benign polyQ sequences in target proteins such as the general transcription factor TBP (Schaffar *et al.*, 2004). In agreement with this view, increased expression of Hsp70, together with Hsp40, has been shown to alleviate polyQ toxicity and neurodegeneration in various cellular and animal models, presumably by redirecting the aggregation process towards the formation of non-fibrillar, amorphous aggregates (Cummings *et al.*, 1998; Warrick *et al.*, 1999; Chan *et al.*, 2000; Muchowski *et al.*, 2000). This mechanism is thought to inhibit the accumulation of certain aggregation intermediates, including soluble polyQ oligomers, which may be the primary toxic agents (Arrasate *et al.*, 2004; Schaffar *et al.*, 2004; Wacker *et al.*, 2004). A reduction in the chaperone capacity due to the ageing process may allow the accumulation of proteotoxic species (Morley *et al.*, 2002; Morley and Morimoto, 2004), thereby possibly explaining the late onset of these diseases.

In the eukaryotic cytosol, the Hsp70 chaperone system cooperates with the chaperonin TRiC in the de novo folding of a subset of newly-synthesized proteins (Frydman, 2001; Hartl and Hayer-Hartl, 2002). Hsp70 members, together with Hsp40 cochaperones, can interact co-translationally with nascent polypeptide chains, protecting them against aggregation, whereas TRiC acts downstream in mediating folding and assisting oligomer assembly. Whether these chaperones also cooperate in preventing the formation of aberrantly folded proteins associated with neurodegenerative diseases, such as HD, has remained largely unexplored. A recent RNA interference (RNAi) screen in *Caenorhabditis elegans*, searching for endogenous regulators of polyQ aggregation, isolated, in addition to Hsp70 and Hsp40, six out of eight TRiC subunits (Nollen *et al.*, 2004), invoking the cytosolic chaperonin TRiC as a previously unknown modulator of polyQ aggregation. Thus, this screen may have uncovered the endogenous chaperone pathway for polyQ proteins. Alternatively, as TRiC folds essential cytoskeletal components, the observed RNAi phenotype could have resulted from indirect effects on the cytoskeleton.

In this study, a series of experiments were conducted to explore the direct interaction of TRiC and polyQ expanded Htt exon 1 fragments. The differential aggregation propensity and toxicity of distinct Htt exon 1 fragments were exploited to dissect the involvement of TRiC in modulating the properties of expanded polyQ proteins and its capacity to suppress their cellular toxicity. These experiments were carried out in the genetic background of wild-type yeast cells instead of *yTBPΔ/hTBP* cells.

4.2.1 TRiC deficiency modulates the properties of polyQ-expanded Htt

Mutations in chaperones have been of great use in analyzing polyQ aggregation (Krobitsch and Lindquist, 2000; Meriin *et al.*, 2002). A possible role of TRiC in modulating polyQ aggregation was investigated taking advantage of the well characterized conditionally TRiC-defective *tcp1-2* yeast strain (Ursic *et al.*, 1994). Because all TRiC subunits are required for function, mutation or depletion of a single subunit is sufficient to impair the function of the complex (Spiess *et al.*, 2004). *tcp1-2* carries a point mutation (G423D) within the equatorial ATP binding domain in the Tcplp subunit of TRiC (Ditzel *et al.*, 1998). The folding of the cytoskeletal proteins tubulin and actin stringently depends on assistance of TRiC (Frydman, 2001). Accordingly, *tcp1-2* cells are hypersensitivity to the microtubule depolymerisation drug benomyl, form large unbudded cells and are temperature-sensitive for growth at 37 °C, indicating that cytoskeletal dysfunction is a consequence of the functional impairment of TRiC (Ursic *et al.*, 1994).

4.2.1.1 Pronounced polyQ aggregation due to TRiC impairment

The effect of TRiC on Htt aggregation was investigated in wild-type and *tcp1-2* mutant yeast. When expressed in wild-type cells, Htt exon 1 with 20 Q (Htt20Q) did not form SDS-resistant aggregates detectable by filter-trap assay (Figure 39A). Htt45Q, close to the threshold-length for polyQ pathology of ~37 Q, formed small amounts of insoluble aggregates, whereas substantial aggregation was observed with Htt96Q (Figure 39A). In *tcp1-2* yeast cells, the amount of SDS-insoluble aggregates increased ~2-fold upon expression of Htt45Q and Htt96Q at the semi-permissive temperature of 30 °C (Figure 39A). Interestingly, immunofluorescence revealed that Htt45Q was diffusely distributed in wild-type cells, while in the *tcp1-2* cells, the protein coalesced into large, well-defined cytoplasmic inclusions (Figure 39B).

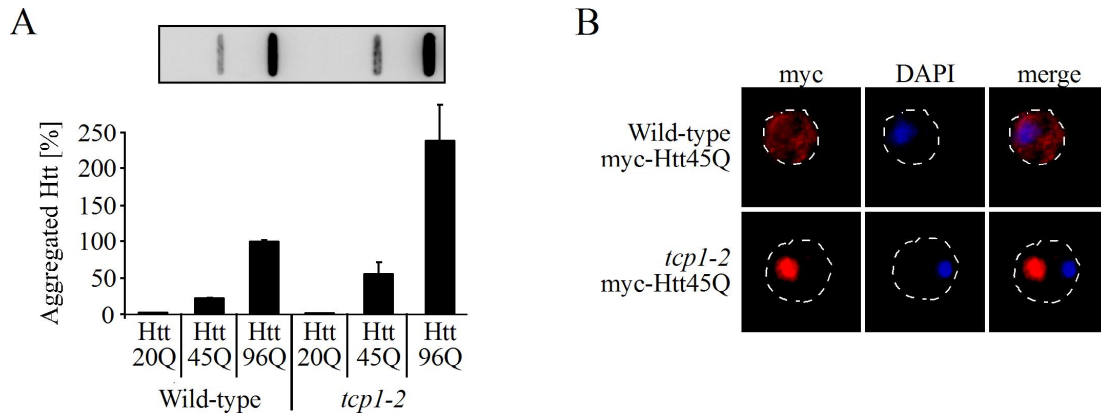


Figure 39: Effect of functional TRiC impairment on Htt aggregation.

(A) Myc-tagged Htt20Q, Htt45Q and Htt96Q were expressed under *CUP1* control for 24 h in wild-type and *tcp1-2* cells at 30 °C. SDS-resistant aggregates in lysates were analyzed by filter assay and detected with anti-myc antibody. The amount of Htt96Q aggregates in wild-type cells was set to 100 %. (B) Cells expressing myc-Htt45Q as in (A) were analyzed by indirect immunofluorescence. myc-Htt45Q was immunolabeled with anti-myc antibody coupled to Cy3-conjugated secondary antibody, and nuclei were counterstained with DAPI.

The enhancement of Htt aggregation due to functional TRiC impairment could be recapitulated with Htt96Q Δ P-GFP. Whereas Htt25Q Δ P-GFP did not aggregate, both in wild-type and in TRiC deficient cells, expression of Htt96Q Δ P-GFP resulted in a ~ 2-fold increase in formation of SDS-resistant aggregates in *tcp1-2* compared to wild-type cells (Figure 40A). Consistently, immunofluorescence analysis showed increased aggregation of Htt96Q Δ P-GFP in *tcp1-2* cells (Figure 40B). Similar results were obtained using the TRiC mutant yeast strain *cct4-1* (Tam *et al.*, 2006).

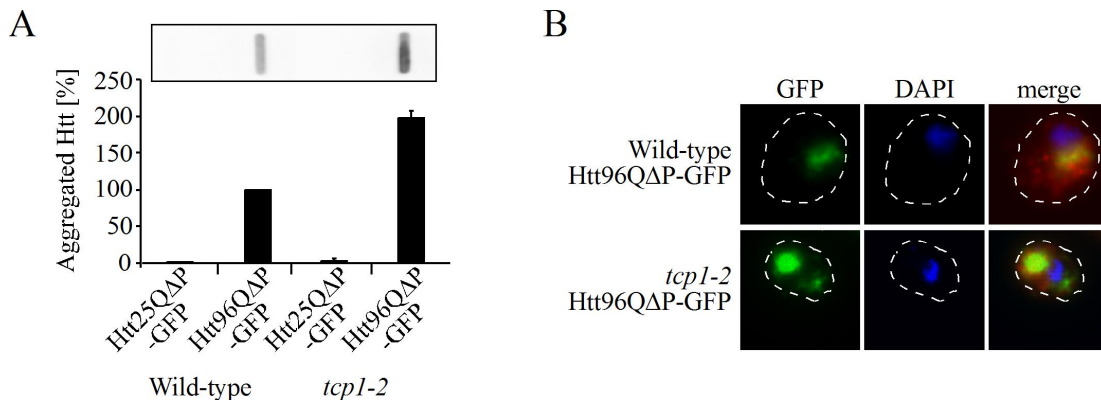


Figure 40: Defective TRiC enhances Htt aggregation.

(A) Htt25Q Δ P-GFP and Htt96Q Δ P-GFP were expressed under *CUP1* control in wild-type and *tcp1-2* for 24 h at 30 °C. SDS-resistant aggregates in lysates were analyzed by filter assay and detected with anti-GFP antibody. The amount of Htt96Q Δ P-GFP aggregates in wild-type cells was set to 100 %. (B) Cells expressing Htt96Q Δ P-GFP as above were analyzed by GFP fluorescence. Nuclei were stained with DAPI.

These findings mirror the observation in *C. elegans* that down-regulation of TRiC subunit expression results in enhanced polyQ aggregation (Nollen *et al.*, 2004). Recently, RNAi-mediated TRiC subunit knockdown in mammalian cells confirmed the role of TRiC in polyQ aggregation (Kitamura *et al.*, 2006; Tam *et al.*, 2006). Enhanced aggregation was unlikely to be a secondary effect of a loss of TRiC function in tubulin biogenesis, because disruption of the tubulin cytoskeleton is known to inhibit formation of large polyQ inclusions (Muchowski *et al.*, 2002). Thus TRiC, at normal levels, profoundly modulates the aggregation properties of polyQ expansion proteins.

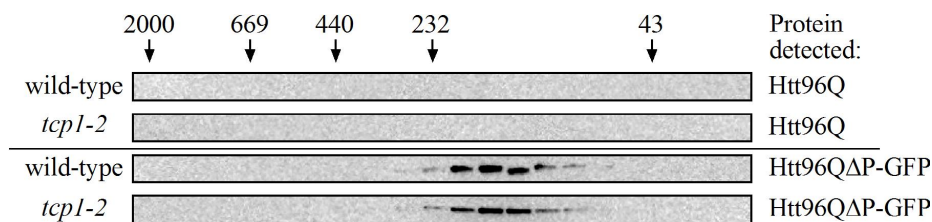


Figure 41: Soluble Htt96QΔP-GFP forms oligomers of ~200 kDa.

Myc-tagged Htt96Q and Htt96QΔP-GFP were expressed under *CUP1* control for 24 h in wild-type and *tcp1-2* cells at 30 °C. Soluble lysate fractions were analyzed by size exclusion chromatography on a Superdex 200 column. Htt proteins were detected by Western blot with anti-myc antibodies. Positions of size markers are indicated in kDa.

To assess whether TRiC impairment had an effect on SDS-solubility of Htt species, the supernatants of lysates derived from wild-type or *tcp1-2* cells expressing either Htt96Q or Htt96QΔP-GFP were subjected to size exclusion chromatography and analyzed by immunoblotting. Whereas no SDS-soluble Htt96Q could be recovered from the gel filtration column regardless of expression in wild-type or *tcp1-2* cells, the amount of ~ 200 kDa Htt96QΔP-GFP oligomers was slightly decreased in *tcp1-2* compared to wild-type cells (Figure 41), consistent with the pronounced formation of detergent-resistant aggregates in *tcp1-2* cells. Thus, TRiC deficiency appears to modulate the aggregation pathway.

4.2.1.2 Ambivalent effect of TRiC impairment on polyQ toxicity

The fact that TRiC impairment increases the formation of detergent-resistant aggregates stimulated the further investigation of its effect on cell viability. The growth defect caused by expression of Htt96QΔP-GFP in wild-type cells was slightly suppressed in *tcp1-2* cells (Figure 42A), consistent with the reduced amount of soluble, presumably toxic, ~200 kDa Htt96QΔP-GFP oligomers and increased formation of SDS-insoluble aggregates by the

same protein. In contrast, expression of Htt96Q is tolerated by wild-type yeast under standard growth conditions without overt toxicity (Figure 42B). However, in TRiC deficient *tcp1-2* cells, expression of Htt96Q markedly aggravated the growth defect of *tcp1-2* cells at 37°C (Figure 42B), which was rescued by expression of wild-type *TCPI* (Figure 42C). Increased polyQ toxicity was also observed in neuroblastoma cells upon downregulation of TRiC subunits by RNA interference (Kitamura *et al.*, 2006). Thus, different Htt exon 1 constructs may exert distinct mechanisms of toxicity under certain conditions.

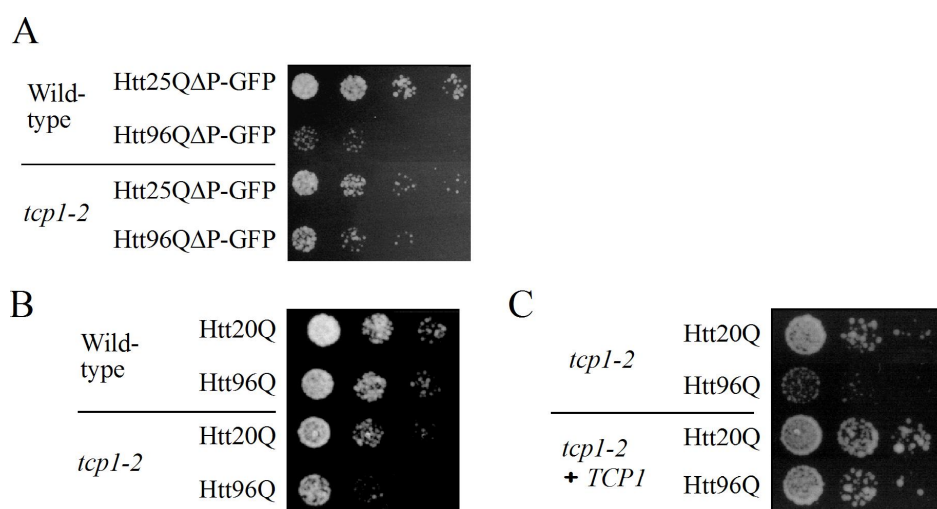


Figure 42: Increased polyQ toxicity in TRiC-impaired yeast.

(A) Wild-type and *tcp1-2* cells expressing Htt25QΔP-GFP or Htt96QΔP-GFP were cultured in liquid media and growth was examined by 5-fold serial dilutions on SC plates at 37 °C after 2 days. (B) Growth of cells expressing Htt20Q or Htt96Q was analyzed as in (A). (C) Htt20Q and Htt96Q were coexpressed for 24 h at 30 °C together with either empty vector or *TCPI* under its endogenous promoter, and growth of yeast cells was monitored as in (A).

In the case of toxicity conferred by Htt96Q, either Htt becomes toxic when TRiC function is partially impaired, or re-localization of TRiC to Htt aggregates causes a critical reduction in available TRiC activity in *tcp1-2* cells. In order to test the latter hypothesis, sequestration of TRiC subunits was analyzed in wild-type and *tcp1-2* cells. The TRiC subunit Tcp5p and Tcp1p were diffusely distributed in the cytoplasm of wild-type and *tcp1-2* mutant cells upon expression of Htt20Q, but co-localized partially with aggregates of Htt96Q in both cell types (Figure 43 and data not shown). Notably, similar results were obtained for Tcp1p in neuronal N2a cells upon transient expression of Htt96Q-GFP (data not shown). Thus, the chaperonin TRiC seems to be recruited into Htt aggregates.

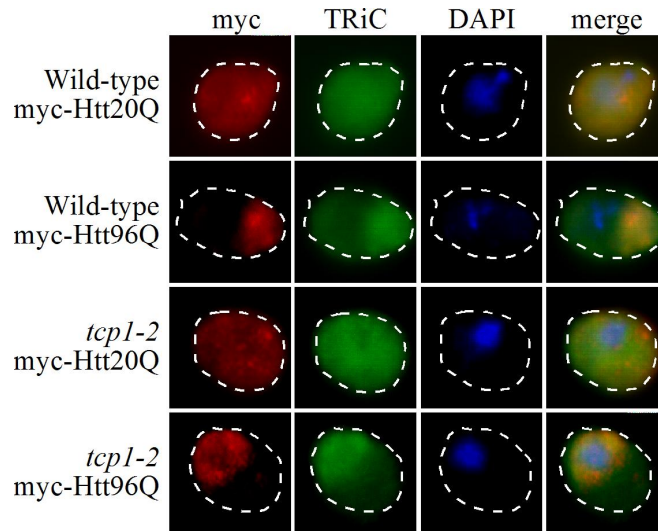


Figure 43: Colocalization of TRiC subunits with aggregates.

Wild-type and *tcp1-2* mutant cells expressing myc-Htt20Q or myc-Htt96Q for 24 h at 30 °C were analyzed by indirect immunofluorescence. myc-Htt constructs were immunolabeled with anti-myc antibody coupled to Cy3-conjugated secondary antibody, TRiC was immunostained with anti-Tcp5p antibody coupled to FITC-conjugated secondary antibody, and nuclei were counterstained with DAPI.

In order to quantify the amount of sequestered TRiC subunits, the endogenous TRiC subunit *TCP2* was functionally replaced by C-terminally HA-tagged *TCP2* in wild-type and *tcp1-2* mutant yeast. SDS-insoluble TRiC subunit Tcp2p was detected in Htt96Q expressing cells by filter-trap assay, presumably reflecting stable incorporation into the aggregates. This effect was more pronounced in *tcp1-2* cells (Figure 44A).

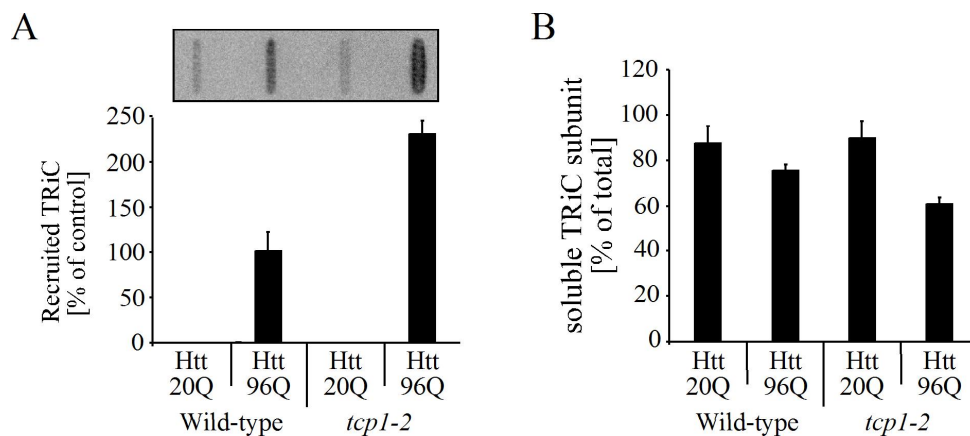


Figure 44: Recruitment of TRiC subunit into aggregates.

(A) myc-Htt20Q and myc-Htt96Q were expressed in wild-type and *tcp1-2* cells carrying chromosomal HA-tagged *TCP2* for 24 h at 30 °C. SDS-resistant aggregates in lysates containing Tcp2p-HA were analyzed by filter trap assay and detected with anti-HA antibody. Non-specific interaction of anti-HA antibody with Htt aggregates was excluded. Amounts of aggregated Tcp2p in cells expressing Htt96Q was set to 100 %. (B) Lysates derived from (A) were separated by centrifugation at 100,000 x g for 30 min and analyzed by Western blot. Tcp2p-HA was detected in fractions with anti-HA antibody. Total amount of Tcp2p-HA was set to 100 %.

However, ~75 % of TRiC remained soluble, arguing against a functionally significant depletion of available chaperonin, at least in wild-type cells. In *tcp1-2* cells, the amount of soluble TRiC was further reduced upon expression of Htt96Q to ~ 60 % of the total amount of TRiC (Figure 44B). Thus, enhanced Htt aggregation due to TRiC deficiency likely results in increased TRiC recruitment, possibly leading to a vicious circle that might severely engage the cellular chaperone activity.

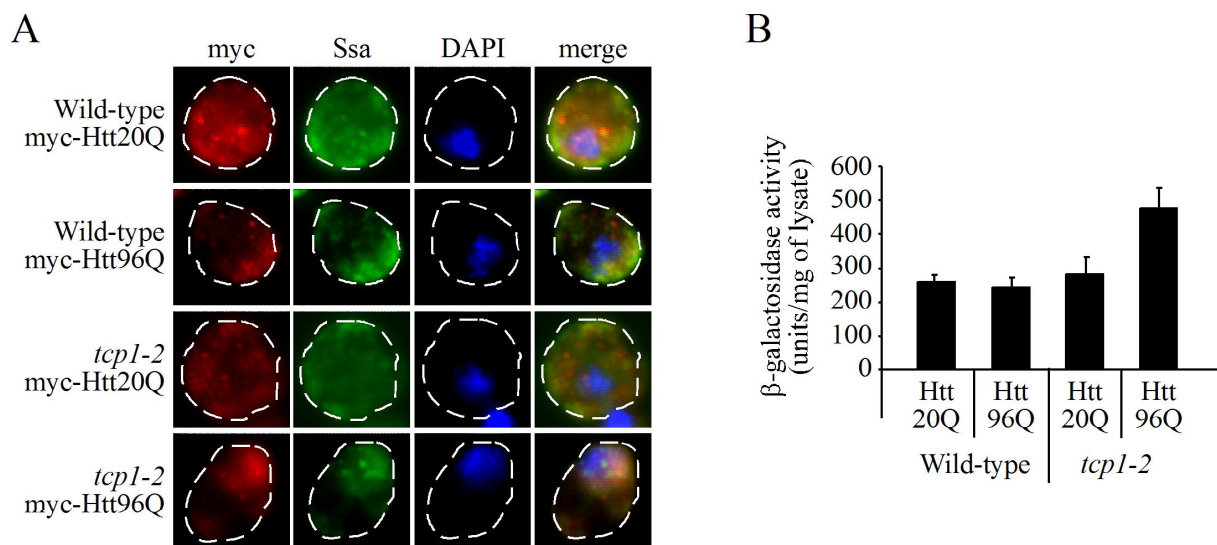


Figure 45: Changes in localization and induction of Ssa proteins upon Htt aggregation.

(A) Wild-type and *tcp1-2* cells expressing myc-tagged Htt20Q and Htt96Q for 24 h at 30 °C were analyzed by indirect immunofluorescence. myc-Htt constructs were immunolabeled with anti-myc antibody coupled to Cy3-conjugated secondary antibody, Ssa1p was immunostained with anti-Ssa1p antibody coupled to FITC-conjugated secondary antibody and nuclei were counterstained with DAPI. Note that anti-Ssa1p recognize all 4 Ssa proteins. (B) Induction of *SSA3* upon expression of Htt. myc-Htt20Q, myc-Htt96Q and HSE-*SSA3-LacZ* reporter were coexpressed in wild-type and *tcp1-2* cells for 24 h at 30 °C. Lysates were assayed for β -galactosidase activity.

Intriguingly, besides TRiC subunits, the cytosolic Hsp70s of the Ssa class co-localized partially with aggregates of Htt96Q in wild-type and *tcp1-2* cells, while being diffusely distributed in the cytoplasm upon expression of Htt20Q (Figure 45A). Importantly, in contrast to TRiC, two members of the Ssa class of Hsp70s, namely Ssa3p and Ssa4p, are stress-inducible. To investigate whether Htt expression leads to Hsp70 induction, the heat shock element (HSE) of the Ssa3p promoter was fused to the *lacZ* gene and induction of Ssa3p was quantified by measuring β -galactosidase activity (Boorstein and Craig, 1990). While Htt96Q did not affect β -galactosidase activity in wild-type yeast, *tcp1-2* cells showed 1.5 – 2 fold increase in activity upon expression of Htt96Q compared to Htt20Q (Figure 45B). Thus, the induction of the stress-inducible Ssa might counteract sequestration of Ssa proteins.

Accordingly, sequestration of TRiC could potentially lead to its functional depletion since TRiC is not stress-inducible and of low abundance compared to Hsp70 (Hartl, 1996; Siegers *et al.*, 1999).

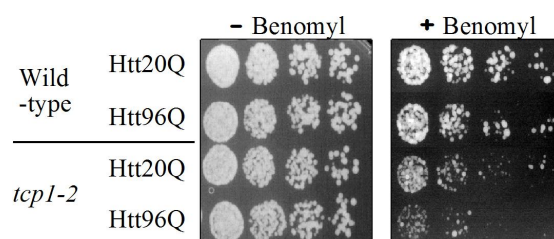


Figure 46: TRiC-impairment upon Htt expression in *tcp1-2* mutant cells.

Sensitivity to the microtubules depolymerisation drug Benomyl. Wild-type and *tcp1-2* cells expressing myc-Htt20Q or myc-Htt96Q were cultured in liquid media, and growth was examined by 5-fold serial dilutions on YPD plates with or without 40 mg/ml Benomyl at 34 °C after 4 days.

Consequently, in order to test whether recruitment of TRiC into Htt aggregates leads to further TRiC impairment, cells were assayed for sensitivity to the microtubule-depolymerizing drug benomyl. The growth defect displayed on benomyl containing plates was initially used to describe TRiC dysfunction in *tcp1-2* mutant cells (Ursic *et al.*, 1994). Wild-type cells expressing Htt96Q did not show increased sensitivity to benomyl compared to cells expressing Htt20Q (Figure46). *tcp1-2* mutant cells expressing Htt20Q possessed a slight growth defect compared to wild-type cells, reflecting TRiC deficiency conferred by mutation in the *TCP1* gene. Remarkably, Htt96Q caused a profound growth defect in *tcp1-2* cells (Figure 46). Thus, TRiC activity seems to be further reduced via recruitment of TRiC subunits (or the TRiC complex) into Htt aggregates, likely accounting for the increased polyQ toxicity in *tcp1-2* cells.

Based on these results, TRiC is an important modulator of polyQ aggregation and toxicity. Generally, decreased TRiC activity facilitates the formation of detergent-resistant inclusions. Depending on the properties of polyQ expansion proteins, this increased aggregate formation appears to have different consequences for cellular toxicity. Increased aggregation can either reduce the accumulation of toxic, soluble species, as in the case of Htt96Q-GFP, or even generate toxic species, as presumably in the case of Htt96Q. Moreover, increased aggregation might also compromise the quality control system, especially those components that are of low abundance and cannot be up-regulated, such as the chaperonin TRiC.

4.2.2 Influence of TRiC overexpression on the properties of mutant Htt

Like the mutational analysis of chaperones, overexpression of chaperones in yeast has also been helpful in elucidating their role in modulating polyQ protein aggregation and toxicity (Krobitsch and Lindquist, 2000; Muchowski *et al.*, 2000; Meriin *et al.*, 2002). Although several members of different chaperone families are known to affect polyQ aggregation and toxicity, overexpression of TRiC has not been investigated.

4.2.2.1 Suppression of detergent-resistant aggregate formation

To test whether TRiC is involved in suppressing aggregation and toxicity of polyQ proteins, a yeast strain overexpressing all eight TRiC subunits was constructed. To this end, *TCP1* and *TCP7*, *TCP2* and *TCP3*, *TCP4* and *TCP5* as well as *TCP6* and *TCP8* were cloned pairwise, with each gene under an individual galactose inducible promoter, into yeast expression vectors. Wild-type cells were cotransformed with these four plasmids and induction and assembly of TRiC was analyzed. These cells produced significantly increased amounts of TRiC subunits (Figure 47A), and size exclusion chromatography revealed that the overexpressed subunits assembled into a complex with similar fractionation properties but 5 – 10-fold more abundant as endogenous TRiC (Figure 47B).

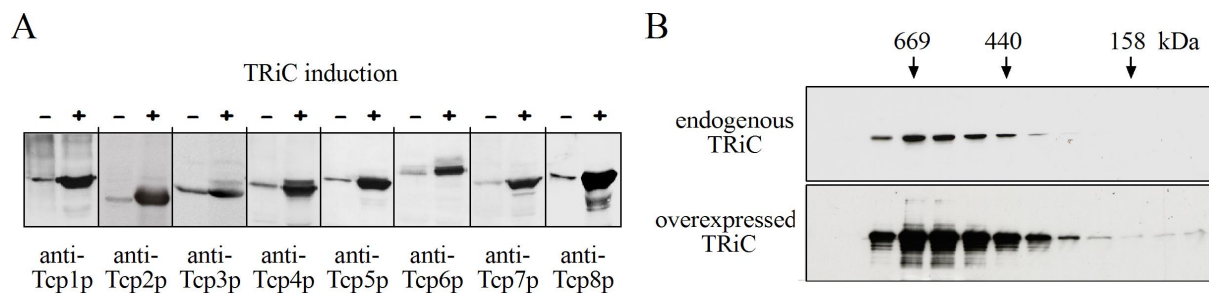


Figure 47: TRiC overexpression in wild-type yeast.

(A) Wild-type cells were grown with and without overexpression of TRiC subunits from galactose-inducible promoters for 20 h at 30 °C. Induction of TRiC subunits was analyzed by Western blot with indicated antibodies. (B) Soluble fractions derived from (A) were subjected to size exclusion chromatography on a Superose 6 column. Tcp5p was detected by Western blot with anti-Tcp5p antibody. Positions of size markers are indicated in kDa. This experiment was performed in cooperation with Dr. Ulrike Böttcher.

TRiC has been described to cooperate with Hsp70 in de novo folding of substrate proteins and in assisting their oligomeric assembly (Frydman *et al.*, 1994; Melville *et al.*, 2003; Siegers *et al.*, 2003). Whether these chaperones also cooperate in modulating polyQ protein aggregation and toxicity remains unclear. In order to address this, TRiC was overexpressed in yeast cells with reduced amount of cytosolic Hsp70s of the Ssa class

(*ssa1Δ/ssa2Δ*) or lacking the non-canonical, ribosome-associated Hsp70s Ssb1p and Ssb2p (*ssb1Δ/ssb2Δ*) (Figure 48A). Similar to wild-type yeast, these cells produced 5 – 10-fold higher levels of TRiC upon induction compared to uninduced cells (Figure 48B).



Figure 48: TRiC overexpression in chaperone deletion yeast.

(A) Wild-type, *ssa1Δ/ssa2Δ* and *ssb1Δ/ssb2Δ* cells were grown as above. The absence of Ssa1p/Ssa2p and Ssb1p/Ssb2p was confirmed by Western blot with indicated antibodies. Note that anti-Ssa1p and anti-Ssb1p also recognize Ssa2p, Ssa3p, Ssa4p and Ssb2p, respectively. (B) Cells were grown as in (A) with and without TRiC overexpression. Induction of TRiC was analyzed in lysates by Western blot with anti-Tcp5p antibody.

The effect of TRiC overexpression on polyQ protein aggregation was analyzed in wild-type, *ssa1Δ/ssa2Δ* and *ssb1Δ/ssb2Δ* yeast cells. In addition to the four *TCP* expression vectors, the corresponding cells were transformed with different Htt constructs under control of copper-inducible promoters and formation of SDS-insoluble aggregates was analyzed by filter retardation assay. Increased expression of TRiC in wild-type yeast cells markedly inhibited the formation of SDS-insoluble aggregates of Htt96Q and of Htt96QΔP-GFP (Figure 49A). Similar results have been reported in mammalian cells (Kitamura *et al.*, 2006).

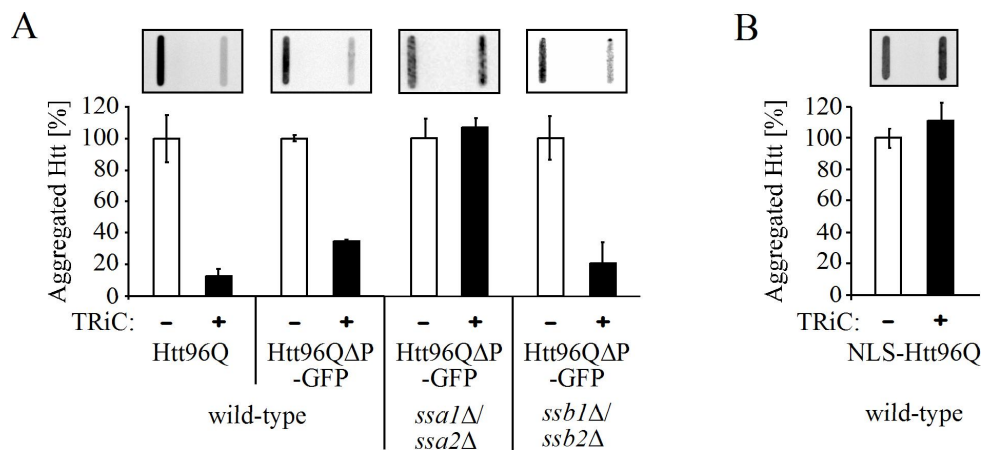


Figure 49: TRiC overexpression affects Htt aggregation.

(A) myc-tagged Htt96Q and Htt96QΔP-GFP were expressed under *CUP1* control in wild-type, *ssa1Δ/ssa2Δ* and *ssb1Δ/ssb2Δ* yeast cells for 24 h at 30 °C with and without TRiC overexpression. SDS-insoluble aggregates in lysates were analyzed by filter assay and myc-Htt96Q and Htt96QΔP-GFP were immunodetected with anti-myc and anti-GFP antibody, respectively. Amounts of aggregates without TRiC overexpression were set to 100 %. (B) SDS-insoluble aggregates from wild-type cells expressing myc-tagged NLS-Htt96Q were analyzed as in (A).

In *ssa1Δ/ssa2Δ* cells, however, TRiC overexpression failed to reduce Htt aggregation (Figure 49A). In contrast, normal inhibition of Htt aggregation by TRiC was observed in *ssb1Δ/ssb2Δ* cells (Figure 49A). Intriguingly, TRiC overexpression in the cytosol did not affect formation of SDS-insoluble aggregates of NLS-Htt96Q, which is targeted to the nucleus via a nuclear localization sequence (NLS) (Figure 49B). Thus, TRiC modulates polyQ aggregation in cooperation with the canonical Hsp70s only in the cytosol. In agreement with this result, TRiC and Hsp70/Hsp40 have also been demonstrated to alter polyQ aggregation cooperatively *in vitro* (Behrends *et al.*, 2006).

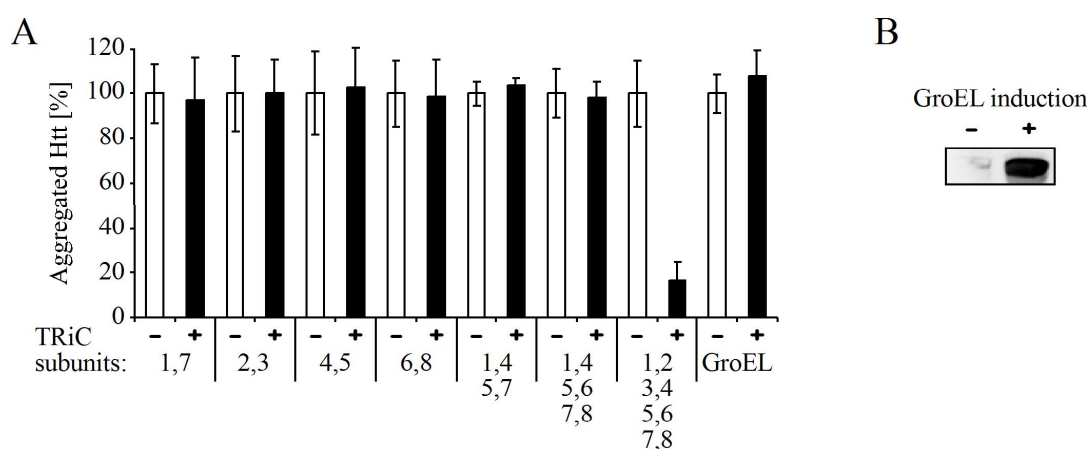


Figure 50: Overexpression of various TRiC subunit combinations does not affect Htt aggregation.

(A) myc-tagged Htt96Q was expressed under *CUP1* control in wild-type cells for 24 h at 30 °C with and without overexpression of indicated TRiC subunits or bacterial GroEL. SDS-insoluble Htt aggregates were analyzed by filter assay following immunodetection with anti-myc antibody. Amounts of aggregates without TRiC overexpression were set to 100 %. (B) GroEL was detected in lysates by Western blot with anti-GroEL antibody.

To exclude the possibility that the observed modulation of polyQ aggregation is mediated by single and distinct TRiC subunits rather than the complete TRiC complex, various subunit combinations were analyzed regarding their effect on formation of SDS-insoluble aggregates by Htt. Remarkably, TRiC-dependent inhibition of Htt aggregation was only seen upon overexpression of all TRiC subunits but not of various TRiC subunit combinations (Figure 50A). Moreover, expression of the bacterial chaperonin, GroEL, a distant homolog of TRiC, also failed to reduce the formation of SDS-resistant Htt aggregates (Figure 50A), although GroEL was expressed (Figure 50B) and is functionally active in yeast (Kerner *et al.*, 2005). Similarly, *in vitro*, GroEL fail to prevent the formation of SDS-resistant aggregates (G. Schaffar and C. Langer, personal communication). Thus, the TRiC complex and not single TRiC subunits mediate the inhibitory effect on Htt aggregation. Furthermore,

the eukaryotic chaperonin TRiC appears to interact with certain structural features in substrate proteins that are not recognized by the bacterial chaperonin GroEL.

4.2.2.2 Generation and accumulation of detergent-soluble polyQ oligomers

Since TRiC inhibited Htt aggregation, it was of interest to determine whether the amount of SDS-soluble Htt exon 1 fragments increased in the presence of overexpressed TRiC. Western blot analysis revealed that there were 2 – 3 fold higher amounts of SDS-soluble Htt96Q and Htt96Q Δ P-GFP upon TRiC induction (Figure 51A). In contrast, the expression level of Htt25Q Δ P-GFP was unchanged, indicating that TRiC overexpression did not unspecifically affect the expression of polyQ constructs (Figure 51A). Consistent with the inability of TRiC to suppress the aggregation of NLS-Htt96Q, the amount of SDS-soluble NLS-Htt96Q did not increase (Figure 51A). Immunofluorescence analysis showed that whereas Htt96Q and Htt96Q Δ P-GFP formed large aggregates in wild-type cells, both constructs displayed diffuse cytoplasmic staining in TRiC overexpressing cells (Figure 51B). Thus, TRiC inhibits the formation of SDS-insoluble aggregates and favors the formation of SDS-soluble species.

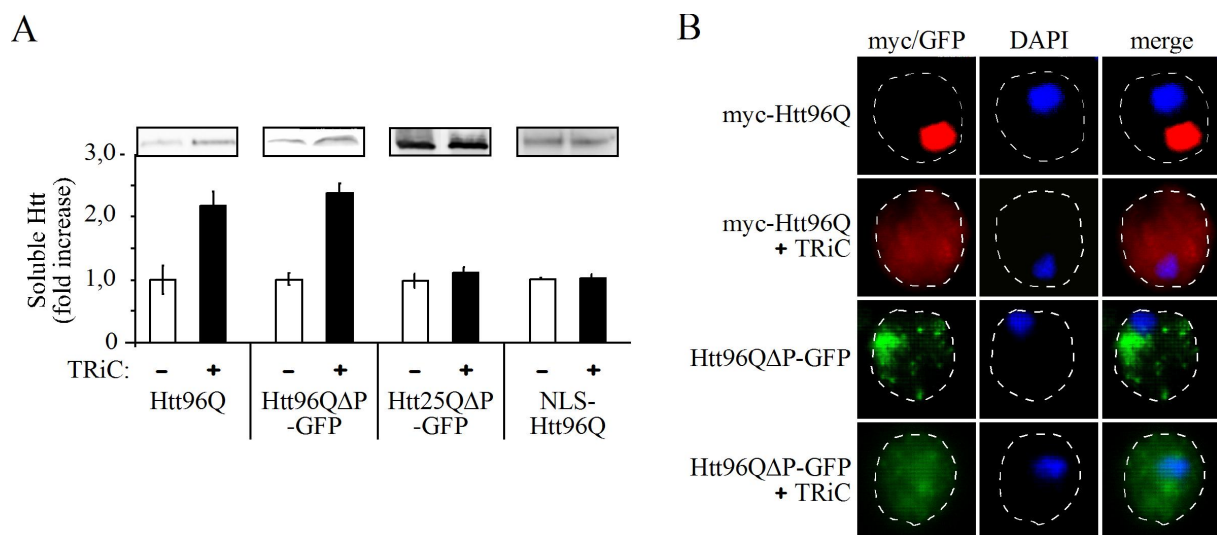


Figure 51: TRiC overexpression increases fraction of SDS-soluble Htt.

(A) myc-tagged Htt96Q, myc-tagged NLS-Htt96Q, Htt25Q Δ P-GFP and Htt96Q Δ P-GFP constructs were expressed under control of *CUPI* in wild-type cells for 24 h at 30 °C with and without TRiC overexpression. The amount of SDS-soluble Htt in lysates was analyzed by Western blot, and myc-tagged Htt and Htt-GFP were detected with anti-myc or anti-GFP antibody, respectively. The amount of Htt without TRiC overexpression was set to 1. **(B)** Cells derived from (A) were analyzed by indirect immunofluorescence with anti-myc antibody coupled to Cy3-conjugated secondary antibody and by GFP fluorescence, respectively. Nuclei were counterstained with DAPI.

Small amounts of polyQ protein were co-immunoprecipitated with antibodies against various TRiC subunits (Figure 52A). Intriguingly, Htt96Q Δ P-GFP but not Htt25Q Δ P-GFP was pulled down together with overexpressed His-tagged TRiC from lysates (Figure 52B). The N-terminal His-tag on TRiC subunit Tcp1p did not interfere with assembly of the overexpressed TRiC. His-tagged Tcp1p fractionated at a similar size as shown for the endogenous TRiC complex (Figure 52C and Figure 47B), and Tcp5p cofractionated with His-tagged Tcp1p (Figure 52C). Hence, the chaperonin TRiC interacts weakly with soluble expanded polyQ protein.

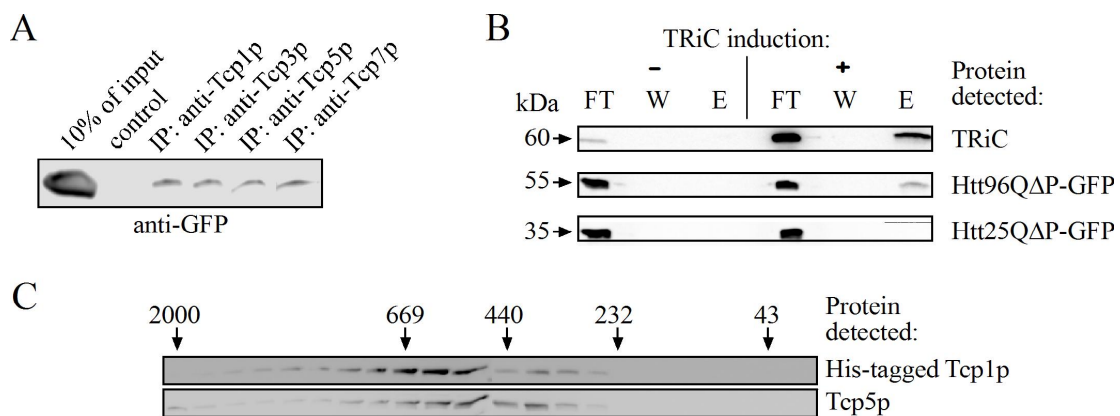


Figure 52: A fraction of soluble Htt associates with TRiC.

(A) Htt96Q Δ P-GFP and TRiC were coexpressed in wild-type cells for 24 h at 30 °C. Soluble lysates (20,000 x g) were immunoprecipitated with antibodies against Tcp1p, Tcp3p, Tcp5p and Tcp7p or control antibody. Precipitates were Western blot with anti-GFP antibody. 10 % of input is shown for comparison. (B) Htt25Q Δ P-GFP, Htt96Q Δ P-GFP and His-tagged TRiC were coexpressed as in (A). NiNTA pull down from soluble lysates via His-tagged Tcp1p was analyzed by Western blot. Htt-GFP and Tcp5p were detected with anti-GFP and anti-Tcp5 antibodies, respectively. Flow through (FT), wash (W) and eluate (E) are shown. (C) Size exclusion chromatography (Superose 6 column) of lysate derived from (B) followed by Western blot and detection of His-tagged Tcp1p and Tcp5p with anti-His and anti-Tcp5p antibodies, respectively. Positions of size markers are indicated in kDa.

The effect of TRiC overexpression on the SDS-soluble fraction of Htt exon 1 fragments was analyzed in more detail by centrifugation and size exclusion chromatography. In wild-type cells, Htt96Q was almost absent from the supernatant and exclusively found in the pellet fraction. Upon TRiC induction, Htt96Q was largely recovered in the supernatant fraction upon centrifugation (Figure 53A). While no soluble Htt96Q was recovered upon size exclusion chromatography of extracts in the absence of TRiC overexpression, TRiC overexpressing cells contained large amounts of Htt96Q that fractionated around 440 kDa (Figure 53B). The distribution of TRiC and of cytosolic Hsp70 (Ssa proteins) did not overlap with that of the polyQ oligomers. Strikingly, gel filtration analysis of *in vitro* Htt aggregation

in the combined presence of TRiC and Hsp70/Hsp40 but not with any of these chaperones alone revealed the formation of similar sized Htt oligomers (Behrends *et al.*, 2006). Thus, the two chaperone systems seem to cooperatively modulate Htt aggregation.

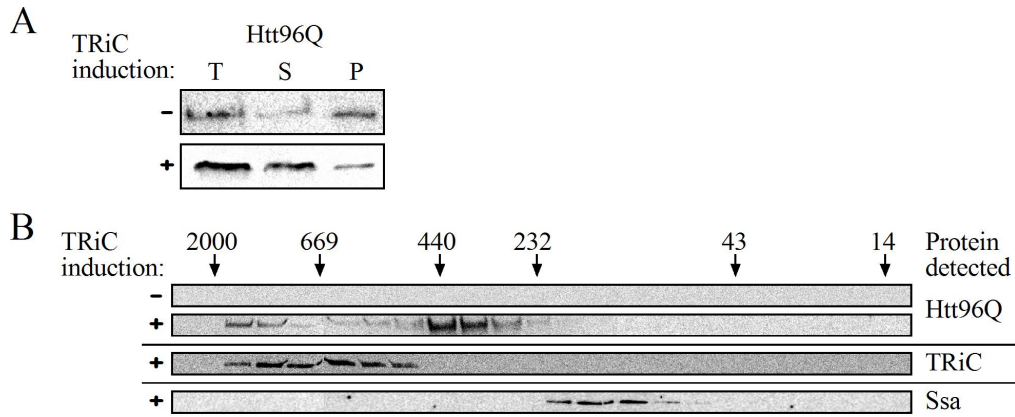


Figure 53: Characterization of TRiC modulated soluble Htt species.

(A) myc-tagged Htt96Q was expressed under control of *CUP1* in wild-type cells with and without TRiC overexpression for 24 h at 30 °C. Distribution of myc-Htt96Q upon centrifugation at 20,000 x g (30 min) was analyzed by Western blot followed detection with anti-myc antibody. Total (T), supernatant (S) and pellet (P) fractions are shown. (B) Soluble fractions analyzed in (A) were subjected to size exclusion chromatography on a Superdex 200 column followed by Western blot. Htt96Q was detected with anti-myc antibody and TRiC and Ssa protein with anti-Tcp5p and anti-Ssa antibody, respectively. Positions of size markers are indicated in kDa.

4.2.2.3 Cooperative and effective modulation of toxic, oligomeric aggregation intermediates

Htt96Q Δ P-GFP, unlike Htt96Q, is known to cause a polyQ-length dependent growth defect of yeast cells (Meriin *et al.*, 2002) (Figure 54A). This distinct property of Htt96Q Δ P-GFP was exploited to address whether TRiC is able to suppress polyQ toxicity. Remarkably, overexpression of TRiC efficiently suppressed the growth defect caused by Htt96Q Δ P-GFP. In contrast, overexpression of Ssa1p and its Hsp40 co-chaperone, Ydj1p, did not rescue the growth defect, suggesting that TRiC is limiting in suppressing polyQ protein toxicity. Strikingly, overexpression of TRiC in *ssa1* Δ /*ssa2* Δ but not in *ssb1* Δ /*ssb2* Δ cells failed to suppress the growth defect caused by Htt96Q Δ P-GFP, in support of the conclusion that TRiC and the canonical Hsp70 must cooperate in alleviating polyQ proteotoxicity in the yeast system. The growth defect of Htt96Q Δ P-GFP in wild-type yeast depends on the prion state of Rnq1, which is indicated by the insolubility of Rnq1 protein (Meriin *et al.*, 2002; Duennwald *et al.*, 2006a) (Figure 54B). Importantly, TRiC suppressed toxicity of Htt96Q Δ P-GFP without affecting the solubility of Rnq1p (Figure 54B).

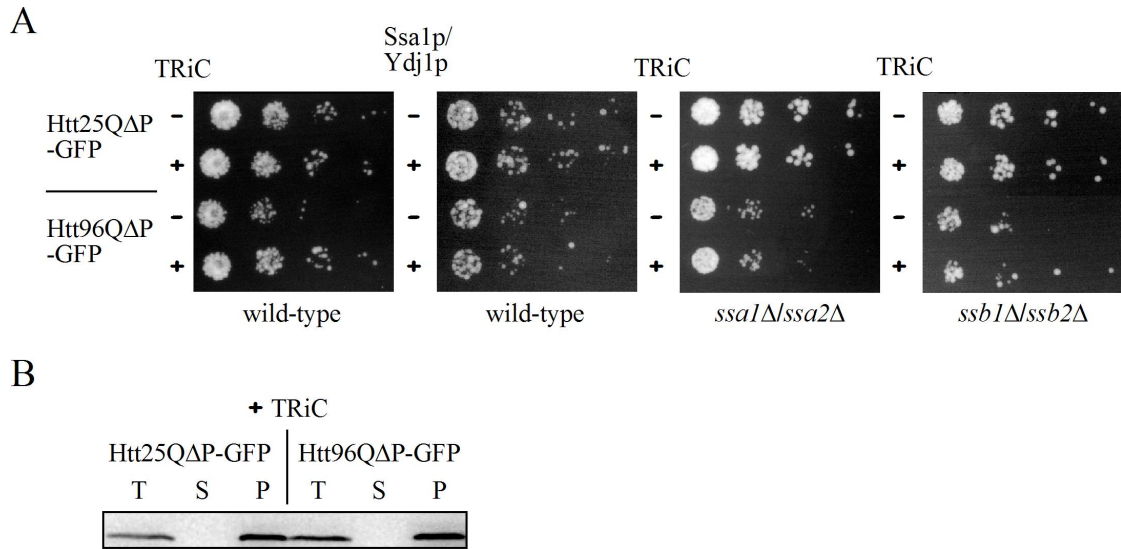


Figure 54: Effect of TRiC overexpression on polyQ toxicity.

(A) Growth of wild-type, *ssa1Δ/ssa2Δ* or *ssb1Δ/ssb2Δ* cells expressing Htt25Q-GFP or Htt103Q-GFP under control of *CUP1* with and without overexpression of TRiC or Ssa1p/Ydj1p was examined by 5-fold serial dilutions on SC plates after 2 days at 37 °C. (B) Htt25Q-GFP, Htt103Q-GFP and TRiC were coexpressed in wild-type cells for 24 h at 30 °C. The distribution of Rnq1p upon centrifugation at 100,000 x g was analyzed by Western blot with anti-Rnq1p antibody. Total (T), supernatant (S) and pellet (P) fractions are shown.

Failure of suppression of toxicity by the Hsp70 and Hsp40 chaperones, Ssa1p and Ydj1p, was not due to inefficient overexpression of the two chaperones. Cells produced ~3-fold higher levels of Ssa1p and Ydj1p upon induction compared to uninduced cells (Figure 55A). Likewise, Ssa1p and Ydj1p markedly inhibited the formation of SDS-insoluble Htt aggregates (Figure 55B).

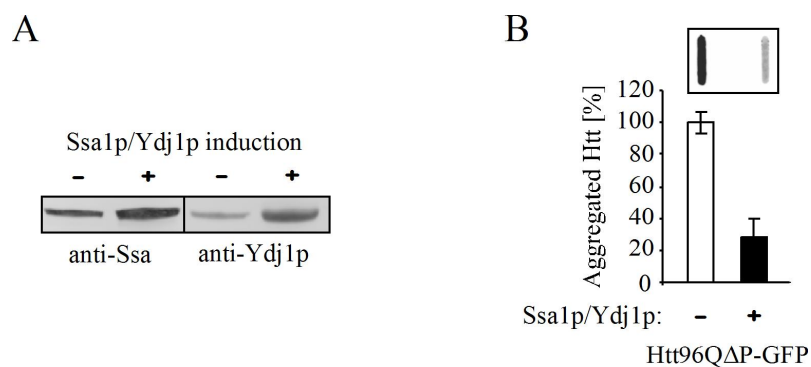


Figure 55: Ssa1 and Ydj1 overexpression reduces Htt aggregation.

(A) Wild-type cells were grown with and without overexpression of Ssa1p and Ydj1p from galactose-inducible promoters for 24 h at 30 °C. Induction of Ssa1p and Ydj1p was analyzed by Western blot followed detection with indicated antibodies. (B) Htt96QΔP-GFP was expressed under control of *CUP1* as in (A). SDS-insoluble aggregates in lysates were analyzed by filter assay followed by immunodetection with anti-GFP antibody. Amounts of Htt aggregates without TRiC overexpression were set to 100 %.

To understand how TRiC suppresses toxicity, lysates derived from cells expressing Htt96Q Δ P-GFP were analyzed by centrifugation. In cells with endogenous TRiC levels, Htt96Q Δ P-GFP was largely present in the pellet and only a minor amount was recovered in the supernatant fraction. TRiC overexpression reversed this ratio. Htt96Q Δ P-GFP was mainly found in the supernatant and to some smaller extent in the pellet fraction (Figure 56A).

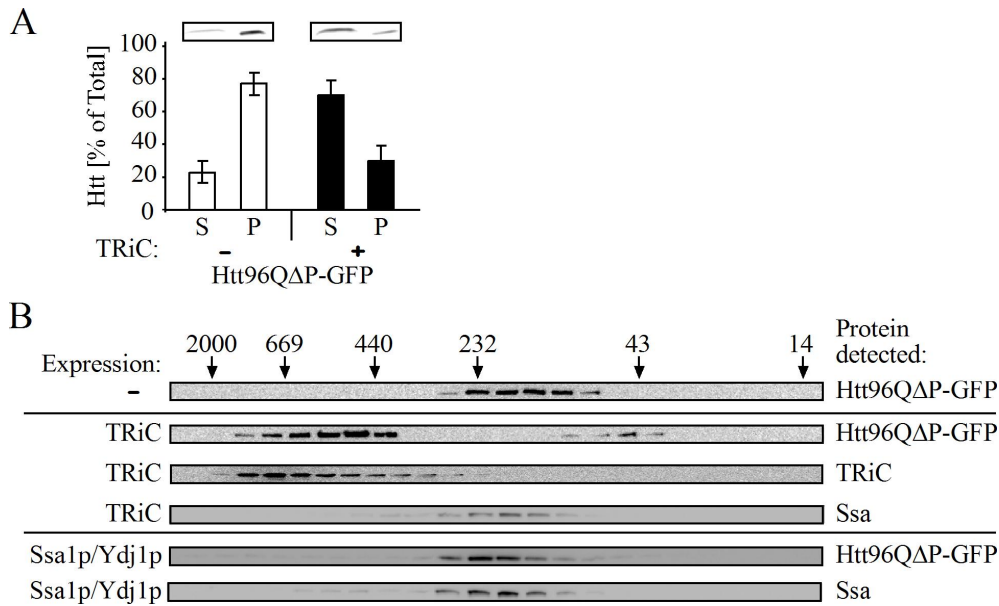


Figure 56: TRiC modulates toxic soluble Htt species.

(A) Htt96Q Δ P-GFP was expressed under control of *CUPI* in wild-type cells with and without TRiC overexpression for 24 h at 30 °C. Distribution of Htt96Q Δ P-GFP upon centrifugation at 20,000 x g (30 min) was analyzed by Western blot followed by detection with anti-GFP antibody and quantification. Supernatant (S) and pellet (P) fraction are shown. (B) Htt96Q Δ P-GFP was expressed as in (A) with and without overexpression of TRiC or Ssa1p/Ydj1p. Soluble fractions were subjected to size exclusion chromatography followed by Western blot. Htt96Q Δ P-GFP was detected with anti-GFP antibody and TRiC and Ssa protein with anti-Tcp5p and anti-Ssa antibody, respectively. Positions of size markers are indicated in kDa.

Size exclusion chromatography of extracts from cells with normal TRiC levels showed the presence of Htt96Q Δ P-GFP oligomers of ~200 kDa, which were not populated upon expression of Htt96Q (Figure 56B and Figure 53B). Strikingly, overexpression of TRiC prevented the formation of ~200 kDa Htt96Q Δ P-GFP species and produced an increased amount of Htt96Q Δ P-GFP fractionating at ~500 kDa, comparable to the oligomers of Htt96Q formed upon TRiC overexpression (Figure 56B and Figure 53B). A minor fraction of unassembled Htt96Q Δ P-GFP was detected at ~50 kDa. Overexpression of Ssa1p/Ydj1p at normal TRiC levels did not prevent the formation of ~200 kDa oligomers, in line with the failure of Ssa1p/Ydj1p to rescue the growth defect caused by Htt96Q Δ P-GFP (Figure 56B).

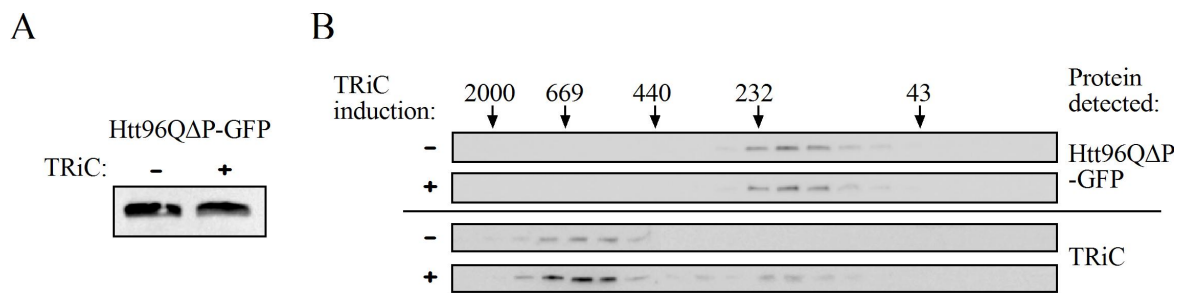


Figure 57: TRiC requires cooperation with Ssa for modulation of toxic soluble Htt species.

(A) Htt96QΔP-GFP was expressed in *ssa1Δ/ssa2Δ* cells with and without TRiC overexpression as before. Lysates were analyzed by Western blot and Htt96QΔP-GFP was detected with anti-GFP antibody. (B) Soluble fractions from (A) were subjected to size exclusion chromatography followed by Western blot. Htt96QΔP-GFP was detected with anti-GFP antibody and TRiC with anti-Tcp5p. Positions of size markers are indicated in kDa.

Consistent with the result above, overexpression of TRiC in *ssa1Δ/ssa2Δ* cells neither changed the level of SDS-soluble Htt96QΔP-GFP (Figure 57A), nor reduced the amount of the ~200 kDa oligomers (Figure 57B). Despite the fact that these cells produced 5 – 10-fold higher levels of TRiC compared to uninduced cells (Figure 57B). Thus, TRiC appears to profoundly modulate the aggregation pathway of mutant Htt in cooperation with the canonical Hsp70, resulting in the elimination of presumably toxic oligomeric species in favour of the generation of apparently benign Htt oligomers.

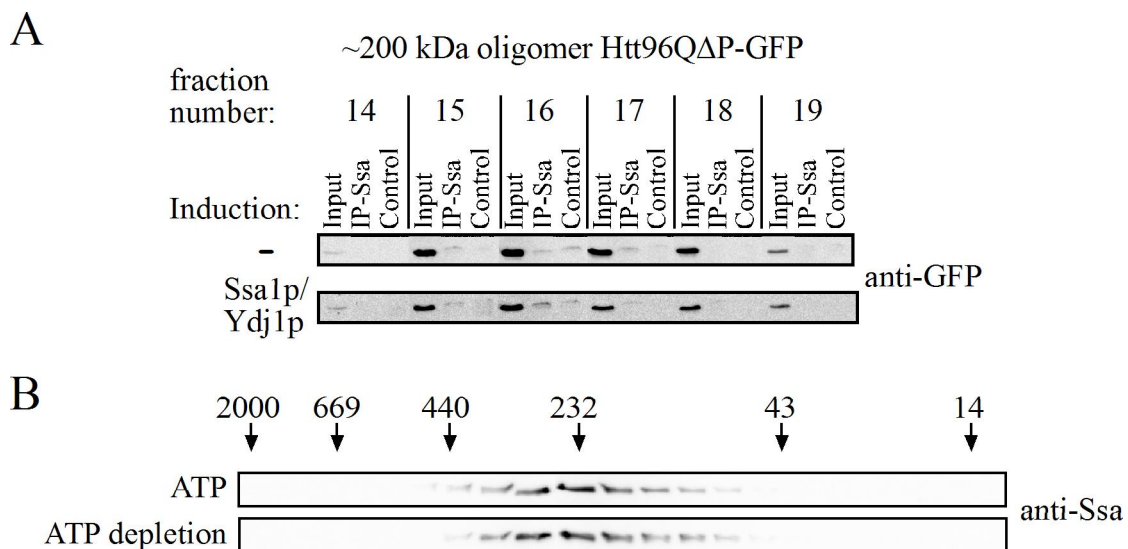


Figure 58: Toxic soluble Htt oligomers are not associated with Ssa.

(A) Htt96QΔP-GFP was expressed in wild-type cells with and without Ssa1p/Ydj1p overexpression as before. Soluble fractions were subjected to size exclusion chromatography followed by immunoprecipitation of the ~200 kDa peak fraction (14-19) with anti-Ssa1p or control antibodies. Precipitates were immunoblotted with anti-GFP antibody. 10 % of input is shown for comparison. (B) Wild-type cells from (A) were lysed in the presence of 10 mM ATP or 10 mM glucose, 20 U/ml hexokinase and 10 mM ADP (ATP depletion). Soluble fractions were subjected to size exclusion chromatography followed by Western blot with anti-Ssa1 antibody. Positions of size markers are indicated in kDa

The ~200 kDa and ~500 kDa Htt96Q Δ P-GFP oligomers partially co-fractionated with the Ssa Hsp70 chaperones and TRiC, respectively, (Figure 56B) but could neither be co-immunoprecipitated with anti-Ssa nor with anti-Tcp antibodies from the corresponding gel filtration fractions (Figures 58A and data not shown). Neither was the fractionation of Ssa altered by the presence of ATP or by ATP depletion (Figure 58B), suggesting that the Htt oligomers formed are no longer efficiently recognized by the ATP-dependent chaperone.

4.2.2.4 Structural differences between toxic and benign Htt oligomers

To characterize the ~200 kDa and ~500 kDa oligomers formed in the absence and presence of TRiC overexpression, respectively, in more detail, the corresponding gel filtration fractions were subjected to centrifugation at 100,000 x g. Remarkably, the ~200 kDa and ~500 kDa Htt96Q Δ P-GFP oligomers remained soluble and dissociated in SDS (Figure 59A).

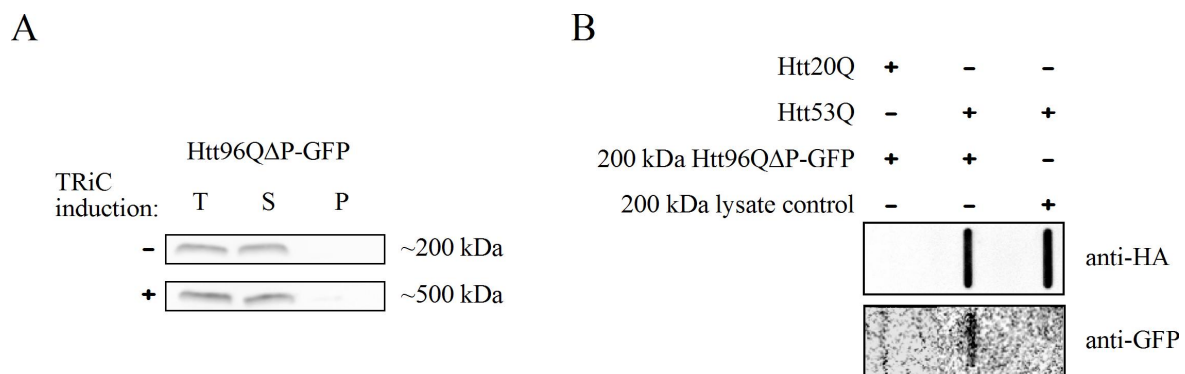


Figure 59: Solubility of Htt96Q Δ P-GFP oligomers and recruitment of oligomer into Htt aggregates.

(A) Distribution upon centrifugation at 100,000 x g (1 h) of ~200 and ~500 kDa Htt96Q Δ P-GFP oligomers obtained by size exclusion chromatography was analyzed by Western blot with anti-GFP antibody. Total (T), supernatant (S) and pellet (P) fractions are shown. (B) Proteins (3 μ M GST-Htt20Q and GST-Htt53Q) and gel filtration fractions (~200 kDa fraction of Htt96Q Δ P-GFP and lysate control) were incubated in the indicated combination. Aggregation reactions were started at 30 °C by addition of PreScission protease and stopped after 5 h by addition of SDS. Aggregated proteins were analyzed by filter assay and immunodetection as indicated.

To address whether the ~200 kDa Htt96Q Δ P-GFP oligomers are aggregation competent, recruitment of this species into Htt aggregates was analyzed *in vitro*. HA-tagged Htt20Q and Htt53Q were produced as N-terminal GST-fusion cleavable with PreScission protease. Upon incubation with PreScission protease, GST-Htt53Q but not GST-Htt20Q, formed SDS-insoluble Htt aggregates detectable by filter assay (Figure 59B) (Schaffar *et al.*, 2004). The ~200 kDa Htt96Q Δ P-GFP gel filtration fraction coaggregated with Htt53Q, but not with Htt20Q (Figure 59B). Consistently, the corresponding ~200 kDa gel filtration

fraction derived from lysate without Htt96Q Δ P-GFP expression did not show any SDS-insoluble aggregates (Figure 59B). Hence, the ~200 kDa Htt96Q Δ P-GFP oligomer likely represents an intermediate species on the aggregation pathway. Whether these oligomers are on- or off-pathway to aggregate formation remains to be established.

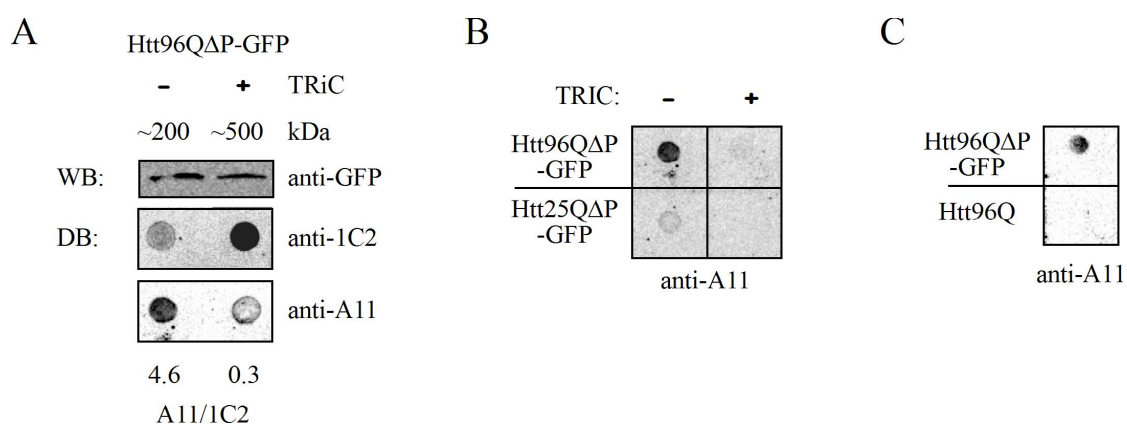


Figure 60: Epitope mapping of ~200 and ~500 kDa Htt96Q Δ P-GFP oligomers.

(A) Analysis of ~200 and ~500 kDa oligomers obtained by size exclusion chromatography of soluble lysates fractions, derived from cells expressing Htt96Q Δ P-GFP in the presence and absence of overexpressed TRiC, by Western blot (WB) with anti-GFP antibody and by dot blot (DB) with antibodies 1C2 and A11. The ratio of A11 to 1C2 signal is given below. (B) Dot blot analysis of ~200 kDa gel filtration fractions of Htt25Q Δ P-GFP and Htt96Q Δ P-GFP in the presence or absence of overexpressed TRiC with anti-A11 antibody. (C) Dot blot analysis of ~200 kDa gel filtration fractions of Htt96Q Δ P-GFP and Htt96Q by with anti-A11 antibody.

The conformational status of a protein can be judged by its aggregation state, which is determined by its solubility or by the size of the oligomer according to exclusion chromatography and gel electrophoresis. Size measurements can lack the desired resolution, however, and do not necessarily reflect the aggregation state under more physiological circumstances. Conformation-dependent antibodies have the potential to provide more detailed and sensitive information about the conformation of misfolded proteins.

A structural differentiation between the ~200 kDa and ~500 kDa Htt96Q Δ P-GFP oligomers was achieved based on their immunoreactivity with two different antibodies. Antibody 1C2 interacts with an epitope formed by expanded polyQ sequences (Trottier et al., 1995) and antibody A11 recognizes a sequence-independent structural feature common to soluble amyloid oligomers associated with toxicity (Kayed *et al.*, 2003). Comparable amounts of the two oligomers were analyzed, as determined by immunoblotting with anti-GFP antibody (Figure 60A). Strikingly, dot blot analysis in the absence of SDS showed that the ~200 kDa oligomers reacted only weakly with antibody 1C2 but were highly reactive with

A11 antibody, whereas the ~500 kDa oligomers were efficiently recognized by antibody 1C2 but essentially lacked A11 reactivity (Figure 60A). The immunoreactivity of the ~200 kDa oligomers with antibody A11 was specific since it depended on the presence of these oligomers in the absence of TRiC overexpression (Figure 60B). Likewise, corresponding gel filtration fractions of Htt25Q Δ P-GFP or Htt96Q did not show reactivity to antibody A11 above background in dot blot analysis (Figure 60B and Figure 60C). Thus, the two types of oligomer are clearly conformationally distinct with regard to exposure of the polyQ sequence. Moreover, reactivity with the generic amyloid oligomer antibody A11 would support the view that the ~200 kDa Htt96Q Δ P-GFP species is cytotoxic.

The interaction of the chaperonin TRiC with polyQ expanded fragments of huntingtin, implicated in HD, was explored in a yeast model. TRiC was found to interfere with polyQ fibril formation and proved to be a limiting factor in suppressing polyQ toxicity. Remarkably, the chaperonin cooperated with Hsp70 and Hsp40 in promoting the assembly of benign Htt oligomers of ~500 kDa. In combination with *in vitro* experiments (Behrends *et al.*, 2006), this process is reminiscent of the sequential action of Hsp70/Hsp40 and TRiC in assisting the folding of newly-synthesized proteins.

5 Discussion

In amyloid diseases, specific peptides or proteins misfold and give rise to highly ordered fibrillar aggregates. In Alzheimer's disease (AD), extracellular A β peptide deposition is thought to be intimately associated with the initiation of disease, whereas in certain forms of Parkinson's disease (PD), it is the intracellular formation of aggregates of the protein α -synuclein. Huntington's disease (HD) is caused by a mutant version of huntingtin (Htt), which results in an expansion of its polyglutamine (polyQ) segment and renders the protein aggregation-prone. The same type of mutation in otherwise unrelated proteins gives rise to a collection of other neurodegenerative polyQ diseases. Perinuclear inclusions of mutant Htt, or other polyQ-containing disease proteins, in brain tissue are a key feature of these disorders. However, the poor overlap between neurons with visible inclusions and neurons actually undergoing degeneration indicates that aggregates, although a hallmark of these diseases, are not sufficient to provoke neuronal damage. In addition, polyQ toxicity can be dissociated from the formation of inclusions in several cellular and animal model systems. The exact mechanism by which protein misfolding and aggregation is linked to disease is still unclear. In any case, misfolded disease proteins are supposed to act through a gain-of-function mechanism that eventually leads to cell death.

Increasing evidence indicates that the main toxic agents are soluble precursors of the disease proteins generated through the process of aggregation, rather than the mature insoluble fibrils. In a model for AD, A β oligomers instead of the mature amyloid fibrils have been demonstrated to exert neurotoxicity (Walsh *et al.*, 2002). Furthermore, the suppression of fibril deposition in intranuclear inclusions has even been shown to exacerbate the cellular toxicity of polyQ proteins, assigning a protective role to the mature fibrils (Saudou *et al.*, 1998). Thus, the oligomeric species formed in the pathway towards mature fibrils, present in a wide variety of misfolding diseases, may be the principal agents of toxicity. However, the possibility that mature fibrils may also contribute to neuronal toxicity should not be ruled out. In fact, soluble and aggregated polyQ might harm neurons via non-exclusive mechanisms (Michalik and Van Broeckhoven, 2003).

Although a number of different cellular events are known to be associated with HD, the actual pathogenic mechanisms remain unclear. Transcriptional dysregulation is hypothesized to be a common theme in polyQ pathogenesis (Cha, 2000; Sakahira *et al.*, 2002; Sugars and Rubinsztein, 2003). Such dysregulation might be mediated by several mechanisms. PolyQ proteins can directly interact with numerous transcription regulators, which have been found in polyQ inclusions. The expanded polyQ stretch in mutant Htt may result in sequestration of these proteins into perinuclear aggregates, leading to their functional depletion (Kazantsev *et al.*, 1999). However, given the evidence for a protective role of inclusions in disease, toxicity might be exerted by soluble aggregate precursors via aberrant interaction with transcription factors, thereby rendering them non-functional and disrupting transcriptional pathways. Molecular chaperones might counteract these aberrant protein interactions, presumably by shielding hydrophobic surfaces. Finally, the association of aggregating polyQ proteins with the quality control machinery may itself contribute to cellular toxicity (Sherman and Goldberg, 2001; Sakahira *et al.*, 2002). Misfolded proteins may sequester and/or non-productively engage components of the chaperone (and degradation) systems and consequently reduce their activity in the cell. The increased expression of chaperones frequently relieves toxicity associated with aggregation diseases.

The present study mechanistically dissected the contribution of aggregated and soluble, misfolded polyQ expansion proteins to cellular toxicity (Figure 61). Soluble oligomers of mutant Htt exon 1 deactivate transcription factors with normal polyQ repeats by a polyQ-mediated aberrant interaction. Importantly, this mechanism is independent of the formation of insoluble coaggregates. Furthermore, the analysis of how chaperones modulate polyQ-expanded proteins was expanded to a chaperone class previously not described in this context. The interaction of the chaperonin TRiC with mutant Htt and its cooperation with the Hsp70/Hsp40 chaperone system in modulating Htt aggregation and toxicity was analyzed in detail. TRiC interferes with polyQ fibril formation and proves to be limiting in suppressing polyQ toxicity. In cooperation with Hsp70/Hsp40, TRiC promotes the assembly of benign Htt oligomers. Thus, the mechanistic principles of chaperone cooperation between Hsp70 and TRiC employed in the pathway of de novo protein folding may also be utilized in the cellular defense against potentially toxic, amyloidogenic proteins.

5.1 PolyQ-induced transcriptional dysregulation

Transcriptional alterations have been reported to occur early in disease progression for various polyQ diseases (Sugars and Rubinsztein, 2003). Coordinated transcription requires the synchronization of many events and mechanisms that depend on the regulated trafficking and interaction of numerous proteins. Such proteins include DNA-binding transcription factors, non-DNA-binding co-regulators and components of the basal RNA-polymerase apparatus. In addition to the components involved in transcription, eukaryotic gene expression depends on other multi-protein complexes that carry out the additional steps of pre-messenger RNA processing and export of mRNA to the cytoplasm. These processes involved in gene expression are believed to form an extensive coupled network with proteins participating in more than one step (Maniatis and Reed, 2002; Reed, 2003). Notably, many regulators of transcription contain glutamine-rich activation domains that are typical of an extensive family of highly conserved transcriptional activators. These glutamine-rich activation domains are an important class of protein–protein interacting motifs that enable transcription factors to interact with one another and thus regulate gene expression (Tanese and Tjian, 1993).

The TATA-binding protein (TBP) is a general transcription factor and a crucial component of the core transcriptional complex, TFIID, which plays two important roles in the initiation of transcription for most eukaryotic genes (Gill and Tjian, 1992). Assembly of the TFIID complex is dependent on interactions between TBP and multiple TBP-associated factors. The TFIID complex is the first general transcription complex to bind to DNA, and this step is essential for initiating transcription by RNA polymerase II. TBP is the component of the TFIID complex that directs the complex to DNA by binding to the TATA-box (Roeder, 1991). Recently, a role for TBP in neurodegeneration has been described. TBP contains a polyQ stretch of 38 Q at its N-terminus, and expansion of this polyQ tract beyond 42 Q results in an autosomal dominant form of SCA17 (Koide *et al.*, 1999; Rolfs *et al.*, 2003). Furthermore, TBP is associated with aggregates in several polyQ disorders (Perez *et al.*, 1998; van Roon-Mom *et al.*, 2002). Thus, a reduction of the available TBP activity contributes to cellular toxicity in polyQ diseases.

5.1.1 Contribution of aggregated polyQ-expanded Htt

In HD, the elongated CAG repeat encoding a stretch of glutamines (Q) is located within the first exon of the gene encoding the protein Htt. PolyQ repeats in Htt below the threshold value of 35 are not associated with HD; repeats over 36 residues cause neurodegenerative dysfunction, and longer repeats are characterized by an earlier age of onset (Zoghbi and Orr, 2000). Expression of Htt exon 1 carrying the expanded CAG stretch recapitulates toxicity in transgenic mice and *C. elegans*, causing HD-like phenotypes (Mangiarini *et al.*, 1996; Morley *et al.*, 2002). *In vitro*, mutant Htt exon 1 typically forms large, SDS-resistant aggregates, which can be detected by membrane filtration through a 200 nm pore-sized membrane (Scherzinger *et al.*, 1997). For *in vivo* analysis of the aggregation of polyQ proteins, yeast and murine neuronal cells were used as model systems as described previously (Wang *et al.*, 1999; Krobitch and Lindquist, 2000).

Htt exon 1 with 20 Q was diffusely distributed in the cytoplasm and did not form aggregates regardless of the model system in which it was expressed. In contrast, expression of Htt exon 1 with an expanded polyQ tract resulted in the formation of SDS-insoluble perinuclear aggregates in both model systems (Figure 15 and 16). In yeast cells, the amount of Htt aggregates was found to correlate with the length of the polyQ stretch (Becher *et al.*, 1998), whereas in neuroblastoma cells aggregation of Htt53Q was most pronounced. This discrepancy may be attributed to the altered aggregation propensity of the distinct polyQ-expansion proteins in neuroblastoma cells, possibly due to protein modification or interaction with other proteins, and requires further investigation.

In addition to repeat length, the aggregation propensity of the polyQ repeat protein/peptide depends on sequence context (Nozaki *et al.*, 2001; Steffan *et al.*, 2004; Bhattacharyya *et al.*, 2006; Duennwald *et al.*, 2006b). *In vitro*, fusion of expanded Htt exon 1 to GST prevents its aggregation, allowing the expression and purification of mutant Htt as a soluble protein from *E. coli*; subsequent cleavage of the GST-part permits analysis of Htt aggregation under controlled conditions (Scherzinger *et al.*, 1997; Schaffar *et al.*, 2004). In yeast and neuroblastoma cells, aggregation of polyQ expanded Htt exon 1 with up to 96 Q has been found to be likewise inhibited in the sequence context of the GST fusion (Figure 15 and 16). Remarkably, the polyQ repeats in these GST fusion proteins are solvent-exposed, based on their ability to mediate recruitment into Htt aggregates, in contrast to GST alone (Figure

17). Consistently, GST-Htt53Q is accessible to protease digestion *in vitro* (Schaffar *et al.*, 2004). How the GST domain stabilizes the polyQ sequence of Htt exon 1 in a nontoxic conformation remains to be established, but it is an attractive possibility that the context of the authentic full-length huntingtin provides a similar protective effect. Intriguingly, aberrant Htt proteolysis and/or dysfunctional clearance of Htt fragments are suggested to underlie the neuropathology of HD, since N-terminal Htt fragments have been found to accumulate intracellularly in HD and mouse models (Gutekunst *et al.*, 1999; Kim *et al.*, 2001).

5.1.1.1 Sequestration and co-aggregation of TBP

Aggregates in polyQ disease patient's brains are not solely composed of the respective disease proteins, but rather contain a plethora of additional cellular proteins, including transcription factors carrying non-pathogenic polyQ repeats (Suhr *et al.*, 2001). This observation led to the hypothesis that sequestration into aggregates might deplete these factors away from their usual localization, thereby compromising their function and leading to toxicity (Cha, 2000). In fact, transcriptional dysregulation has been demonstrated to occur in polyQ diseases, but much remains to be elucidated to understand the underlying mechanisms.

In order to mechanistically dissect the recruitment of transcription factors into polyQ protein inclusions, co-aggregation of TBP was analyzed in the herein established cellular models systems for Htt aggregation. In yeast and murine neuronal cells, exogenous human TBP was located in the nucleus upon coexpression with normal Htt, whereas it was dislocated to the cytoplasm and coalesced with aggregates upon coexpression with mutant Htt. These co-aggregates were SDS-resistant and the amount of co-aggregated TBP correlated with the propensity of the expanded polyQ stretch to aggregate (Figure 15 and 16). In Htt-TBP co-aggregation reactions *in vitro*, TBP is almost exclusively recovered in the pellet fraction upon centrifugation. However, the majority of aggregated TBP can be solubilized with SDS, in contrast to aggregated Htt53Q (Schaffar *et al.*, 2004). Consistently, *in vivo* FRET experiments failed to detect an interaction of co-aggregated TBP and mutant Htt (Kim *et al.*, 2002), suggesting that the nature of TBP interaction with polyQ aggregates is markedly distinct from the self-association of polyQ expansion proteins. The recruitment process appears to be mediated by the polyQ segment in human TBP, since a mutant version of TBP, lacking the polyQ tract, fails to mislocalize and co-aggregate with mutant Htt (Schaffar *et al.*, 2004). While preexisting Htt inclusions have been shown to be recruitment incompetent, recruitment

seems to depend on the ongoing synthesis of mutant Htt (Schaffar *et al.*, 2004). Newly synthesized, diffusible Htt presumably drives the aberrant interaction with TBP. Consistent with the prevention of SDS-resistant aggregation, fusion to GST inhibits polyQ expanded Htt exon 1 fragments from sequestering TBP. The transcription factor is located in the nucleus regardless which GST-Htt construct is coexpressed (Figure 15 and 16). The toxic property of an expanded polyQ sequence, i.e., to interact aberrantly with the benign polyQ repeats of other proteins, seems to be structurally linked with its ability to nucleate self-oligomerization.

5.1.1.2 Prerequisites for Htt aggregation and TBP co-aggregation

The toxicity of the mutant protein in HD is believed to be unmasked upon proteolytic cleavage to release N-terminal fragments containing the expanded repeats (Luo *et al.*, 2005; Graham *et al.*, 2006). PolyQ repeats up to at least 53 Q are in an unstructured conformation when attached to GST (Masino *et al.*, 2002). Based on the *in vivo* observations herein, the polyQ segment in GST-Htt53Q is assumed to be solvent exposed. Analogous to *in vitro* experiments (Scherzinger *et al.*, 1997), aggregation of formerly soluble polyQ-expanded Htt exon 1 fragment fused to GST is initiated *in vivo*, in yeast cells, upon cleavage of the Htt part from the GST moiety (Figure 18). Similarly, aggregation of full-length polyQ expanded Ataxin-3 has been demonstrated to be initiated by proteolytic cleavage at an engineered, internal TEV protease cleavage site (Haacke *et al.*, 2006). Intramolecular FRET experiments *in vitro* indicate that a conformational rearrangement occurs in the polyQ-expanded Htt fragment upon its proteolytic release from its protective sequence context (GST), compatible with a compaction due to the formation of intramolecular β sheet structure in the mutant polyQ segment (Schaffar *et al.*, 2004). Consistent with this observation, the epitope of expanded-polyQ tracts has been shown to become rapidly inaccessible for the anti-polyQ antibody MW1 in an *in vitro* aggregation assay (Ehrnhoefer *et al.*, 2006). A similar conformational change may occur when N-terminal fragments resembling Htt exon1 are produced by proteolytic processing of full-length huntingtin.

Concomitant with the initiation of self-association, mutant Htt acquires the ability to induce the co-aggregation of TBP upon its proteolytic release from the GST part *in vivo* in the yeast model system (Figure 19). The structural rearrangement in the mutant polyQ segment presumably renders the expanded polyQ repeat capable of interacting with the benign polyQ segment in TBP. *In vitro*, intermolecular FRET between polyQ-expanded Htt molecules

monitors early events during Htt oligomerization (Schaffar *et al.*, 2004). TBP interferes with this FRET efficiency, consistent with the idea that ongoing Htt production is required for recruitment. Interaction with soluble polyQ-expanded Htt may be sufficient to affect the functional properties of the transcription factor, and sequestration into co-aggregates is likely to represent a secondary phenomenon. In fact, the co-aggregation of polyQ-expanded Htt and TBP observed *in vivo* may result from the expression of both proteins to high levels.

5.1.2 Contribution of soluble, misfolded polyQ-expanded Htt to toxicity

Alternative to the sequestration of transcription factors by recruitment into Htt aggregates, their concerted interactions among each other and/or with other cellular factors may be disrupted by soluble, misfolded polyQ expansion proteins. A number of nuclear transcription factors has been shown to interact directly with mutant Htt (Okazawa, 2003). DNA microarray studies have detected changes in gene expression profiles in HD transgenic mice, which are not necessarily associated with the formation of Htt aggregates (Luthi-Carter *et al.*, 2002a; Luthi-Carter *et al.*, 2002b). Altered expression levels in cell models can occur in the absence of inclusions (Kita *et al.*, 2002; Sipione *et al.*, 2002). To understand the mechanism by which soluble mutant Htt may interact with transcription factors to mediate early pathological changes prior to the formation of large inclusions, a cellular model system was established in yeast. Although yeast and human TBP share considerable homology, the N-terminal region encompassing the polyQ stretch is absent in yeast TBP (Kao *et al.*, 1990). Importantly, yeast TBP is essential for growth but can be functionally replaced by human TBP carrying the point mutation R231K in the C-terminal DNA binding domain (Cormack *et al.*, 1994). The TBP-dependent polyQ-toxicity model system consists of the *yTBPΔ/hTBP* yeast strain, in which yeast TBP is deleted and mutated human TBP (R231K) is expressed under control of the endogenous yeast TBP promoter (Schaffar *et al.*, 2004). These cells depend on the transcriptional activity of human TBP (Figure 21).

Expression of Htt exon 1 fragments with expanded polyQ in the cytoplasm resulted only in a mild growth defect of *yTBPΔ/hTBP* cells. However, targeting mutant Htt to the nucleus caused a pronounced, polyQ length-dependent growth impairment, which could be suppressed by the coexpression of yeast TBP (Figure 23). In wild-type yeast, mutant Htt did not result in toxicity whether its expression was directed to the cytosol or the nucleus. Thus, toxicity can be attributed to a polyQ-mediated deactivation of human TBP. Mutant Htt fused

to GST was without any effect on growth regardless of its cellular localization. Hence, the growth impairment by mutant Htt detected in the yeast model appears to require a conformational rearrangement of Htt upon its release from the GST moiety, as predicted based on the *in vivo* and *in vitro* experiments discussed above.

5.1.2.1 Influence of cellular localization on polyQ aggregation and toxicity

Cellular localization appears to influence the aggregation propensity of polyQ-expanded proteins. Mutant Htt with 53 Q and 96 Q formed substantially higher amounts of SDS-insoluble aggregates in the cytosol than in the nucleus (Figure 22). Consistently, polyQ aggregation has been observed to be most pronounced in the cytosol (Rousseau *et al.*, 2004). Neither a difference in expression levels between the nuclear and cytoplasmic Htt proteins nor aggregation inhibition by attachment of the nuclear localization sequence (NLS) could account for this effect. Thus, the formation of insoluble Htt aggregates appears to be retarded in the nuclear environment relative to the cytoplasm. Consistently, soluble polyQ-expanded Htt species were most abundant in the nucleus and almost absent in the cytosol (Figure 22). Expression of mutant Htt in the cytosol and nucleus of mouse and human neuroblastoma cells confirmed that Htt aggregation and the partitioning between aggregated and soluble polyQ species depended on cellular localization (Figure 30 and 32). Intriguingly, the amount of soluble but not aggregated Htt correlated with toxicity in *yTBPΔ/hTBP* cells. Moreover, not only the accumulation of soluble mutant Htt *per se* seemed to be necessary for toxicity but also its conformationally altered state (i.e. the acquisition of harmful intramolecular β -sheet structure) and its exclusive presence in the nuclear compartment (Figure 24 and 26). Consistent with the latter, nuclear translocation is an early step in pathogenesis in a HD mouse model and is required for neurotoxicity of other polyQ disease proteins (Klement *et al.*, 1998; Saudou *et al.*, 1998; Van Raamsdonk *et al.*, 2005).

Modification of mutant Htt in the nucleus might contribute to the observed modulation of Htt aggregation. In fact, mutant Htt can be modified either by ubiquitin or the small ubiquitin-like modifier SUMO-1 on identical lysine residues (Waelter *et al.*, 2001; Steffan *et al.*, 2004). Ubiquitination appears to reduce polyQ toxicity, presumably by promoting degradation (Tsai *et al.*, 2003), whereas SUMOylation stabilizes mutant Htt, reduces its ability to form aggregates and promotes its capacity to repress transcription. Furthermore SUMOylation exacerbates neurodegeneration in a *Drosophila* model of HD (Steffan *et al.*,

2004). Likewise, the absence of a microtubule-mediated process that concentrates microaggregates into large aggresome-type inclusions in the cytoplasm may play a role in the retardation of aggregation in the nucleus (Waelter *et al.*, 2001; Muchowski *et al.*, 2002). Alternatively, cytosolic factors, such as prions, might assist or catalyze expanded polyQ aggregation (Osherovich and Weissman, 2001; Meriin *et al.*, 2002). On the other hand, specific nuclear protein-protein interactions might contribute to the inhibition of aggregation in the nucleus (Cattaneo *et al.*, 2001).

5.1.2.2 *Significance of soluble, misfolded polyQ intermediates*

The amount of diffuse mutant Htt has been demonstrated to predict whether and when inclusion formation or cell death in neurons occur (Arrasate *et al.*, 2004). Likewise, kinetic analysis of the growth impairment relative to the progression of polyQ aggregation in *yTBPΔ/hTBP* yeast turned out to be highly informative concerning the contribution to toxicity of cytoplasmic and nuclear as well as soluble and aggregated polyQ species (Figure 25). Growth impairment has been observed shortly after induction of nuclear polyQ-expanded Htt but not upon expression of cytosolic Htt. In contrast, SDS-insoluble aggregates were formed almost immediately upon expression of cytosolic mutant Htt and only with a substantial delay upon expression of nuclear Htt. Concomitantly, while cytosolic polyQ-expanded Htt was essentially all insoluble, nuclear polyQ-expanded Htt was exclusively found in the soluble cellular fraction (Figure 26). Analysis of the oligomeric state of soluble polyQ-expanded Htt revealed a size between 70 and 120 kDa (Figure 26). These species may represent monomers and/or small oligomers of Htt (dimers and trimers), given that Htt constructs exhibit atypical physical properties and tend to fractionate greater than their nominal mass (Kazantsev *et al.*, 1999; Schaffar, 2004). Notably, NLS-Htt96Q has a calculated molecular mass of 23 kDa but migrates at 45 kDa in SDS-PAGE. However, association of polyQ-expanded Htt with other cellular factors cannot be ruled out at this point. Mutant Htt with the same fractionation properties was also observed in the nucleus of mouse and human neuroblastoma cells (Figure 30 and 32), suggesting a general role of the nuclear environment in allowing the accumulation and/or generation of such species.

Whether these oligomers are on- or off-pathway with regard to fibril formation remains to be determined. However, accumulating evidence has raised the possibility that precursors to amyloid fibrils, such as low-molecular weight oligomers and/or structured

protofibrils, are the primary pathogenic species in neurodegenerative disease (Caughey and Lansbury, 2003; Chiti and Dobson, 2006). For example, the severity of neurodegeneration in AD correlates with the levels of low-molecular-weight species of A β including small oligomers (McLean *et al.*, 1999). Moreover, the aggressive ‘Arctic’ mutation of the amyloid β precursor protein, associated with a heritable early-onset manifestation of AD, has been found to enhance protofibril formation (Nilsberth *et al.*, 2001). The toxic nature of prefibrillar aggregates extends far beyond AD and the A β peptide. Early, non fibrillar aggregates of transthyretin (TTR) associated with familiar amyloid polyneuropathy are toxic to neuronal cells (Sousa *et al.*, 2001). Recently, such toxicity has been demonstrated to originate from low-molecular-weight oligomers of TTR of up to \sim 100 kDa in size (Reixach *et al.*, 2004). In support of the relevance of these findings, prefibrillar forms of nondisease-related proteins are also highly toxic to cultured neurons, whereas the monomeric native states and the amyloid-like fibrils display no substantial toxicity (Bucciantini *et al.*, 2002).

5.1.2.3 Mechanism of transcription factor deactivation

The mechanism by which oligomers or prefibrillar aggregates exert toxicity to cells is a matter of intensive research. The conversion of a protein from its soluble state into oligomeric forms will invariably generate a wide distribution of nonnative, misfolded species that expose an array of structural features on their surfaces that are normally buried in globular proteins or dispersed in highly unfolded peptides or proteins (Chiti and Dobson, 2006). In the crowded and highly organized cellular environment, the nonnative character of misfolded oligomers likely triggers aberrant events resulting from their inappropriate interactions with other cellular factors (Ellis and Minton, 2006), possibly leading to the malfunctioning of crucial aspects of the cellular machinery.

Notably, toxicity in *yTBP Δ /hTBP* cells was most effective when the polyQ-expanded model protein was targeted to the nucleus, where small soluble oligomers reach apparently high local concentrations close to the sites of transcription. Indeed, the size fractionation properties of the transcription factor TBP in these cells were affected by nuclear polyQ-expanded Htt, but not by cytosolic mutant Htt or by fusion of GST to the nuclear polyQ-expanded protein (Figure 27). Upon expression of mutant Htt in the nucleus, TBP shifted from a well-defined complex of \sim 200 kDa in size to high molecular weight fractions between 200 and 800 kDa. A similar alteration of the fractionation properties was observed for

endogenous TBP in the presence of polyQ-expanded Htt in the nucleus of human neuroblastoma cells (Figure 32). This conformational interference of TBP (or TBP-containing transcription complexes) with polyQ-expanded Htt was found to be associated with impairment of the transcription initiation function of TBP in yeast and neuroblastoma cells. Furthermore, mutant Htt transiently associated with TBP and did not cause the formation of insoluble TBP/Htt coaggregates (Figure 29 and 31). In agreement with this, soluble rather than aggregated forms of mutant Htt have been demonstrated to directly dysregulate transcription by interfering with specific components of the transcription initiation complex (Zhai *et al.*, 2005). Deactivation of TBP depended on the presence of its polyQ segment, emphasizing the role of aberrant polyQ-polyQ interactions (Figure 29). Transcription factor molecules that are functionally compromised may populate misfolded and partially aggregated states or, alternatively, may be degraded.

The N-terminal part of TBP encompassing the polyQ-stretch has been presumed to regulate the DNA binding activity of the protein (Lescure *et al.*, 1994). Strikingly, *in vitro*, mutant Htt affects the function of TBP by inhibiting its binding to DNA (Schaffar *et al.*, 2004). The kinetics of TBP deactivation *in vitro* resembles that of the conformational change and early oligomer formation in mutant Htt detected by intramolecular FRET and is considerably faster than the formation of insoluble TBP/Htt coaggregates (Schaffar *et al.*, 2004). Moreover, polyQ-expanded Htt increases the protease sensitivity of TBP (Schaffar *et al.*, 2004). Thus, impairment of the functional conformation of TBP is likely to result from a structural destabilization of the protein induced by a transient, polyQ-mediated interaction with small, soluble oligomers of mutant Htt, before sequestration into aggregates occurs. This is consistent with observations of polyQ-mediated interference with transcription in the apparent absence of inclusions (Sugars and Rubinsztein, 2003).

The general relevance of this observation is supported by the fact that the soluble form of nuclear polyQ-expanded Htt similarly modulated the size fractionation properties of endogenous CREB binding protein (CBP) in human neuroblastoma cells concomitant with an impairment of cAMP-responsive-element (CRE)-mediated transcription in these cells (Figure 32). Of the transcription pathways that are affected in HD, the CRE-mediated pathway, in which CBP plays a central role as co-activator, is perhaps the most interesting because of its role in neuronal survival (Lonze and Ginty, 2002). Also, early downregulation of CRE-regulated genes is a feature of early human HD, and CRE-mediated transcription is

compromised by polyQ proteins (McCampbell *et al.*, 2000; Nucifora *et al.*, 2001; Wytenbach *et al.*, 2001; Jiang *et al.*, 2006). Since colocalization of CBP with polyQ aggregates yielded mixed results (Nucifora *et al.*, 2001; Yu *et al.*, 2002), soluble interactions between polyQ-expanded proteins and CBP may account for the dysregulation of CBP. Whether the described impairment of functional CBP conformation leads to toxicity remains to be demonstrated.

5.1.2.4 Influence of sequence context on polyQ aggregation and toxicity

Besides HD, there are eight other known neurodegenerative diseases caused by expanded CAG repeats, each involving the repeat expansion of polyQ in a different protein (Zoghbi and Orr, 2000). Similar conditions can be induced in animal models by expression of the polyQ sequence alone or in other protein contexts (Mangiarini *et al.*, 1996; Morley *et al.*, 2002). Apart from the polyQ sequence, the cellular context of the disease protein and the sequence context of the polyQ tract within the disease protein are both likely to contribute to the physical behavior of the polyQ protein and to pathology (Nozaki *et al.*, 2001; de Chiara *et al.*, 2005; Wetzel, 2005; Duennwald *et al.*, 2006b). Domains adjacent to the polyQ expansion are clearly important given the fact that polyQ proteins, both native and unnatural fusions, tend to aggregate more aggressively when non-glutamine domains are removed by proteolysis (Scherzinger *et al.*, 1997; Schaffar *et al.*, 2004; Haacke *et al.*, 2006).

In addition to the modulating effect of other domains on conformation, it seems possible that short sequence elements directly adjacent to the polyQ sequence, retained in protease-resistant fragments, may modulate aggregation efficiency (Nozaki *et al.*, 2001). One particularly interesting flanking sequence is the oligo-proline sequence found immediately C-terminal to the polyQ tract in Htt exon 1. A single proline residue interrupting an amyloidogenic sequence can decrease the ability of that sequence to aggregate (Thakur and Wetzel, 2002; Williams *et al.*, 2004). The presence of a proline-rich extension C-terminal to a polyQ tract modulates its conformational behavior and decreases its tendency to aggregate (Bhattacharyya *et al.*, 2006; Dehay and Bertolotti, 2006). From an evolutionary perspective, the oligo-proline sequences may help proteins avoid aggregation during synthesis and folding in the cell. In agreement with these findings, deletion of the proline-rich segment adjacent to the polyQ expansion has been found to enhance Htt aggregation in wild-type yeast cells (Figure 35). Importantly, increased aggregation did not correlate with enhanced toxicity in these cells (Figure 34), which are known to tolerate the expression of polyQ-expanded Htt

without overt growth impairment (Krobitsch and Lindquist, 2000; Muchowski *et al.*, 2000). This is in line with the assumption that cellular toxicity is unlikely to be conferred by aggregates of the disease protein themselves but rather by the process of their formation. Enhanced aggregation presumably alters the aggregation pathway depleting possible toxic aggregation intermediates.

Intriguingly, deletion of the proline-rich segment flanking the polyQ tract in Htt exon 1 in combination with heterologous fusion to GFP (Htt96Q Δ P-GFP) causes a pronounced growth defect, as reported previously (Meriin *et al.*, 2002). In contrast to recent observations (Duennwald *et al.*, 2006b), the toxicity of this construct did not depend on its N-terminal epitope tag but arose rather from the combined effect of deletion of the proline rich domain and fusion to GFP (Figure 34). Moreover, this particular polyQ-expanded Htt chimera not only displayed reduced aggregation propensity, but also accumulated in detergent-soluble form and was present in an oligomeric state of ~ 200 kDa (100 – 230 kDa) in size (Figure 35 and 36). Thus, the combined effect of deletion of the proline segment and fusion to GFP seems to impose a block on the path towards fibrillar Htt aggregates, retarding the formation of detergent-resistant inclusions and allowing the formation and accumulation of presumably toxic, oligomeric intermediates. These oligomers could not be recruited into aggregates when coexpressed with an aggregation prone mutant Htt construct, and thus toxicity persisted (Figure 37). The formation of these oligomers likely represents either a kinetically trapped intermediate in the polyQ aggregation pathway or an off-pathway oligomerization reaction.

These Htt oligomers resemble those generated by targeting polyQ-expanded Htt to the nucleus in *yTBP Δ /hTBP* cells. Strikingly, in these cells, the toxicity of Htt96Q Δ P-GFP was significantly increased compared to wild-type cells (Figure 38), indicating a partially similar mechanism of proteotoxicity as suggested for the oligomers formed by NLS-Htt96Q. Whether Htt96Q Δ P-GFP can also be found in the nucleus remains to be demonstrated. Intriguingly, fusion to a hydrophobic peptide converts polyQ-expanded Htt from a benign aggregation-prone species into a toxic, soluble species, which accumulate likewise as a ~ 200 kDa oligomer both *in vitro* and *in vivo* (Sarah Broadley, personal communication). Thus, several distinct polyQ-expansion proteins exert their toxicity in yeast through the formation of soluble oligomers, supporting the hypothesis that the soluble oligomeric form of amyloidogenic proteins might represent the principle pathogenic species (Caughey and Lansbury, 2003).

5.2 Molecular chaperones and polyQ expansion proteins

Chaperones assist proteins in folding into their native conformation, refold abnormally folded proteins and rescue previously aggregated proteins (Fink, 1999; Hartl and Hayer-Hartl, 2002). Consistently, the aggregation of various polyQ-containing disease proteins are modulated by chaperones (Cummings *et al.*, 1998; Chai *et al.*, 1999; Chan *et al.*, 2000; Krobisch and Lindquist, 2000; Muchowski *et al.*, 2000; Schaffar *et al.*, 2004). Hsp70 and Hsp40 chaperones can divert the polyQ aggregation pathway from the formation of fibrils to the generation of amorphous aggregates (Muchowski *et al.*, 2000; Schaffar *et al.*, 2004; Wacker *et al.*, 2004). FRET experiments suggest that the toxic oligomerization of mutant Htt begins with an intramolecular structural rearrangement of monomeric Htt (Schaffar *et al.*, 2004). Hsp70 and Hsp40 inhibit this intramolecular rearrangement, presumably by preventing monomeric Htt from achieving the β -sheet conformation necessary for the formation of mature fibrils (Schaffar *et al.*, 2004). Although Hsp70 interacts preferentially with extended sequences enriched in hydrophobic residues, glutamine is not excluded from binding (Sakahira *et al.*, 2002). Generally, overexpression of Hsp70 has been shown to improve disease phenotypes without visibly affecting aggregate formation (Warrick *et al.*, 1999; Cummings *et al.*, 2001). Thus, chaperones may not prevent aggregation per se, but rather redirect the aggregation process towards the formation of amorphous, non-amyloidogenic deposits, thereby presumably eliminating potentially toxic species.

In agreement with these observations, rescue of the growth defect in *yTBP Δ /hTBP* cells is achieved by coexpressing mammalian Hsp70 and Hsp40 (Hdj1) without changing the cellular levels of mutant Htt protein (Figure 23). *In vitro*, Hsp70 and Hsp40 preserves the functionality of TBP with regard to DNA binding in the presence of polyQ-expanded Htt (Schaffar *et al.*, 2004). In combination with aforementioned FRET experiments, Hsp70 and Hsp40 appears to interfere early with polyQ toxicity by retarding the conformational compaction of the polyQ disease protein and possibly by transiently shielding benign polyQ sequences in target proteins such as TBP. Through their conformational effect on the polyQ expansion protein, the chaperones may either facilitate the degradation of the potentially toxic agent or mediate its disposal in the form of nonfibrillar, disordered inclusions (Muchowski *et al.*, 2000).

5.2.1 Modulation of polyQ aggregation and toxicity by the chaperonin TRiC

Apart from the Hsp70 and Hsp40 chaperone system, the cytosolic chaperonin TRiC has recently been linked to polyQ aggregation (Nollen *et al.*, 2004). TRiC is a ~900 kDa cylindrical complex with ATPase activity consisting of 8 homologous subunits that are arranged in two octameric rings stacked back-to-back (Hartl and Hayer-Hartl, 2002; Spiess *et al.*, 2004). Unfolded proteins bind in the ring center, contacting multiple apical domains of the TRiC subunits, and are then transiently enclosed in the TRiC central cavity for folding in a process involving ATP-regulated movements of α -helical extensions of the subunits (Meyer *et al.*, 2003). Substrates may be presented to TRiC by Hsp70 and/or the co-chaperone prefoldin (Frydman *et al.*, 1994; Vainberg *et al.*, 1998; Siegers *et al.*, 2003). Moreover, TRiC appears to cooperate with Hsp70 in oligomeric protein assembly by transiently stabilizing protein subunits in assembly-competent conformations (Melville *et al.*, 2003). TRiC substrates include actins, tubulins, several WD40 repeat proteins and the Von-Hippel-Lindau (VHL) tumor suppressor protein (Frydman, 2001; Melville *et al.*, 2003; Siegers *et al.*, 2003). TRiC recognizes hydrophobic β -sheets in VHL and in the trimeric G protein β subunit (G β) and prevents aggregation of the latter *in vitro* (Feldman *et al.*, 2003; Kubota *et al.*, 2006). Given the importance of β -sheet structures in polyQ aggregation, TRiC may play an essential role in antagonizing their aberrant formation, thereby protecting against polyQ toxicity.

5.2.2 TRiC deficiency

Down-regulation of TRiC subunit expression has been shown to result in enhanced polyQ aggregation in *C. elegans* (Nollen *et al.*, 2004). This finding was reproduced in conditional TRiC-defective *tcp1-2* yeast cells. These cells have reduced TRiC activity due to a mutation in the equatorial ATP binding domain of the TRiC subunit Tcp1p (Ursic *et al.*, 1994). The formation of SDS-insoluble Htt aggregates was increased substantially upon expression of polyQ-expanded Htt in these cells. Immunofluorescence analysis of a Htt construct with polyQ-expansion close to the threshold-length of polyQ pathology of ~37 Q has nicely demonstrated this effect (Figure 39). Aggregation of the distinct Htt96Q Δ P-GFP construct was likewise increased, suggesting a general role of TRiC in modulating polyQ aggregation. Enhanced aggregation is unlikely a secondary effect of a loss of TRiC function in tubulin biogenesis, because disruption of the tubulin cytoskeleton is known to inhibit

formation of large polyQ inclusions (Muchowski *et al.*, 2002). Thus TRiC, at normal levels, profoundly modulates the aggregation properties of polyQ-expansion proteins.

Given the complexity of the cellular environment, it is plausible that chaperone actions may have differential impact on polyQ aggregation. For instance, increased aggregation of Htt96Q Δ P-GFP resulted in a decrease of the potentially toxic polyQ oligomers, consistent with an amelioration of the growth defect (Figure 41 and 42). Thus, preventing the accumulation of certain aggregation intermediates by redirecting the aggregation process is likely to alleviate polyQ toxicity. On the other hand, enhanced aggregation of Htt96Q due to TRiC deficiency caused pronounced toxicity (Figure 42). Similarly, downregulation of TRiC subunit expression by RNA interference has been shown to enhance polyQ aggregation and to cause increased polyQ toxicity in mammalian cells (Kitamura *et al.*, 2006; Tam *et al.*, 2006). In yeast, this phenotype specifically depended on TRiC, since it was suppressed by reintroducing a wild-type copy of the mutant TRiC subunit. In these cells, recruitment of TRiC into polyQ aggregates was considerable (Figure 43 and 44). Notably, TRiC has also been found to colocalize with polyQ aggregates in mammalian neuronal cells (Tam *et al.*, 2006). The increased sensitivity toward the microtubules-depolymerizing drug benomyl suggests that sequestration of TRiC may indeed lead to its functional depletion (Figure 46). Importantly, TRiC is not stress-inducible and of low abundance (Siegers *et al.*, 1999). Furthermore, different chaperone systems appear to be affected differentially by polyQ-mediated sequestration. For instance, colocalization of the cytosolic Hsp70 of the Ssa class into polyQ inclusions seemed to be counteracted by up-regulation of its expression (Figure 45). In addition, proteins trapped or associated with aggregates may exhibit distinct molecular interactions. While association of Hsp70 with polyQ aggregates is dynamic and transient (Kim *et al.*, 2002), detection of TRiC subunits in SDS-resistant Htt aggregates suggests a rather tight incorporation in these inclusions.

Hence, polyQ-expansion proteins may exceed the protective capacity of the cell. The levels of damaged or newly folded proteins and the available chaperone capacity are two sides of a carefully balanced system in cells. An excess of chaperone substrates or diminished chaperone content might induce a relative deficit of available active chaperones (Csermely, 2001). This chaperone overload may become especially prevalent in elderly subjects, in whom general protein damage is abundant (Gray *et al.*, 2003; Trojanowski and Mattson,

2003), and induction and function of quality control mechanisms are likely to be impaired (Keller *et al.*, 2002; Soti and Csermely, 2002). Sequestration of components of the quality control system may partially contribute to the amplification of this effect. Indeed, in a mouse model of HD, sequestration of chaperones into aggregates seems to decrease the amount of soluble chaperones available in the cell, thereby presumably enhancing abnormal protein folding (Hay *et al.*, 2004). Furthermore, in a *C. elegans* model of polyQ aggregation, the chronic expression of a misfolded protein appears to upset the cellular protein folding homeostasis (Gidalevitz *et al.*, 2006). Intriguingly, the human genome harbors numerous polymorphic variants and mutations that might be prevented from exerting deleterious effects by the protein quality control systems of the cell. However, should these mechanisms become overwhelmed, mild folding variants might contribute to disease pathogenesis by perturbing an increasing number of cellular pathways. Therefore, the complexity of pathogenic mechanisms identified for protein conformation diseases could in part result from the imbalance in protein folding homeostasis. These folding-defective proteins may in turn compromise the overall folding capacity of the cell and act as genetic modifiers of disease. In HD, this may contribute to the 40 % of the variance in age of onset that is not attributed to polyQ repeat length but to genes other than the HD gene (Wexler *et al.*, 2004).

5.2.3 TRiC overexpression

TRiC overexpression provided additional insights into the mechanism(s) of polyQ toxicity. The overexpression of TRiC is complicated by the fact that TRiC is a large, hetero-oligomeric complex consisting of two rings with eight orthologous subunits each. Overexpressing all eight TRiC subunits was achieved in yeast cells. Under these conditions, TRiC was significantly more abundant than in uninduced cells. Importantly, overexpressed TRiC assembled into a similar, high molecular weight complex as ‘wild-type’ TRiC (Figure 47). Thus, overexpression of TRiC likely produces an active chaperonin complex.

5.2.3.1 Modulation of aggregated polyQ-expanded Htt

Contrary to the situation in TRiC deficient yeast cells, overexpression of TRiC reduced the formation of detergent-resistant Htt aggregates (Figure 49). Secondary effects are unlikely to contribute to this inhibition, since the cytosolic chaperonin TRiC neither alters the level of Htt expression nor affects the aggregation of nuclear targeted polyQ-expanded Htt.

Similar results have recently been reported in mammalian neuronal cells (Kitamura *et al.*, 2006). The inhibitory effect on Htt aggregation required the functional TRiC complex and not single TRiC subunits (Figure 50). In contrast, a recent study suggests that single subunits could also contribute to the modulation of Htt aggregation (Tam *et al.*, 2006). This apparent contradiction is probably due to different overexpression conditions. Tam and colleagues expressed single subunits in wild-type cells to high amounts and large excess of unassembled TRiC subunits might interfere with Htt aggregation to some extent by unspecific binding. In the present study, combinations of single TRiC subunits were expressed in the genetic background of the TRiC overexpression strain, resulting in slower growth of these cells and lower amounts of overexpressed subunits. Under these conditions, unspecific interactions were likely reduced. Notably, GroEL from *E. coli* did not prevent the formation of Htt aggregates. Thus, the eukaryotic chaperonin TRiC appears to interact with certain structural features in substrate proteins that are not recognized by the bacterial chaperonin GroEL.

In vitro, purified bovine TRiC reduces the aggregation of polyQ-expanded Htt exon 1 fragment (Htt53Q) at equimolar and even at substoichiometric concentrations of TRiC relative to Htt (Behrends *et al.*, 2006). This effect is equally observed in the presence of ATP and in the absence of nucleotide. Aggregation prevention is mildly enhanced in the presence of ADP or the non-hydrolyzable ATP analog AMP-PNP. Intriguingly, these nucleotides are known to stabilize the acceptor state of the chaperonin for protein substrate (Meyer *et al.*, 2003). TRiC appears to function in this reaction by transiently binding the Htt protein with low affinity. Consistent with the proposed mechanism of chaperone-mediated modulation of polyQ aggregation (Scherzinger *et al.*, 1997; Muchowski *et al.*, 2000), TRiC blocks the formation of large polyQ fibrils in favor of shorter fibrillar structures *in vitro* (Behrends *et al.*, 2006). In this aggregation reaction, TRiC does not lead to the accumulation of considerable amounts of soluble polyQ-expanded Htt protein (Behrends *et al.*, 2006).

However, in the cellular context and concomitant with the inhibition of aggregate formation by Htt96Q, TRiC overexpression resulted in accumulation of SDS-soluble species, which were diffusely distributed throughout the cell (Figure 51). These soluble polyQ expansion proteins were present in an oligomeric complex of ~440 kDa (Figure 53). Importantly, this fractionation behavior cannot be attributed to association of polyQ-expanded Htt with TRiC or cytosolic Hsp70 (Ssa proteins), since the distribution of these chaperones did not overlap with that of the polyQ oligomers. Furthermore, the Htt oligomers seemed to

be no longer efficiently recognized by these chaperones. The discrepancy with the *in vitro* situation might be explained by the contribution of additional factors, possibly including other chaperones, to the modulation of Htt aggregation.

TRiC interacted directly with the soluble polyQ-expanded proteins (Figure 52). However, this interaction must be weak and transient, since it did not persist upon size exclusion chromatography. TRiC seems to interact with polyQ proteins via its substrate binding regions, since binding of denatured actin reduces the activity of TRiC in the aggregation assay (Behrends *et al.*, 2006). Thus, TRiC likely functions in this inhibitory reaction by transiently binding the Htt protein with relatively low affinity.

5.2.3.2 Modulation of soluble, misfolded and toxic polyQ-expanded Htt

Cytosolic TRiC not only prevents the formation of detergent-resistant Htt aggregates, but also acts on polyQ-expanded oligomeric species. Overexpression of TRiC inhibited the formation of the ~200 kDa oligomers formed by Htt96QΔP-GFP. In accordance with chaperone-mediated redirection of Htt aggregation, prevention of the formation of ~200 kDa oligomers concomitantly produced an increased amount of polyQ-expanded Htt fractionating at ~500 kDa (Figure 56). Neither of these oligomeric mutant Htt species was found to be associated with Hsp70 or TRiC, suggesting that these polyQ oligomers are not recognized anymore by those chaperones. Remarkably, these higher molecular weight oligomers are comparable to the oligomers of Htt96Q formed upon TRiC overexpression. Additionally, a minor fraction of Htt96QΔP-GFP may represent unassembled Htt.

Expression of Htt96QΔP-GFP caused a pronounced growth defect in wild-type cells that correlated with the presence of ~200 kDa Htt oligomers. Consistent with the elimination of this potentially toxic oligomeric species, overexpression of TRiC suppressed growth impairment (Figure 54). The ~500 kDa oligomers are likely benign, since they are not associated with toxicity. Notably, the toxicity of Htt96QΔP-GFP depends on the protein Rnq1p (Meriin *et al.*, 2002). Rnq1p is rich in asparagines and glutamines and belongs to a small class of proteins known as yeast prions. They are capable of adopting an alternate, self-perpetuating conformational state (Sondheimer *et al.*, 2001). Htt96QΔP-GFP only causes growth impairment, when Rnq1p is in its prion conformation (Meriin *et al.*, 2002). Importantly, overexpression of TRiC did not affect the prion conformation of Rnq1p,

suggesting that TRiC-mediated suppression of toxicity directly depends on its action on polyQ-expansion proteins. Thus, TRiC appears to profoundly modulate the aggregation pathway of mutant Htt, resulting in the elimination of presumably toxic oligomeric species in favour of the generation of apparently benign Htt oligomers.

5.2.4 Cooperation of TRiC with Hsp70 in altering aggregation and toxicity

Several studies have demonstrated an important role of the Hsp70/Hsp40 system in modulating polyQ aggregation and cytotoxicity (Muchowski and Wacker, 2005). Mammalian Hsp70 and Hsp40 (Hdj1) are known to slow polyQ aggregation and to increase the amount of proto-fibrillar oligomers and amorphous aggregates in an ATP-dependent manner (Muchowski *et al.*, 2000; Schaffar *et al.*, 2004; Wacker *et al.*, 2004). The cytosolic chaperonin TRiC cooperates with Hsp70 chaperones in de novo folding of a subset of newly synthesized polypeptides and in assisting the assembly of oligomeric protein complexes (Hartl and Hayer-Hartl, 2002; Melville *et al.*, 2003). A similar cooperation between TRiC and Hsp70 chaperone systems appears to exist for handling misfolded, aggregation-prone proteins. Overexpression of TRiC failed to suppress polyQ aggregation in cells having a reduced amount of cytosolic Hsp70 of the Ssa class (*ssa1Δ/ssa2Δ*), but not in cells lacking the noncanonical, ribosome-associated Hsp70 of the Ssb class (*ssb1Δ/ssb2Δ*) (Figure 49). Consistently, Htt exon 1 has been demonstrated to interact with TRiC and Ssa but not with Ssb *in vitro* (Tam *et al.*, 2006). Thus, TRiC seems to modulate polyQ aggregation in cooperation with the canonical Hsp70.

Likewise *in vitro*, addition of Hsp70/Hsp40, TRiC and ATP to an aggregation reaction of polyQ-expanded Htt (Htt53Q) produces almost exclusively SDS-soluble polyQ protein, which represented Htt oligomers of ~500 kDa (440-700 kDa), as revealed by size exclusion chromatography (Behrends *et al.*, 2006). Strikingly, these oligomers resemble those observed upon overexpression of TRiC *in vivo*, in yeast cells. In contrast, the presence of Hsp70/Hsp40/ATP or TRiC/ATP alone during *in vitro* Htt aggregation yields either reduced amounts of soluble protein co-fractionating with Hsp70 or hardly any polyQ protein, respectively (Behrends *et al.*, 2006). Thus, the ~500 kDa Htt oligomers form only in the presence of both chaperone systems and ATP. Furthermore, preincubation of aggregating mutant Htt with Hsp70 and Hsp40 followed by delayed addition of TRiC results in the production of ~500 kDa Htt oligomers, whereas such oligomers are absent when the order of chaperone addition is reversed (Behrends *et al.*, 2006). Thus, Hsp70/Hsp40 likely stabilizes

monomers or small oligomers of polyQ-expanded Htt in a conformation competent for subsequent interaction with TRiC, which then mediates formation of the ~500 kDa species.

Intramolecular FRET experiments with a fluorescence labeled Htt exon 1 fragment provide mechanistic insight into the synergistic activity of the two chaperone systems. While TRiC alone is unable to interfere with the conformational collapse of the protein that occurs during the nucleation phase of aggregation (Schaffar *et al.*, 2004), TRiC and Hsp70/Hsp40 in combination completely prevents this conformational change (Behrends *et al.*, 2006). In this reaction, TRiC may modulate structural properties of Htt by acting either on the polyQ segment itself and/or its flanking sequences. Transient, ATP-regulated enclosure in the central cavity of TRiC might be involved in this activity. The end products of the reaction are presumably 'folded' Htt exon 1 monomers that assemble into soluble oligomers of ~500 kDa, reminiscent of the role of TRiC in the folding and assembly of proteins such as actin, tubulin or VHL. It is tempting to speculate that TRiC may also be involved in the de novo folding of proteins with polyQ repeats of normal length.

Consistent with this cooperative modulation of Htt aggregation by TRiC and Hsp70 *in vitro*, the prevention of formation of toxic ~200 kDa Htt96QΔP-GFP oligomers in yeast cells in favour of benign ~500 kDa oligomers similarly requires the cooperation of the two chaperone systems. TRiC overexpression failed to eliminate the ~ 200 kDa oligomeric Htt species in cells that had a reduced amount of Ssa. Furthermore, overexpression of Ssa1p and its Hsp40 co-chaperone, Ydj1p at normal TRiC levels did not prevent the formation of ~200 kDa oligomers. Apparently, TRiC is not only limiting in modulating polyQ protein aggregation and oligomer formation, but also in suppressing its toxicity. In line with the failure of Ssa1p and Ydj1p to eliminate the ~200 kDa Htt oligomers, overexpression of these two chaperones could not suppress the growth defect caused by Htt96QΔP-GFP. Moreover, overexpression of TRiC in *ssa1Δ/ssa2Δ* but not in *ssb1Δ/ssb2Δ* cells failed to suppress the growth defect caused by Htt96QΔP-GFP (Figure 54, 56 and 57). Thus, in the yeast system, TRiC appears to cooperate with the canonical Hsp70 in modulating the aggregation pathway and alleviating polyQ proteotoxicity.

The interaction of Hsp70/Hsp40 and TRiC with polyQ-expanded proteins resembles the sequential action of these chaperones in de novo folding. In both reactions, the more abundant Hsp70 stabilizes the substrate protein in a conformation that is appropriate for

productive interaction with the chaperonin, which then promotes folding to the native state. In both processes, the chaperones act early in the folding/assembly pathway, either on nascent polypeptide chains or on aggregation-prone conformers during the incipient stage of polyQ aggregation, which may be initiated by processing of the full-length disease protein.

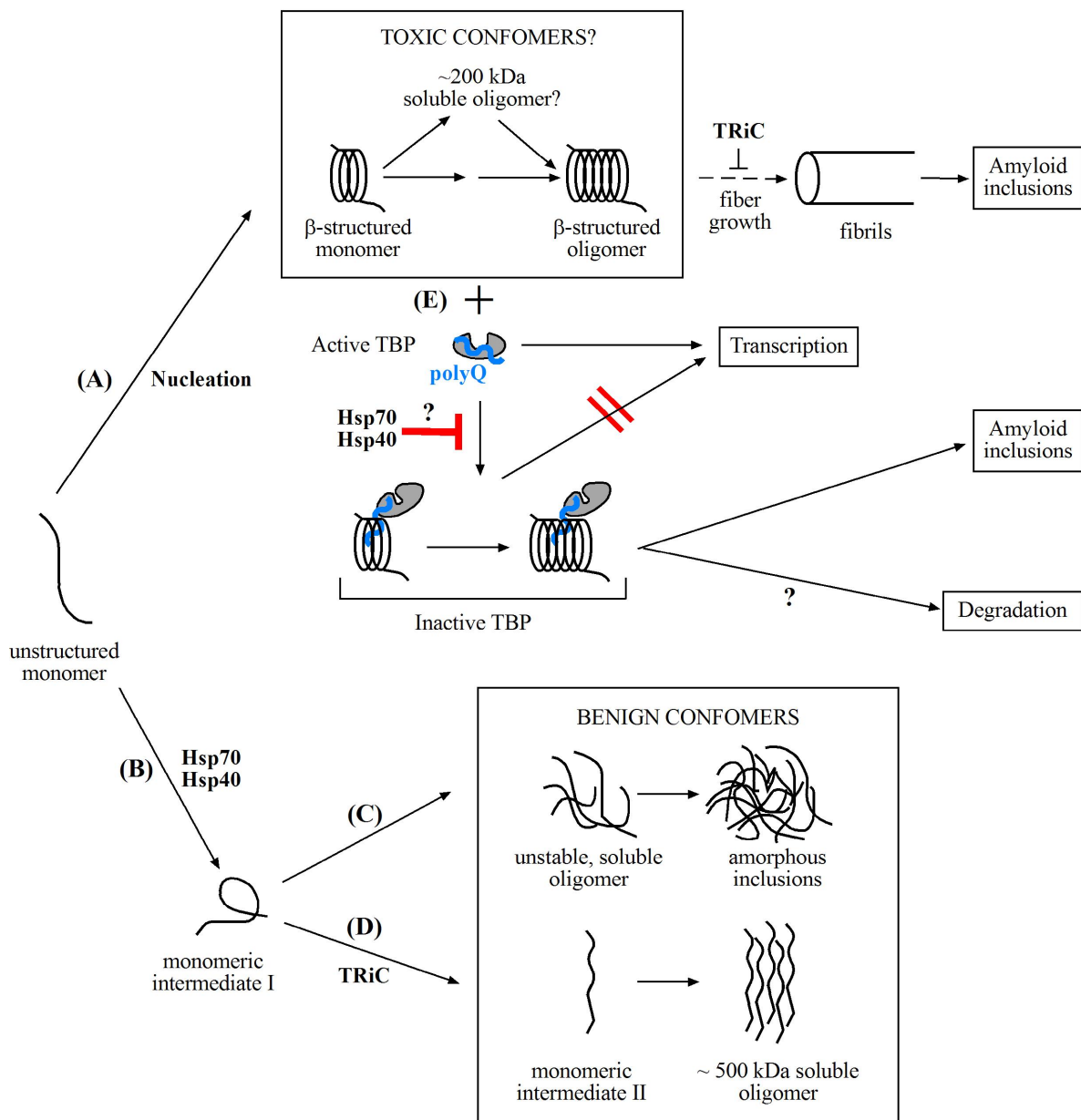


Figure 61: Working model of chaperone-mediated modulation of polyQ aggregation and toxicity.

Nucleation of aggregation may occur at the level of polyQ-expanded monomers of the Htt exon 1 fragment. Early oligomers include prefibrillar forms with cytotoxic properties, such as the ~200 kDa oligomer, which may be off pathway to fibril formation. Reaction (A) with TRiC alone, leading to short polyQ fibrils but not preventing the accumulation of potentially toxic forms; (B) with Hsp70/Hsp40, favoring the formation of amorphous aggregates (C); and (D) with Hsp70/Hsp40 and TRiC combined, leading to soluble, benign ~500 kDa oligomers. (E) Toxic species may aberrantly interact with proteins containing non-pathogenic polyQ tracts such as TBP, leading to conformational destabilization and functional deactivation.

5.3 Existence of distinct polyQ oligomeric states

The variety of oligomer sizes and prefibrillar structures, coupled with the implication that they might represent the primary species suspected to cause toxicity in degenerative disease, implicates the challenge of determining the conformational status of misfolded proteins. The polyQ disease proteins can access conformationally distinct, soluble oligomer states, which may be on- or off-pathway with respect to the formation of fibrillar inclusions. An initial structural differentiation between the toxic ~200 kDa and the benign ~500 kDa Htt96QΔP-GFP oligomers was achieved based on their immunoreactivity with the two conformation-dependent antibodies 1C2 and A11 under native-like conditions (Figure 60).

1C2 antibody interacts with an epitope formed by polyQ expansion sequences (Trottier *et al.*, 1995b). Interestingly, 1C2 was originally raised against the N-terminus of TBP encompassing its polyQ stretch (Lescure *et al.*, 1994). This monoclonal antibody has recognition properties that mimic the clinical severity of polyQ diseases. In HD, the recognition signal appears to increase over the whole length range of polyQ tracts, with no obvious threshold effect. The strong length dependence suggests that the antibody detects with high affinity a unique conformation, which requires a minimum length of polyQ and which is stabilized by further increase in length. However, multiple bivalent binding of the antibody on the homopolymeric epitopes could not be excluded. Notably, 1C2 is also able to detect intracellular inclusions containing polyQ expansion proteins (Paulson *et al.*, 1997).

On the other hand, the antibody A11 specifically recognizes soluble A β amyloid oligomers and prefibrillar aggregates, but not natively folded APP, low molecular weight monomers or dimers of A β , or mature amyloid fibrils (Kayed *et al.*, 2003). This reactivity indicates that the oligomeric aggregates display a common epitope, which is distinct from that displayed by mature fibrils. Furthermore, the anti-oligomer antibody recognizes soluble oligomers of different amyloids, including α -synuclein, islet amyloid polypeptide, PrP and polyQ (Kayed *et al.*, 2003). Because antibody recognition is independent of the amino acid sequence, the epitope is likely to be a common peptide backbone motif, such as the array of hydrogen bond donors and acceptors at the edge of a β -sheet or a turn motif. This epitope seems to be greatly reduced in the fibril structure. In keeping with the latter, the edge of the β -sheet is likely being exposed only at the ends of fibrils; thus, the amount of this epitope would decrease as the average length of the fibrils increased.

The size exclusion chromatography fractions containing the ~200 kDa oligomers were highly reactive with A11 antibody but only weakly reactive with antibody 1C2. In contrast, the ~500 kDa oligomers were efficiently recognized by antibody 1C2 but essentially lacked A11 reactivity. Importantly, comparable amounts of the two oligomers were analyzed in this assay and A11 reactivity depended on the presence of ~200 kDa oligomers. Thus, the two types of oligomers, while being identical in sequence, are clearly distinct with regard to the conformational properties of the polyQ repeat. Whether epitope masking by posttranslational modifications or association with other cellular factors might contribute to the different reactivity of the two oligomeric species, remains to be investigated.

The anti-oligomer antibody A11 has been found to block toxicity of all of the above mentioned oligomers (Kayed *et al.*, 2003). This observation is in line with the widely accepted hypothesis that the soluble oligomeric forms of amyloids might represent the principal pathogenic species (Caughey and Lansbury, 2003). Based on immunoreactivity with the anti-oligomer antibody, the ~200 kDa polyQ oligomers may resemble the potentially toxic, prefibrillar states formed by other amyloidogenic disease proteins and peptides. Strikingly, Htt oligomers of similar size were found to undergo aberrant interactions with the transcription factor TBP and their accumulation correlated with toxicity in the yeast model system (Figure 25, 26 and 27). Furthermore, polyQ-expanded Htt fused to a hydrophobic peptide likewise accumulates as ~200 kDa oligomer, inhibits the ubiquitin proteasome system and causes toxicity in yeast (Sarah Broadley, personal communication). Whether these toxic oligomers also show reactivity to the anti-oligomer antibody remains to be determined. In addition, it would be interesting to test whether all of these toxic polyQ oligomers also lead to cytotoxicity when applied to mammalian cells, as previously reported for other non-fibrillar pre-aggregates (Bucciantini *et al.*, 2002). In contrast, the ~500 kDa polyQ oligomers produced by the cooperative action of Hsp70/Hsp40 and TRiC are conformationally distinct and may be more comparable to the native assembled state of other oligomeric proteins. They lack reactivity with the A11 antibody and are not associated with proteotoxicity in the yeast model. Thus, in the ~500 kDa assembly, the polyQ expansion sequence is presumably prevented from adopting structural features enabling aberrant interactions with other proteins.

5.4 Implications in neurodegenerative diseases

Failure of the cooperative Hsp70/Hsp40-TRiC pathway to prevent certain proteins from accessing potentially toxic, amyloidogenic conformations may be critical in the onset of CAG-repeat diseases and perhaps other neurodegenerative folding disorders. In fact, this function may be more generally relevant in protein quality control considering that the ability to form amyloid structures is not an unusual feature of the small number of proteins associated with diseases, but instead may be a more general property of polypeptide chains (Stefani and Dobson, 2003). The factors that may be responsible for the failure of chaperone defense in neurodegenerative disease remain to be determined.

In a *C. elegans* model of HD, the age-1 mutation, which extends the lifespan of the worms, causes a significant delay in polyQ toxicity and protein aggregation (Morley *et al.*, 2002). A delay in ageing in mice caused by caloric restriction, lead to a significant reduction in polyQ aggregation, reduced brain atrophy and a delay in development of behavioral symptoms of the disease (Duan *et al.*, 2003). Dietary restriction is known to reduce oxidative stress and increase the production of chaperones (Mattson and Magnus, 2006). Thus, the rate of progression for proteinopathies seems to be linked with the genetic regulation of ageing. Intriguingly, the heat shock response appears to be poorly induced during ageing (Amici *et al.*, 1992; Soti and Csermely, 2002). Hence, the ability of chaperone networks to respond to the appearance of misfolded and aggregation-prone proteins during ageing would be compromised, which is consistent with genetic approaches that have identified molecular chaperones as suppressors in models of ageing and protein aggregation related diseases (Nollen *et al.*, 2004). In fact, the capacity of the stress protein network, which is regulated by the master transcription regulator heat shock factor (HSF1), may decrease as part of the ageing program (Morley and Morimoto, 2004), thus favoring the accumulation of toxic protein species. Interestingly, the regulation of TRiC and several other chaperones involved in *de novo* folding differs from that of stress-inducible Hsp70 members in that it is HSF1-independent (Albanese and Frydman, 2002). It will therefore be important to see how TRiC is regulated and whether the level of functional chaperonin changes during ageing.

5.5 Perspective

While the formation of large inert aggregates (inclusions, aggresome) seems to be part of the cellular protective response against misfolded proteins, it is clear that the aggregation process itself is related to toxicity. An important issue that remains is to determine the exact nature of the toxic species: whether this is some form of soluble aggregate such as a small oligomer or the misfolded monomer itself. A detailed understanding of toxicity mechanisms will depend on information concerning the molecular composition, reactivity and structure of these forms. A related question is whether soluble oligomeric species are on the pathway to fibre formation or represent an off-pathway step. Dissecting and ordering the pathway of fibril formation *in vivo* will help to elucidate the underlying pathomechanism and to guide the development of therapeutic strategies. It is important to realize in this context that, contrary to present belief, interfering with the aggregation process may not be generally advantageous but could increase the accumulation of toxic species.

Molecular chaperones and other components of the protein quality control system are remarkably efficient in ensuring the neutralization of potentially toxic protein species. These protective mechanisms likely involve the ability of chaperones to alter the partitioning between harmful and harmless forms of aggregates. Therefore, a plausible therapeutic strategy would be to seek ways to enhance the cellular defense mechanisms. Drugs such as geldanamycin can increase the level of chaperones (Sittler *et al.*, 2001). Small molecules may be similarly able to target the misfolding proteins directly. Congo red has been shown to bind to proteins with β -sheet structure and reduce toxicity *in vivo* (Sanchez *et al.*, 2003). It is conceivable that small molecule inhibitors can be identified that mimic the combined effect of the Hsp70/Hsp40 and TRiC chaperones in converting toxic oligomers into benign forms. Drug screens may take advantage of the ability of conformation-specific antibodies to differentiate these forms.

6 References

- Adachi, H., Katsuno, M., Minamiyama, M., Sang, C., Pagoulatos, G., Angelidis, C., Kusakabe, M., Yoshiki, A., Kobayashi, Y., Doyu, M., and Sobue, G. (2003). Heat shock protein 70 chaperone overexpression ameliorates phenotypes of the spinal and bulbar muscular atrophy transgenic mouse model by reducing nuclear-localized mutant androgen receptor protein. *J Neurosci* *23*, 2203-2211.
- Agashe, V. R., and Hartl, F. U. (2000). Roles of molecular chaperones in cytoplasmic protein folding. *Semin Cell Dev Biol* *11*, 15-25.
- Albanese, V., and Frydman, J. (2002). Where chaperones and nascent polypeptides meet. *Nat Struct Biol* *9*, 716-718.
- Altschuler, E. L., Hud, N. V., Mazrimas, J. A., and Rupp, B. (1997). Random coil conformation for extended polyglutamine stretches in aqueous soluble monomeric peptides. *J Pept Res* *50*, 73-75.
- Amici, C., Sistonen, L., Santoro, M. G., and Morimoto, R. I. (1992). Antiproliferative prostaglandins activate heat shock transcription factor. *Proc Natl Acad Sci U S A* *89*, 6227-6231.
- Anfinsen, C. B. (1973). Principles that govern the folding of protein chains. *Science* *181*, 223-230.
- Arrasate, M., Mitra, S., Schweitzer, E. S., Segal, M. R., and Finkbeiner, S. (2004). Inclusion body formation reduces levels of mutant huntingtin and the risk of neuronal death. *Nature* *431*, 805-810.
- Ban, N., Nissen, P., Hansen, J., Moore, P. B., and Steitz, T. A. (2000). The complete atomic structure of the large ribosomal subunit at 2.4 Å resolution. *Science* *289*, 905-920.
- Barral, J. M., Hutagalung, A. H., Brinker, A., Hartl, F. U., and Epstein, H. F. (2002). Role of the myosin assembly protein UNC-45 as a molecular chaperone for myosin. *Science* *295*, 669-671.
- Bates, G. (2000). Huntington's disease. In reverse gear. *Nature* *404*, 944-945.
- Bates, G. (2003). Huntingtin aggregation and toxicity in Huntington's disease. *Lancet* *361*, 1642-1644.
- Bates, G. P. (2006). BIOMEDICINE: One Misfolded Protein Allows Others to Sneak By. *Science* *311*, 1385-1386.
- Becher, M. W., Kotzok, J. A., Sharp, A. H., Davies, S. W., Bates, G. P., Price, D. L., and Ross, C. A. (1998). Intranuclear neuronal inclusions in Huntington's disease and dentatorubral and pallidoluysian atrophy: correlation between the density of inclusions and IT15 CAG triplet repeat length. *Neurobiol Dis* *4*, 387-397.
- Beckmann, R. P., Mizzen, L. E., and Welch, W. J. (1990). Interaction of Hsp 70 with newly synthesized proteins: implications for protein folding and assembly. *Science* *248*, 850-854.
- Behrends, C., Langer, C. A., Boteva, R., Böttcher, U. M., Stemp, M. J., Schaffar, G., Rao, B. V., Giese, A., Kretschmar, H., Siegers, K., and Hartl, F. U. (2006). Chaperonin TRiC Promotes the Assembly of polyQ Expansion Proteins into Nontoxic Oligomers. *Mol Cell* *23*, 887-897.
- Bence, N. F., Sampat, R. M., and Kopito, R. R. (2001). Impairment of the ubiquitin-proteasome system by protein aggregation. *Science* *292*, 1552-1555.
- Bennett, E. J., Bence, N. F., Jayakumar, R., and Kopito, R. R. (2005). Global impairment of the ubiquitin-proteasome system by nuclear or cytoplasmic protein aggregates precedes inclusion body formation. *Mol Cell* *17*, 351-365.
- Benzinger, T. L., Gregory, D. M., Burkoth, T. S., Miller-Auer, H., Lynn, D. G., Botto, R. E., and Meredith, S. C. (2000). Two-dimensional structure of beta-amyloid(10-35) fibrils. *Biochemistry* *39*, 3491-3499.
- Ben-Zvi, A. P., and Goloubinoff, P. (2001). Review: mechanisms of disaggregation and refolding of stable protein aggregates by molecular chaperones. *J Struct Biol* *135*, 84-93.

- Berke, S. J., and Paulson, H. L. (2003). Protein aggregation and the ubiquitin proteasome pathway: gaining the UPPer hand on neurodegeneration. *Curr Opin Genet Dev* 13, 253-261.
- Bhattacharyya, A., Thakur, A. K., Chellgren, V. M., Thiagarajan, G., Williams, A. D., Chellgren, B. W., Creamer, T. P., and Wetzel, R. (2006). Oligoproline effects on polyglutamine conformation and aggregation. *J Mol Biol* 355, 524-535.
- Bonini, N. M. (2002). Chaperoning brain degeneration. *Proc Natl Acad Sci U S A* 99, 16407-16411.
- Boorstein, W. R., and Craig, E. A. (1990). Transcriptional regulation of SSA3, an HSP70 gene from *Saccharomyces cerevisiae*. *Mol Cell Biol* 10, 3262-3267.
- Bouchard, M., Zurdo, J., Nettleton, E. J., Dobson, C. M., and Robinson, C. V. (2000). Formation of insulin amyloid fibrils followed by FTIR simultaneously with CD and electron microscopy. *Protein Sci* 9, 1960-1967.
- Boutell, J. M., Thomas, P., Neal, J. W., Weston, V. J., Duce, J., Harper, P. S., and Jones, A. L. (1999). Aberrant interactions of transcriptional repressor proteins with the Huntington's disease gene product, huntingtin. *Hum Mol Genet* 8, 1647-1655.
- Bowman, A. B., Yoo, S. Y., Dantuma, N. P., and Zoghbi, H. Y. (2005). Neuronal dysfunction in a polyglutamine disease model occurs in the absence of ubiquitin-proteasome system impairment and inversely correlates with the degree of nuclear inclusion formation. *Hum Mol Genet* 14, 679-691.
- Bradford, M. M. (1976). A rapid and sensitive method for the quantitation of microgram quantities of protein utilizing the principle of protein-dye binding. *Anal Biochem* 72, 248-254.
- Bryngelson, J. D., Onuchic, J. N., Socci, N. D., and Wolynes, P. G. (1995). Funnels, pathways, and the energy landscape of protein folding: a synthesis. *Proteins* 21, 167-195.
- Bucciantini, M., Giannoni, E., Chiti, F., Baroni, F., Formigli, L., Zurdo, J., Taddei, N., Ramponi, G., Dobson, C. M., and Stefani, M. (2002). Inherent toxicity of aggregates implies a common mechanism for protein misfolding diseases. *Nature* 416, 507-511.
- Bukau, B., and Horwich, A. L. (1998). The Hsp70 and Hsp60 chaperone machines. *Cell* 92, 351-366.
- Camasses, A., Bogdanova, A., Shevchenko, A., and Zachariae, W. (2003). The CCT chaperonin promotes activation of the anaphase-promoting complex through the generation of functional Cdc20. *Mol Cell* 12, 87-100.
- Cashikar, A. G., Duennwald, M., and Lindquist, S. L. (2005). A chaperone pathway in protein disaggregation. Hsp26 alters the nature of protein aggregates to facilitate reactivation by Hsp104. *J Biol Chem* 280, 23869-23875.
- Cattaneo, E., Rigamonti, D., Goffredo, D., Zuccato, C., Squitieri, F., and Sipione, S. (2001). Loss of normal huntingtin function: new developments in Huntington's disease research. *Trends Neurosci* 24, 182-188.
- Cattaneo, E. (2003). Dysfunction of wild-type huntingtin in Huntington disease. *News Physiol Sci* 18, 34-37.
- Caughey, B., and Lansbury, P. T. (2003). Protofibrils, pores, fibrils, and neurodegeneration: separating the responsible protein aggregates from the innocent bystanders. *Annu Rev Neurosci* 26, 267-298.
- Cha, J. H. (2000). Transcriptional dysregulation in Huntington's disease. *Trends Neurosci* 23, 387-392.
- Chai, Y., Koppenhafer, S. L., Bonini, N. M., and Paulson, H. L. (1999). Analysis of the role of heat shock protein (Hsp) molecular chaperones in polyglutamine disease. *J Neurosci* 19, 10338-10347.
- Chai, Y., Shao, J., Miller, V. M., Williams, A., and Paulson, H. L. (2002). Live-cell imaging reveals divergent intracellular dynamics of polyglutamine disease proteins and supports a sequestration model of pathogenesis. *Proc Natl Acad Sci U S A* 99, 9310-9315.

- Chan, H. Y., Warrick, J. M., Gray-Board, G. L., Paulson, H. L., and Bonini, N. M. (2000). Mechanisms of chaperone suppression of polyglutamine disease: selectivity, synergy and modulation of protein solubility in *Drosophila*. *Hum Mol Genet* *9*, 2811-2820.
- Chen, S., Berthelie, V., Yang, W., and Wetzel, R. (2001). Polyglutamine aggregation behavior in vitro supports a recruitment mechanism of cytotoxicity. *J Mol Biol* *311*, 173-182.
- Chen, S., and Wetzel, R. (2001). Solubilization and disaggregation of polyglutamine peptides. *Protein Sci* *10*, 887-891.
- Chen, S., Ferrone, F. A., and Wetzel, R. (2002). Huntington's disease age-of-onset linked to polyglutamine aggregation nucleation. *Proc Natl Acad Sci U S A* *99*, 11884-11889.
- Chiti, F., Webster, P., Taddei, N., Clark, A., Stefani, M., Ramponi, G., and Dobson, C. M. (1999). Designing conditions for in vitro formation of amyloid protofilaments and fibrils. *Proc Natl Acad Sci U S A* *96*, 3590-3594.
- Chiti, F., Taddei, N., Baroni, F., Capanni, C., Stefani, M., Ramponi, G., and Dobson, C. M. (2002). Kinetic partitioning of protein folding and aggregation. *Nat Struct Biol* *9*, 137-143.
- Chiti, F., and Dobson, C. M. (2006). Protein misfolding, functional amyloid, and human disease. *Annu Rev Biochem* *75*, 333-366.
- Ciechanover, A., and Brundin, P. (2003). The ubiquitin proteasome system in neurodegenerative diseases: sometimes the chicken, sometimes the egg. *Neuron* *40*, 427-446.
- Cohen, F. E., and Kelly, J. W. (2003). Therapeutic approaches to protein-misfolding diseases. *Nature* *426*, 905-909.
- Colby, D. W., Chu, Y., Cassady, J. P., Duennwald, M., Zazulak, H., Webster, J. M., Messer, A., Lindquist, S., Ingram, V. M., and Wittrup, K. D. (2004). Potent inhibition of huntingtin aggregation and cytotoxicity by a disulfide bond-free single-domain intracellular antibody. *Proc Natl Acad Sci U S A* *101*, 17616-17621.
- Cormack, B. P., Strubin, M., Stargell, L. A., and Struhl, K. (1994). Conserved and nonconserved functions of the yeast and human TATA-binding proteins. *Genes Dev* *8*, 1335-1343.
- Creighton, T. E. (1990). Protein folding. *Biochem J* *270*, 1-16.
- Csermely, P. (2001). Chaperone overload is a possible contributor to 'civilization diseases'. *Trends Genet* *17*, 701-704.
- Cummings, C. J., Mancini, M. A., Antalffy, B., DeFranco, D. B., Orr, H. T., and Zoghbi, H. Y. (1998). Chaperone suppression of aggregation and altered subcellular proteasome localization imply protein misfolding in SCA1. *Nat Genet* *19*, 148-154.
- Cummings, C. J., Reinstein, E., Sun, Y., Antalffy, B., Jiang, Y., Ciechanover, A., Orr, H. T., Beudet, A. L., and Zoghbi, H. Y. (1999). Mutation of the E6-AP ubiquitin ligase reduces nuclear inclusion frequency while accelerating polyglutamine-induced pathology in SCA1 mice. *Neuron* *24*, 879-892.
- Cummings, C. J., Sun, Y., Opal, P., Antalffy, B., Mestrl, R., Orr, H. T., Dillmann, W. H., and Zoghbi, H. Y. (2001). Over-expression of inducible HSP70 chaperone suppresses neuropathology and improves motor function in SCA1 mice. *Hum Mol Genet* *10*, 1511-1518.
- Cyr, D. M., Hohfeld, J., and Patterson, C. (2002). Protein quality control: U-box-containing E3 ubiquitin ligases join the fold. *Trends Biochem Sci* *27*, 368-375.
- Daggett, V., and Fersht, A. R. (2003). Is there a unifying mechanism for protein folding? *Trends Biochem Sci* *28*, 18-25.
- Davies, S. W., Turmaine, M., Cozens, B. A., DiFiglia, M., Sharp, A. H., Ross, C. A., Scherzinger, E., Wanker, E. E., Mangiarini, L., and Bates, G. P. (1997). Formation of neuronal intranuclear inclusions underlies the neurological dysfunction in mice transgenic for the HD mutation. *Cell* *90*, 537-548.

- de Almeida, L. P., Ross, C. A., Zala, D., Aebischer, P., and Deglon, N. (2002). Lentiviral-mediated delivery of mutant huntingtin in the striatum of rats induces a selective neuropathology modulated by polyglutamine repeat size, huntingtin expression levels, and protein length. *J Neurosci* 22, 3473-3483.
- de Chiara, C., Menon, R. P., Dal Piaz, F., Calder, L., and Pastore, A. (2005). Polyglutamine is not all: the functional role of the AXH domain in the ataxin-1 protein. *J Mol Biol* 354, 883-893.
- Dehay, B., and Bertolotti, A. (2006). Critical role of the proline-rich region in huntingtin for aggregation and cytotoxicity in yeast. *J Biol Chem*.
- Demand, J., Alberti, S., Patterson, C., and Hohfeld, J. (2001). Cooperation of a ubiquitin domain protein and an E3 ubiquitin ligase during chaperone/proteasome coupling. *Curr Biol* 11, 1569-1577.
- DiFiglia, M., Sapp, E., Chase, K., Schwarz, C., Meloni, A., Young, C., Martin, E., Vonsattel, J. P., Carraway, R., Reeves, S. A., and et al. (1995). Huntingtin is a cytoplasmic protein associated with vesicles in human and rat brain neurons. *Neuron* 14, 1075-1081.
- DiFiglia, M., Sapp, E., Chase, K. O., Davies, S. W., Bates, G. P., Vonsattel, J. P., and Aronin, N. (1997). Aggregation of huntingtin in neuronal intranuclear inclusions and dystrophic neurites in brain. *Science* 277, 1990-1993.
- Dill, K. A., and Chan, H. S. (1997). From Levinthal to pathways to funnels. *Nat Struct Biol* 4, 10-19.
- Ding, Q., Lewis, J. J., Strum, K. M., Dimayuga, E., Bruce-Keller, A. J., Dunn, J. C., and Keller, J. N. (2002). Polyglutamine expansion, protein aggregation, proteasome activity, and neural survival. *J Biol Chem* 277, 13935-13942.
- Dinner, A. R., Sali, A., Smith, L. J., Dobson, C. M., and Karplus, M. (2000). Understanding protein folding via free-energy surfaces from theory and experiment. *Trends Biochem Sci* 25, 331-339.
- Ditzel, L., Lowe, J., Stock, D., Stetter, K. O., Huber, H., Huber, R., and Steinbacher, S. (1998). Crystal structure of the thermosome, the archaeal chaperonin and homolog of CCT. *Cell* 93, 125-138.
- Dobson, C. M., and Ellis, R. J. (1998). Protein folding and misfolding inside and outside the cell. *Embo J* 17, 5251-5254.
- Dobson, C. M., and Hore, P. J. (1998). Kinetic studies of protein folding using NMR spectroscopy. *Nat Struct Biol* 5 *Suppl*, 504-507.
- Dobson, C. M., and Karplus, M. (1999). The fundamentals of protein folding: bringing together theory and experiment. *Curr Opin Struct Biol* 9, 92-101.
- Dobson, C. M. (2002). Getting out of shape. *Nature* 418, 729-730.
- Dobson, C. M. (2003). Protein folding and misfolding. *Nature* 426, 884-890.
- Dobson, C. M. (2004). Principles of protein folding, misfolding and aggregation. *Semin Cell Dev Biol* 15, 3-16.
- Dragovic, Z., Broadley, S. A., Shomura, Y., Bracher, A., and Hartl, F. U. (2006). Molecular chaperones of the Hsp110 family act as nucleotide exchange factors of Hsp70s. *Embo J* 25, 2519-2528.
- Duan, W., Guo, Z., Jiang, H., Ware, M., Li, X. J., and Mattson, M. P. (2003). Dietary restriction normalizes glucose metabolism and BDNF levels, slows disease progression, and increases survival in huntingtin mutant mice. *Proc Natl Acad Sci U S A* 100, 2911-2916.
- Duennwald, M. L., Jagadish, S., Giorgini, F., Muchowski, P. J., and Lindquist, S. (2006a). A network of protein interactions determines polyglutamine toxicity. *Proc Natl Acad Sci U S A* 103, 11051-11056.
- Duennwald, M. L., Jagadish, S., Muchowski, P. J., and Lindquist, S. (2006b). Flanking sequences profoundly alter polyglutamine toxicity in yeast. *Proc Natl Acad Sci U S A* 103, 11045-11050.

- Dunah, A. W., Jeong, H., Griffin, A., Kim, Y. M., Standaert, D. G., Hersch, S. M., Mouradian, M. M., Young, A. B., Tanese, N., and Krainc, D. (2002). Sp1 and TAFIII130 transcriptional activity disrupted in early Huntington's disease. *Science* 296, 2238-2243.
- Eanes, E. D., and Glenner, G. G. (1968). X-ray diffraction studies on amyloid filaments. *J Histochem Cytochem* 16, 673-677.
- Ecker, D. J., Khan, M. I., Marsh, J., Butt, T. R., and Crooke, S. T. (1987). Chemical synthesis and expression of a cassette adapted ubiquitin gene. *J Biol Chem* 262, 3524-3527.
- Ehrnhoefer, D. E., Duennwald, M., Markovic, P., Wacker, J. L., Engemann, S., Roark, M., Legleiter, J., Marsh, J. L., Thompson, L. M., Lindquist, S., *et al.* (2006). Green tea (-)-epigallocatechin-gallate modulates early events in huntingtin misfolding and reduces toxicity in Huntington's disease models. *Hum Mol Genet*.
- Ellis, R. J., van der Vies, S. M., and Hemmingsen, S. M. (1989). The molecular chaperone concept. *Biochem Soc Symp* 55, 145-153.
- Ellis, R. J., and Hartl, F. U. (1996). Protein folding in the cell: competing models of chaperonin function. *Faseb J* 10, 20-26.
- Ellis, R. J., and Hartl, F. U. (1999). Principles of protein folding in the cellular environment. *Curr Opin Struct Biol* 9, 102-110.
- Ellis, R. J. (2001). Macromolecular crowding: an important but neglected aspect of the intracellular environment. *Curr Opin Struct Biol* 11, 114-119.
- Ellis, R. J., and Minton, A. P. (2006). Protein aggregation in crowded environments. *Biol Chem* 387, 485-497.
- Evans, I. H. (1996). Yeast Protocols. In *Methods in Molecular Biology*, I. H. Evans, ed. (Totowa, New Jersey, Humana Press).
- Fandrich, M., Fletcher, M. A., and Dobson, C. M. (2001). Amyloid fibrils from muscle myoglobin. *Nature* 410, 165-166.
- Fandrich, M., and Dobson, C. M. (2002). The behaviour of polyamino acids reveals an inverse side chain effect in amyloid structure formation. *Embo J* 21, 5682-5690.
- Farr, G. W., Scharl, E. C., Schumacher, R. J., Sondak, S., and Horwich, A. L. (1997). Chaperonin-mediated folding in the eukaryotic cytosol proceeds through rounds of release of native and nonnative forms. *Cell* 89, 927-937.
- Faux, N. G., Bottomley, S. P., Lesk, A. M., Irving, J. A., Morrison, J. R., de la Banda, M. G., and Whisstock, J. C. (2005). Functional insights from the distribution and role of homopeptide repeat-containing proteins. *Genome Res* 15, 537-551.
- Feany, M. B., and La Spada, A. R. (2003). Polyglutamines stop traffic: axonal transport as a common target in neurodegenerative diseases. *Neuron* 40, 1-2.
- Feldman, D. E., Thulasiraman, V., Ferreyra, R. G., and Frydman, J. (1999). Formation of the VHL-elongin BC tumor suppressor complex is mediated by the chaperonin TRiC. *Mol Cell* 4, 1051-1061.
- Feldman, D. E., and Frydman, J. (2000). Protein folding in vivo: the importance of molecular chaperones. *Curr Opin Struct Biol* 10, 26-33.
- Feldman, D. E., Spiess, C., Howard, D. E., and Frydman, J. (2003). Tumorigenic mutations in VHL disrupt folding in vivo by interfering with chaperonin binding. *Mol Cell* 12, 1213-1224.
- Fernandez-Funez, P., Nino-Rosales, M. L., de Gouyon, B., She, W. C., Luchak, J. M., Martinez, P., Turiegano, E., Benito, J., Capovilla, M., Skinner, P. J., *et al.* (2000). Identification of genes that modify ataxin-1-induced neurodegeneration. *Nature* 408, 101-106.

- Fersht, A. R. (2000). Transition-state structure as a unifying basis in protein-folding mechanisms: contact order, chain topology, stability, and the extended nucleus mechanism. *Proc Natl Acad Sci U S A* *97*, 1525-1529.
- Fink, A. L. (1999). Chaperone-mediated protein folding. *Physiol Rev* *79*, 425-449.
- Frydman, J., Nimmesgern, E., Ohtsuka, K., and Hartl, F. U. (1994). Folding of nascent polypeptide chains in a high molecular mass assembly with molecular chaperones. *Nature* *370*, 111-117.
- Frydman, J., and Hartl, F. U. (1996). Principles of chaperone-assisted protein folding: differences between in vitro and in vivo mechanisms. *Science* *272*, 1497-1502.
- Frydman, J. (2001). Folding of newly translated proteins in vivo: the role of molecular chaperones. *Annu Rev Biochem* *70*, 603-647.
- Gafni, J., and Ellerby, L. M. (2002). Calpain activation in Huntington's disease. *J Neurosci* *22*, 4842-4849.
- Gao, Y., Thomas, J. O., Chow, R. L., Lee, G. H., and Cowan, N. J. (1992). A cytoplasmic chaperonin that catalyzes beta-actin folding. *Cell* *69*, 1043-1050.
- Gautschi, M., Lilie, H., Funfschilling, U., Mun, A., Ross, S., Lithgow, T., Rucknagel, P., and Rospert, S. (2001). RAC, a stable ribosome-associated complex in yeast formed by the DnaK-DnaJ homologs Ssz1p and zuotin. *Proc Natl Acad Sci U S A* *98*, 3762-3767.
- Gautschi, M., Mun, A., Ross, S., and Rospert, S. (2002). A functional chaperone triad on the yeast ribosome. *Proc Natl Acad Sci U S A* *99*, 4209-4214.
- Geissler, S., Siegers, K., and Schiebel, E. (1998). A novel protein complex promoting formation of functional alpha- and gamma-tubulin. *Embo J* *17*, 952-966.
- Gerber, H. P., Seipel, K., Georgiev, O., Hofferer, M., Hug, M., Rusconi, S., and Schaffner, W. (1994). Transcriptional activation modulated by homopolymeric glutamine and proline stretches. *Science* *263*, 808-811.
- Gething, M. J., and Sambrook, J. (1992). Protein folding in the cell. *Nature* *355*, 33-45.
- Gidalevitz, T., Ben-Zvi, A., Ho, K. H., Brignull, H. R., and Morimoto, R. I. (2006). Progressive disruption of cellular protein folding in models of polyglutamine diseases. *Science* *311*, 1471-1474.
- Gill, G., and Tjian, R. (1992). Eukaryotic coactivators associated with the TATA box binding protein. *Curr Opin Genet Dev* *2*, 236-242.
- Glabe, C. G. (2004). Conformation-dependent antibodies target diseases of protein misfolding. *Trends Biochem Sci* *29*, 542-547.
- Glass, M., Dragunow, M., and Faull, R. L. (2000). The pattern of neurodegeneration in Huntington's disease: a comparative study of cannabinoid, dopamine, adenosine and GABA(A) receptor alterations in the human basal ganglia in Huntington's disease. *Neuroscience* *97*, 505-519.
- Goldsbury, C. S., Wirtz, S., Muller, S. A., Sunderji, S., Wicki, P., Aebi, U., and Frey, P. (2000). Studies on the in vitro assembly of a beta 1-40: implications for the search for a beta fibril formation inhibitors. *J Struct Biol* *130*, 217-231.
- Gosal, W. S., Morten, I. J., Hewitt, E. W., Smith, D. A., Thomson, N. H., and Radford, S. E. (2005). Competing pathways determine fibril morphology in the self-assembly of beta2-microglobulin into amyloid. *J Mol Biol* *351*, 850-864.
- Graham, R. K., Deng, Y., Slow, E. J., Haigh, B., Bissada, N., Lu, G., Pearson, J., Shehadeh, J., Bertram, L., Murphy, Z., *et al.* (2006). Cleavage at the caspase-6 site is required for neuronal dysfunction and degeneration due to mutant huntingtin. *Cell* *125*, 1179-1191.
- Gray, D. A., Tsirigotis, M., and Woulfe, J. (2003). Ubiquitin, proteasomes, and the aging brain. *Sci Aging Knowledge Environ* *2003*, RE6.

- Grewal, S. I., and Moazed, D. (2003). Heterochromatin and epigenetic control of gene expression. *Science* 301, 798-802.
- Gutekunst, C. A., Li, S. H., Yi, H., Ferrante, R. J., Li, X. J., and Hersch, S. M. (1998). The cellular and subcellular localization of huntingtin-associated protein 1 (HAP1): comparison with huntingtin in rat and human. *J Neurosci* 18, 7674-7686.
- Gutekunst, C. A., Li, S. H., Yi, H., Mulroy, J. S., Kuemmerle, S., Jones, R., Rye, D., Ferrante, R. J., Hersch, S. M., and Li, X. J. (1999). Nuclear and neuropil aggregates in Huntington's disease: relationship to neuropathology. *J Neurosci* 19, 2522-2534.
- Gutsche, I., Essen, L. O., and Baumeister, W. (1999). Group II chaperonins: new TRiC(k)s and turns of a protein folding machine. *J Mol Biol* 293, 295-312.
- Haacke, A., Broadley, S. A., Boteva, R., Tzvetkov, N., Hartl, F. U., and Breuer, P. (2006). Proteolytic cleavage of polyglutamine-expanded ataxin-3 is critical for aggregation and sequestration of non-expanded ataxin-3. *Hum Mol Genet* 15, 555-568.
- Hahn, S., Buratowski, S., Sharp, P. A., and Guarente, L. (1989). Isolation of the gene encoding the yeast TATA binding protein TFIID: a gene identical to the SPT15 suppressor of Ty element insertions. *Cell* 58, 1173-1181.
- Hanahan, D. (1983). Studies on transformation of *Escherichia coli* with plasmids. *J Mol Biol* 166, 557-580.
- Hansen, W. J., Cowan, N. J., and Welch, W. J. (1999). Prefoldin-nascent chain complexes in the folding of cytoskeletal proteins. *J Cell Biol* 145, 265-277.
- Harjes, P., and Wanker, E. E. (2003). The hunt for huntingtin function: interaction partners tell many different stories. *Trends Biochem Sci* 28, 425-433.
- Harrison, C. J., Hayer-Hartl, M., Di Liberto, M., Hartl, F., and Kuriyan, J. (1997). Crystal structure of the nucleotide exchange factor GrpE bound to the ATPase domain of the molecular chaperone DnaK. *Science* 276, 431-435.
- Hartl, F. U. (1996). Molecular chaperones in cellular protein folding. *Nature* 381, 571-579.
- Hartl, F. U., and Hayer-Hartl, M. (2002). Molecular chaperones in the cytosol: from nascent chain to folded protein. *Science* 295, 1852-1858.
- Hay, D. G., Sathasivam, K., Tobaben, S., Stahl, B., Marber, M., Mestril, R., Mahal, A., Smith, D. L., Woodman, B., and Bates, G. P. (2004). Progressive decrease in chaperone protein levels in a mouse model of Huntington's disease and induction of stress proteins as a therapeutic approach. *Hum Mol Genet* 13, 1389-1405.
- HDCRG (1993). A novel gene containing a trinucleotide repeat that is expanded and unstable on Huntington's disease chromosomes. The Huntington's Disease Collaborative Research Group. *Cell* 72, 971-983.
- Hershko, A., and Ciechanover, A. (1998). The ubiquitin system. *Annu Rev Biochem* 67, 425-479.
- Heydari, A. R., Takahashi, R., Gutschmann, A., You, S., and Richardson, A. (1994). Hsp70 and aging. *Experientia* 50, 1092-1098.
- Hohfeld, J., Minami, Y., and Hartl, F. U. (1995). Hip, a novel cochaperone involved in the eukaryotic Hsc70/Hsp40 reaction cycle. *Cell* 83, 589-598.
- Hohfeld, J., Cyr, D. M., and Patterson, C. (2001). From the cradle to the grave: molecular chaperones that may choose between folding and degradation. *EMBO Rep* 2, 885-890.
- Holbert, S., Denghien, I., Kiechle, T., Rosenblatt, A., Wellington, C., Hayden, M. R., Margolis, R. L., Ross, C. A., Dausset, J., Ferrante, R. J., and Neri, C. (2001). The Gln-Ala repeat transcriptional activator CA150 interacts with huntingtin: neuropathologic and genetic evidence for a role in Huntington's disease pathogenesis. *Proc Natl Acad Sci U S A* 98, 1811-1816.

- Hrnčić, R., Wall, J., Wolfenbarger, D. A., Murphy, C. L., Schell, M., Weiss, D. T., and Solomon, A. (2000). Antibody-mediated resolution of light chain-associated amyloid deposits. *Am J Pathol* *157*, 1239-1246.
- Huang, P., Gautschi, M., Walter, W., Rospert, S., and Craig, E. A. (2005). The Hsp70 Ssz1 modulates the function of the ribosome-associated J-protein Zuo1. *Nat Struct Mol Biol* *12*, 497-504.
- Iwata, A., Christianson, J. C., Bucci, M., Ellerby, L. M., Nukina, N., Forno, L. S., and Kopito, R. R. (2005). Increased susceptibility of cytoplasmic over nuclear polyglutamine aggregates to autophagic degradation. *Proc Natl Acad Sci U S A* *102*, 13135-13140.
- Jaenicke, R. (1991). Protein folding: local structures, domains, subunits, and assemblies. *Biochemistry* *30*, 3147-3161.
- Jana, N. R., Tanaka, M., Wang, G., and Nukina, N. (2000). Polyglutamine length-dependent interaction of Hsp40 and Hsp70 family chaperones with truncated N-terminal huntingtin: their role in suppression of aggregation and cellular toxicity. *Hum Mol Genet* *9*, 2009-2018.
- Jiang, H., Poirier, M. A., Liang, Y., Pei, Z., Weiskittel, C. E., Smith, W. W., Defranco, D. B., and Ross, C. A. (2006). Depletion of CBP is directly linked with cellular toxicity caused by mutant huntingtin. *Neurobiol Dis*.
- Johnson, J. L., and Craig, E. A. (2001). An essential role for the substrate-binding region of Hsp40s in *Saccharomyces cerevisiae*. *J Cell Biol* *152*, 851-856.
- Kao, C. C., Lieberman, P. M., Schmidt, M. C., Zhou, Q., Pei, R., and Berk, A. J. (1990). Cloning of a transcriptionally active human TATA binding factor. *Science* *248*, 1646-1650.
- Karplus, M., and Weaver, D. L. (1976). Protein-folding dynamics. *Nature* *260*, 404-406.
- Karplus, M. (1997). The Levinthal paradox: yesterday and today. *Fold Des* *2*, S69-75.
- Kayed, R., Head, E., Thompson, J. L., McIntire, T. M., Milton, S. C., Cotman, C. W., and Glabe, C. G. (2003). Common structure of soluble amyloid oligomers implies common mechanism of pathogenesis. *Science* *300*, 486-489.
- Kaytor, M. D., Wilkinson, K. D., and Warren, S. T. (2004). Modulating huntingtin half-life alters polyglutamine-dependent aggregate formation and cell toxicity. *J Neurochem* *89*, 962-973.
- Kazantsev, A., Preisinger, E., Dranovsky, A., Goldgaber, D., and Housman, D. (1999). Insoluble detergent-resistant aggregates form between pathological and nonpathological lengths of polyglutamine in mammalian cells. *Proc Natl Acad Sci U S A* *96*, 11404-11409.
- Kazemi-Esfarjani, P., and Benzer, S. (2000). Genetic suppression of polyglutamine toxicity in *Drosophila*. *Science* *287*, 1837-1840.
- Keller, J. N., Gee, J., and Ding, Q. (2002). The proteasome in brain aging. *Ageing Res Rev* *1*, 279-293.
- Kerner, M. J., Naylor, D. J., Ishihama, Y., Maier, T., Chang, H. C., Stines, A. P., Georgopoulos, C., Frishman, D., Hayer-Hartl, M., Mann, M., and Hartl, F. U. (2005). Proteome-wide analysis of chaperonin-dependent protein folding in *Escherichia coli*. *Cell* *122*, 209-220.
- Khan, F., Chuang, J. I., Gianni, S., and Fersht, A. R. (2003). The kinetic pathway of folding of barnase. *J Mol Biol* *333*, 169-186.
- Kim, P. S., and Baldwin, R. L. (1982). Specific intermediates in the folding reactions of small proteins and the mechanism of protein folding. *Annu Rev Biochem* *51*, 459-489.
- Kim, S., Willison, K. R., and Horwich, A. L. (1994). Cytosolic chaperonin subunits have a conserved ATPase domain but diverged polypeptide-binding domains. *Trends Biochem Sci* *19*, 543-548.
- Kim, S., Nollen, E. A., Kitagawa, K., Bindokas, V. P., and Morimoto, R. I. (2002). Polyglutamine protein aggregates are dynamic. *Nat Cell Biol* *4*, 826-831.

- Kim, Y. J., Yi, Y., Sapp, E., Wang, Y., Cuiffo, B., Kegel, K. B., Qin, Z. H., Aronin, N., and DiFiglia, M. (2001). Caspase 3-cleaved N-terminal fragments of wild-type and mutant huntingtin are present in normal and Huntington's disease brains, associate with membranes, and undergo calpain-dependent proteolysis. *Proc Natl Acad Sci U S A* *98*, 12784-12789.
- Kita, H., Carmichael, J., Swartz, J., Muro, S., Wyttenbach, A., Matsubara, K., Rubinsztein, D. C., and Kato, K. (2002). Modulation of polyglutamine-induced cell death by genes identified by expression profiling. *Hum Mol Genet* *11*, 2279-2287.
- Kitamura, A., Kubota, H., Pack, C. G., Matsumoto, G., Hirayama, S., Takahashi, Y., Kimura, H., Kinjo, M., Morimoto, R. I., and Nagata, K. (2006). Cytosolic chaperonin prevents polyglutamine toxicity with altering the aggregation state. *Nat Cell Biol.*
- Klement, I. A., Skinner, P. J., Kaytor, M. D., Yi, H., Hersch, S. M., Clark, H. B., Zoghbi, H. Y., and Orr, H. T. (1998). Ataxin-1 nuclear localization and aggregation: role in polyglutamine-induced disease in SCA1 transgenic mice. *Cell* *95*, 41-53.
- Klumpp, M., Baumeister, W., and Essen, L. O. (1997). Structure of the substrate binding domain of the thermosome, an archaeal group II chaperonin. *Cell* *91*, 263-270.
- Koide, R., Kobayashi, S., Shimohata, T., Ikeuchi, T., Maruyama, M., Saito, M., Yamada, M., Takahashi, H., and Tsuji, S. (1999). A neurological disease caused by an expanded CAG trinucleotide repeat in the TATA-binding protein gene: a new polyglutamine disease? *Hum Mol Genet* *8*, 2047-2053.
- Koo, E. H., Lansbury, P. T., Jr., and Kelly, J. W. (1999). Amyloid diseases: abnormal protein aggregation in neurodegeneration. *Proc Natl Acad Sci U S A* *96*, 9989-9990.
- Krobitsch, S., and Lindquist, S. (2000). Aggregation of huntingtin in yeast varies with the length of the polyglutamine expansion and the expression of chaperone proteins. *Proc Natl Acad Sci U S A* *97*, 1589-1594.
- Kubota, S., Kubota, H., and Nagata, K. (2006). Cytosolic chaperonin protects folding intermediates of Gbeta from aggregation by recognizing hydrophobic beta-strands. *Proc Natl Acad Sci U S A* *103*, 8360-8365.
- Kuemmerle, S., Gutekunst, C. A., Klein, A. M., Li, X. J., Li, S. H., Beal, M. F., Hersch, S. M., and Ferrante, R. J. (1999). Huntington aggregates may not predict neuronal death in Huntington's disease. *Ann Neurol* *46*, 842-849.
- Laemmli, U. K. (1970). Cleavage of structural proteins during the assembly of the head of bacteriophage T4. *Nature* *227*, 680-685.
- Landles, C., and Bates, G. P. (2004). Huntingtin and the molecular pathogenesis of Huntington's disease. Fourth in molecular medicine review series. *EMBO Rep* *5*, 958-963.
- Lashuel, H. A., Hartley, D., Petre, B. M., Walz, T., and Lansbury, P. T., Jr. (2002). Neurodegenerative disease: amyloid pores from pathogenic mutations. *Nature* *418*, 291.
- Lescure, A., Lutz, Y., Eberhard, D., Jacq, X., Krol, A., Grummt, I., Davidson, I., Chambon, P., and Tora, L. (1994). The N-terminal domain of the human TATA-binding protein plays a role in transcription from TATA-containing RNA polymerase II and III promoters. *Embo J* *13*, 1166-1175.
- Li, S. H., Cheng, A. L., Zhou, H., Lam, S., Rao, M., Li, H., and Li, X. J. (2002). Interaction of Huntington disease protein with transcriptional activator Sp1. *Mol Cell Biol* *22*, 1277-1287.
- Li, S. H., and Li, X. J. (2004). Huntingtin-protein interactions and the pathogenesis of Huntington's disease. *Trends Genet* *20*, 146-154.
- Llorca, O., McCormack, E. A., Hynes, G., Grantham, J., Cordell, J., Carrascosa, J. L., Willison, K. R., Fernandez, J. J., and Valpuesta, J. M. (1999). Eukaryotic type II chaperonin CCT interacts with actin through specific subunits. *Nature* *402*, 693-696.

- Llorca, O., Martin-Benito, J., Ritco-Vonsovici, M., Grantham, J., Hynes, G. M., Willison, K. R., Carrascosa, J. L., and Valpuesta, J. M. (2000). Eukaryotic chaperonin CCT stabilizes actin and tubulin folding intermediates in open quasi-native conformations. *Embo J* *19*, 5971-5979.
- Llorca, O., Martin-Benito, J., Gomez-Puertas, P., Ritco-Vonsovici, M., Willison, K. R., Carrascosa, J. L., and Valpuesta, J. M. (2001a). Analysis of the interaction between the eukaryotic chaperonin CCT and its substrates actin and tubulin. *J Struct Biol* *135*, 205-218.
- Llorca, O., Martin-Benito, J., Grantham, J., Ritco-Vonsovici, M., Willison, K. R., Carrascosa, J. L., and Valpuesta, J. M. (2001b). The 'sequential allosteric ring' mechanism in the eukaryotic chaperonin-assisted folding of actin and tubulin. *Embo J* *20*, 4065-4075.
- Lonze, B. E., and Ginty, D. D. (2002). Function and regulation of CREB family transcription factors in the nervous system. *Neuron* *35*, 605-623.
- Lonze, B. E., Riccio, A., Cohen, S., and Ginty, D. D. (2002). Apoptosis, axonal growth defects, and degeneration of peripheral neurons in mice lacking CREB. *Neuron* *34*, 371-385.
- Lunkes, A., Lindenberg, K. S., Ben-Haiem, L., Weber, C., Devys, D., Landwehrmeyer, G. B., Mandel, J. L., and Trottier, Y. (2002). Proteases acting on mutant huntingtin generate cleaved products that differentially build up cytoplasmic and nuclear inclusions. *Mol Cell* *10*, 259-269.
- Luo, S., Vacher, C., Davies, J. E., and Rubinsztein, D. C. (2005). Cdk5 phosphorylation of huntingtin reduces its cleavage by caspases: implications for mutant huntingtin toxicity. *J Cell Biol* *169*, 647-656.
- Luthi-Carter, R., Strand, A., Peters, N. L., Solano, S. M., Hollingsworth, Z. R., Menon, A. S., Frey, A. S., Spektor, B. S., Penney, E. B., Schilling, G., *et al.* (2000). Decreased expression of striatal signaling genes in a mouse model of Huntington's disease. *Hum Mol Genet* *9*, 1259-1271.
- Luthi-Carter, R., Hanson, S. A., Strand, A. D., Bergstrom, D. A., Chun, W., Peters, N. L., Woods, A. M., Chan, E. Y., Kooperberg, C., Krainc, D., *et al.* (2002a). Dysregulation of gene expression in the R6/2 model of polyglutamine disease: parallel changes in muscle and brain. *Hum Mol Genet* *11*, 1911-1926.
- Luthi-Carter, R., Strand, A. D., Hanson, S. A., Kooperberg, C., Schilling, G., La Spada, A. R., Merry, D. E., Young, A. B., Ross, C. A., Borchelt, D. R., and Olson, J. M. (2002b). Polyglutamine and transcription: gene expression changes shared by DRPLA and Huntington's disease mouse models reveal context-independent effects. *Hum Mol Genet* *11*, 1927-1937.
- Mangiarini, L., Sathasivam, K., Seller, M., Cozens, B., Harper, A., Hetherington, C., Lawton, M., Trottier, Y., Lehrach, H., Davies, S. W., and Bates, G. P. (1996). Exon 1 of the HD gene with an expanded CAG repeat is sufficient to cause a progressive neurological phenotype in transgenic mice. *Cell* *87*, 493-506.
- Maniatis, T., and Reed, R. (2002). An extensive network of coupling among gene expression machines. *Nature* *416*, 499-506.
- Mantamadiotis, T., Lemberger, T., Bleckmann, S. C., Kern, H., Kretz, O., Martin Villalba, A., Tronche, F., Kellendonk, C., Gau, D., Kapfhammer, J., *et al.* (2002). Disruption of CREB function in brain leads to neurodegeneration. *Nat Genet* *31*, 47-54.
- Martin-Benito, J., Boskovic, J., Gomez-Puertas, P., Carrascosa, J. L., Simons, C. T., Lewis, S. A., Bartolini, F., Cowan, N. J., and Valpuesta, J. M. (2002). Structure of eukaryotic prefoldin and of its complexes with unfolded actin and the cytosolic chaperonin CCT. *Embo J* *21*, 6377-6386.
- Masino, L., Kelly, G., Leonard, K., Trottier, Y., and Pastore, A. (2002). Solution structure of polyglutamine tracts in GST-polyglutamine fusion proteins. *FEBS Lett* *513*, 267-272.
- Mattson, M. P., and Magnus, T. (2006). Ageing and neuronal vulnerability. *Nat Rev Neurosci* *7*, 278-294.

- McCallum, C. D., Do, H., Johnson, A. E., and Frydman, J. (2000). The interaction of the chaperonin tailless complex polypeptide 1 (TCP1) ring complex (TRiC) with ribosome-bound nascent chains examined using photo-cross-linking. *J Cell Biol* *149*, 591-602.
- McC Campbell, A., Taylor, J. P., Taye, A. A., Robitschek, J., Li, M., Walcott, J., Merry, D., Chai, Y., Paulson, H., Sobue, G., and Fischbeck, K. H. (2000). CREB-binding protein sequestration by expanded polyglutamine. *Hum Mol Genet* *9*, 2197-2202.
- McC Campbell, A., Taye, A. A., Whitty, L., Penney, E., Steffan, J. S., and Fischbeck, K. H. (2001). Histone deacetylase inhibitors reduce polyglutamine toxicity. *Proc Natl Acad Sci U S A* *98*, 15179-15184.
- McLean, C. A., Cherny, R. A., Fraser, F. W., Fuller, S. J., Smith, M. J., Beyreuther, K., Bush, A. I., and Masters, C. L. (1999). Soluble pool of Abeta amyloid as a determinant of severity of neurodegeneration in Alzheimer's disease. *Ann Neurol* *46*, 860-866.
- Melville, M. W., McClellan, A. J., Meyer, A. S., Darveau, A., and Frydman, J. (2003). The Hsp70 and TRiC/CCT chaperone systems cooperate in vivo to assemble the von Hippel-Lindau tumor suppressor complex. *Mol Cell Biol* *23*, 3141-3151.
- Meriin, A. B., Zhang, X., He, X., Newnam, G. P., Chernoff, Y. O., and Sherman, M. Y. (2002). Huntington toxicity in yeast model depends on polyglutamine aggregation mediated by a prion-like protein Rnq1. *J Cell Biol* *157*, 997-1004.
- Meyer, A. S., Gillespie, J. R., Walther, D., Millet, I. S., Doniach, S., and Frydman, J. (2003). Closing the folding chamber of the eukaryotic chaperonin requires the transition state of ATP hydrolysis. *Cell* *113*, 369-381.
- Michalik, A., and Van Broeckhoven, C. (2003). Pathogenesis of polyglutamine disorders: aggregation revisited. *Hum Mol Genet* *12 Spec No 2*, R173-186.
- Michimoto, T., Aoki, T., Toh-e, A., and Kikuchi, Y. (2000). Yeast Pdr13p and Zuo1p molecular chaperones are new functional Hsp70 and Hsp40 partners. *Gene* *257*, 131-137.
- Minami, Y., Hohfeld, J., Ohtsuka, K., and Hartl, F. U. (1996). Regulation of the heat-shock protein 70 reaction cycle by the mammalian DnaJ homolog, Hsp40. *J Biol Chem* *271*, 19617-19624.
- Minton, A. P. (2001). The influence of macromolecular crowding and macromolecular confinement on biochemical reactions in physiological media. *J Biol Chem* *276*, 10577-10580.
- Mizushima, S., and Nagata, S. (1990). pEF-BOS, a powerful mammalian expression vector. *Nucleic Acids Res* *18*, 5322.
- Morley, J. F., Brignull, H. R., Weyers, J. J., and Morimoto, R. I. (2002). The threshold for polyglutamine-expansion protein aggregation and cellular toxicity is dynamic and influenced by aging in *Caenorhabditis elegans*. *Proc Natl Acad Sci U S A* *99*, 10417-10422.
- Morley, J. F., and Morimoto, R. I. (2004). Regulation of longevity in *Caenorhabditis elegans* by heat shock factor and molecular chaperones. *Mol Biol Cell* *15*, 657-664.
- Muchowski, P. J., Schaffar, G., Sittler, A., Wanker, E. E., Hayer-Hartl, M. K., and Hartl, F. U. (2000). Hsp70 and hsp40 chaperones can inhibit self-assembly of polyglutamine proteins into amyloid-like fibrils. *Proc Natl Acad Sci U S A* *97*, 7841-7846.
- Muchowski, P. J., Ning, K., D'Souza-Schorey, C., and Fields, S. (2002). Requirement of an intact microtubule cytoskeleton for aggregation and inclusion body formation by a mutant huntingtin fragment. *Proc Natl Acad Sci U S A* *99*, 727-732.
- Muchowski, P. J., and Wacker, J. L. (2005). Modulation of neurodegeneration by molecular chaperones. *Nat Rev Neurosci* *6*, 11-22.
- Mumberg, D., Muller, R., and Funk, M. (1994). Regulatable promoters of *Saccharomyces cerevisiae*: comparison of transcriptional activity and their use for heterologous expression. *Nucleic Acids Res* *22*, 5767-5768.

- Nakamura, K., Jeong, S. Y., Uchihara, T., Anno, M., Nagashima, K., Nagashima, T., Ikeda, S., Tsuji, S., and Kanazawa, I. (2001). SCA17, a novel autosomal dominant cerebellar ataxia caused by an expanded polyglutamine in TATA-binding protein. *Hum Mol Genet* *10*, 1441-1448.
- Nasir, J., Floresco, S. B., O'Kusky, J. R., Diewert, V. M., Richman, J. M., Zeisler, J., Borowski, A., Marth, J. D., Phillips, A. G., and Hayden, M. R. (1995). Targeted disruption of the Huntington's disease gene results in embryonic lethality and behavioral and morphological changes in heterozygotes. *Cell* *81*, 811-823.
- Netzer, W. J., and Hartl, F. U. (1997). Recombination of protein domains facilitated by co-translational folding in eukaryotes. *Nature* *388*, 343-349.
- Nielsen, D. A., Chou, J., MacKrell, A. J., Casadaban, M. J., and Steiner, D. F. (1983). Expression of a preproinsulin-beta-galactosidase gene fusion in mammalian cells. *Proc Natl Acad Sci U S A* *80*, 5198-5202.
- Nilsberth, C., Westlind-Danielsson, A., Eckman, C. B., Condron, M. M., Axelman, K., Forsell, C., Sten, C., Luthman, J., Teplow, D. B., Younkin, S. G., *et al.* (2001). The 'Arctic' APP mutation (E693G) causes Alzheimer's disease by enhanced A β protofibril formation. *Nat Neurosci* *4*, 887-893.
- Nollen, E. A., Garcia, S. M., van Haften, G., Kim, S., Chavez, A., Morimoto, R. I., and Plasterk, R. H. (2004). Genome-wide RNA interference screen identifies previously undescribed regulators of polyglutamine aggregation. *Proc Natl Acad Sci U S A* *101*, 6403-6408.
- Nozaki, K., Onodera, O., Takano, H., and Tsuji, S. (2001). Amino acid sequences flanking polyglutamine stretches influence their potential for aggregate formation. *Neuroreport* *12*, 3357-3364.
- Nucifora, F. C., Jr., Sasaki, M., Peters, M. F., Huang, H., Cooper, J. K., Yamada, M., Takahashi, H., Tsuji, S., Troncoso, J., Dawson, V. L., *et al.* (2001). Interference by huntingtin and atrophin-1 with cbp-mediated transcription leading to cellular toxicity. *Science* *291*, 2423-2428.
- Okazawa, H. (2003). Polyglutamine diseases: a transcription disorder? *Cell Mol Life Sci* *60*, 1427-1439.
- O'Nuallain, B., and Wetzel, R. (2002). Conformational Abs recognizing a generic amyloid fibril epitope. *Proc Natl Acad Sci U S A* *99*, 1485-1490.
- Orr, H. T., and Zoghbi, H. Y. (2001). SCA1 molecular genetics: a history of a 13 year collaboration against glutamines. *Hum Mol Genet* *10*, 2307-2311.
- Osherovich, L. Z., and Weissman, J. S. (2001). Multiple Gln/Asn-rich prion domains confer susceptibility to induction of the yeast [PSI(+)] prion. *Cell* *106*, 183-194.
- Otto, H., Conz, C., Maier, P., Wolfle, T., Suzuki, C. K., Jenö, P., Rucknagel, P., Stahl, J., and Rospert, S. (2005). The chaperones MPP11 and Hsp70L1 form the mammalian ribosome-associated complex. *Proc Natl Acad Sci U S A* *102*, 10064-10069.
- Paulson, H. L., Perez, M. K., Trotter, Y., Trojanowski, J. Q., Subramony, S. H., Das, S. S., Vig, P., Mandel, J. L., Fischbeck, K. H., and Pittman, R. N. (1997). Intranuclear inclusions of expanded polyglutamine protein in spinocerebellar ataxia type 3. *Neuron* *19*, 333-344.
- Perez, M. K., Paulson, H. L., Pendse, S. J., Saionz, S. J., Bonini, N. M., and Pittman, R. N. (1998). Recruitment and the role of nuclear localization in polyglutamine-mediated aggregation. *J Cell Biol* *143*, 1457-1470.
- Perutz, M. F., Johnson, T., Suzuki, M., and Finch, J. T. (1994). Glutamine repeats as polar zippers: their possible role in inherited neurodegenerative diseases. *Proc Natl Acad Sci U S A* *91*, 5355-5358.
- Perutz, M. F., Finch, J. T., Berriman, J., and Lesk, A. (2002a). Amyloid fibers are water-filled nanotubes. *Proc Natl Acad Sci U S A* *99*, 5591-5595.
- Perutz, M. F., Pope, B. J., Owen, D., Wanker, E. E., and Scherzinger, E. (2002b). Aggregation of proteins with expanded glutamine and alanine repeats of the glutamine-rich and asparagine-rich

- domains of Sup35 and of the amyloid beta-peptide of amyloid plaques. *Proc Natl Acad Sci U S A* *99*, 5596-5600.
- Peters, M. F., Nucifora, F. C., Jr., Kushi, J., Seaman, H. C., Cooper, J. K., Herring, W. J., Dawson, V. L., Dawson, T. M., and Ross, C. A. (1999). Nuclear targeting of mutant Huntingtin increases toxicity. *Mol Cell Neurosci* *14*, 121-128.
- Peterson, M. G., Tanese, N., Pugh, B. F., and Tjian, R. (1990). Functional domains and upstream activation properties of cloned human TATA binding protein. *Science* *248*, 1625-1630.
- Pickart, C. M., and Cohen, R. E. (2004). Proteasomes and their kin: proteases in the machine age. *Nat Rev Mol Cell Biol* *5*, 177-187.
- Poirier, M. A., Li, H., Macosko, J., Cai, S., Amzel, M., and Ross, C. A. (2002). Huntingtin spheroids and protofibrils as precursors in polyglutamine fibrilization. *J Biol Chem* *277*, 41032-41037.
- Pratt, W. B., and Toft, D. O. (2003). Regulation of signaling protein function and trafficking by the hsp90/hsp70-based chaperone machinery. *Exp Biol Med (Maywood)* *228*, 111-133.
- Preisinger, E., Jordan, B. M., Kazantsev, A., and Housman, D. (1999). Evidence for a recruitment and sequestration mechanism in Huntington's disease. *Philos Trans R Soc Lond B Biol Sci* *354*, 1029-1034.
- Prodromou, C., Siligardi, G., O'Brien, R., Woolfson, D. N., Regan, L., Panaretou, B., Ladbury, J. E., Piper, P. W., and Pearl, L. H. (1999). Regulation of Hsp90 ATPase activity by tetratricopeptide repeat (TPR)-domain co-chaperones. *Embo J* *18*, 754-762.
- Ptitsyn, O. B., and Rashin, A. A. (1975). A model of myoglobin self-organization. *Biophys Chem* *3*, 1-20.
- Quist, A., Doudevski, I., Lin, H., Azimova, R., Ng, D., Frangione, B., Kagan, B., Ghiso, J., and Lal, R. (2005). Amyloid ion channels: a common structural link for protein-misfolding disease. *Proc Natl Acad Sci U S A* *102*, 10427-10432.
- Radford, S. E., Dobson, C. M., and Evans, P. A. (1992). The folding of hen lysozyme involves partially structured intermediates and multiple pathways. *Nature* *358*, 302-307.
- Radford, S. E. (2000). Protein folding: progress made and promises ahead. *Trends Biochem Sci* *25*, 611-618.
- Rattan, S. I., and Derwentzi, A. (1991). Altered cellular responsiveness during ageing. *Bioessays* *13*, 601-606.
- Ravikumar, B., and Rubinsztein, D. C. (2004). Can autophagy protect against neurodegeneration caused by aggregate-prone proteins? *Neuroreport* *15*, 2443-2445.
- Reed, R. (2003). Coupling transcription, splicing and mRNA export. *Curr Opin Cell Biol* *15*, 326-331.
- Reiner, A., Del Mar, N., Meade, C. A., Yang, H., Dragatsis, I., Zeitlin, S., and Goldowitz, D. (2001). Neurons lacking huntingtin differentially colonize brain and survive in chimeric mice. *J Neurosci* *21*, 7608-7619.
- Reixach, N., Deechongkit, S., Jiang, X., Kelly, J. W., and Buxbaum, J. N. (2004). Tissue damage in the amyloidoses: Transthyretin monomers and nonnative oligomers are the major cytotoxic species in tissue culture. *Proc Natl Acad Sci U S A* *101*, 2817-2822.
- Richter, K., and Buchner, J. (2001). Hsp90: chaperoning signal transduction. *J Cell Physiol* *188*, 281-290.
- Rideout, H. J., Lang-Rollin, I., and Stefanis, L. (2004). Involvement of macroautophagy in the dissolution of neuronal inclusions. *Int J Biochem Cell Biol* *36*, 2551-2562.
- Rigamonti, D., Bauer, J. H., De-Fraja, C., Conti, L., Sipione, S., Sciorati, C., Clementi, E., Hackam, A., Hayden, M. R., Li, Y., *et al.* (2000). Wild-type huntingtin protects from apoptosis upstream of caspase-3. *J Neurosci* *20*, 3705-3713.

- Rochet, J. C., and Lansbury, P. T., Jr. (2000). Amyloid fibrillogenesis: themes and variations. *Curr Opin Struct Biol* 10, 60-68.
- Roder, H., and Colon, W. (1997). Kinetic role of early intermediates in protein folding. *Curr Opin Struct Biol* 7, 15-28.
- Roeder, R. G. (1991). The complexities of eukaryotic transcription initiation: regulation of preinitiation complex assembly. *Trends Biochem Sci* 16, 402-408.
- Rolfs, A., Koeppen, A. H., Bauer, I., Bauer, P., Buhlmann, S., Topka, H., Schols, L., and Riess, O. (2003). Clinical features and neuropathology of autosomal dominant spinocerebellar ataxia (SCA17). *Ann Neurol* 54, 367-375.
- Ross, C. A. (2002). Polyglutamine pathogenesis: emergence of unifying mechanisms for Huntington's disease and related disorders. *Neuron* 35, 819-822.
- Ross, C. A., Poirier, M. A., Wanker, E. E., and Amzel, M. (2003). Polyglutamine fibrillogenesis: the pathway unfolds. *Proc Natl Acad Sci U S A* 100, 1-3.
- Ross, C. A., and Poirier, M. A. (2004). Protein aggregation and neurodegenerative disease. *Nat Med* 10 Suppl, S10-17.
- Ross, C. A., and Poirier, M. A. (2005). Opinion: What is the role of protein aggregation in neurodegeneration? *Nat Rev Mol Cell Biol* 6, 891-898.
- Rousseau, E., Dehay, B., Ben-Haiem, L., Trottier, Y., Morange, M., and Bertolotti, A. (2004). Targeting expression of expanded polyglutamine proteins to the endoplasmic reticulum or mitochondria prevents their aggregation. *Proc Natl Acad Sci U S A* 101, 9648-9653.
- Rudiger, S., Germeroth, L., Schneider-Mergener, J., and Bukau, B. (1997). Substrate specificity of the DnaK chaperone determined by screening cellulose-bound peptide libraries. *Embo J* 16, 1501-1507.
- Rutherford, S. L., and Lindquist, S. (1998). Hsp90 as a capacitor for morphological evolution. *Nature* 396, 336-342.
- Sakahira, H., Breuer, P., Hayer-Hartl, M. K., and Hartl, F. U. (2002). Molecular chaperones as modulators of polyglutamine protein aggregation and toxicity. *Proc Natl Acad Sci U S A* 99, 16412-16418.
- Sambrook J., F. E. F., Maniatis T (1989). *Molecular Cloning*, 2nd edn, Cold Spring Harbor Laboratory Press).
- Sanchez, I., Mahlke, C., and Yuan, J. (2003). Pivotal role of oligomerization in expanded polyglutamine neurodegenerative disorders. *Nature* 421, 373-379.
- Sanchez, I. E., and Kiefhaber, T. (2003). Evidence for sequential barriers and obligatory intermediates in apparent two-state protein folding. *J Mol Biol* 325, 367-376.
- Saudou, F., Finkbeiner, S., Devys, D., and Greenberg, M. E. (1998). Huntingtin acts in the nucleus to induce apoptosis but death does not correlate with the formation of intranuclear inclusions. *Cell* 95, 55-66.
- Schaffar, G. (2004) *Inhibition der Polyglutamin-induzierten Inaktivierung von Transkriptionsfaktoren durch molekulare Chaperone*, Ludwig-Maximilians-Universität, München.
- Schaffar, G., Breuer, P., Boteva, R., Behrends, C., Tzvetkov, N., Strippel, N., Sakahira, H., Siegers, K., Hayer-Hartl, M., and Hartl, F. U. (2004). Cellular toxicity of polyglutamine expansion proteins: mechanism of transcription factor deactivation. *Mol Cell* 15, 95-105.
- Scherzinger, E., Lurz, R., Turmaine, M., Mangiarini, L., Hollenbach, B., Hasenbank, R., Bates, G. P., Davies, S. W., Lehrach, H., and Wanker, E. E. (1997). Huntingtin-encoded polyglutamine expansions form amyloid-like protein aggregates in vitro and in vivo. *Cell* 90, 549-558.
- Scherzinger, E., Sittler, A., Schweiger, K., Heiser, V., Lurz, R., Hasenbank, R., Bates, G. P., Lehrach, H., and Wanker, E. E. (1999). Self-assembly of polyglutamine-containing huntingtin fragments into

- amyloid-like fibrils: implications for Huntington's disease pathology. *Proc Natl Acad Sci U S A* *96*, 4604-4609.
- Scheufler, C., Brinker, A., Bourenkov, G., Pegoraro, S., Moroder, L., Bartunik, H., Hartl, F. U., and Moarefi, I. (2000). Structure of TPR domain-peptide complexes: critical elements in the assembly of the Hsp70-Hsp90 multichaperone machine. *Cell* *101*, 199-210.
- Serio, T. R., Cashikar, A. G., Kowal, A. S., Sawicki, G. J., Moslehi, J. J., Serpell, L., Arnsdorf, M. F., and Lindquist, S. L. (2000). Nucleated conformational conversion and the replication of conformational information by a prion determinant. *Science* *289*, 1317-1321.
- Sharp, A. H., Loev, S. J., Schilling, G., Li, S. H., Li, X. J., Bao, J., Wagster, M. V., Kotzok, J. A., Steiner, J. P., Lo, A., and et al. (1995). Widespread expression of Huntington's disease gene (IT15) protein product. *Neuron* *14*, 1065-1074.
- Sherman, M. Y., and Goldberg, A. L. (2001). Cellular defenses against unfolded proteins: a cell biologist thinks about neurodegenerative diseases. *Neuron* *29*, 15-32.
- Shi, X., Parthun, M. R., and Jaehning, J. A. (1995). The yeast EGD2 gene encodes a homologue of the alpha NAC subunit of the human nascent-polypeptide-associated complex. *Gene* *165*, 199-202.
- Shimohata, T., Nakajima, T., Yamada, M., Uchida, C., Onodera, O., Naruse, S., Kimura, T., Koide, R., Nozaki, K., Sano, Y., et al. (2000). Expanded polyglutamine stretches interact with TAFII130, interfering with CREB-dependent transcription. *Nat Genet* *26*, 29-36.
- Shimohata, T., Onodera, O., and Tsuji, S. (2001). Expanded polyglutamine stretches lead to aberrant transcriptional regulation in polyglutamine diseases. *Hum Cell* *14*, 17-25.
- Shomura, Y., Dragovic, Z., Chang, H. C., Tzvetkov, N., Young, J. C., Brodsky, J. L., Guerriero, V., Hartl, F. U., and Bracher, A. (2005). Regulation of Hsp70 function by HspBP1: structural analysis reveals an alternate mechanism for Hsp70 nucleotide exchange. *Mol Cell* *17*, 367-379.
- Siegers, K., Waldmann, T., Leroux, M. R., Grein, K., Shevchenko, A., Schiebel, E., and Hartl, F. U. (1999). Compartmentation of protein folding in vivo: sequestration of non-native polypeptide by the chaperonin-GimC system. *Embo J* *18*, 75-84.
- Siegers, K., and Schiebel, E. (2000). Purification of GimC from *Saccharomyces cerevisiae*. *Methods Mol Biol* *140*, 185-193.
- Siegers, K., Bolter, B., Schwarz, J. P., Bottcher, U. M., Guha, S., and Hartl, F. U. (2003). TRiC/CCT cooperates with different upstream chaperones in the folding of distinct protein classes. *Embo J* *22*, 5230-5240.
- Sigler, P. B., Xu, Z., Rye, H. S., Burstson, S. G., Fenton, W. A., and Horwich, A. L. (1998). Structure and function in GroEL-mediated protein folding. *Annu Rev Biochem* *67*, 581-608.
- Sikorski, R. S., and Hieter, P. (1989). A system of shuttle vectors and yeast host strains designed for efficient manipulation of DNA in *Saccharomyces cerevisiae*. *Genetics* *122*, 19-27.
- Sikorski, R. S., and Boeke, J. D. (1991). In vitro mutagenesis and plasmid shuffling: from cloned gene to mutant yeast. *Methods Enzymol* *194*, 302-318.
- Sipione, S., and Cattaneo, E. (2001). Modeling Huntington's disease in cells, flies, and mice. *Mol Neurobiol* *23*, 21-51.
- Sipione, S., Rigamonti, D., Valenza, M., Zuccato, C., Conti, L., Pritchard, J., Kooperberg, C., Olson, J. M., and Cattaneo, E. (2002). Early transcriptional profiles in huntingtin-inducible striatal cells by microarray analyses. *Hum Mol Genet* *11*, 1953-1965.
- Sittler, A., Lurz, R., Lueder, G., Priller, J., Lehrach, H., Hayer-Hartl, M. K., Hartl, F. U., and Wanker, E. E. (2001). Geldanamycin activates a heat shock response and inhibits huntingtin aggregation in a cell culture model of Huntington's disease. *Hum Mol Genet* *10*, 1307-1315.

- Slow, E. J., Graham, R. K., Osmand, A. P., Devon, R. S., Lu, G., Deng, Y., Pearson, J., Vaid, K., Bissada, N., Wetzel, R., *et al.* (2005). Absence of behavioral abnormalities and neurodegeneration in vivo despite widespread neuronal huntingtin inclusions. *Proc Natl Acad Sci U S A* *102*, 11402-11407.
- Sondheimer, N., Lopez, N., Craig, E. A., and Lindquist, S. (2001). The role of Sis1 in the maintenance of the [RNQ+] prion. *Embo J* *20*, 2435-2442.
- Soti, C., and Csermely, P. (2002). Chaperones and aging: role in neurodegeneration and in other civilizational diseases. *Neurochem Int* *41*, 383-389.
- Sousa, M. M., Cardoso, I., Fernandes, R., Guimaraes, A., and Saraiva, M. J. (2001). Deposition of transthyretin in early stages of familial amyloidotic polyneuropathy: evidence for toxicity of nonfibrillar aggregates. *Am J Pathol* *159*, 1993-2000.
- Spiess, C., Meyer, A. S., Reissmann, S., and Frydman, J. (2004). Mechanism of the eukaryotic chaperonin: protein folding in the chamber of secrets. *Trends Cell Biol* *14*, 598-604.
- Stefani, M., and Dobson, C. M. (2003). Protein aggregation and aggregate toxicity: new insights into protein folding, misfolding diseases and biological evolution. *J Mol Med* *81*, 678-699.
- Steffan, J. S., Kazantsev, A., Spasic-Boskovic, O., Greenwald, M., Zhu, Y. Z., Gohler, H., Wanker, E. E., Bates, G. P., Housman, D. E., and Thompson, L. M. (2000). The Huntington's disease protein interacts with p53 and CREB-binding protein and represses transcription. *Proc Natl Acad Sci U S A* *97*, 6763-6768.
- Steffan, J. S., Bodai, L., Pallos, J., Poelman, M., McCampbell, A., Apostol, B. L., Kazantsev, A., Schmidt, E., Zhu, Y. Z., Greenwald, M., *et al.* (2001). Histone deacetylase inhibitors arrest polyglutamine-dependent neurodegeneration in *Drosophila*. *Nature* *413*, 739-743.
- Steffan, J. S., Agrawal, N., Pallos, J., Rockabrand, E., Trotman, L. C., Slepko, N., Illes, K., Lukacsovich, T., Zhu, Y. Z., Cattaneo, E., *et al.* (2004). SUMO modification of Huntingtin and Huntington's disease pathology. *Science* *304*, 100-104.
- Stevanin, G., Fujigasaki, H., Lebre, A. S., Camuzat, A., Jeannequin, C., Dode, C., Takahashi, J., San, C., Bellance, R., Brice, A., and Durr, A. (2003). Huntington's disease-like phenotype due to trinucleotide repeat expansions in the TBP and JPH3 genes. *Brain* *126*, 1599-1603.
- Strubin, M., and Struhl, K. (1992). Yeast and human TFIID with altered DNA-binding specificity for TATA elements. *Cell* *68*, 721-730.
- Sugars, K. L., and Rubinsztein, D. C. (2003). Transcriptional abnormalities in Huntington disease. *Trends Genet* *19*, 233-238.
- Suhr, S. T., Senut, M. C., Whitelegge, J. P., Faull, K. F., Cuizon, D. B., and Gage, F. H. (2001). Identities of sequestered proteins in aggregates from cells with induced polyglutamine expression. *J Cell Biol* *153*, 283-294.
- Sunde, M., and Blake, C. (1997). The structure of amyloid fibrils by electron microscopy and X-ray diffraction. *Adv Protein Chem* *50*, 123-159.
- Tam, S., Geller, R., Spiess, C., and Frydman, J. (2006). The chaperonin TRiC controls polyglutamine aggregation and toxicity through subunit-specific interactions. *Nat Cell Biol*.
- Tan, S. Y., and Pepys, M. B. (1994). Amyloidosis. *Histopathology* *25*, 403-414.
- Tanese, N., and Tjian, R. (1993). Coactivators and TAFs: a new class of eukaryotic transcription factors that connect activators to the basal machinery. *Cold Spring Harb Symp Quant Biol* *58*, 179-185.
- Taylor, J. P., Tanaka, F., Robitschek, J., Sandoval, C. M., Taye, A., Markovic-Plese, S., and Fischbeck, K. H. (2003). Aggresomes protect cells by enhancing the degradation of toxic polyglutamine-containing protein. *Hum Mol Genet* *12*, 749-757.

- Terry, R. D., Masliah, E., Salmon, D. P., Butters, N., DeTeresa, R., Hill, R., Hansen, L. A., and Katzman, R. (1991). Physical basis of cognitive alterations in Alzheimer's disease: synapse loss is the major correlate of cognitive impairment. *Ann Neurol* *30*, 572-580.
- Thakur, A. K., and Wetzel, R. (2002). Mutational analysis of the structural organization of polyglutamine aggregates. *Proc Natl Acad Sci U S A* *99*, 17014-17019.
- Tobin, A. J., and Signer, E. R. (2000). Huntington's disease: the challenge for cell biologists. *Trends Cell Biol* *10*, 531-536.
- Tompkins, M. M., and Hill, W. D. (1997). Contribution of somal Lewy bodies to neuronal death. *Brain Res* *775*, 24-29.
- Towbin, H., Staehelin, T., and Gordon, J. (1979). Electrophoretic transfer of proteins from polyacrylamide gels to nitrocellulose sheets: procedure and some applications. *Proc Natl Acad Sci U S A* *76*, 4350-4354.
- Trojanowski, J. Q., and Mattson, M. P. (2003). Overview of protein aggregation in single, double, and triple neurodegenerative brain amyloidoses. *Neuromolecular Med* *4*, 1-6.
- Trottier, Y., Devys, D., Imbert, G., Saudou, F., An, I., Lutz, Y., Weber, C., Agid, Y., Hirsch, E. C., and Mandel, J. L. (1995a). Cellular localization of the Huntington's disease protein and discrimination of the normal and mutated form. *Nat Genet* *10*, 104-110.
- Trottier, Y., Lutz, Y., Stevanin, G., Imbert, G., Devys, D., Cancel, G., Saudou, F., Weber, C., David, G., Tora, L., and et al. (1995b). Polyglutamine expansion as a pathological epitope in Huntington's disease and four dominant cerebellar ataxias. *Nature* *378*, 403-406.
- Tsai, Y. C., Fishman, P. S., Thakor, N. V., and Oyler, G. A. (2003). Parkin facilitates the elimination of expanded polyglutamine proteins and leads to preservation of proteasome function. *J Biol Chem* *278*, 22044-22055.
- Ursic, D., Sedbrook, J. C., Himmel, K. L., and Culbertson, M. R. (1994). The essential yeast Tcp1 protein affects actin and microtubules. *Mol Biol Cell* *5*, 1065-1080.
- Vacher, C., Garcia-Oroz, L., and Rubinsztein, D. C. (2005). Overexpression of yeast hsp104 reduces polyglutamine aggregation and prolongs survival of a transgenic mouse model of Huntington's disease. *Hum Mol Genet* *14*, 3425-3433.
- Vainberg, I. E., Lewis, S. A., Rommelaere, H., Ampe, C., Vandekerckhove, J., Klein, H. L., and Cowan, N. J. (1998). Prefoldin, a chaperone that delivers unfolded proteins to cytosolic chaperonin. *Cell* *93*, 863-873.
- Van Raamsdonk, J. M., Murphy, Z., Slow, E. J., Leavitt, B. R., and Hayden, M. R. (2005). Selective degeneration and nuclear localization of mutant huntingtin in the YAC128 mouse model of Huntington disease. *Hum Mol Genet* *14*, 3823-3835.
- van Roon-Mom, W. M., Reid, S. J., Jones, A. L., MacDonald, M. E., Faull, R. L., and Snell, R. G. (2002). Insoluble TATA-binding protein accumulation in Huntington's disease cortex. *Brain Res Mol Brain Res* *109*, 1-10.
- Vendruscolo, M., Paci, E., Dobson, C. M., and Karplus, M. (2001). Three key residues form a critical contact network in a protein folding transition state. *Nature* *409*, 641-645.
- Venkatachalam, C. M., and Ramachandran, G. N. (1969). Conformation of polypeptide chains. *Annu Rev Biochem* *38*, 45-82.
- Verhoef, L. G., Lindsten, K., Masucci, M. G., and Dantuma, N. P. (2002). Aggregate formation inhibits proteasomal degradation of polyglutamine proteins. *Hum Mol Genet* *11*, 2689-2700.
- Vonsattel, J. P., Myers, R. H., Stevens, T. J., Ferrante, R. J., Bird, E. D., and Richardson, E. P., Jr. (1985). Neuropathological classification of Huntington's disease. *J Neuropathol Exp Neurol* *44*, 559-577.

- Wacker, J. L., Zareie, M. H., Fong, H., Sarikaya, M., and Muchowski, P. J. (2004). Hsp70 and Hsp40 attenuate formation of spherical and annular polyglutamine oligomers by partitioning monomer. *Nat Struct Mol Biol* *11*, 1215-1222.
- Waelter, S., Boeddrich, A., Lurz, R., Scherzinger, E., Lueder, G., Lehrach, H., and Wanker, E. E. (2001). Accumulation of mutant huntingtin fragments in aggresome-like inclusion bodies as a result of insufficient protein degradation. *Mol Biol Cell* *12*, 1393-1407.
- Walsh, D. M., Klyubin, I., Fadeeva, J. V., Cullen, W. K., Anwyl, R., Wolfe, M. S., Rowan, M. J., and Selkoe, D. J. (2002). Naturally secreted oligomers of amyloid beta protein potently inhibit hippocampal long-term potentiation in vivo. *Nature* *416*, 535-539.
- Wang, G. H., Mitsui, K., Kotliarova, S., Yamashita, A., Nagao, Y., Tokuhira, S., Iwatsubo, T., Kanazawa, I., and Nukina, N. (1999). Caspase activation during apoptotic cell death induced by expanded polyglutamine in N2a cells. *Neuroreport* *10*, 2435-2438.
- Warrick, J. M., Chan, H. Y., Gray-Board, G. L., Chai, Y., Paulson, H. L., and Bonini, N. M. (1999). Suppression of polyglutamine-mediated neurodegeneration in *Drosophila* by the molecular chaperone HSP70. *Nat Genet* *23*, 425-428.
- Wegrzyn, R. D., Hofmann, D., Merz, F., Nikolay, R., Rauch, T., Graf, C., and Deuerling, E. (2006). A conserved motif is prerequisite for the interaction of NAC with ribosomal protein L23 and nascent chains. *J Biol Chem* *281*, 2847-2857.
- Wellington, C. L., Ellerby, L. M., Gutekunst, C. A., Rogers, D., Warby, S., Graham, R. K., Loubser, O., van Raamsdonk, J., Singaraja, R., Yang, Y. Z., *et al.* (2002). Caspase cleavage of mutant huntingtin precedes neurodegeneration in Huntington's disease. *J Neurosci* *22*, 7862-7872.
- Wetlaufer, D. B. (1973). Nucleation, rapid folding, and globular intrachain regions in proteins. *Proc Natl Acad Sci U S A* *70*, 697-701.
- Wetzel, R. (2005). Chemical and physical properties of polyglutamine deposits in brain tissue. In *Genetic Instabilities and Neurological Diseases*, R. Wells, and T. Ashizawa, eds. (San Diego, Elsevier).
- Wexler, N. S., Lorimer, J., Porter, J., Gomez, F., Moskowitz, C., Shackell, E., Marder, K., Penchaszadeh, G., Roberts, S. A., Gayan, J., *et al.* (2004). Venezuelan kindreds reveal that genetic and environmental factors modulate Huntington's disease age of onset. *Proc Natl Acad Sci U S A* *101*, 3498-3503.
- Wiedmann, B., Sakai, H., Davis, T. A., and Wiedmann, M. (1994). A protein complex required for signal-sequence-specific sorting and translocation. *Nature* *370*, 434-440.
- Williams, A. D., Portelius, E., Kheterpal, I., Guo, J. T., Cook, K. D., Xu, Y., and Wetzel, R. (2004). Mapping abeta amyloid fibril secondary structure using scanning proline mutagenesis. *J Mol Biol* *335*, 833-842.
- Wolynes, P. G., Onuchic, J. N., and Thirumalai, D. (1995). Navigating the folding routes. *Science* *267*, 1619-1620.
- Won, K. A., Schumacher, R. J., Farr, G. W., Horwich, A. L., and Reed, S. I. (1998). Maturation of human cyclin E requires the function of eukaryotic chaperonin CCT. *Mol Cell Biol* *18*, 7584-7589.
- Wytenbach, A., Carmichael, J., Swartz, J., Furlong, R. A., Narain, Y., Rankin, J., and Rubinsztein, D. C. (2000). Effects of heat shock, heat shock protein 40 (HDJ-2), and proteasome inhibition on protein aggregation in cellular models of Huntington's disease. *Proc Natl Acad Sci U S A* *97*, 2898-2903.
- Wytenbach, A., Swartz, J., Kita, H., Thykjaer, T., Carmichael, J., Bradley, J., Brown, R., Maxwell, M., Schapira, A., Orntoft, T. F., *et al.* (2001). Polyglutamine expansions cause decreased CRE-mediated transcription and early gene expression changes prior to cell death in an inducible cell model of Huntington's disease. *Hum Mol Genet* *10*, 1829-1845.

- Yaffe, M. B., Farr, G. W., Miklos, D., Horwich, A. L., Sternlicht, M. L., and Sternlicht, H. (1992). TCP1 complex is a molecular chaperone in tubulin biogenesis. *Nature* *358*, 245-248.
- Yamamoto, A., Lucas, J. J., and Hen, R. (2000). Reversal of neuropathology and motor dysfunction in a conditional model of Huntington's disease. *Cell* *101*, 57-66.
- Yan, W., Schilke, B., Pfund, C., Walter, W., Kim, S., and Craig, E. A. (1998). Zuo1, a ribosome-associated DnaJ molecular chaperone. *Embo J* *17*, 4809-4817.
- Young, J. C., Moarefi, I., and Hartl, F. U. (2001). Hsp90: a specialized but essential protein-folding tool. *J Cell Biol* *154*, 267-273.
- Young, J. C., Hoogenraad, N. J., and Hartl, F. U. (2003). Molecular chaperones Hsp90 and Hsp70 deliver preproteins to the mitochondrial import receptor Tom70. *Cell* *112*, 41-50.
- Young, J. C., Agashe, V. R., Siegers, K., and Hartl, F. U. (2004). Pathways of chaperone-mediated protein folding in the cytosol. *Nat Rev Mol Cell Biol* *5*, 781-791.
- Yu, Z. X., Li, S. H., Nguyen, H. P., and Li, X. J. (2002). Huntingtin inclusions do not deplete polyglutamine-containing transcription factors in HD mice. *Hum Mol Genet* *11*, 905-914.
- Zhai, W., Jeong, H., Cui, L., Krainc, D., and Tjian, R. (2005). In vitro analysis of huntingtin-mediated transcriptional repression reveals multiple transcription factor targets. *Cell* *123*, 1241-1253.
- Zhang, X., Smith, D. L., Meriin, A. B., Engemann, S., Russel, D. E., Roark, M., Washington, S. L., Maxwell, M. M., Marsh, J. L., Thompson, L. M., *et al.* (2005). A potent small molecule inhibits polyglutamine aggregation in Huntington's disease neurons and suppresses neurodegeneration in vivo. *Proc Natl Acad Sci U S A* *102*, 892-897.
- Zhu, X., Zhao, X., Burkholder, W. F., Gragerov, A., Ogata, C. M., Gottesman, M. E., and Hendrickson, W. A. (1996). Structural analysis of substrate binding by the molecular chaperone DnaK. *Science* *272*, 1606-1614.
- Ziegelhoffer, T., Lopez-Buesa, P., and Craig, E. A. (1995). The dissociation of ATP from hsp70 of *Saccharomyces cerevisiae* is stimulated by both Ydj1p and peptide substrates. *J Biol Chem* *270*, 10412-10419.
- Zimmerman, S. B., and Trach, S. O. (1991). Estimation of macromolecule concentrations and excluded volume effects for the cytoplasm of *Escherichia coli*. *J Mol Biol* *222*, 599-620.
- Zoghbi, H. Y., and Orr, H. T. (2000). Glutamine repeats and neurodegeneration. *Annu Rev Neurosci* *23*, 217-247.

7 Appendix

7.1 Abbreviations

Units are expressed according to the international system of units (SI), including outside units accepted for use with the SI. Amino acids are abbreviated with their one or three letter symbols. Protein and gene names are abbreviated according to their SWISSPROT database entries.

3-AT	3-Amino-1,2,4-triazole
ADP	adenosine 5'-diphosphate
APS	ammonium peroxodisulfate
ATP	adenosine 5'-triphosphate
bp	base pair
<i>C. elegans</i>	<i>Caenorhabditis elegans</i>
CMV	cytomegalovirus immediate-early promotor
Da	Dalton
ddH ₂ O	double distilled water
DAPI	4,6-diamidin-2-phenylindol
DNA	deoxyribonucleic acid
dNTP	dideoxy-nucleoside triphosphate
DMSO	dimethylsulfoxid
DTT	dithiothreitol
DMEM	Dulbecco's Modified Eagle's Medium
ECL	enhance chemiluminescence
<i>E.coli</i>	<i>Escherichia coli</i>
EDTA	ethylenediaminetetraacetic acid
FCS	fetal calf serum
FITC	fluorescein-isothiocyanate
FPLC	fast performance liquid chromatography
FRET	fluorescence resonance energy transfer
g	acceleration of gravity, 9.81 m/s ²
hr	hours
LB	Luria-Bertani
min	minutes
Ni-NTA	nickel-nitrilotriacetic acid
OD	optical density
P _i	inorganic Phosphate
PBS	phosphate-buffered saline
PEG	polyethylene glycol
PMSF	phenylmethylsulfonyl fluoride
pH	reverse logarithm of relative hydrogen proton (H ⁺) concentration
RT	room temperature
<i>S. cerevisiae</i>	<i>Saccharomyces cerevisiae</i>
SDS	sodium dodecylsulfate
TCA	trichloroacetic acid
TEMED	N,N,N',N'-tetramethylethylenediamine
Tris	Tris(hydroxymethyl)aminomethane
Triton X-100	octyl phenol ethoxylate
Tween 20	polyoxyethylen-sorbitan-monolaurate

7.2 Publications and Presentations

Publications

Behrends C., Langer C. A., Boteva R., Böttcher U. M., Stemp M. J., Schaffar G., Rao B. V., Giese A., Kretschmar H., Siegers K., and Hartl F. U. (2006). Chaperonin TRiC promotes the assembly of polyQ expansion proteins into nontoxic oligomers. *Molecular Cell* Vol.23, pp.887-897.

Schaffar G., Breuer P., Boteva R., Behrends C., Tzvetkov N., Strippel N., Sakahira H., Siegers K., Hayer-Hartl M., and Hartl F. U. (2004). Cellular toxicity of polyglutamine expansion proteins: Mechanism of transcription factor deactivation. *Molecular Cell* Vol.15, pp.95-105.

Harnasch M., Grau S., Behrends C., Dove S. L., Hochschild A., Iskandar M. K., Xia W., and Ehrmann M. (2004). Characterization of presenilin-amyloid precursor interaction using bacterial expression and two-hybrid systems for human membrane proteins. *Molecular Membrane Biology* Vol.21, pp.373-383.

Oral Presentations

Symposium of the SFB (Collaborative Research Center) 596 “Molecular mechanisms of neurodegeneration“, October 2006, LMU, Munich, Germany
“Chaperonin TRiC promotes the assembly of polyQ proteins into nontoxic oligomers”

Symposium of the SFB 596, October 2005, LMU, Munich, Germany
“The role of TRiC as a modulator in polyQ aggregation”

Symposium of the SFB 596, May 2005, LMU, Munich, Germany
“Mechanisms of polyQ protein toxicity and modulation by chaperones”

Poster Presentations and Conferences

EMBO (European Molecular Biology Organization) – FEBS (Federation of European Biochemical Societies) Conference on “Amyloid Formation“, March 2006, Florence, Italy
“Role of chaperonin TRiC as a suppressor of aggregation and cytotoxicity of polyglutamine expansion proteins”

GBM (Society for Biochemistry and Molecular Biology) Meeting on “Molecular Machines“, March 2005, Mosbach, Germany
“Soluble polyQ protein impairs transcription factor function”

Survey of the SFB 596 by the German Research Foundation, February 2004, Munich, Germany
“Pathomechanisms of Huntington’s disease: Effects of molecular chaperones”

7.3 Curriculum vitae

Personal Details

Name	Christian Behrends
Date of Birth	June 20, 1975
Place of Birth	Frankfurt (Main)
Nationality	German
Martial Status	single

Education

09/02-03/07	PhD thesis at the Max-Planck-Institute of Biochemistry, Martinsried, Germany Department of Cellular Biochemistry (Prof. F. U. Hartl) Subject: "Proteotoxicity of polyglutamine expansion proteins: Cellular mechanisms and their modulation by molecular chaperones"
12/01	Diplom (Master) in Biology, University of Konstanz, Germany
01/01-12/01	Diplom thesis at the School of Bioscience, Cardiff University, UK Molecular Cell Biology Research Group (Prof. M. Ehrmann), Subject: "Characterization of protein-protein interactions in <i>E.coli</i> "
09/96-12/01	Studies in Biology, University of Konstanz, Germany Focus: Genetics, Biochemistry, Microbiology and Molecular Toxicology
07/95-08/96	Civil service, Youth Hostel, Bad Endorf, Germany
07/95	Abitur (High School Diploma), Humboldtschule, Bad Homburg, Germany

